

UNIVERSITY OF GDAŃSK
FACULTY OF OCEANOGRAPHY AND GEOGRAPHY

Anna Fidor

**Peptides produced by the Baltic cyanobacterium
Nostoc edaphicum CCNP1411 –
structure and biological activity**

Peptydy produkowane przez bałtycką cyjanobakterię
Nostoc edaphicum CCNP1411 – struktura i aktywność biologiczna

PhD thesis under the supervision of
Prof. dr hab. Hanna Mazur-Marzec
in the Department of Marine Biotechnology
University of Gdańsk

Gdynia 2022

Podziękowania

Pragnę podziękować tym wszystkim, bez pomocy i wsparcia których praca ta nie mogłaby powstać...



Serdecznie dziękuję Pani Prof. dr hab. Hannie Mazur-Marzec za wieloletnią współpracę oraz możliwość realizacji badań zaprezentowanych w niniejszej rozprawie doktorskiej. Dziękuję za przyjęcie mnie pod swoje skrzydła w 2015 roku, gdy byłam jeszcze na studiach licencyjnych. Dziękuję za merytoryczne wsparcie i motywację; za zaufanie, cierpliwość i wyrozumiałość; za przestrzeń do bycia naukowcem. Dziękuję za wprowadzenie mnie do niesamowitego świata Błękitnej Biotechnologii.



Dziękuję Wszystkim Pracownikom Zakładu Biotechnologii Morskiej za okazaną pomoc podczas prowadzenia badań. Dziękuję za każdą naukową i nienaukową dyskusję przy kawie, za Waszą radę i słowa wsparcia. Dziękuję za atmosferę, którą tworzycie. Realizacja doktoratu w takim Zespole była wielką przyjemnością!



Ogromnie dziękuję osobie, która w 2018 roku podjęła ze mną studia doktoranckie w Zakładzie Biotechnologii Morskiej – Robertowi Konkel. Dziękuję Ci za wszystkie długie godziny spędzone w laboratorium; za wspólne stanie przy zlewie podczas mycia tysięcy kolb i probówek. Dziękuję za to, że naprawiłeś wszystko, co niechcący “samo” się popsuło; za pomoc w każdym “nie da się”; za muzykę, sarkazm i żart. Dziękuję za to, że każdy problem stawał się wyzwaniem, każdy nieudany eksperyment stawał się motywacją, a każdy mikroskopijny sukces był przełomem na miarę samej Nagrody Nobla! Dziękuję!



Pragnę serdecznie podziękować Marcie Cegłowskiej (Instytut Oceanologii PAN) za okazaną pomoc i wsparcie w prowadzonych badaniach. Dziękuję Ci za wspólnie przeprowadzone (i niezliczone) rozdziały chromatograficzne; za zawsze miłe spędzony czas; za Nasze rozmowy; za wspólny śmiech; i za to, że zawsze mogę na Ciebie liczyć. Dziękuję!

Mojemu kuzynowi, Michałowi Szematowicz, dziękuję za ogromne wsparcie i bycie moim coach'em.

Dziękuję za to, że każdy mój ciężki czas potrafisz przekuć w przełom. Brat – dziękuję!



Składałam ogromne podziękowania mojej przyjaciółce, Sandrze Borejszą-Chmura. Dziękuję Ci kochana za to,

że od czasów szkolnych jesteś zawsze przy mnie. Dziękuję za Twoje wsparcie i wiarę we mnie.

Za to, że w chwilach słabości dodajesz mi skrzydeł.



Dziękuję moim Rodzicom.

Dziękuję za Wasze poświęcenie, wsparcie i wiarę we mnie;

za każde "przeczytaj" i "sprawdź";

i za to, że zawsze mogę na Was liczyć.



Mojej drugiej połowie, Dawidowi Ebel, z całego serca dziękuję.

Dziękuję, że zawsze przy mnie jesteś i we mnie wierzysz;

za to, że nigdy nie pozwoliłeś mi się poddać

i za to, że w chwilach słabości przypominasz mi kim jestem.

Pracę dedykuję tym, którzy od zawsze skłaniali mnie do zadawania pytań

– RODZICOM

STRESZCZENIE

Cyjanobakterie to fotosyntetyzujące Gram-ujemne bakterie. Uważane są za jedną z najstarszych form życia na Ziemi. Organizmy te są bogatym źródłem biologicznie aktywnych metabolitów, w tym toksyn oraz związków o potencjalnym biotechnologicznym i farmakologicznym zastosowaniu. Z uwagi na wykazaną aktywność, szczególną rolę przypisuje się peptydom oraz ich pochodnym. W tym zakresie badań, najwięcej prac dotyczy tropikalnych szczepów cyjanobakterii, jednak wyniki uzyskane w ramach niniejszej pracy doktorskiej wskazują na podobny potencjał mikroorganizmów pochodzących z Morza Bałtyckiego.

Do przeprowadzenia badań wykorzystano szczep *Nostoc edaphicum* CCNP1411 wyizolowany z Zatoki Gdańskiej (Morze Bałtyckie) i hodowany w warunkach laboratoryjnych. Na podstawie analiz widm fragmentacyjnych pozyskanych metodą tandemowej spektrometrii mas zidentyfikowano dziesięć wariantów strukturalnych peptydów z klasy nostocyclopeptydów (Ncps), zbudowanych (z jednym wyjątkiem) z siedmiu reszt aminokwasowych. Wyróżniono sześć nieznanych wcześniej struktur. Wśród nich, potwierdzono obecność związków zarówno o budowie cyklicznej, jak i liniowej. Wykazano, iż cztery cykliczne Ncps mają swoje odpowiedniki w postaci liniowych analogów zawierających C-końcową grupę aldehydową. Ponadto, liniowe analogi występowały w znacznie większej ilości niż ich cykliczne odpowiedniki. Fakt ten wskazuje, iż pomimo konformacyjnych uwarunkowań wynikających z obecności Gly oraz Gln, proces makrocyklizacji Ncps jest zależny także od pozostałych reszt aminokwasowych.

Sześć Ncps poddano badaniom pod kątem aktywności względem ludzkiego proteasomu 20S (h20S). Aktywność chymotrypsynopodobna (CH-L) h20S została zahamowana w obecności liniowych form Ncps, ale tylko takich, które w swojej strukturze zawierały C-końcową grupę aldehydową. W przypadku jednej z cyklicznych form zaobserwowano hamowanie aktywności trypsynopodobnej (T-L). Uzyskane wyniki stanowią pierwsze doniesienie o aktywności biologicznej Ncps względem proteasomu. Proteasom 20S jest kompleksem proteolitycznym, który uczestniczy w regulacji podstawowych procesów komórkowych w organizmach eukariotycznych. Nieprawidłowe działanie tej struktury prowadzi do wielu zaburzeń, w tym nowotworów. Ponieważ w ramach niniejszej pracy potwierdzono selektywne działanie Ncps względem h20S, związki te, jako nowe inhibitory tego kompleksu białkowego, mogą być brane pod uwagę jako narzędzia w badaniach nad regulacją procesów komórkowych.

Drugą grupą peptydów produkowanych przez bałtycki szczep *N. edaphicum* CCNP1411 były cyjanopeptoliny (Cps). Stwierdzono, że zidentyfikowane związki różnią się składem aminokwasowym oraz modyfikacjami w łańcuchu bocznym. Przeprowadzone testy z zastosowaniem kluczowych enzymów metabolicznych wykazały zależność aktywności Cps od aminokwasu ulokowanego między Thr i Aph. W przypadku Cps zawierających w tym miejscu Arg, zaobserwowano silny efekt względem trypsyny oraz umiarkowany względem chymotrypsyny. Z kolei peptydy zawierające Tyr, były selektywnie aktywne tylko względem chymotrypsyny. Enzymy należące do grupy proteaz są zaangażowane w szereg procesów metabolicznych, dlatego poszukuje się regulatorów (aktywatorów i inhibitorów) tych białek celem zastosowania ich w terapiach medycznych. Cps, jako inhibitory trypsyny i chymotrypsyny, mogą zatem stanowić wyjściowe związki do opracowania nowych leków.

Wyniki dotychczasowych badań niewątpliwie ujawniają potencjał bałtyckiego szczepu *Nostoc edaphicum* CCNP1411, jako źródła związków o istotnej aktywności biologicznej oraz stanowią silne podstawy do dalszych badań nad ich farmaceutycznym lub biotechnologicznym wykorzystaniem.

ABSTRACT

Cyanobacteria are photosynthetic Gram-negative bacteria. They are considered as one of the oldest life forms on the Earth. These organisms constitute a rich source of biologically active metabolites, including toxins and compounds with potential biotechnological and pharmaceutical applications. Due to their biological activity, peptides and their derivatives have attracted the attention of scientific community. The greatest interest in this field of research has been focused on cyanobacteria originating from tropical regions. However, the results obtained within this PhD thesis indicate a similar potential of microorganisms from the Baltic Sea.

In this study, *Nostoc edaphicum* strain CCNP1411 isolated from the Gulf of Gdańsk (Baltic Sea) was used and cultured for biomass. The analyses of mass fragmentation spectra obtained with application of tandem mass spectrometry allowed for identification of ten peptides classified to nostocyclopeptide (Ncp) group of compounds. This includes six new analogues containing (with one exception) seven amino acid residues, occurring in cyclic as well as in linear form. It was shown that four cyclic Ncps have their linear counterparts with a C-terminal aldehyde group. Moreover, the linear analogues were present in higher concentrations than their cyclic forms. This fact indicated that despite the conformational determinants resulting from the presence of Gly and Gln, the macrocyclization process is also dependent on other amino acid residues.

Six Ncps were tested for their activity against the human 20S proteasome (h20S). The chymotrypsin-like (CH-L) activity of h20S was inhibited in the presence of linear forms of Ncps, but only those that contained a C-terminal aldehyde group in their structure. For the cyclic variants, no such effect was observed. In contrast, one of the cyclic forms inhibited the trypsin-like (T-L) activity of the h20S proteasome. This is the first report on Ncps activity against proteasome. The 20S proteasome is a proteolytic complex that takes part in the regulation of basic cellular processes in eukaryotic organisms. Dysfunction of this proteolytic complex leads to many pathological disorders, including cancer. Since the selective activity of Ncps against h20S was confirmed within this PhD thesis, these compounds, as novel inhibitors, may be considered as tools in studies on the regulation of cellular processes.

The other group of peptides produced by the Baltic strain of *N. edaphicum* CCNP1411 were cyanopeptolins (Cps). The identified compounds (thirteen analogues) were found to differ in amino acid composition and side chain modifications. Biochemical assays using key metabolic enzymes indicated the effect of the amino acid located between Thr and Aph on biological activity of these peptides. In the case of Cps containing Arg at this position, a strong activity against trypsin and moderate against chymotrypsin was observed. In contrast, peptides containing Tyr were selectively active only against chymotrypsin. Proteases are known to be involved in a number of metabolic processes, therefore regulators (activators and inhibitors) of these proteins are sought for their application in medical therapies. Cps, as trypsin and chymotrypsin inhibitors, can be therefore the starting material for development of new drugs.

The results of the present study undoubtedly reveal the potential of the Baltic strain *Nostoc edaphicum* CCNP1411, as a source of compounds with significant biological activity and provide a strong basis for further research into the possible pharmaceutical or biotechnological application.

CONTENTS

1. INTRODUCTION	8
1.1. Peptides produced by cyanobacteria of the genus <i>Nostoc</i> – structure and activity	8
2. MAIN AIMS OF THE STUDY	10
3. MATERIALS AND METHODS.....	11
3.1. Cyanobacterium <i>Nostoc edaphicum</i> CCNP1411 – isolation, purification and culture	11
3.2. Genetic analyses	12
3.3. Extraction and isolation	12
3.4. LC-MS/MS analysis	13
3.5. NMR analysis	13
3.6. Enzymatic inhibition assay	13
3.7. Cytotoxicity assay.....	14
3.8. Human 20S proteasome assays.....	15
4. RESULTS AND DISCUSSION	15
4.1. Analysis of structure	15
4.1.1. Cyanopeptolins	15
4.1.2. Nostocyclopeptides	17
4.2. Biological activity.....	20
4.2.1. Cyanopeptolins	20
4.2.2. Nostocyclopeptides	21
5. CONCLUSIONS.....	22
6. REFERENCES	23
7. PUBLICATIONS.....	30
7.1. Publication 1	31
7.2. Publication 2	55
7.3. Publication 3	111
7.3. Publication 4	141
8. APPENDIX.....	158

1. INTRODUCTION

Cyanobacteria, photosynthetic Gram-negative bacteria, belong to one of the oldest forms of life. The earliest evidence of their occurrence is dated back to over three billion years (stromatolites in Western Australia and Greenland). As first organisms capable of producing oxygen, they had a significant impact on the evolution of life on the Earth (Schirrmeister et al., 2016). Cyanobacteria occur in various environments, including fresh and marine waters as well as terrestrial habitats (Hallenbeck, 2017). Their abundant occurrence and production of toxins by some species pose a high risk to aquatic organisms and human health. In the Baltic Sea, the dense blooms are formed in summer by three taxa, *Nodularia spumigena*, *Aphanizomenon flosaquae* and *Dolichospermum* spp. (Olofsson et al., 2020; Kahru et al., 2020). Apart from toxins, cyanobacteria can also produce a large number of biologically active metabolites with potential biotechnological significance (Shah et al., 2017; Khalifa et al., 2021; Singh et al., 2005; Singh et al., 2017).

Compounds produced by cyanobacteria have attracted the attention of scientists from different sectors of biotechnology. The *Synechocystis* sp. and *Synechococcus* sp. are producers of polyhydroxyalkanoates (PHAs), one of the most promising bioplastic materials (Troschl et al., 2017). Several species including *Anabaena oryzae* or *Spirulina platensis* have been extensively explored for wastewater treatment use (Ansari et al., 2015). *Arthrospira maxima* can be applied as an alternative energy source by production of hydrogen during autofermentation of glycogen under dark anaerobic conditions (Ananyev et al., 2012). Due to the high content of proteins, vitamins, minerals, fatty acids and pigments, *Arthrospira platensis* is commonly used as a food and dietary supplement for humans and animals (Demarco et al., 2022).

The pharmacological potential of cyanobacterial metabolites has also been documented. Numerous compounds have been tested in preclinical studies or entered clinical trials. Brentuximab vedotin 63 (Adcetris™) is an example of cyanometabolite that was approved by the U.S. Food and Drug Administration (FDA) and European Medicines Evaluation Agency (EMA). This synthetic analog of dolastatin 10, isolated from *Symploca hydnoidea* (Luesch et al., 2001), is applied in the treatment of lymphoma in adults (van de Donk et al., 2012).

1.1. Peptides produced by cyanobacteria of the genus *Nostoc* – structure and activity

The species of the genus *Nostoc* (order Nostocales) belong to the most common cyanobacteria. They can be found in a wide range of environmental conditions, from tropics to the polar regions, in aquatic (sea-, brackish- and fresh water bodies) and terrestrial habitats (Dodds et al., 1995; Sand-Jensen et al., 2014; Arima et al., 2012). *Nostoc* can form micro- or macroscopic colonies, living as free forms or as symbionts in association with other organisms i.e. marine sponges, cycads, or fungi (Kobayashi et al., 1994; Yamada et al., 2012; Kaasalainen et al., 2012; Oksanen et al., 2004). *Nostoc* was reported to produce biologically active compounds, mainly classified to peptides, lipopeptides, alkaloids or polysaccharides. Peptides and peptide-like compounds are composed of proteogenic and non-proteogenic amino acids, as well as other unique units (Dittmann et al., 2001; Dembitsky et al., 2005; Nowruzi et al., 2012; Řezanka et al., 2003; Welker et al., 2006). In this thesis, the structures and biological activities of peptides produced by *Nostoc edaphicum* CCNP1411 from the Baltic Sea were studied.

Non-ribosomal peptides (NRPs) constitute an important group of secondary metabolites produced by *Nostoc* species (Dittmann et al., 2015). They are synthesized on multifunctional enzyme complexes called non-ribosomal peptide synthetases (NRPSs). NRPSs are composed of proteins responsible for selection, activation, transport, incorporation of amino acids, peptide-bond formation, as well as a release of the final product from the biosynthetic machinery. Post-translational structural modifications catalyzed by tailoring enzymes are important part of the multi-step biosynthetic pathway. They include oxygenation, methylation, epimerization or cyclization reactions (Weber et al., 2001; Finking et al., 2004; Dittmann et al., 2015). These modifications increase the structural diversity of NRPs and provide an abundant chemical space for exploration (Felngle et al., 2008).

In addition to the NRPs, *Nostoc* as well as other cyanobacteria has the ability to produce polyketides (PKs) (e.g. nosperin) which are assembled by polyketide synthases (PKSs) (Kampa et al., 2013). PKS resembles NRPS in modular organization. As in the case of non-ribosomal peptides, products of polyketide synthesis also undergoes various modifications (Dittmann et al., 2001). It was demonstrated that cyanobacteria of the genus *Nostoc* also produce NRPs and PKs hybrids (NRPs/PKs) (i.e. cryptophycins, nostophycin) (Magarvey et al., 2006; Fewer et al., 2011).

Nostoc-derived peptides have been widely screened for the possible use (Khalifa et al., 2021). The cyclic depsipeptides classified to cryptophycins (Crs) are known for their potent cytotoxic effects against cancer cells. Three strains of *Nostoc* sp. ATCC53789 (Scotland), GSV-224 (India) and ASN_M (Iran), were confirmed to produce this class of compounds. There are 28 naturally occurring Crs, and many other structural variants of the compounds were chemically synthesized. These metabolites consist of four non-proteogenic units enclosed in cyclic form by an ester bond. They showed strong anticancer activity against several cell lines, including multidrug-resistant (MDR) cancer cells. Crs cause cell cycle arrest in the G2/M phase leading to apoptosis (Golakoti et al., 1995; Schwartz et al., 1990). Recently, the pharmaceutical potential of Cr-52 and Cr-55, as antibody drug conjugates (ADC), has been explored (Lai et al., 2020). Cyanovirin-N (CV-N), a lectin isolated from *Nostoc ellipsosporum*, is an antiviral polypeptide. The molecule consists of 101 amino acids, including four cysteine residues, which form disulfide bonds stabilizing the structure.

CV-N has potent *in vitro* and *in vivo* activity against human immunodeficiency virus (HIV-1 and -2), simian immunodeficiency virus (SIV), and several other enveloped viruses (Boyd et al., 1997; Gustafson et al., 1997). This lectin interacts with the viral envelop glycoprotein gp120 and blocks the cell-to-cell transmission of the virus between infected and uninfected cells. As the compound is chemically stable and non-toxic, it is considered as an important candidate for antiviral drug development (Dey et al., 2000).

Nostoc is a source of other non-ribosomal peptides that are not exclusively produced by cyanobacteria of this genus. These include toxins such as microcystins (MC). The difference between analogues produced by *Nostoc* and by other cyanobacteria is the presence of *O*-acetyl-demethyl Adda (ADMAdda) instead of Adda (Sivonen et al., 1990; Oksanen et al., 2004). In addition, *Nostoc* sp. 65.1 and *Nostoc* sp. 73.1 (Australia) were confirmed as nodularin and *L*-Har nodularin producers, respectively (Gehringer et al., 2010; Gehringer et al., 2012). Cyanobacteria of the genus also constitute a source of cyanopeptolins (Cps), the potent protease inhibitors (Publication 2), which among other are produced by species of *Microcystis* and *Planktothrix* (Jakobi et al., 1996; Welker et al., 2004a and 2004b; Bister et al., 2004; Martin et al., 1993). The biological activity of Cps depends on their amino acid composition and chemical character of the residues, as shown in Publication 2. In addition, cyanopeptolin-like peptides such as nostopeptins or insulapeptolides were isolated from *Nostoc* strains (Ploutno et al., 2002; Mehner et al., 2008; Okino et al., 1997).

As a part of this dissertation, the existing knowledge on structural diversity and biological activity of peptides produced by cyanobacteria of the genus *Nostoc* was reviewed (Publication 1).

2. MAIN AIMS OF THE STUDY

The main aim of the work was structure elucidation and biological activity assessment of peptides (nostocyclopeptides, Ncps; cyanopeptolins; Cps) produced by the Baltic Sea cyanobacterium *Nostoc edaphicum* CCNP1411 (Fig. 1). Liquid chromatography techniques (analytical/flash/preparative), tandem mass spectrometry (MS/MS) and Nuclear Magnetic Resonance (NMR) spectroscopy were used to isolate pure peptides and identify their structures (Publication 2-4). To determine the activity of compounds, biochemical assays (enzyme inhibition, h2OS proteasome inhibition and MTT assay) (Publication 2 and 4) were applied. The genome of CCNP1411 was sequenced and nostocyclopeptide gene cluster was characterized (Publication 3). The existing knowledge about the peptides and peptide-like compounds produced by *Nostoc* species was reviewed (Publication 1).

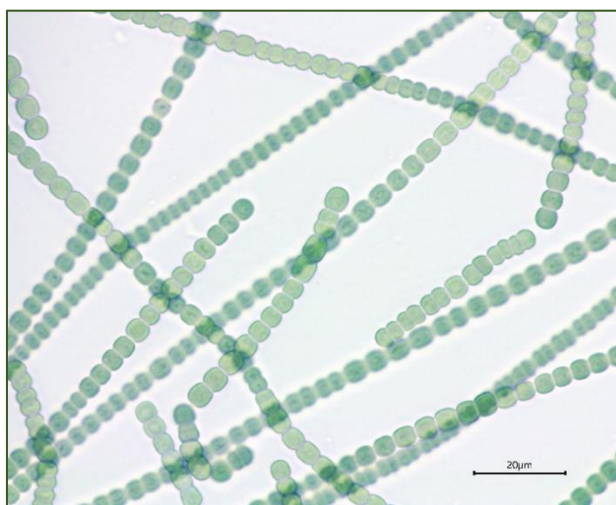


Figure 1. *Nostoc edaphicum* CCNP1411

3. MATERIALS AND METHODS

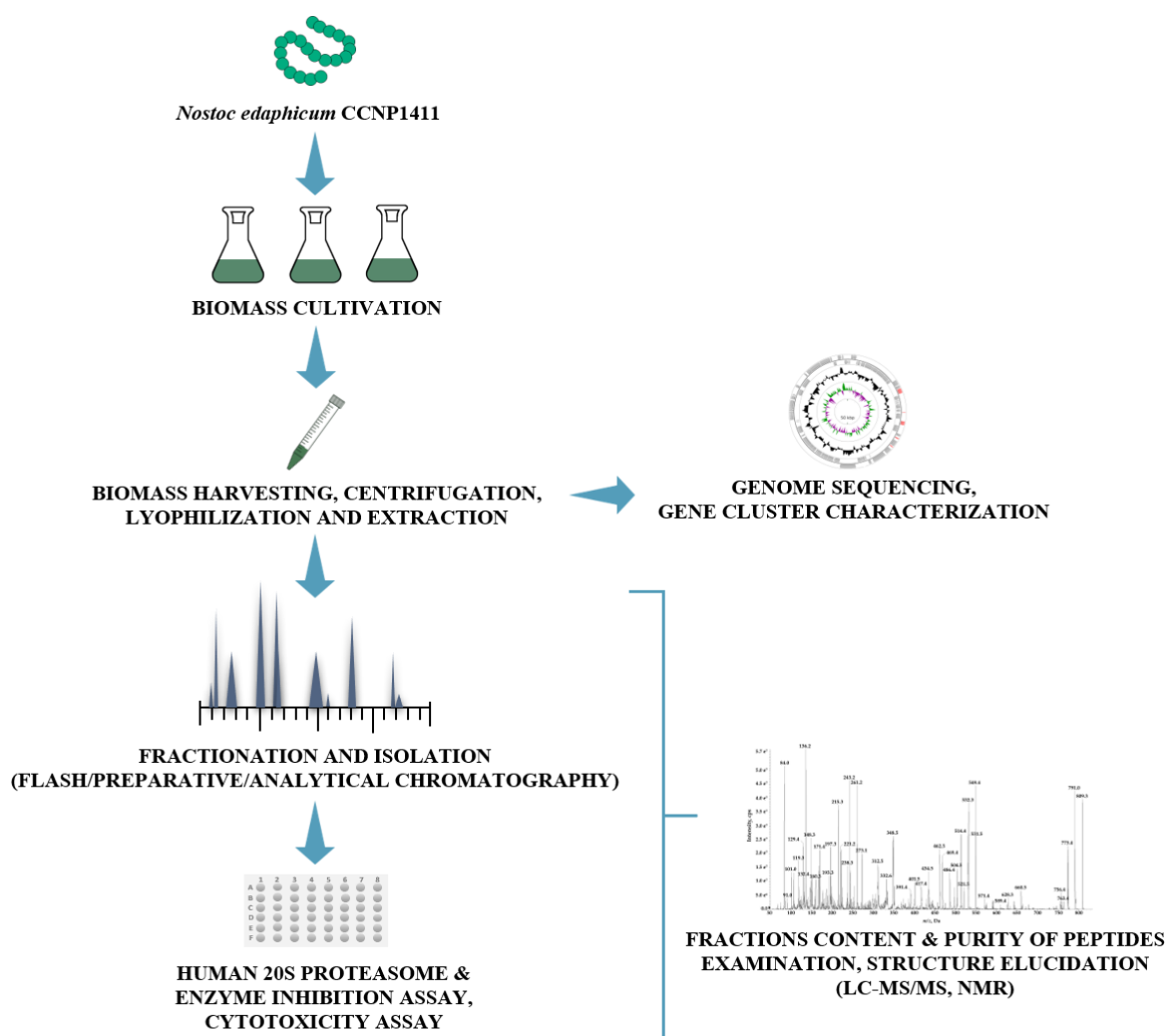


Figure 2. A flowchart presenting a sequence of procedures applied in the study

3.1. Cyanobacterium *Nostoc edaphicum* CCNP1411 – isolation, purification and culture

Nostoc edaphicum strain CCNP1411 was isolated in 2010 from the Gulf of Gdańsk (southern Baltic Sea) by Dr Justyna Kobos (University of Gdańsk). The strain belongs to filamentous cyanobacteria of Nostocales order characterized by spherical or barrel-shaped cells ($4.56 \pm 0.30 \mu\text{m}$ wide and $4.12 \pm 0.72 \mu\text{m}$ long) and lack of akinetes. CCNP1411 was grown in Z8 medium (2 and 5 L flasks) enriched with NaCl (Kotai, 1972) at $22 \text{ }^\circ\text{C} \pm 1 \text{ }^\circ\text{C}$ and light intensity of $5\text{-}10 \mu\text{mol photons m}^{-2} \text{ s}^{-1}$. After three weeks, cyanobacterial biomass was harvested using a nylon net (mesh size $25 \mu\text{m}$) and freeze-dried (Alpha 2-4 LSCbasic, Martin Christ Gefriertrocknungsanlagen GmbH, Osterode am Harz, Germany) before further processing. A ceftriaxone ($100 \mu\text{g mL}^{-1}$) (Pol-Aura, Olsztyn, Poland), a third-generation cephalosporin, was applied to purify the strain by reducing the number of accompanying heterotrophic bacteria. The purity of the culture was verified by microscopic examinations and inoculation on agar, including LA-agar (solid LB medium enriched 1.5% agar) (Bertani, 1951) and highly nutritious Columbia agar with 5% sheep blood (BTL Ltd., Łódź, Poland).

3.2. Genetic analyses

Genetic analyses were performed by Michał Grabski (University of Gdańsk), Jan Gawor and Robert Gromadka (Polish Academy of Sciences). Genomic DNA of *Nostoc edaphicum* CCNP1411 was isolated according to method described by Nowak et. al (2019). A control of DNA quality was performed by measurements of the absorbance (260/230 nm) using fluorimeter (Thermo Fisher Scientific, Waltham, MA, USA). The integrity of genetic material was analyzed via electrophoresis and by PFGE using Biorad CHEF-III instrument (BioRad, Hercules, CA, USA). NEB Ultra II FS Preparation Kit was applied to construct a paired-end sequencing library. To sequence the library an Illumina MiSeq platform (Illumina, San Diego, CA, USA) and MinION sequencer were used. To assemble the genome of CCNP1411, raw data were filtered using Guppy v3.2.2 (Oxford Nanopore Technologies, Oxford, UK), then the quality of dataset was improved using Nanofilt according to de Coster et al. (2018) and NanoPlot. The assembling was conducted by Flye v2.6 (Kolmogorov et al., 2019). NRPS cluster was confirmed with BLAST_n, BLAST_p and antiSMASH (Altschul et al., 1997; Medema et al., 2011). Genomic sequences generated in the study were deposited in the GenBank database (PRJNA638531).

3.3. Extraction and isolation

The freeze-dried biomass of *N. edaphicum* CCNP1411 was homogenized (by mortar and pestle) and extracted four times with 75% methanol (MeOH) by vortexing for 30 min. Following centrifugation at 12,000 *g* for 15 min at 4 °C, supernatants were combined and diluted in MilliQ water to achieve the concentration of MeOH below 10%. Flash column chromatography technique was the first step of the cyanobacterial extract separation. It was performed by loading the sample onto 120 g SNAP KP-C18-HC column (100 Å, 30 µm) (Biotage, Uppsala, Sweden) using mainly Shimadzu HPLC system (Shimadzu Corporation, Kyoto, Japan) (Publication 3 and 4), and an Isolera flash chromatography system (Biotage, Uppsala, Sweden) (Publication 2). The elution was conducted with a mobile phase consisting of MilliQ water (phase A) and 100% MeOH (phase B) using a step gradient (10-100% B) at a flow rate 12-40 mL min⁻¹ (depending on the column and instrument). The volume of collected fractions was in the range of 40-60 mL, depending on the chromatographic run. During all chromatographic runs the absorbance was monitored at 210 and 270 nm.

After flash chromatography, Ncps- and Cps-containing fractions were obtained. In the second step of the isolation process, a preparative chromatography technique was applied (Shimadzu Corporation, Kyoto, Japan). For this purpose, Ncps- and Cps-containing fractions were combined (each class of compounds separately) and loaded onto XBridge BEH C18 OBD Prep column (250 × 19 mm; 10 µm; 130 Å) (Waters, Elstree, UK) (Publication 2) or Jupiter Proteo C12 column (250 × 21.2 mm; 4 µm; 90 Å) (Phenomenex, Torrance, CA, USA) (Publication 3 and 4). The mobile phase was composed of 5% acetonitrile (ACN) in MilliQ water (phase A) and 100% ACN (phase B), both containing 0.1% formic acid (FA). For most of the compounds, one preparative run was not sufficient and subsequent runs under modified conditions (gradient, flow rate) were performed. In general, Cps and Ncps were isolated when the content of phase B was 15-80% and 15-19%, respectively. In the case of four Ncps, an Agilent HPLC 1200 Series (Agilent Technologies, Santa Clara, CA, USA) analytical system was used to obtain pure peptides. In these cases, the separation was performed using Jupiter Proteo C12 column (250 × 4.6 mm; 4 µm; 90 Å) (Phenomenex, Torrance, CA, USA) and Zorbax Eclipse XDB-C18 column (150 × 4.6 mm; 5 µm; 80 Å) (Agilent Technologies, Santa Clara, CA, USA). Compounds were eluted in the range of 16-43% of phase B.

3.4. LC-MS/MS analysis

The analyses of collected fractions/subfractions, purity verification and compounds identification were performed by two systems, LC-MS/MS and UPLC-MS/MS. For LC-MS/MS analyses, an Agilent 1200 HPLC (Agilent Technologies, Santa Clara, CA, USA) coupled to a QTRAP5500 triple-quadrupole/linear ion trap mass spectrometer (Applied Biosystems MDS Sciex, Concord, ON, Canada) was used (Publication 3 and 4). Peptides and peptide-like compounds were separated using Zorbax Eclipse XDB-C18 column (150 × 4.6 mm; 5 μm; 80 Å) (Agilent Technologies, Santa Clara, CA, USA). A mobile phase A contained 5% ACN in water and phase B contained 100% ACN, both with the 0.1% FA. The content of phase B changed from 10% to 100% and a flow rate 0.6 mL min⁻¹ was applied. The mass spectrometer operated under the positive Turbo Ion Spray ionization mode and MS/MS fragmentation spectra were acquired within the range of *m/z* from 50 to 1100 Da. A Waters Acquity UPLC system (UPLC-MS/MS) coupled to a photodiode array detector (PDA) and a Xevo quadrupole time of flight mass detector (Waters, Elstree, UK) was used in Publication 2. Separation of compounds was conducted on an ethylene-bridged hybrid C18 column (100 × 2.1 mm; 1.7 μm; 130 Å) (Waters, Elstree, UK) with the application of the same mobile phases like in the case of LC-MS/MS, but under modified elution conditions (gradient elution 20-100% B, 0.3 mL min⁻¹). A positive ion electrospray scanning in the range of *m/z* from 50 to 2000 Da was used. Data acquisition in the case of the two systems was accomplished with the Analyst[®] Software (version 1.5.1 and 1.7) (Applied Biosystems, Concord, ON, Canada).

3.5. NMR analysis

NMR analysis was performed by Ewa Wiczerzak (University of Gdańsk). Two Bruker Avance III spectrometers, 500 MHz and 700 MHz, were applied to acquire 1D ¹H NMR and 2D homo- and heteronuclear NMR (COSY, TOCSY, ROESY, HSQC, HMBC) data collected for one Ncp and two Cps. Spectra were recorded in H₂O:D₂O (9:1) and DMSO-d₆. NMR data were processed and analyzed using TopSpin (Bruker, Billerica, MA, USA) and SPARKY Software (version 3.114, Goddard and Kneller, freeware www.cgl.ucsf.edu/home/sparky).

3.6. Enzymatic inhibition assay

Five enzymatic inhibition assays including proteases (chymotrypsin, trypsin, elastase, thrombin) and protein phosphatase-1 (PP1) were performed (Publication 2). All experiments were conducted in triplicate at 37 °C in 96-well plates. Conditions of the assays i.e. substrates, inhibitors, buffers and references are presented in Table 1. MilliQ water, buffer and substrate were used as a negative control in each assay. The absorbance was measured using SpectraMax M3 microplate reader (Molecular Devices, Sunnyvale, CA, USA) at 405 nm. Reagents were mainly from Sigma-Aldrich (St. Louis, MO, USA); PP1 was from England Biolabs (Hitchin, UK) and microcystin-LR was from Enzo Life Sciences (Lausen, Switzerland).

In addition, samples with the highest concentration of CP962 and CP985 (45.4 μg mL⁻¹) (containing and not containing enzymes) obtained during chymotrypsin and trypsin inhibition assays, were analyzed by LC-MS/MS for the Cps content verification.

Table 1. Reagents, solutions and procedures applied during enzyme inhibition assays.

Enzyme	Substrate	Inhibitor	Buffer	Reference
chymotrypsin (C4129) (0.1 mg mL ⁻¹)	<i>N</i> -Suc-Gly-Gly- <i>p</i> - nitroanilide (2 mM)		50 mM TrisHCl, 100 mM NaCl, 1 mM CaCl ₂ ; pH 7.5	Ploutno et al., 2005
trypsin (T0303) (0.1 mg mL ⁻¹)	<i>N</i> - α-benzoyl-DL- arginine- <i>p</i> - nitroanilide hydrochloride (BAPNA) (2 mM)	aprotinin (1.5-200 μg mL ⁻¹)		
elastase (E0258) (75 μg mL ⁻¹)	<i>N</i> -Suc-Ala-Ala- Ala- <i>p</i> -nitroanilide (2 mM)	elastatinal (5-125 μg mL ⁻¹)	0.2 M TrisHCl; pH 8.0	Kwan et al., 2009
thrombin (T4648) (0.5 mg mL ⁻¹)	(<i>N</i> - <i>p</i> -tosyl-Gly-L- Pro-L-Lys- <i>p</i> - nitroanilide acetate salt (0.5 mg mL ⁻¹)	(4-(2-aminoethyl)benzene- sulfonyl fluoride hydrochloride (AEBSF) (60-2400 μg mL ⁻¹)	0.2 M TrisHCl; pH 8.0	Bennett, 2007
protein phosphatase-1 (754S) (1 mg mL ⁻¹)	<i>p</i> -nitrophenyl phosphate disodium salt hexahydrate (<i>p</i> -NPP) (5.5 mg mL ⁻¹)	microcystin-LR (0.125-4.0 ng mL ⁻¹)	<u>Enzyme solution:</u> 50 mM Tris; 1 mg mL ⁻¹ BSA, 1 mM MnCl ₂ , 2 mM DTT; pH 7.4 <u>Substrate solution:</u> 5.5 mg mL ⁻¹ , 50 mM Tris, 0.5 mg mL ⁻¹ BSA; 20 mM MgCl ₂ ×6H ₂ O; 200 mM MnCl ₂ ×4H ₂ O; pH 8.1	Rapala et al., 2002

3.7. Cytotoxicity assay

Two Cps, CP962 and CP985, representing Arg- and Tyr-containing structures, were selected for the cytotoxicity assays. MCF-7 breast cancer cell line was used. Cells were seeded at a density of 7.5×10^3 cells/100 μL in a 96-well plates. The incubation was carried out at 37 °C, 5% CO₂ for 24 h. Then, cells were treated with Cps for a further 24 h in the range of concentration from 0 to 500 μg mL⁻¹. Next, a sterile and filtered solution of 3-(4,5-dimethylthiazol-2-yl)-2,5-diphenyltetrazolium bromide (MTT, 1 mg mL⁻¹) was added to each well. The incubation lasted 4 h (at 37°C, in the dark), then, the MTT solution was removed and formazan crystals solubilized in DMSO (1%). Before the absorbance was measured in microplate reader (at 560 nm) (Synergy/HT, BIOTEK, Wnooski, VT, USA), the 96-well plates were shaken in the dark, at room temperature for 20 min. Untreated cells constituted a negative control of the assay representing 100% cell viability. The experiment was performed in three independent assays – in each assay samples were tested in six replicates.

3.8. Human 20S proteasome assays

The activity of Ncps against human 20S (h20S) proteasome was conducted according to Czerwonka et al. (2020). The human-derived proteolytic complex applied in the assays was isolated from erythrocytes and purified by Professor Elżbieta Jankowska's group at the Department of Biomedical Chemistry (University of Gdańsk). A 0.01% sodium dodecyl sulfate was used as an activator of latent h20S. The final concentration of proteasome was $1 \mu\text{g mL}^{-1}$ (1.4 nM). To determine the inhibitory effect of Ncps (10 mM of stock solution prepared in DMSO; tested in the concentration range 5-50 μM), the fluorogenic substrates, Suc-LLVY-AMC, Boc-LRR-AMC and Z-LLE-AMC (at final concentration of 100 μM) were used in the chymotrypsin-, trypsin- and caspase-like activity assays (Enzo Life Sciences Inc., NY, USA). The content of DMSO was maintained below 3% of the final reaction volume. The assays were performed in 96-well plates in 50 mM TrisHCl (pH 8.0) at 37 °C. Fluorescence measurements (λ 380-460 nm) were performed in 2-min intervals for 60 with a Tecan Trading AG spectrofluorimeter (Männedorf, Switzerland). DMSO and PR11 (known proteasome inhibitor) (Gaczyńska et al., 2003) were used as a negative and positive control of the assay, respectively.

4. RESULTS AND DISCUSSION

4.1. Analysis of structure

4.1.1. Cyanopeptolins

In the Baltic strain *Nostoc edaphicum* CCNP1411 thirteen cyanopeptolins were detected. Of this, twelve analogues have been identified for the first time (Fig.3, Tab. 2). Structures were elucidated based on mass fragmentation spectra and NMR. These NRPs are composed of a six-amino acid cyclic part and two-residue side chain. The basic feature of all Cps is the presence of 3-amino-6-hydroxy-2-piperidone (Ahp) in position 3 (Fig. 3). Position 1 is conserved and occupied by *L*-Thr containing β -hydroxy group linked by an ester bond to carboxy terminus of the residue in position 6. Because of the presence of an ester bond Cps are classified to depsipeptides, more specifically, to peptidolactones. Positions 4 (Phe) and 6 (Val), and Asp in the side chain are conserved. Depending on the residue in position 2 (Arg or Tyr), compounds were classified to Arg-containing (Arg²-Cps) and Tyr-containing (Tyr²-Cps) Cps. Position 5 is occupied by *N*-methylated aromatic amino acids, MePhe, MeTyr or its homo-variant, MeHty. In the side chain of the Cps produced by CCNP1411, butanoic acid (BA), hexanoic acid (HA) or octanoic acid (OA), linked to Asp were present.

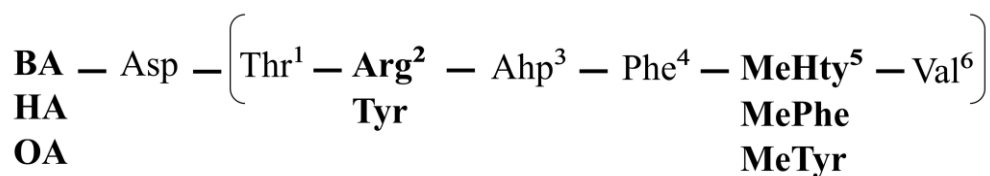


Figure 3. General structure of cyanopeptolins detected in *N. edaphicum* CCNP1411

Table 2. Structures, molecular masses and m/z values of the cyanopeptolins identified in *N. edaphicum* CCNP1411. The variable residues in position 2 and 5 of the cyclic part, and residue in the peptide chain, are marked in blue, green and orange, respectively.

Cyanopeptolin	Structure	Mass [Da]	m/z of $[M+H]^+$ (Arg^2 -Cp) or $[M+H-H_2O]^+$ (Tyr^2 -Cp)
CP1048	[Thr ¹ + Arg ² + Ahp ³ + Phe ⁴ + MeHty ⁵ + Val ⁶]Asp+OA	1048	1049
CP1020	[Thr ¹ + Arg ² + Ahp ³ + Phe ⁴ + MeHty ⁵ + Val ⁶]Asp+HA	1020	1021
CP1018	[Thr ¹ + Arg ² + Ahp ³ + Phe ⁴ + MePhe ⁵ + Val ⁶]Asp+OA	1018	1019
CP1006	[Thr ¹ + Arg ² + Ahp ³ + Phe ⁴ + MeTyr ⁵ + Val ⁶]Asp+HA	1006	1007
CP992	[Thr ¹ + Arg ² + Ahp ³ + Phe ⁴ + MeHty ⁵ + Val ⁶]Asp+BA	992	993
CP990	[Thr ¹ + Arg ² + Ahp ³ + Phe ⁴ + MePhe ⁵ + Val ⁶]Asp+HA	990	991
CP978	[Thr ¹ + Arg ² + Ahp ³ + Phe ⁴ + MeTyr ⁵ + Val ⁶]Asp+BA	978	979
CP962	[Thr ¹ + Arg ² + Ahp ³ + Phe ⁴ + MePhe ⁵ + Val ⁶]Asp+BA	962	963
CP1027	[Thr ¹ + Tyr ² + Ahp ³ + Phe ⁴ + MeHty ⁵ + Val ⁶]Asp+HA	1027	1010
CP1013	[Thr ¹ + Tyr ² + Ahp ³ + Phe ⁴ + MeTyr ⁵ + Val ⁶]Asp+HA	1013	996
CP999	[Thr ¹ + Tyr ² + Ahp ³ + Phe ⁴ + MeHty ⁵ + Val ⁶]Asp+BA	999	982
CP985	[Thr ¹ + Tyr ² + Ahp ³ + Phe ⁴ + MeTyr ⁵ + Val ⁶]Asp+BA	985	968
CP969	[Thr ¹ + Tyr ² + Ahp ³ + Phe ⁴ + MePhe ⁵ + Val ⁶]Asp+BA	969	952

The Tyr²-containing Cps were detected as dehydrated protonated molecules $[M + H - H_2O]^+$ and observed at m/z within the range of 952-1049 (Tab. 2). The occurrence of this ion form in Tyr²-containing cyanopeptolin-like (Cp-like) peptides was previously reported in aeruginopeptins by Harada et al. (2001). The process of structure elucidation was supported by the presence of immonium ions in MS/MS spectra. For example, the Tyr-immonium ion (m/z 136) was always present in Tyr²-Cps spectra. Two ion-derived peaks, corresponding to the longest residues sequence common to the spectra of all Cp analogues, were observed at m/z 297 $[Asp + Thr + Val + H - H_2O]^+$ and m/z 269 $[Asp + Thr + Val + H - H_2O - CO]^+$. To confirm the structure elucidation, CP962 and CP985 were purified in sufficient quantities for NMR analyses. The COSY, TOCSY and HMBC experiments proved the presence of Thr, Tyr, Ahp, Val, Asp, BA (CP985) and Thr, Arg, Ahp, Phe, MePhe, Val, BA (CP962). The presence of aromatic amino acid residues was recognized by the signals occurring in the aromatic region of the spectrum and the ¹H – ¹³C long range correlation led to recognize methylation as their modifications. Ahp residue was detected by the characteristic OH proton signal. A cyclic part of the compound containing an ester bond between Thr and Val was confirmed by HMBC correlations. NMR results were found to be consistent with structure elucidation based on mass fragmentation spectra. Among all compounds identified in this study, only one was previously reported, i.e. CP1006 and its chlorinated derivative (CP1040A) were identified in *Microcystis* (Welker et al., 2004a; Cadel-Six et al., 2008).

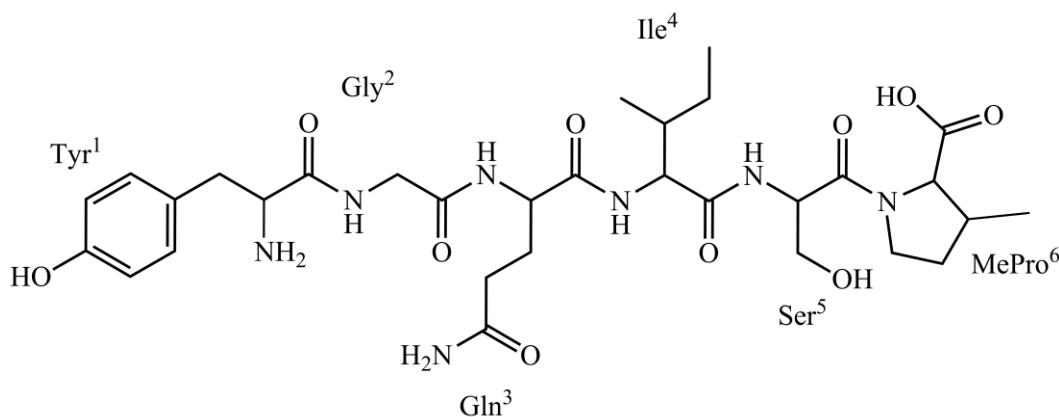
Apart from Cps, *Nostoc* produces a number of cyanopeptolin-like (Cp-like) peptides. As Cps, these compounds contain six-amino acid cyclic component and Ahp in position 3. The differences are mainly in position 1 and 2, e.g. in insulapeptolides from *Nostoc insulare*, Hmp (3-hydroxy-4-methyl-proline) and Leu/Hph (homophenylalanine) were documented (Mehner et al., 2008). In nostopeptin A and B, Hmp and Leu were also present, but in nostopeptin BN920 (in addition to Leu in position 2) position 1 was occupied by Thr, as in standard Cps analogues (Okino et al., 1997; Ploutno et al., 2002). Modifications are also present in the side chain. In nostocyclin identified by Kaya et al. (1996), three residues including Hse (homoserine), Ile and Hpla (p-hydroxyphenyllactic acid) were reported. In four insulapeptolides, two-component side chain was found containing citrulline (Cit) and acetic acid (Ac) residues (Mehner et al., 2008).

4.1.2. Nostocyclopeptides

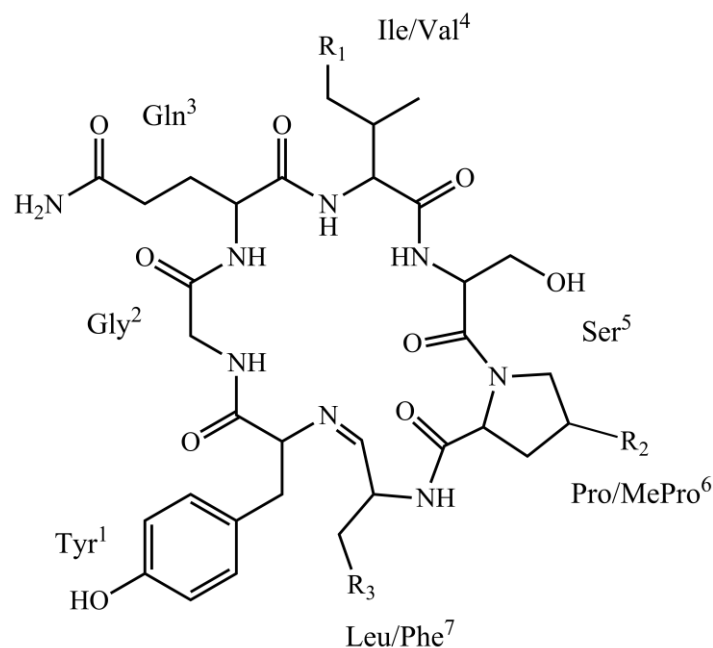
The application of mass spectrometry and NMR technique allowed the identification of ten nostocyclopeptide analogues in the Baltic Sea *Nostoc edaphicum* CCNP1411 (Tab. 3) (Publication 3). Of these, six compounds i.e. Ncp-E1, Ncp-E1-L, Ncp-E2, Ncp-E2-L, Ncp-E3 and Ncp-E4-L were detected for the first time. These compounds occur in two forms – as cyclic or linear structures. In addition, linear forms contain the aldehyde functional group in the C-terminus instead of the carboxyl group, so these compounds belong to the peptide-aldehyde class of compounds. Ncp-E4-L is the only Ncp having typical peptide structure with C-terminal carboxyl group. The masses of Ncps produced by the Baltic *Nostoc* strain ranges from 676 to 808 Da. With one exception (Ncp-E4-L) (Fig. 4A), these compounds are composed of seven amino acid residues (Fig. 4B-C). Of these, four are conserved including Tyr, Gly, Gln and Ser, occurring at positions 1, 2, 3 and 5, respectively (Fig. 4A-C). Among the detected peptides, five cyclic Ncps are characterized by the presence of a unique imine bond, identified for the first time in this class of compounds by Golakoti et al., (2001). An imine bond is formed between the N-terminal amine group of the conserved Tyr and the C-terminal aldehyde group of a residue at position 7. The three cyclic Ncps, Ncp-A1, Ncp-A2 and Ncp-E3, contain a methylated Pro at position 6, while Ncp-E1 and Ncp-E2 contain an unmodified form of this amino acid. In addition, these cyclic peptides contain Leu (Ncp-A1, Ncp-E2, Ncp-E3) or Phe (Ncp-A2, Ncp-E1) at position 7. Almost all detected cyclic forms have their linear aldehyde analogues. The only exception is a Val⁴-containing Ncp-E3, which occur only in a cyclic form.

Table 3. Structures of nostocyclopeptides (Ncps) detected in *Nostoc edaphicum* CCNP1411. The variable residues in position in 4, 6 and 7 are marked in blue, green and orange, respectively.

Nostocyclopeptide	Structure	Molecular Mass [Da]	
		Cyclic Form	Linear Form
Ncp-A1	[Tyr ¹ + Gly ² + Gln ³ + Ile ⁴ + Ser ⁵ + MePro ⁶ + Leu ⁷]	756	
Ncp-A1-L	Tyr ¹ + Gly ² + Gln ³ + Ile ⁴ + Ser ⁵ + MePro ⁶ + Leu ⁷		774
Ncp-A2	[Tyr ¹ + Gly ² + Gln ³ + Ile ⁴ + Ser ⁵ + MePro ⁶ + Phe ⁷]	790	
Ncp-A2-L	Tyr ¹ + Gly ² + Gln ³ + Ile ⁴ + Ser ⁵ + MePro ⁶ + Phe ⁷		808
Ncp-E1	[Tyr ¹ + Gly ² + Gln ³ + Ile ⁴ + Ser ⁵ + Pro ⁶ + Phe ⁷]	776	
Ncp-E1-L	Tyr ¹ + Gly ² + Gln ³ + Ile ⁴ + Ser ⁵ + Pro ⁶ + Phe ⁷		794
Ncp-E2	[Tyr ¹ + Gly ² + Gln ³ + Ile ⁴ + Ser ⁵ + Pro ⁶ + Leu ⁷]	742	
Ncp-E2-L	Tyr ¹ + Gly ² + Gln ³ + Ile ⁴ + Ser ⁵ + Pro ⁶ + Leu ⁷		760
Ncp-E3	[Tyr ¹ + Gly ² + Gln ³ + Val ⁴ + Ser ⁵ + MePro ⁶ + Leu ⁷]	742	
Ncp-E4-L	Tyr ¹ + Gly ² + Gln ³ + Ile ⁴ + Ser ⁵ + MePro ⁶		676

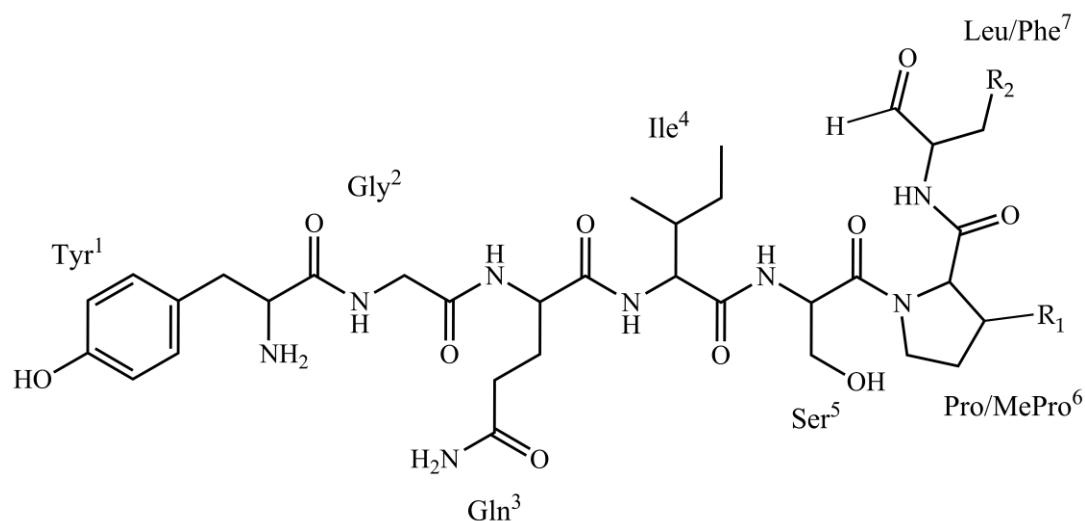


A



R₁: CH₃ (Ile) (Ncp: A1,A2, E1,E2); H (Val) (Ncp: E3)
 R₂: H (Pro) (Ncp: E1, E2); CH₃ (MePro) (Ncp: A1, A2, E3)
 R₃: C₃H₇ (Leu) (Ncp: A1, E2, E3); C₆H₅ (Phe) (Ncp: A2, E1)

B



R₁: H (Pro) (Ncp: E1-L, E2-L); CH₃ (MePro) (Ncp: A1-L, A2-L)
 R₂: C₄H₉ (Leu) (Ncp: A1-L, E2-L); C₇H₇ (Phe) (Ncp: A2-L, E1-L)

C

Figure 4. General structures of nostocyclopeptides: linear Ncp-E4-L (A), cyclic form (B) and linear (aldehyde) form (C)

In the *N. edaphicum* CCNP1411 genome (Tab. 1 and Fig. 2 in Publication 3), the non-ribosomal peptide synthetase (NRPS) cluster, containing genes coding for enzymes involved in Ncps synthesis was identified (Tab. 2 and Fig.3-5 in Publication 3). In the process, 35 complete cyanobacterial nucleotide sequence clusters were used and the antiSMASH analysis was employed. It was found, that the main part of the Ncp gene cluster, located between positions 7,609,981-7,643,289 bps of the

chromosome, is composed of two large genes – *ncpA* and *ncpB*. They are over 80% homologous to genes found in the *ncp* cluster in *Nostoc* sp. ATCC53789 (Fig.6 in Publication 3) (Becker et al., 2004). These two genes code for enzymes consisting of repetitive modules (condensation, adenylation and peptidyl carrier protein domains) which are responsible for peptide elongation by adding single residues. Substrate specificity of NRPS adenylation domains were recognized and present in Table 2 in Publication 3.

The results of chemical analyses (LC-MS/MS and NMR) were consistent with the analysis of *ncp* gene cluster (Publication 3). The process of structure identification of the peptides (Tab. 3) was carried out manually, on the basis of a series of *b* and *y* fragment ions produced by a cleavage of the peptide bonds. In addition, during the analysis, the presence of peaks originating from immonium ions, e.g. *m/z* 70 for Pro, 84 for MePro or 136 for Tyr), and peaks formed by loss of water (18 Da) or ammonia (NH₃) (17 Da) indicated the presence of specific residues. The identification of structures was additionally supported by the previously published spectra of Ncps (Nowruzi et al., 2012). The detailed characterization of fragmentation pathways of Ncps detected in the CCNP1411 strain is presented in the main text (Fig.7-9) and in supplementary materials (Fig.S1-S7) in Publication 3. Due to the insufficient amount of the isolated compounds, NMR analysis was possible to perform only for Ncp-A2-L (Fig.1 and Tab. 2 in Publication 4). The peptide sequence and the presence of Gly, Gln, Ile, Ser and the aromatic amino acids, Tyr and Phe, was confirmed by COSY, TOCSY and HMBC experiments. In addition, on the basis of ¹H NMR doublet signal at δ 0.82 ppm and the HMBC correlation between the methyl protons with carbons, the 4-methyl group of the Pro residue was identified. The lack of ROESY correlation between the aromatic residues occupying position 1 and 7 confirmed the linearity of the peptide.

During the study, the relative amounts of the individual Ncps produced by *N. edaphicum* CCNP1411 were determined. Due to lack of Ncps standards, the relative concentrations of the peptides were determined based on the peak areas of the parent ions in the extracted ion chromatograms. The experiment was carried out using different solvents and pH (Fig. 10 and Fig. S8 in Publication 3). According to Becker et al. (2004) Ncps are synthesized by NRPS as linear aldehydes and the process of formation of cyclic forms is enzyme independent and spontaneous phenomenon. However, according to Enck et al. (2008) the equilibrium between linear and cyclic forms can be controlled by pH and temperature. In the experiments performed within this thesis, the same temperature was used, but to exclude a spontaneous linearization during sample processing, fresh and lyophilized biomass was applied. Of the eight analyzed compounds, the linear Ncp-A2-L was the most abundant structural analogue. The highest ratios of linear (Ncp-A1-L, Ncp-A2-L) to cyclic (Ncp-A1, Ncp-A2) forms of Ncp were observed when the pH was in the intermediate range (pH 6 and 8). That was not in the agreement with the results obtained by Enck et al. (2008) where aldehydes were dominant mainly at low pH (pH 3). However, the cellular content of the linear Ncp aldehydes variants was generally higher than the cyclic ones, independently on the pH values or kind of the solvent (Fig. 10 and Fig. S8 in Publication 3). It was proven by Kopp et al. (2006) that macrocyclization process of Ncps is determined by the aldehyde geometry, especially by the conformation of amino acids such as *D*-Gln and Gly. Structural arrangement of these residues is crucial for the imino bond formation between the *N*-terminal amine group of Tyr and *C*-terminal aldehyde hydrate. As these two residues were present in all detected Ncps (including the linear forms), then, probably other elements of the structure affected the ring formation.

4.2. Biological activity

4.2.1. Cyanopeptolins

Among the thirteen cyanopeptolin variants (Tab. 2) detected in *N. edaphicum* CCNP1411, six were isolated in sufficient amounts for the assessment of activity against serine proteases (chymotrypsin, trypsin, elastase, thrombin) and protein phosphatase 1 (PP1) (Publication 2). Neither of the peptides was active against elastase, thrombin and PP1. In studies performed within this PhD thesis, Arg²-Cps significantly inhibited trypsin. In the case of four Arg-containing compounds (CP1020, CP1018, CP992, CP978) the effect was in the narrow range of IC₅₀ values, from 0.24 to 0.26 μM (Tab. 2 in Publication 2). The activity of other Arg²-containing peptides (CP1048, CP1006, CP990, CP962) was defined as medium. Five Arg²-Cps affecting trypsin were also active against chymotrypsin, but at the lower level of activity (IC₅₀ > 3.1 μM). The inhibitory activity of Arg²-Cps was probably also affected by the residue in position 5. Only when MeTyr⁵ or MeHty⁵ occurred the activity against two serine proteases was observed. When MePhe⁵ was present, Arg²-Cps were inactive against chymotrypsin. All Tyr²-Cps were selectively and potently active against chymotrypsin showing strong or moderate activity against the enzyme (IC₅₀ for CP1027 and CP985 was 0.26 μM ; Tab. 2 in Publication 2).

Based on the obtained results, it can be concluded that *N. edaphicum* CCNP1411 produces Cps with protease inhibition activity determined mainly by the residue in position 2 of the peptide (i.e. Arg or Tyr). This conclusion is consistent with results achieved in other studies. According to Gademann et al. (2010) and Choi et al. (2008), Arg in position 2 is important for the inhibitory activity against trypsin, while Tyr²-containing Cps are more potent and selective inhibitors of chymotrypsin (Bister et al., 2004; Yamaki et al., 2005). Cyanobacteria produce other Ahp-containing inhibitors of proteases. For example, *Symploca* sp. derived symplocamide A, with Cit (citrulline) in position 2, showed strong activity against chymotrypsin (IC₅₀ 0.38 μM) and 200-fold weaker activity against trypsin (IC₅₀ 80.2 μM). The similarity in the structure of Cit and Arg as well as similar activity of Arg²-Cps and symplocamide A confirm the crucial role of amino acid in position 2 on cyanopeptides activity against serine proteases (Linington et al., 2008).

Changes in the relative concentration of Arg²-containing CP962 and Tyr²-containing CP985 during 20-min exposure to serine proteases were measured by LC-MS/MS. No significant losses of these peptides were observed. These results are in agreement with Yamaki et al. (2005) who suggested that cyanopeptolins, as serine proteases inhibitors, block the active centers of the enzymes and do not undergo hydrolysis during the reaction. The same two Cps, CP962 and CP985, were used in the cytotoxicity assay (MTT) on MCF-7 breast cancer cells, but no effects were observed (Fig. 5 in Publication 2). Cps-like peptide isolated from *Symploca* sp., symplocamide A, had no cytotoxic activity to NCI H460 lung cancer cells and neuro-2A neuroblastoma cells (Linington et al., 2008). However, in the experiments conducted by Faltermann et al (2016), cyanopeptolin CP-1020, with an identical cyclic part of the molecule to CP1006 from CCNP1411, showed anti-inflammatory activity in Human Hepatoma Cell Line Huh7.

Peptides that modify the activity of serine proteases, such as trypsin or chymotrypsin, have already been used in medicine. For example, trypsin inhibitors are applied in the acute pancreatitis treatment (Mao, et al., 2021). de Lima et al. (2019) proposed the use of trypsin inhibitors in obesity and other metabolic disorders, while according to de Souza Nascimento et al. (2021), peptide trypsin inhibitors can be used in treatment of bacterial infections.

Inhibitors of proteases such as cyanopeptolins can also have some ecological functions, e.g. they can protect cyanobacteria from grazers as it was documented in the case of oscillapeptin J, CP SS and CP-1020 (Jakobi et al., 1996; Gademann et al., 2010; Blom et al., 2003). The toxic effects of these cyanopeptides on crustaceans *Daphnia magna* and *Thamnocephalus platyurus* were reported. Also for *N. edaphicum* CCNP1411, these peptides can constitute an element of defense or play role

of signaling molecules. Similarly to other bioactive cyanopeptides, the ecological role of Cps is still a matter of scientific debate and should be further explored.

4.2.2. Nostocyclopeptides

Among ten Ncps produced by *N. edaphicum* CCNP1411, six compounds, including cyclic (Ncp-A1, Ncp-A2, Ncp-E2) and linear forms (Ncp-A2-L, Ncp-E2-L, Ncp-E4-L) were isolated and their inhibitory activity against human 20S (h20S) proteasome was investigated (Publication 4). The study revealed a selective effects of the compounds. The chymotrypsin-like (CT-L) activity of the h20S proteasome was inhibited (IC_{50} ca. 50 μ M) in the presence of the linear forms of Ncps that contained a C-terminal aldehyde group, i.e. Ncp-A2-L (Fig. 1 in Publication 4) and Ncp-E2-L. Due to the limited amounts of the isolated compounds, their effect on the trypsin-like (T-L) and caspase-like (C-L) activity of the h20S proteasome was examined with no replications. For the cyclic Ncp-A2, an inhibitory and concentration-dependent effect on the T-L activity, and weak effect on C-L activity, were observed. Two cyclic Ncps, Ncp-A1 and Ncp-E2, and the linear hexapeptide Ncp-E4-L did not inhibit the catalytic sites of the h20S proteasome.

Ncp-E2-L, similarly to the widely used synthetic proteasome inhibitor MG-132 (Guo et al., 2013; Zhang et al., 2011), contains an aldehyde group at the C-terminal Leu. The inhibitory activity of MG-132 (IC_{50} 0.11 μ M) was explained by the formation of a hemiacetal covalent bond between an aldehyde group of Leu and a hydroxyl group of Thr1 located in the active site of the proteasome (Kisselev et al., 2001; Adams et al., 2003). Since both, Ncp-A2-L and Ncp-E2-L, are small peptides containing a C-terminal aldehyde group, the importance of this moiety in CT-L inhibition can be inferred. The inhibition level of the isolated Ncps was moderate (approx. IC_{50} ca. 50 μ M) (Fig. 2A in Publication 4). However, it was compensated by the specificity of their action. Ncp-A2-L and Ncp-E2-L did not inhibit two other activities (Fig. 2B and 2C in Publication 4), while Ncp-A2 affected only T-L active site of the h20S proteasome (Fig. 2A-C in Publication 4). Many other naturally occurring peptide aldehydes interact with more than one active site of the proteasome. For example, fellutamide B produced by marine fungus *Peicillum fellutanum*, interacts potently, but with all three active sites of proteasome, i.e. CT-L (IC_{50} 9.4 nM), T-L (IC_{50} 2.0 μ M) and C-L (IC_{50} 1.2 μ M), respectively (Hines et al., 2008).

Inhibitors reacting selectively with specific active centers are valuable tools in studies on the mechanism of their action (Kisselev et al., 2003; Mirabella et al., 2011; Harer et al., 2012). CT-L activity of proteasome was proved to be crucial, and its inhibition blocks the 20S proteasome functions. For example, the boronic acid moiety in bortezomib binds to and forms a complex with the hydroxyl group of Thr in the β 5-subunit of the CT-L active site, blocking the 20S complex (Kisselev et al., 2012; Groll et al., 2006). However, Mirabella et al. (2011) demonstrated that CT-L and T-L active sites may constitute target and co-target of the anticancer therapy, respectively. According to the authors, inhibition of T-L active site of h20S proteasome may sensitize myeloma cells to CT-L activity inhibitors, increasing the effectiveness of the applied inhibitors.

Proteasome regulators are explored as promising therapeutic agents, especially in the case of cancer or autoimmune disorders (Goldberg et al., 2012; Field-Smith et al., 2006; Verbrugge et al., 2015). Many of them belongs to peptide-based structures (de Bettignies et al., 2010). It was shown that Ncp-A2-L or Ncp-E2-L cannot be used for therapeutic purposes due to the presence of a highly reactive aldehyde group (Beck et al., 2012; de Bettignies et al., 2010). However, structural modifications of the peptides can optimize their activity, so that these compounds still may be used as tools in 20S proteasome inhibition studies. Such strategy was applied in the case of a widely used 20S proteasome inhibitor, MG-132 (Kisselev et al., 2012; Guo et al., 2013).

5. CONCLUSIONS

The basic aim of the PhD thesis was to characterize the structure and biological activity of metabolites produced by *Nostoc edaphicum* CCNP1411 isolated from the Gulf of Gdańsk (southern Baltic Sea). The results of the study are presented in Publication 2, 3 and 4. In addition, the current state of knowledge of bioactive peptides from *Nostoc* genus was reviewed and described in Publication 1. Based on the published data and results obtained during few years of research focused on cyanometabolites from *N. edaphicum* CCNP1411, the following statements can be concluded:

- i) *Nostoc edaphicum* CCNP1411 is a producer of at least two groups of nonribosomal compounds classified as nostocyclopeptides (Ncps) and cyanopeptolins (Cps).
- ii) The peptides produced by *N. edaphicum* CCNP1411 were revealed to be either serine protease inhibitors (Cps) or human 20S proteasome inhibitors (Ncps). The amino acid composition and form of the compounds was proved to have significant effect on their activity.
- iii) Results of this study revealed that *N. edaphicum* CCNP1411 produces Ncps mainly as linear aldehydes, in contrast to other *Nostoc* strains reported to be a source of cyclic Ncps analogues.
- iv) Both classes of compounds showed selective activity against the tested targets. This is an important feature of molecules considered as lead compounds in drug discovery process.
- v) The activity of Ncps against h20S proteasome was discovered in the work for the first time.
- vi) The structural diversity and the related selective biological activity of Ncps and Cps isolated from *Nostoc edaphicum* CCNP1411 provide a basis for further research on the biotechnological application of Baltic cyanobacteria metabolites.

6. REFERENCES

1. Adams, J. The proteasome: structure, function, and role in the cell. *Cancer Treatment Reviews*, 2003, 29, 3-9. (doi:10.1016/S0305-7372(03)00081-1)
2. Altschul, S.; Madden, T.; Schäffer, A.; Zhang, J.; Zhang, Z.; Miller, W.; Lipman, D. Gapped BLAST and PSI-BLAST: A new generation of protein database search programs. *Nucleic Acids Research*, 1997, 25, 3389-3402. (doi:10.1093/nar/25.17.3389)
3. Ananyev, G. M.; Skizim, N. J.; Dismukes, G. C. Enhancing biological hydrogen production from cyanobacteria by removal of extracted products. *Journal of Biotechnology*, 2012, 162, 97-104. (doi:10.1016/j.jbiotec.2012.03.026)
4. Arima, H.; Horiguchi, N.; Takaichi, S.; Kofuji, R.; Ishida, K-I.; Wada, K.; Sakamoto, T. Molecular genetic and chemotaxonomic characterization of the terrestrial cyanobacterium *Nostoc commune* and its neighboring species. *FEMS Microbiology Ecology*, 2012, 79 (1), 34-45. (doi:10.1111/j.1574-6941.2011.01195.x.)
5. Ansari, A. A.; Gill, S.; Gill, R.; Lanza, G. R.; Newman, L. (editors). *Phytoremediation. Management of environmental contaminants, volume 2*. Springer International Publishing Switzerland, 2015.
6. Beck, P.; Dubiella, C.; Groll, M. Covalent and non-covalent reversible proteasome inhibition. *Biological Chemistry*, 2012, 393 (10), 1101-1120. (doi:10.1515/hsz-2012-0212)
7. Becker, J. E.; Moore, R. E.; Moore, B. S. Cloning, sequencing, and biochemical characterization of the nostocyclopeptide biosynthetic gene cluster: molecular basis for imine macrocyclization. *Gene*, 2004, 325, 35-42. (doi:10.1016/j.gene.2003.09.034)
8. Bertani, G. Studies on lysogenesis. I. The mode of phage liberation by lysogenic *Escherichia coli*. *Journal of Bacteriology*, 1951, 62, 293-300. (doi:10.1128/jb.62.3.293-300.1951)
9. Bister, B.; Keller, S.; Baumann, H. I.; Nicholson, G.; Weist, S, Jung, G.; Süßmuth, R. D.; Jüttner, F. Cyanopeptolin 963A, a chymotrypsin inhibitor of *Microcystis* PCC 7806. *Journal of Natural Products*, 2004, 67, 1755-1757. (doi:10.1021/np049828f)
10. Blom, J. F.; Bister, B.; Bischoff, D.; Nicholson, G.; Jung, G.; Süßmuth, R. D.; Jüttner, F. Oscillapeptin J, a new grazer toxin of the freshwater cyanobacterium *Planktothrix rubescens*. *Journal of Natural Products*, 2003, 66, 431-434. (doi:10.1021/np020397f)
11. Boyd, M. R.; Gustafson, K. R.; McMahon, J. B.; Shoemaker, R. H.; O'keefe, B. R.; Mori, T.; Gułakowski, R. J.; Wu, L.; Rivera, M. I.; Laurencot, C. M.; Currens, M. J.; Cardellin aII, J. H.; Buckeit, R. W.; Nara, P. L.; Pannell, L. K.; Sowder II, R. C.; Henderson, L. E. Discovery of cyanovirin-N, a novel human immunodeficiency virus-inactivating protein that binds viral surface envelope glycoprotein gp120: potential applications to microbicide development. *Antimicrobial Agents and Chemotherapy*, 1997, 41 (7), 1521-1530. (doi:10.1128/AC.41.7.152)
12. Cadel-Six, S.; Dauga, C.; Castets, A. M.; Rippka, R.; Bouchier, C.; de Marsac, N.; Welker, M. Halogenase genes in nonribosomal peptide synthetase gene clusters of *Microcystis* (cyanobacteria): sporadic distribution and evolution. *Molecular Biology and Evolution*, 2008, 25 (9), 2031-2041. (doi:10.1093/molbev/msn150)
13. Choi, H.; Oh, S. K.; Yih, W.; Chin, J.; Kang, H.; Rho, J-R. Cyanopeptolin CB071: a cyclic depsipeptide isolated from the freshwater cyanobacterium *Aphanocapsa* sp. *Chemical and Pharmaceutical Bulletin*, 2008, 56 (8), 1191-1193. (doi:10.1248/cpb.56.1191)
14. Czerwonka, A.; Fiołka, M. J.; Jędrzejewska, K.; Jankowska, E.; Zając, A.; Rzeski, W. Pro-apoptotic action of protein-carbohydrate fraction isolated from coelomic fluid of the

- earthworm *Dendrobaena veneta* against human colon adenocarcinoma cells. *Biomedicine and Pharmacotherapy*, 2020, *126*, 110035. (doi:10.1016/j.biopha.2020.110035)
- 15.de Bettignies, G.; Coux, O. Proteasome inhibitors: dozens of molecules and still counting. *Biochimie*, 2010, *92*, 1530-1545. (doi:10.1016/j.biochi.2010.06.023)
 - 16.de Coster, W.; D'Hert, S.; Schultz, D.; Cruts, M.; Van Broeckhoven, C. NanoPack: Visualizing and processing long-read sequencing data. *Bioinformatics*, 2018, *34*, 2666-2669. (doi:10.1093/bioinformatics/bty149)
 - 17.de Lima, V. C. O.; Piuvezam, G.; Maciel, B. L. L.; de Araujo Morais, A. H. Trypsin inhibitors: promising candidate satietogenic proteins as complementary treatment for obesity and metabolic disorders. *Journal of Enzyme Inhibition and Medicinal Chemistry*, 2019, *34* (1), 405-419. (doi:10.1080/14756366.2018.1542387)
 - 18.de Souza Nascimento, A. M.; Matias, L. L. R.; de Oliveira Segundo, V. H.; Piuvezam, G.; Passos, T. S.; Damasceno, K. S.; de Araujo Morais, A. H. Antibacterial action mechanism of trypsin inhibitors. A protocol for synthetic review and meta-analysis. *Journal of Enzyme Inhibition and Medicinal Chemistry*, 2022, *37* (1), 749-759. (doi:10.1080/14756366.2022.2039918)
 - 19.Demarco, M.; de Moraes, J. O.; Ferrari, M. C.; de Farias Neves, F.; Laurindo, J. B.; Tribuzi, G. Production of Spirulina (*Arthrospira platensis*) powder by innovative and traditional techniques. *Journal of Food Process Engineering*, 2022, *45*, e13919. (doi:10.1111/jfpe.13919)
 - 20.Dembitsky, V. M.; Řezanka, T. Metabolites produced by nitrogen-fixing *Nostoc* species. *Folia Microbiologica*, 2005, *50* (5), 363-391. (doi:10.1007/BF02931419)
 - 21.Dey, B.; Lerner, D. L.; Lusso, P.; Boyd, M. R.; Elder, J. H.; Berger, E. A. Multiple antiviral activities of cyanovirin-N: blocking of human immunodeficiency virus type 1 gp120 interaction with CD4 and coreceptor and inhibition of diverse enveloped viruses. *Journal of Virology*, 2000, *74* (10), 4562-4569. (doi:10.1128/jvi.74.10.4562-4569.2000)
 - 22.Dittmann, E.; Gugger, M.; Sivonen, K.; Fewer, D. P. Natural product biosynthetic diversity and comparative genomics of the cyanobacteria. *Trends in Microbiology*, 2015, *23* (10), 642-652. (doi:10.1016/j.tim.2015.07.008)
 - 23.Dittmann, E.; Neilan, B. A.; Börner, T. Molecular biology of peptide and polyketide biosynthesis in cyanobacteria. *Applied Microbiology and Biotechnology*, 2001, *57*, 467-473. (doi:10.1007/s002530100810)
 - 24.Dodds, W.; Gudder, D.; Mollenhauer, D. The ecology of *Nostoc*. *Journal of Phycology*, 1995, *31*, 2-18. (doi:10.1111/j.0022-3646.1995.00002.x)
 - 25.Enck, S.; Kopp, F.; Marahiel, M. A.; Geyer, A. The entropy balance of nostocyclopeptide macrocyclization analysed by NMR spectroscopy. *ChemBioChem*, 2008, *9*, 2597-2601. (doi:10.1002/cbic.200800314)
 - 26.Faltermann, S.; Hutter, S.; Christen, V.; Hettich, T.; Fent, K. Anti-inflammatory activity of cyanobacterial serine protease inhibitors aeruginosin 828A and cyanopeptolin 1020 in human hepatoma cell line Huh7 and effects in zebrafish (*Danio rerio*). *Toxins*, 2016, *8*, 219. (doi:10.3390/toxins8070219)
 - 27.Felnagle, E. A.; Jackson, E. E., Chan, Y. A.; Podevels, A. M.; Berti, A. D.; McMahon, M. D.; Thomas, M. G. Nonribosomal peptide synthetases involved in the production of medically relevant natural products. *Molecular Pharmaceutics*, 2008, *5* (2), 191-211. (doi:10.1021/mp700137g)

28. Fewer, D. P.; Österholm, J.; Rouhiainen, L.; Jokela, J.; Wahlsten, M.; Sivonen, K. Nostophycin biosynthesis is directed by a hybrid polyketide synthase-nonribosomal peptide synthetase in the toxic cyanobacterium *Nostoc* sp. strain 152. *Applied and Environmental Microbiology*, 2011, 77 (22), 8034-8040. (doi:0.1128/AEM.05993-11)
29. Field-Smith, A.; Morgan, G. J.; Davies, F. E. Bortezomib (Velcade) in the treatment of multiple myeloma. *Therapeutics and Clinical Risk Management*, 2006, 2 (3), 271-279. (doi:10.2147/tcrm.2006.2.3.271)
30. Finking, R.; Marahiel, M. A. Biosynthesis of nonribosomal peptides. *Annual Review of Microbiology*, 2004, 58, 453-488. (doi:10.1146/annurev.micro.58.030603.123615)
31. Gaczyńska, M.; Osmulski, P.A.; Gao, Y.; Post, M.J.; Simons, M. Proline- and arginine-rich peptides constitute a novel class of allosteric inhibitors of proteasome activity. *Biochemistry*, 2003, 42, 8663-8670. (doi:10.1021/bi034784f)
32. Gademann, K.; Portmann, C.; Blom, J. F.; Zeder, M.; Jüttner, F. Multiple toxin production in the cyanobacterium *Microcystis*: isolation of the toxic protease inhibitor cyanopeptolin 1020. *Journal of Natural Products*, 2010, 73, 980-984. (doi: 10.1021/np900818c)
33. Gehringer, M. M.; Adler, L.; Roberts, A. A.; Moffitt, M. C.; Mihali, T. K.; Mills, T. J. T.; Fieker, C.; Neilan, B. A. Nodularin-R, a cyanobacterial toxin, is synthesized in *planta* by symbiotic *Nostoc* sp. *International Society for Microbial Ecology Journal*, 2012, 6, 1834-1847. (doi:10.1038/ismej.2012.25)
34. Gehringer, M. M.; Pengelly, J. J. L.; Cuddy, W. S.; Fieker, C.; Forster, P. I.; Neilan, B. A. Host selection of symbiotic cyanobacteria in 31 species of the Australian cycad genus: *Macrozamia* (Zamiaceae). *Molecular Plant-Microbe Interactions*, 2010, 23 (6), 811-822. (doi:10.1094/MPMI-23-6-0811)
35. Golakoti, T.; Ogino, J.; Heltzel, C. E.; Le Husebo, T.; Jensen, C. M.; Larsen, L. K.; Patterson, G. M. L.; Moore, R. E.; Mooberry, S. L.; Corbett, T. H.; Valeriote, F. A. Structure determination, conformational analysis, chemical stability studies, and antitumor evaluation of the cryptophycins. Isolation of 18 new analogs from *Nostoc* sp. strain GSV 224. *Journal of the American Chemical Society*, 1995, 117, 12030-12049. (doi:10.1021/ja965401m)
36. Golakoti, T.; Yoshida, W. Y.; Chaganty, S.; Moore, R. E. Isolation and structure determination of nostocyclopeptides A1 and A2 from the terrestrial cyanobacterium *Nostoc* sp. ATCC53789. *Journal of Natural Products*, 2001, 64, 54-59. (doi:10.1021/np000316k)
37. Goldberg, A. L. Development of proteasome inhibitors as research tools and cancer drugs. *Journal of Cell Biology*, 2012, 199 (4), 583-588. (doi:10.1083/jcb.201210077)
38. Groll, M.; Götz, M.; Kaiser, M.; Weyher, E.; Moroder, L. TMC-95-based inhibitor design provides evidence for the catalytic versatility of the proteasome. *Chemistry & Biology*, 2006, 13, 607-614. (doi:10.1016/j.chembiol.2006.04.005)
39. Guo, N.; Zhilan, P. MG 132, a proteasome inhibitor, induces apoptosis in tumor cells. *Asia-Pacific Journal of Clinical Oncology*, 2013, 9, 6-11. (doi:10.1111/j.17437563.2012.01535.x)
40. Gustafson, K. R.; Sowder II, R. C.; Henderson, L. E.; Cardellina II, J. H.; McMahon, J. B.; Rajamani, U.; Pannell, L. K.; Boyd, M. R. Isolation, primary sequence determination, and disulfide bond structure of cyanovirin-N, an anti-HIV (Human Immunodeficiency Virus) protein from the cyanobacterium *Nostoc ellipsosporum*. *Biochemical and Biophysical Research Communications*, 1997, 238, 223-228. (doi:10.1006/bbrc.1997.7203)

41. Hallenbeck, P. C. (editor). Modern topics in the phototrophic prokaryotes. Environmental and applied aspects. Springer International Publishing Switzerland, 2017.
42. Harada, K.; Mayumi, T.; Park, H.; Watanabe, M. Co-production of microcystins and aeruginopeptins by natural cyanobacterial bloom. *Environmental Toxicology*, 2001, 16 (4), 298-305. (doi:10.1002/tox.1036)
43. Harer, S. L.; Bhatia, M. S.; Bhatia, N. M. Proteasome inhibitors mechanism; source for design of newer therapeutic agents. *Journal of Antibiotics*, 2012, 65, 279-288. (doi:10.1038/ja.2011.84)
44. Hines, J.; Groll, M.; Fahnestock, M.; Crews, C. M. Proteasome inhibition by fellutamide B induces nerve growth factor synthesis. *Chemistry & Biology*, 2008, 15 (5), 501-512. (doi:10.1016/j.chembiol.2008.03.020)
45. Jakobi, C.; Rinehart, K. L.; Neuber, R.; Mez, K.; Weckesser, J. Cyanopeptolin SS, a disulphated depsipeptide from a water bloom: structural elucidation and biological activities. *Phycologia*, 1996, 35, 111-116. (doi:10.2216/i0031-8884-35-6S-111.1)
46. Kaasalainen, U.; Fewer, D. P.; Jokela, J.; Wahlsten, M.; Sivonen, K.; Rikkinen, J. Cyanobacteria produce a high variety of hepatotoxic peptides in lichen symbiosis. *Proceedings of the National Academy of Sciences*, 2012, 109 (15), 5886-5891. (doi:10.1073/pnas.1200279109)
47. Kahru, M.; Elmgren, R.; Kaiser, J.; Wasmund, N.; Savchuk, O. Cyanobacterial blooms in the Baltic Sea: correlations with environmental factors. *Harmful Algae*, 2020, 92, 101739. (doi: 10.1016/j.hal.2019.101739)
48. Kampa, A.; Gagunashvili, A. N.; Gulder, T. A. M.; Morinaka, B. I.; Daolio, C.; Godejohann, M.; Miao, V. P. W.; Piel, J.; Andrésón, Ó. S. Metagenomic natural product discovery in lichen provides evidence for a family of biosynthetic pathways in diverse symbioses. *PNAS*, 2013, 110 (33), 3129-3137. (doi:10.1073/pnas.1305867110)
49. Kaya, K.; Sano, T.; Beattie, K. A.; Codd, G. A. Nostocyclin, a novel 3-amino-6-hydroxy-2-piperidone-containing cyclic depsipeptide from the cyanobacterium *Nostoc* sp. *Tetrahedron Letters*, 1996, 37 (37), 6725-6728. (doi:10.1016/S0040-4039(96)01452-9)
50. Khalifa, S. A. M.; Shedid, E. S.; Saied, E. M.; Jassbi, A. R.; Jamebozorgi, F. H.; Rateb, M. E.; Du, M.; Abdel-Daim, M. M.; Kai, G-Y.; Al-Hammady, M. A. M.; Xiao, J.; Guo, Z.; El-Seedi, H. R. Cyanobacteria – from the oceans to the potential biotechnological and biomedical applications. *Marine Drugs*, 2021, 19, 241. (doi:10.3390/md19050241)
51. Kisselev, A. F.; Garcia-Calvo, M.; Overkleeft, H. S.; Peterson, E.; Pennington, M. W.; Ploegh, H. L.; Thornberry, N. A.; Goldberg, A. L. The caspase-like sites of proteasomes, their substrate specificity, new inhibitors and substrates, and allosteric interactions with the trypsin-like sites. *Journal of Biological Chemistry*, 2003, 278 (38), 35869-35877. (doi:10.1074/jbc.M303725200)
52. Kisselev, A. F.; Golberg, A. L. Proteasome inhibitors: from research tools to drug candidates. *Chemistry and Biology*, 2001, 8, 739-758. (doi:10.1016/s1074-5521(01)00056-4)
53. Kisselev, A. F.; van der Linden, W. A.; Overkleeft, H. S. Proteasome inhibitors: an expanding army attacking a unique target. *Chemistry & Biology*, 2012, 19 (1), 99-115. (doi:10.1016/j.chembiol.2012.01.003)
54. Kobayashi, M.; Aoki, S.; Ohyabu, N.; Kurosu, M.; Wang, W.; Kitagawa, I. Arenastatin A, a potent cytotoxic depsipeptide from the Okinawan marine sponge *Dysidea arenaria*. *Tetrahedron Letters*, 1994, 35 (43), 7969-7972. (doi:10.1016/0040-4039(94)80024-3)
55. Kolmogorov, M.; Yuan, J.; Lin, Y.; Pevzner, P. Assembly of long, error-prone reads using repeat graphs. *Nature Biotechnology*, 2019, 37, 540-546. (doi:10.1038/s41587-019-0072-8)

56. Kopp, F.; Mahler, C.; Grünwald, J.; Marahiel, M. A. Peptide macrocyclization: the reductase of the nostocyclopeptide synthetase triggers the self-assembly of a macrocyclic imine. *Journal of the American Chemical Society Communications*, 2006, 128, 16478-16479. (doi:10.1021/ja0667458)
57. Kotai, J. Instructions for Preparation of Modified Nutrient Solution Z8 for Algae; Norwegian Institute for Water Research: Oslo, Norway, 1972; p. 5.
58. Kwan, J. C.; Eksioğlu, E. A.; Liu, C. Paul, V. J.; Luesch, H. Grassystatins A-C from marine cyanobacteria, potent cathepsin E inhibitors that reduce antigen presentation. *Journal of Medicinal Chemistry*, 2009, 52, 5732-5747. (doi:10.1021/jm9009394)
59. Lai, Q.; Wu, M.; Wang, R.; Lai, W.; Tao, Y.; Lu, Y.; Wang, Y.; Yu, L.; Zhang, R.; Peng, Y.; Jiang, X.; Fu, Y.; Wang, X.; Zhang, Z.; Guo, C.; Liao, W.; Zhang, Y.; Kang, T.; Chen, H.; Yao, Y.; Gou, L.; Yang, J. Cryptophycin-55/52 based antibody-drug conjugates: synthesis, efficacy, and mode of action studies. *European Journal of Medicinal Chemistry*, 2020, 199, 112364. (doi:10.1016/j.ejmech.2020.112364)
60. Linington, R. G.; Edwards, D. J.; Shuman, C. F.; McPhail, K. L.; Maitainaho, T.; Gerwick, W. H. Symplocamide A, a potent cytotoxin and chymotrypsin inhibitor from the marine cyanobacterium *Symploca* sp. *Journal of Natural Products*, 2008, 71, 22-27. (doi:10.1021/np070280x)
61. Luesch, H.; Moore, R. E.; Paul, V. J.; Mooberry, S. L.; Corbett, T. H. Isolation of dolastatin 10 from the marine cyanobacterium *Symploca* species VP642 and total stereochemistry and biological evaluation of its analogue symplostatin 1. *Journal of Natural Products*, 2001, 64, 907-910. (doi:10.1021/np010049y)
62. Magarvey, N. A.; Beck, Z. Q.; Golakoti, T.; Ding, Y.; Huber, U.; Hemscheidt, T. K.; Abelson, D.; Moore, R. E.; Sherman, D. H. Biosynthetic characterization and chemoenzymatic assembly of the cryptophycins. Potent anticancer agents from *Nostoc* cyanobionts. *ACS Chemical Biology*, 2006, 1 (12), 766-779. (doi:10.1021/cb6004307)
63. Mao, X.; Yang, Z. Current usage status of somatostatin and its analogs and trypsin inhibitors: a real-world study of 34,654 Chinese adult patients with acute pancreatitis. *Annals of Palliative Medicine*, 2021, 10 (2), 1325-1335. (doi:10.21037/apm-19-363)
64. Martin, C.; Oberer, L.; Ino, T.; König, W. A.; Busch, M.; Weckesser, J. Cyanopeptolins, new depsipeptides from the cyanobacterium *Microcystis* sp. PCC 7806. *Journal of Antibiotics*, 1993, 46 (10), 1550-1556. (doi:10.7164/antibiotics.46.1550)
65. Medema, M.; Blin, K.; Cimermanic, P.; de Jager, V.; Zakrzewski, P.; Fischbach, M.; Weber, T.; Takano, E.; Breitling, R. antiSMASH: Rapid identification, annotation and analysis of secondary metabolites biosynthesis gene clusters in bacterial and fungal genome sequences. *Nucleic Acids Research*, 2011, 39, w339-w346. (doi:10.1093/nar/gkr466)
66. Mehner, C.; Müller, D.; Kehraus, S.; Hautmann, S.; Gütschow, M.; König, G. M. New peptolides from the cyanobacterium *Nostoc insulare* as selective and potent inhibitors of human leukocyte elastase. *ChemBioChem*, 2008, 9, 2692-2703. (doi:10.1002/cbic.200800415)
67. Mirabella, A. C.; Pletnev, A. A.; Downey, S. L.; Florea, B. I.; Shabaneh, T. B.; Britton, M.; Verdoes, M.; Filippov, D. V.; Overkleeft, H. S.; Kisselev, A. F. Specific cell-permeable inhibitor of proteasome trypsin-like sites selectively sensitizes myeloma cells to bortezomib and carfilzomib. *Chemistry & Biology*, 2011, 18 (5), 608-618. (doi:10.1016/j.chembiol.2011.02.015)
68. Nowak, R.; Jastrzębski, J.; Kuśmirek, W.; Sałamatin, R.; Rydzanicz, M.; Sobczyk-Kopcioł, A.; Sulima-Celińska, A.; Pauksto, Ł.; Makowaczenko, K.; Płoski, R.; Tkach, V. V.; Basała, K.;

- Młocicki, D. Hybrid *de novo* whole genome assembly and annotation of the model tapeworm *Hymenolepis diminuta*. *Scientific Data*, 2020, 7, 52. (doi:10.1038/s41597-019-0311-3)
69. Nowruzi, B.; Khavari-Nejad, R.-A.; Sivonen, K.; Kazemi, B.; Najafi, F.; Nejadstattari, T. Identification and toxigenic potential of a *Nostoc* sp. *Algae*, 2012, 27 (4), 303-313. (doi:10.4490/algae.2012.27.4.303)
70. Ocampo Bennet, X. Peptide au Seiner Cyanobakterien Wasserblütte (1998) aus dem Wannsee/Berli: Strukturen and Biologische Wirksamkeit. University of Freiburg: Freiburg, Germany, 2007; 28p.
71. Okino, T.; Qi, S.; Matsuda, H.; Murakami, M.; Yamaguchi, K. Nostopeptins A and B, elastase inhibitors from the cyanobacterium *Nostoc minutum*. *Journal of Natural Products*, 1997, 60, 158-161. (doi:10.1021/np960649a)
72. Oksanen, I.; Jokela, J.; Fewer, D. P.; Wahlsten, M.; Rikkinen, J.; Sivonen, K. Discovery of rare and highly toxic microcystins from lichen-associated cyanobacterium *Nostoc* sp. strain IO-102-I. *Applied and Environmental Microbiology*, 2004, 70 (10), 5756-5763. (doi:10.1128/AEM.70.10.5756-5763.2004)
73. Olofsson, M.; Suikkanen, S.; Kobos, J.; Wasmund, N.; Karlson, B. Basin-specific changes in filamentous cyanobacteria community composition across four decades in the Baltic Sea. *Harmful Algae*, 2020, 91, 101685. (doi:10.1016/j.hal.2019.101685)
74. Ploutno, A.; Carmeli, S. Modified peptides from a water bloom of the cyanobacterium *Nostoc* sp. *Tetrahedron*, 2002, 58, 9949-9957. (doi:10.1016/S0040-4020(02)01326-1)
75. Ploutno, A.; Carmeli, S. Banyasin A and banyasides A and B, three novel modified peptides from a water bloom of the cyanobacterium *Nostoc* sp. *Tetrahedron*, 2005, 61, 575-583. (doi: 10.1016/j.tet.2004.11.016)
76. Rapala, J.; Erkomaa, K.; Kukkonen, J.; Sivonen, K.; Lahti, K. Detection of microcystins with protein phosphatase inhibition assay, high-performance liquid chromatography–UV detection and enzyme-linked immunosorbent assay. Comparison of methods. *Analytica Chimica Acta*, 2002, 466, 213–231. (doi:10.1016/S0003-2670(02)00588-3)
77. Řezanka, T.; Dor, I.; Prell, A.; Dembitsky, V. M. Fatty acid composition of six freshwater wild cyanobacterial species. *Folia Microbiologica*, 2003, 48 (1), 71-75. (doi:10.1007/BF02931279)
78. Sand-Jensen, K. Ecophysiology of gelatinous *Nostoc* colonies: unprecedented slow growth and survival in resource-poor and harsh environments. *Annals of Botany*, 2014, 114, 17-33. (doi: 10.1093/aob/mcu085)
79. Schirrmeister, B. E.; Sanchez-Baracaldo, P.; Wacey, D. Cyanobacterial evolution during the Precambrian. *International Journal of Astrobiology*, 2016, 15 (3), 187-204. (doi: 10.1017/S1473550415000579)
80. Schwartz, R. E.; Hirsch, C. F.; Sesin, D. F.; Flor, J. E.; Chartrain, M.; Fromtling, R. E.; Harris, G. H.; Salvatore, M. J.; Liesch, J. M.; Yudin, K. Pharmaceuticals from cultured algae. *Journal of Industrial Microbiology*, 1990, 5, 113-124. (doi:10.1007/bf01573860)
81. Shah, S. A. A.; Akhter, N.; Auckloo, B. N.; Khan, I.; Lu, Y.; Wang, K.; Wu, B.; Guo, Y.-W. Structural diversity, biological properties and applications of natural products from cyanobacteria. A review. *Marine Drugs*, 2017, 15, 354. (doi: 10.3390/md15110354)
82. Singh, S.; Kate, B. N.; Banerjee, U. C. Bioactive compounds from cyanobacteria and microalgae: an overview. *Critical Reviews in Biotechnology*, 2005, 25, 73-95. (doi: 10.1080/07388550500248498)

83. Singh, R.; Parihar, P.; Singh, M.; Bajguz, A.; Kumar, J.; Singh, S.; Singh, V. P.; Prasad, S. M. Cyanobacteria and algal metabolites in biology, agriculture and medicine: current status and future prospects. *Frontiers in Microbiology*, 2017, 8, 515. (doi: 10.3389/fmicb.2017.00515)
84. Sivonen, K.; Carmichael, W.; Namikoshi, M.; Rinehart, K. L.; Dahlem, A. M.; Niemela, S. I. Isolation and characterization of hepatotoxic microcystin homologs from the filamentous freshwater cyanobacterium *Nostoc* sp. 152. *Applied and Environmental Microbiology*, 1990, 56 (9), 2650-2657. (doi:10.1128/aem.56.9.2650-2657.1990)
85. Troschl, C.; Meixner, K.; Drogg, B. Cyanobacterial PHA production – review of recent advances and a summary of three years' working experience running a pilot plant. *Bioengineering*, 2017, 4, 26. (doi: 10.3390/bioengineering4020026)
86. van de Donk, N. W. C. J.; Dhimolea, E. Brentuximab vedotin. *Landes Bioscience*, 2012, 4 (4), 458-465. (doi: 10.4161/mabs.20776)
87. Verbrugge, S. E.; Scheper, R. J.; Lems, W. F.; de Gruijl, T. D.; Jansen, G. Proteasome inhibitors as experimental therapeutics of autoimmune diseases. *Arthritis Research & Therapy*, 2015, 17, 17. (doi:10.1186/s13075-015-0529-1)
88. Weber, T.; Marahiel, M. A. Exploring the domain structure of modular nonribosomal peptide synthetases. *Structure*, 2001, 9 (1), R3-R9. (doi:10.1016/S0969-2126(00)00560-8)
89. Welker, M.; von Döhren, H. Cyanobacterial peptides – nature's own combinatorial biosynthesis. *FEMS Microbiology Reviews*, 2006, 30, 530-563. (doi:10.1111/j.1574-6976.2006.00022.x)
90. Welker, M.; Brunke, M.; Preussel, K.; Lippert, I.; von Döhren, H. Diversity and distribution of *Microcystis* (Cyanobacteria) oligopeptide chemotypes from natural communities studied by single-colony mass spectrometry. *Microbiology*, 2004a, 150, 1785-1796. (doi:10.1099/mic.0.26947-0)
91. Welker, M.; Christiansen, G.; von Döhren, H. Diversity of coexisting *Planktothrix* (Cyanobacteria) chemotypes deduced by mass spectral analysis of microcystins and other oligopeptides. *Archives of Microbiology*, 2004b, 182, 288-298. (doi:10.1007/s0203-004-071-3)
92. Yamada, S.; Ohkubo, S.; Miyashita, H.; Setoguchi, H. Genetic diversity of symbiotic cyanobacteria in *Cycas revoluta* (Cycadaceae). *FEMS Microbiology Ecology*, 2012, 81 (3), 1-11. (doi:10.1111/j.1574-6941.2012.01403.x)
93. Yamaki, H.; Sitachitta, N.; Sano, T.; Kaya, K. Two new chymotrypsin inhibitors isolated from the cyanobacterium *Microcystis aeruginosa* NIES-88. *Journal of Natural Products*, 2005, 68, 14-18. (doi:10.1021/np0401361)
94. Zhang, L.; Hu, J. J.; Gong, F. MG132 inhibition of proteasome blocks apoptosis induced by severe DNA damage. *Cell Cycle*, 2011, 10 (20), 3515-3518. (doi:10.4161/cc.10.20.17789)

7. PUBLICATIONS

Publication 1

Fidor, A., Konkel, R., Mazur-Marzec, H. Bioactive peptides produced by cyanobacteria of the genus *Nostoc*: A review. *Marine Drugs*, 2019, 17 (10), 1-16.

Publication 2

Mazur-Marzec, H., Fidor, A., Cegłowska, M., Wieczerek, E., Kropidłowska, M., Goua, M., Macaskill, J., Edwards, C. Cyanopeptolins with trypsin and chymotrypsin inhibitory activity from the cyanobacterium *Nostoc edaphicum* CCNP1411. *Marine Drugs*, 2018, 16 (7), 1-19.

Publication 3

Fidor, A., Grabski, M., Gawor, J., Gromadka, R., Węgrzyn, G., Mazur-Marzec, H. *Nostoc edaphicum* CCNP1411 from the Baltic Sea — a new producer of nostocyclopeptides. *Marine Drugs*, 2020, 18 (9) 1-18.

Publication 4


Fidor, A., Cekała, K., Wieczerek, E., Cegłowska, M., Kasprzykowski, F., Edwards, C., Mazur-Marzec, H. Nostocyclopeptides as new inhibitors of 20S proteasome. *Biomolecules*, 2021, 11 (10), 1-10.

Publication 1



Review

Bioactive Peptides Produced by Cyanobacteria of the Genus *Nostoc*: A Review

Anna Fidor ¹, Robert Konkel ¹ and Hanna Mazur-Marzec ^{1,2,*} 

¹ Division of Marine Biotechnology, Faculty of Oceanography and Geography, University of Gdańsk, Marszałka J. Piłsudskiego 46, PL-81378 Gdynia, Poland; anna.fidor@phdstud.ug.edu.pl (A.F.); robert.konkel@phdstud.ug.edu.pl (R.K.)

² Institute of Oceanology, Polish Academy of Sciences, Powstańców Warszawy 55, PL-81712 Sopot, Poland

* Correspondence: biohm@ug.edu.pl; Tel.: +48-58-5236621; Fax: 48-58-5236712

Received: 30 August 2019; Accepted: 27 September 2019; Published: 29 September 2019



Abstract: Cyanobacteria of the genus *Nostoc* are widespread in all kinds of habitats. They occur in a free-living state or in association with other organisms. Members of this genus belong to prolific producers of bioactive metabolites, some of which have been recognized as potential therapeutic agents. Of these, peptides and peptide-like structures show the most promising properties and are of a particular interest for both research laboratories and pharmaceutical companies. *Nostoc* is a sole source of some lead compounds such as cytotoxic cryptophycins, antiviral cyanovirin-N, or the antitoxic nostocyclopeptides. *Nostoc* also produces the same bioactive peptides as other cyanobacterial genera, but they frequently have some unique modifications in the structure. This includes hepatotoxic microcystins and potent proteases inhibitors such as cyanopeptolins, anabaenopeptins, and microginins. In this review, we described the most studied peptides produced by *Nostoc*, focusing especially on the structure, the activity, and a potential application of the compounds.

Keywords: cyanobacteria; *Nostoc*; nonribosomal peptides; bioactivity

1. Introduction

Cyanobacteria, the photosynthetic Gram-negative bacteria, are one of the oldest forms of life on Earth. As oxygen producers, they made a tremendous impact on the evolution of life on our planet. Today, their role as abundant primary producers is also important [1]. The species of the N₂-fixing *Nostoc* genus (order Nostocales) belong to the most common cyanobacteria. They occur in terrestrial ecosystems as well as in fresh, brackish, and marine waters, living in a free form or as symbionts in association with marine sponges [2], cycads [3], or as a component of cyanolichens [4]. *Nostoc* has a wide geographical distribution, and it was reported from different parts of the world—from Arctic and Antarctic to tropical regions [5–9]. The well-developed adaptive strategies enable the cyanobacterium to withstand repeated desiccation, extreme temperatures, salt stress, UV-radiation, and pathogen infections [10–13]. Due to a high tolerance to extreme conditions, *Nostoc* was considered to be a good candidate for extraterrestrial agriculture [14].

For hundreds of years, the cyanobacteria of the genus *Nostoc* have been used as herbs and/or healthy food for people. High contents of fiber, amino acids, proteins, vitamins, and carbohydrates increase their nutritional value. *Nostoc*-containing food products are still consumed in China, India, Indonesia, Peru, Ecuador, and Bolivia [15–18]. *Nostoc* has also been applied as biofertilizer [19,20] and a rich source of bioactive compounds, including anticancer [21], antifungal [22], antibacterial [23], antiviral [24–26], and enzyme inhibiting [27] agents. These metabolites were identified as peptides, lipopeptides, fatty acids, alkaloids, and terpenoids [28–32]. The pharmaceutical application of peptides and peptide-like structures has been explored most widely; the compounds frequently represent a

promising starting point for the design of novel drugs [33]. Peptides tend to bind selectively to cellular targets, reducing the risk of side effects. The drug-like properties of small peptides, such as plasma half-life, bioavailability, and selectivity, can be improved. In addition, some peptides have more than one function, and the combined effects of their activities can be observed, e.g., antimicrobial and immune system stimulating activity [34,35].

This review focuses on the most widely studied peptides produced by cyanobacteria of the genus *Nostoc*. The structure and the biological activity of the biomolecules are described. Both the cyanobacterium and its metabolites represent a high potential for biotechnological application.

2. Non-Ribosomal Peptides (NRPs) and Polyketides (PKs)

A significant part of the metabolites produced by *Nostoc* belongs to nonribosomal peptides (NRPs) or polyketides (PKs). They are characterized by a structural diversity and a broad spectrum of biological activities, including cytotoxic [36], enzyme inhibiting [37], anti-inflammatory [38], antibacterial [39], and antifungal effects [40]. NRPs are mainly synthesized by bacteria (Proteobacteria, Actinobacteria, Firmicutes, and Cyanobacteria) and fungi (Ascomycota) [41]. The ability to produce NRPs and PKs is a strain-specific feature, and in an individual strain, several classes of the compounds can be found. These compounds have linear, cyclic, or branched cyclic structure and are composed of proteogenic and non-proteogenic amino acids. They also contain short fatty acid chains, amines, heterocyclic rings such as thiazole or oxazole, and other residues [32]. NRPs, PKs, and their hybrids (NRPs/PKs) are synthesized on multifunctional enzyme complexes with a modular structure called non-ribosomal peptide synthetases (NRPS) or polyketide synthases (PKS) [28]. Each module of the complex is subdivided into domains catalyzing specific reactions in the multi-step process of residue incorporation into the peptide chain. In NRPS, the adenylation domain selects and activates a specific amino acid residue. Then, the residue is linked to the peptidyl carrier protein via thiol-containing phosphopantetheine. The condensation domain in the final module releases the peptide from the NRPS and terminates the chain elongation [28,42–44]. The structural modifications of NRPs are introduced by tailoring enzymes catalyzing methylation, oxygenation, cyclization, halogenation, glycosylation, and epimerization reactions. The cyanobacterial PKs are assembled on type I PKS with modules consisting of at least three domains: the acyltransferase domain, which recognizes and activates the substrate, the acyl carrier protein, which transports the molecule on the active site of ketosynthase involved in a bond formation [28], and the thioesterase domain which releases the final product [28,42]. Similarly to NRPS, the synthesized PKs are modified by tailoring enzymes, such as ketoreductase, dehydratase, enoylreductase, or methyl transferase. The modifications often lead to increase in the bioactivity and the resistance of NRPs and PKs to enzymatic lysis [45]. They also generate large structural diversity within one class of compounds.

Nostoc is one of the most prolific producers of NRPs/PKs (Table S1) [46]. Some classes of cyanopeptides are common to several cyanobacterial genera (e.g., microcystins, anabaenopeptins, cyanopeptolins), while others have been identified only in species belonging to the genus *Nostoc* (e.g., nostocyclopeptides, cryptophycins, nostopeptolides). In this work, we focus mainly on the peptides produced solely by the genus *Nostoc*, but some examples of the peptides occurring in other cyanobacterial taxa are discussed as well.

3. Cryptophycins

For the first time, cryptophycins [Crs, molecular weight (MW) 604–688 Da], the 16-membered cyclic depsipeptides, were isolated from the lichen associated *Nostoc* sp. ATCC 53789 (Arron Island, Scotland) [47]. The name of this class of peptides is related to their potent antifungal activity against the yeast of the genus *Cryptococcus* [48]. Crs were also found in *Nostoc* sp. GSV-224 (ATCC55483) from a terrestrial sample collected in India [36], in *Nostoc* sp. ASN_M from paddy fields in Iran [30], and in the Okinawan marine sponge *Dysidea arenaria* [2]. The Cr identified in the sponge, arenastatin A, turned out to be identical to Cr-24 from *Nostoc* sp. ATCC 53789. This finding raised the question

about the real origin of the compound. More than 28 natural Crs were identified in *Nostoc*, and many structural variants were synthesized [36,49]. In cyanobacteria, the compounds are assembled on a mixed PKS/NRPS enzyme complex [50]. Their biosynthesis is encoded in two PKS genes (*crpA* and *crpB*), two NRPS genes (*crpC* and *crpD*), and tailoring genes (*crpE-H*) encoding enzymes involved in epoxidation and chlorination reactions. Interestingly, the Cr biosynthetic gene clusters in the two Cr-producing cyanobacteria, ATCC53789 and GSV-224, are identical [50].

The natural Crs consist of four building blocks—ABCD (amino or hydroxycarboxylic acids)—linked in a cyclic sequence through an ester bond between C and D (Figure 1) [51]. Cr-1 belongs to the most abundant natural variants. It contains phenyloctenoic acid (A), 3-chloro-*O*-methyl-*D*-tyrosine (B), methyl- β -alanine (C), and L-leucic acid (D). Crs showed strong antiproliferative and cytotoxic effects against both solid and hematologic tumor cell lines, including multidrug-resistant (MDR) cancer cell lines [52,53]. Crs isolated from *Nostoc* sp. GSV 224 were found to be active against human nasopharyngeal carcinoma (KB), human colorectal adenocarcinoma (LoVo) and human ovarian carcinoma (SKOV3) cells in pM to nM range [36]. Crs also showed activity against a murine leukemia (L1210) cell line [54].

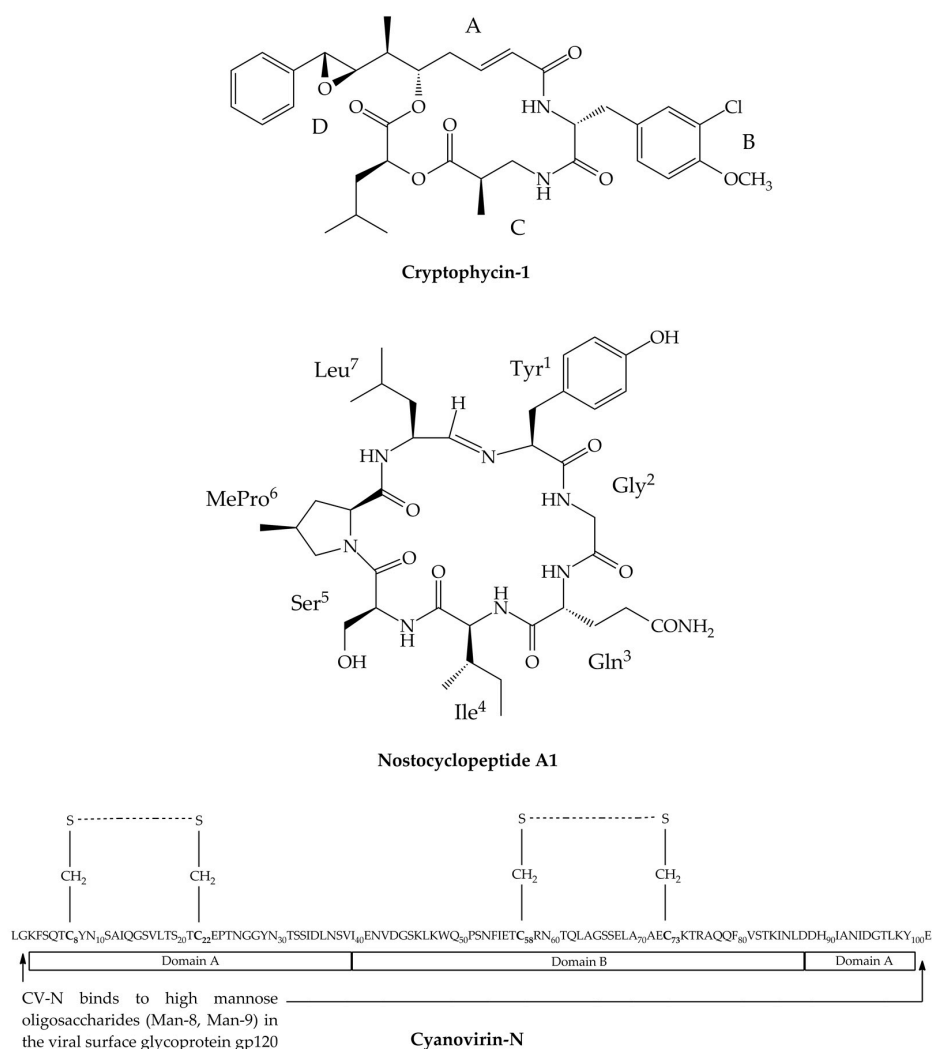


Figure 1. Structure of peptides produced by the genus *Nostoc*: Cryptophycin 1 (Cr-1), nostocyclopeptide A1 (Ncp-A1), and cyanovirin-N (CV-N). In Cr-A, the four building blocks (ABCD) represent phenyloctenoic acid (A), 3-chloro-*O*-methyl-*D*-tyrosine (B), methyl- β -alanine (C), and L-leucic acid (D).

Crs bind to tubulin protein, causing inhibition of microtubule assembly as well as the suppression of microtubule dynamics [54]. These effects lead to cell cycle arrest in the G2/M phase and cell death through apoptosis. Rapid uptake of Crs and accumulation in cells results in a prolonged activity. The compounds are poor substrates for P-glycoprotein (P-gp), the membrane transporter that mediates excretion of xenobiotics out of cells. P-gp are overexpressed in cancer cells, which contributes to the development of MDR [54]. The optimal cytotoxic activity is achieved in the case of cryptophycins with intact 16-membered macrolide structure, reactive epoxide ring in unit A, methyl group in units A (C-6) and C (C-2), *O*-methyl group and chloro-substituent in unit B, and isobutyl group in unit D [36,49]. Modification introduced to the structure by conversion of the epoxide group in unit A into chlorohydrin significantly increased the cytotoxicity of the compounds, but in the aqueous solution, the obtained derivative was found to be unstable [55,56]. This problem was overcome by the synthesis of stable glycinate ester analogues with retained activity of cryptophycin chlorohydrin [53,57]. Cr-52 (LY355703), a synthetic analogue of Cr-1 with an additional methyl group in unit C, was widely explored as a promising anticancer agent. It reached phase II clinical trials for non-small cell lung cancer and in patients with platinum-resistant advanced ovarian cancer. Unfortunately, due to unacceptable toxicity and lack of efficacy *in vivo*, the tests on Cr-52 were discontinued [58,59]. However, the work on Cr as anticancer drug has not been completely ceased. In recent years, the introduction of innovative, highly targeted methods opened new possibilities for drug development. The efficacy of cryptophycins can be improved by conjugation through a cleavable linker with an antibody or small molecule. The non-toxic antibody-drug conjugates (ADCs) or small molecule-drug conjugates (SMDCs) have improved stability in plasma and selectively target cancer cells. In tumor cells, the toxic peptide is released and then initiates the processes of cell death [60,61].

4. Nostocyclopeptides

Nostocyclopeptides (Ncps; MW 756–881 Da) are a small class of nonribosomal heptapeptides. The first two Ncp variants that differ only in one residue, Ncp-A1 (Tyr¹-Gly²-Gln³-Ile⁴-Ser⁵-MePro⁶-Leu⁷) (Figure 1) and Ncp-A2 (Tyr¹-Gly²-Gln³-Ile⁴-Ser⁵-MePro⁶-Phe⁷), were isolated from a terrestrial strain *Nostoc* sp. ATCC 53789 from India [62]. Nostocyclopeptide M1 (Ncp-M1) (Tyr¹-Tyr²-HSer³-Pro⁴-Val⁵-MePro⁶-Tyr⁷) was obtained from *Nostoc* sp. XSPORK 13A isolated from a gastropod collected at the Cape of Porkkala (Baltic Sea) [63]. Ncps are characterized by a unique imino linkage formed between the amine group of the conserved L-Tyr in position 1 and the aldehyde hydrate of the residue in position 7. The head-to-tail intramolecular cyclization reaction is selective and reversible in aqueous solution [64]. In the known Ncps, the C-terminal position is most variable (Leu, Phe, or Tyr), while position 6 is always occupied by a methylated form of Pro (MePro) (Figure 1). The residues in position 3 are D-amino acids [62,63]. The Ncp biosynthetic gene cluster described by Becker et al. [65] contains two large NRPS genes: the *ncpA* gene encoding a three-module protein NcpA1-3 and the *ncpB* gene encoding a four-module protein NcpB1-4. The co-linear arrangement of the gene cluster, the organization of the modules, as well as a substrate specificity of the adenylation domains determine the structure of Ncps. For example, the NcpA3 module contains an epimerase domain, which corresponds to the presence of D-amino acid in position 3, while the terminal part of the NcpB protein contains a reductase domain corresponding to the presence of aldehyde group in the C-terminus of the linear form of Ncp [65].

According to Golakoti et al. [62], Ncp-A1 and Ncp-A2 showed a weak cytotoxic activity (IC₅₀ ca. 1 μM) against a human nasopharyngeal cancer cell line (KB) and a human colorectal cancer adenocarcinoma cell line (LoVo). On the other hand, Ncp-M1 was nontoxic against primary rat hepatocytes [63]. In these cells exposed to microcystin-LR (MC-LR), nostocyclopeptide Ncp-M1 abolished apoptotic effects of the hepatotoxin. It was found that the three nostocyclopeptides as well as the synthetic analogue of Ncp-M1 with all L-amino acid residues and without imino bond blocked the uptake of MC-LR and nodularin (NOD) to rat hepatocytes and to the human embryonic kidney cells (HEK293). The antitoxin activity of Ncps was attributed to the inhibition of the organic ions

transporters OATP1B3 and OATP1B1, which facilitate the uptake of the toxins into the cell [63,66]. Of the tested compounds, Ncp-M1 counteracted the MC-LR-induced apoptosis in the most potent way.

5. Cyanovirin-N

Cyanovirin-N (CV-N; MW 11 kDa) is one of the most widely studied cyanobacterial lectins, with antiviral activity at μM to pM level. CV-N was isolated from *Nostoc ellipsosporum* maintained in the culture collection at the University of Hawaii [24]. This carbohydrate-binding polypeptide consists of 101 amino acids, including four cysteine residues that form two intra-chain disulfide bonds (Cys8-Cys22; Cys58-Cys73) (Figure 1). These bonds stabilize the CV-N structure and determine the antiviral activity of the polypeptide [67]. The molecule represents a unique structure with an extremely low sequence homology to any other known proteins.

CV-N is organized in two domains characterized by a high sequence duplication (32%) and structure identity. Domain A contains residues 1–38 and 90–101, and domain B contains residues 39–89 (Figure 1) [67,68]. In each domain, there are two binding sites for carbohydrates separated by the ~ 40 Å distance and with 10-fold difference in affinity [69]. In solution, the natural CV-N is mainly present as a monomer, while in crystals, dimer is formed by a strand exchange across the two domains [25,68]. Proline in position 51 plays an important role in the swapping of the domains and monomer aggregation. CV-N is a stable compound and preserves its activity even after treatment with denaturants, detergents, organic solvents, or extremely high temperatures (100 °C, 15 min) [24]. Conversion of dimer into monomer is extremely slow, but at higher temperature (>38 °C), the process is accelerated [70].

CV-N showed a potent in-vitro and in-vivo activity against human immunodeficiency virus (HIV-1 and 2), simian immunodeficiency virus (SIV), and other enveloped viruses [24,26,71,72]. It specifically and strongly interacted with the viral envelop glycoprotein gp120 through *N*-linked high mannose glycans (Man-8 and Man-9). Consequently, the gp120 could not bind to the host CD4 T-cell receptor and the chemokine CCR5 and CXCR4 co-receptors. Thus, the viral entry as well as the cell-to-cell fusion and transmission were inhibited [24,26,69,73,74].

Due to good stability, lack of toxic effects (as a 0.5–2% gel), broad spectrum of antiviral activities, and highly specific binding to oligosaccharides, CV-N offers a great potential for prevention of HIV sexual transmission. The female macaques (*Macaca fascicularis*) treated with a CV-N gel as a topical vaginal microbicide were found to be resistant to a pathogenic chimeric SIV/HIV-1 virus, SHIV89.6P [75]. Positive effects and a 63% reduction in the transmission of the virus were also obtained in macaques dosed vaginally with *Lactobacillus jensenii* 1153–1666 expressing CV-N [76,77]. Similar results were reported for CV-N as a preventive measure in rectal transmission of SHIV89.6P in macaques [75,78]. In the macaques models, CV-N was proven to be non-toxic and had no other adverse effects.

In order to obtain CV-N in the amounts required for further studies and at low costs, this polypeptide was expressed in several bacterial hosts (e.g., *Escherichia coli*, *Lactococcus lactis*, *Lactobacillus plantarum*) as well as in yeast and transgenic plants [79]. Cytoplasmic expression of CV-N in *E. coli* gave 3–4 mg of pure and bioactive recombinant protein (rCVN) per g of wet biomass [80,81]. In case of *Nicotiana tabacum*-biosynthesized rCVN, the yield was 130 mg of monomeric form per g fresh leaf tissue [82]. Products with increased activity were obtained by expression of fusion proteins containing CV-N and the plant-derived HIV-neutralizing monoclonal antibody mAb b12 [83] or the *Pseudomonas* exotoxin PE38 [84]. To reduce the immunogenic effects and the risk of proteolysis and to increase the half-life of the molecule in serum, a covalent binding of CV-N to poly(ethylene glycol) (PEGylate) was suggested [85]. As the PEGylation sites were at or near the mannose binding sites of CV-N, in many cases, loss of activity was observed. The in vitro activity was preserved only in the case of the PEGylated mutant Q62C with glutamine 62 replaced by cysteine and with the extra free sulfhydryl group. More successful results were obtained for PEGylated linker-extended CV-N with (Gly4Ser)₃ at the N-terminus designed by Chen et al. [86].

6. Other Peptides Exclusively Produced by *Nostoc*

Cyanobacteria of the genus *Nostoc* produce numerous other peptides, including nostophycin, nostosin, nostopeptolides, nostoweipeptins, and banyasin (Table S1). Some of the peptides have been identified only in cyanobacteria of this genus or even only in one *Nostoc* strain. Therefore, the available data about their structure and activity are scarce and sometimes limited to one to three papers.

Nostophycin (MW 888 Da, Figure 2), the cyclic hexapeptide with a novel β -amino acid residue, was detected only in *Nostoc* sp. 152 isolated from the lake Sääksjärvi in Finland [87]. The general structure of the compound is Ahoa[Pro-Ile-Phe-Pro-Gly-Gln] where Ahoa represents the unique β -amino acid residue, 3-amino-2,5-dihydroxy-8-phenyloctanoic acid (Figure 2). This unit is present only in nostophycin. Other examples of β -amino acids in cyanopeptides include 3-amino-9-methoxy-2,6,8-trimethyl-10-phenyl-4,6-decadienoic acid (ADDA) in microcystins [88], 3-amino-2-methylhexanoic acid (Amha) in medusamide [89], and 2-methyl-3-aminopentanoic acid (Map) in urumamide [90]. Nostophycin is synthesized constitutively on a hybrid PKS/NRPS enzyme complex encoded by the *npn* gene cluster [91]. The relationship between the net production rate of the compound and *Nostoc* sp. 152 growth was observed. However, under physiological stress induced by phosphorous and light limitation, the cell content of nostophycin increased up to 10-fold [92]. Nostophycin was found to be non-toxic (at 20 $\mu\text{g}/\text{mL}$) against bacteria (*Staphylococcus aureus*, *Bacillus subtilis*, *Escherichia coli*) and fungi (*Aspergillus niger*, *Candida albicans*) and showed weak cytotoxicity (10 $\mu\text{g}/\text{mL}$) against the lymphocytic mouse leukemia L1210 cells [87].

The cyclic depsipeptides, nostopeptolides (Np; MW 1033–1080 Da, Figure 2) belong to the MePro-containing peptides. They were found in cryptophycin-producing *Nostoc* sp. GSV224 [93], *Nostoc* sp. UK2almI isolated from lichen [94], and *Nostoc punctiforme* PCC73102 [95]. The general structure of the three Nps (A1–A3) from GSV224 is BA-IleA1/ValA2][Ser-MePro-LeuAc-Leu-Gly-Asn-Tyr-Pro], where MePro and leucylacetate (LeuAc) are the two non-proteinogenic amino acids and BA is a butyryl group. Np A3 was suggested to be either an epimer of Np A1 or an artifact generated during sample processing [93]. The four Nps (L1–L4) from *Nostoc* sp. UK2almI have the following sequence of residues, MHEA[Thr-O-MeSer-PhePr-MeProL1,L2/ProL3,L4-Dhb-Ile-Gln-HypL1,L3/ProL2,L4], where MHEA is 2-methylhex-2-enoic acid, O-MeSer is O-methylated serine, PhePr is phenylalanylpropanoic acid, Dhb is dehydrobutyric acid, and Hyp is hydroxyproline (Figure 2) [94]. As it could be concluded from the presence of non-proteinogenic amino acid residues in the structures, Nps belong to NRPs and are assembled through a mixed NRPS/PKS biosynthetic pathway [96]. Screening of 116 cyanobacterial genomes for the presence of genes involved in the biosynthesis of MePro (nosE and nosF) showed that, in contrast to other cyanobacterial genera, these genes are quite common in *Nostoc* [94].

Besides nostopeptolides, MePro is also present in the structure of nostocyclopeptides and nostoweipeptins (W; MW 1172–1214 Da, Figure 2). The latter class of peptides was found in *Nostoc* sp. XPORK 5A isolated from the Baltic Sea at Porkkala (Gulf of Finland). In four of the seven identified nostoweipeptins, two MePro residues were present. The structure of the major nostoweipeptin W1 is N-MePhe-Ac[Ser-MePro-Leu-Ile-Tyr-Ser-Hyp-Hyp-MePro]; an ester bond is located between MePro and Ser (Figure 2). Similarly as in the case of nostocyclopeptides, nostopeptolides and nostoweipeptins block the transport of microcystin and nodularin to hepatocytes HEK293 through OATP1B1/B3. The inhibition of the hepatotoxin-induced apoptosis by nostopeptolides and nostoweipeptins at μM concentrations indicates a possible application of the peptides as potent antitoxins [94].

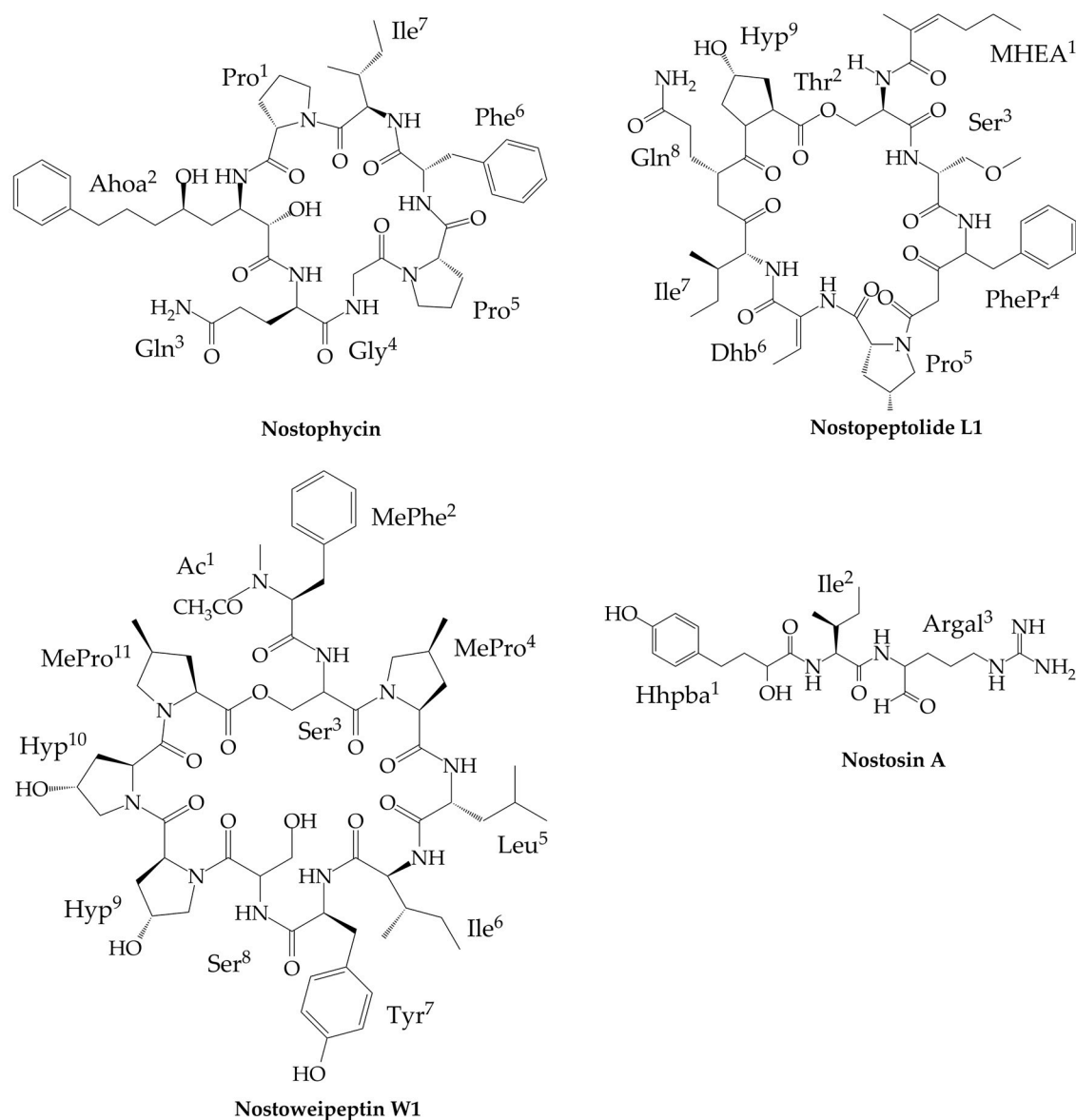


Figure 2. Structures of nostophycin, nostopeptolide L1 (Np-L1), nostoweipeptin W1 (Nwp-W1), and nostosin A (Ns-A) produced exclusively by cyanobacteria of genus *Nostoc*.

Nostosins (Ns-A; MW 449 Da and Ns-B; MW 451 Da, Figure 2), the linear nonribosomal tripeptides, were detected in *Nostoc* sp. FSN from a paddy field in Iran [97]. The peptides are composed of 2-hydroxy-4-(4-hydroxyphenyl)butanoic acid (Hhpba) in N terminus, Ile in the second position, and argininal (Ns-A) or argininal (Ns-B) in C terminus (Figure 2). In the cell extract from *Nostoc* sp. FSN, minor amounts of four other nostosin variants (Ns-C-F) were also detected. In these compounds, Ile was replaced by Val (Ns-D and F), and Hhpba was replaced by deoxyHhpba (Ns-C and E). Nostosins belong to serine proteases inhibitors. Ns-A with argininal is more potent and inhibits the activity of porcine trypsin with IC_{50} of 0.35 μ M, while the IC_{50} value of Ns-B is 0.55 μ M [97]. The strong trypsin-inhibiting activity of Ns-A is in line with similar effects observed for other small linear cyanopeptides with terminal argininal, e.g., spumigin E [98] or aeruginosin [99].

7. Peptides Produced by *Nostoc* and Other Cyanobacteria

As many other cyanobacteria, *Nostoc* produces bioactive nonribosomal peptides such as microcystins, cyanopeptolins, microginins, and anabaenopeptins. There are also reports on the presence

of the ribosomally synthesized microviridins in *Nostoc minutum* NIES-26 [100] and *N. punctiforme* PCC73102 [95] (Table S1). The structure, the activity, and the biosynthetic pathways of the peptides have been described in many scientific papers (e.g., [28,32,101,102]). Here, we refer only to some distinctive features of the peptides produced by cyanobacteria of the genus *Nostoc*.

Microcystins (MCs, Figure 3), the hepatotoxic cyclic heptapeptides, belong to the most widely studied cyanobacterial metabolites. In cyanobacteria of the genus *Nostoc*, microcystin variants with O-acetyl-demethyl Adda (ADMAdda) instead of Adda (Figure 3) are common and almost exclusively present in the members of this genus (Figure 3) [103–107]. The interactions of microcystins with protein phosphatases (PP1 and PP2a) and their toxicity strongly depend on a cyclic structure and the Adda-Glu part of the molecules [108]. In mouse bioassay, the ADMAdda-containing MCs (Figure 3) exhibited similar toxicity as the most potent variants of this class of peptides (LD₅₀ of 100–200 µg/kg) [104]. *Nostoc* is also the rare example of non-*Nodularia* producer of nodularin, the cyclic pentapeptide with a structure similar to microcystins [109,110]. Cyanopeptolins (CPs, Figure 3) constitute another class of peptides commonly detected in different taxonomic groups of cyanobacteria. They are composed of a six-amino acid ring with a unique 3-amino-6-hydroxy-2-piperidone (Ahp) residue (Figure 3). The side chain is linked to the cyclic part via the amino group on Thr [111]. In *Nostoc*, the compounds with similar structures are known as nostopeptins [37,112], insulapeptolides [113], and nostocyclins [114]. Nostopeptins A and B (BA^A/Ac^B-Gln[Hmp-Leu-Ahp-Ile-MeTyr-Ile]) and insulapeptolides (variant D: Ac-Cit[Hmp+Leu+Ahp+Ile+diMeTyr+Ile]) differ from CPs produced by other cyanobacteria in the presence of 3-hydroxy-4-methylproline (Hmp) instead of Thr [37,112,113]. A distinct feature of nostocyclin ([Thr+Hse+Ahp+Phe+MeTyr+Val]Hse+Ile+Hpla) is the presence of hydroxyphenyllactic acid (Hpla) in the side chain and two homoserine residues (Hse)—one in a side chain and one in the ring part of the molecule [114]. The CPs with the structure typical of this class of compounds (Figure 3) identified in other cyanobacteria (e.g., *Microcystis* or *Planktothrix*) were detected in *Nostoc* sp. TAU strain IL-235 from the spring pool of the Banyas stream in Israel [37] and *Nostoc edaphicum* CCNP1411 from the Baltic Sea [27]. Cyanopeptolin-like compounds produced by *Nostoc* inhibited activity of serine proteases (trypsin, chymotrypsin, or/and elastase) at nM to low µM concentrations [37,112,113]. Nostocyclin was active against protein phosphatases PP1 but at a relatively high IC₅₀ value 64 µM [114].

Anabaenopeptins (Aps) were detected in different cyanobacterial genera, including *Nostoc*, strains ASN-M [30], PCC73102 [115,116], and CENA543 [117]. The peptides are composed of a five-amino acid ring with a side chain attached through an ureido linkage (Figure 3). In *Nostoc* sp. CENA543 isolated from a Brazilian saline lake, six APs were found, including four new variants named nostamide with a general structure Ile/Val-CO[Lys-Ile/Val-Hph-MeAla/Ala-Hph/Phe], where Hph is homophenylalanine and MeAla is methylalanine (Figure 3). The strain also produces four namalides with anabaenopeptin-like scaffold but lacking two residues in the ring part (Ile/Val-CO[Lys-Ile/Val-Hph/Hty]) [117]. This type of peptide was earlier reported from marine sponge *Siliquariaspongia mirabilis* collected off Nama Island (Federated States of Micronesia) [118] and from the Brazilian strain of cyanobacterium *Sphaerospermopsis torques-reginae* ITEP-024 [119]. Anabaenopeptins usually inhibit activity of carboxypeptidases [120,121], protein phosphatases [122], or/and serine proteases (trypsin, chymotrypsin) [27,37]. Namalides were found to be active against carboxypeptidase A at submicromolar to micromolar concentrations [117,119].

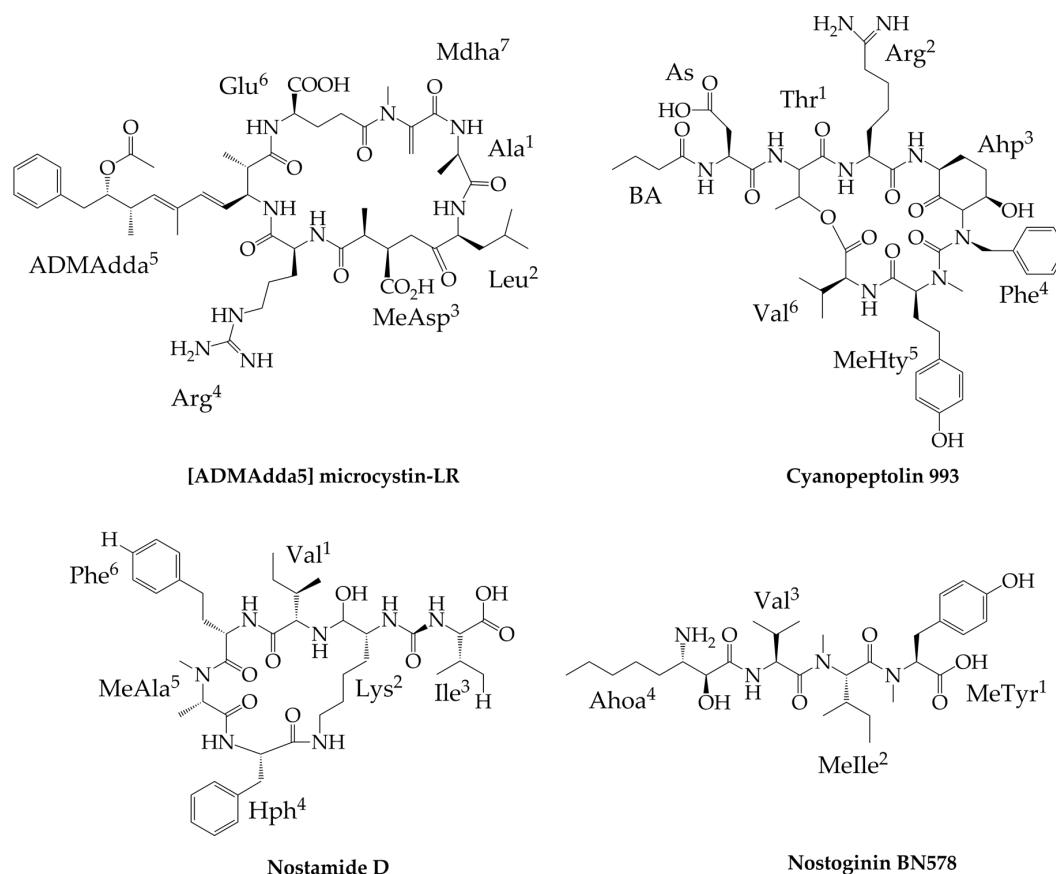


Figure 3. Structures of [ADMAdda5] microcystin-LR ([ADMAdda5]MC-LR), cyanopeptolin 993 (CP993), nostamide D (Na-D), and nostoginin BN578 produced by cyanobacteria of genus *Nostoc* and other cyanobacteria.

Nostoginins, the structural analogues of microginins, are another example of the differences within the same class of peptides produced by *Nostoc* and other cyanobacteria. In the C-terminal position of nostoginins, 3-amino-2-hydroxy decanoic acid (Ahda) residue present in microginins is replaced by 3-amino-2-hydroxy octanoic acid (Ahoa) (e.g., Ahoa-Val-Melle-MeTyr) (Figure 3) [37]. Nostoginin BN741 (MW 741 Da) isolated by Ploutno and Carmeli (2002) inhibited the activity of bovine amino peptidase with IC₉₀ of 1.3 M.

8. Conclusions

A high number of peptides produced by cyanobacteria of the genus *Nostoc*, their unique structures, and a wide spectrum of biological activities indicate a significant biotechnological potential of the organism. In case of already known bioactive peptides of potential pharmaceutical application, efforts are made to improve their drug-like properties by structure modification or conjugation with antibodies or small molecules. To produce sufficient amounts of bioactive agents for preclinical and clinical studies, the effectiveness of chemical synthesis and cloning is explored. In parallel, the search for new peptides produced by *Nostoc* is continued. Surprisingly, despite a wide geographical distribution and common occurrence of *Nostoc*, the most studied metabolites of the genus were detected in a limited number of strains. As new cyanobacterial culture collections with *Nostoc* isolates have recently been established in different institutions, and the use of methods for peptides detection, isolation, and activity screening are more common, further progress in the drug development based on the metabolites produced by *Nostoc* can be expected.

Supplementary Materials: The following are available online at <http://www.mdpi.com/1660-3397/17/10/561/s1>. Table S1: Peptides produced by cyanobacteria of the genus *Nostoc*.

Author Contributions: All authors were equally involved in planning, discussing and writing the article.

Acknowledgments: The work was supported by the National Science Centre in Poland 2016/21/B/NZ9/02304 and 2017/25/B/NZ9/00202.

Conflicts of Interest: The authors declare no conflicts of interest.

References

1. Gademann, K.; Portmann, C. Secondary Metabolites from Cyanobacteria: Complex Structures and Powerful Bioactivities. *Curr. Org. Chem.* **2008**, *12*, 326–341. [[CrossRef](#)]
2. Kobayashi, A.; Kajiyama, S.; Inawaka, K.; Kanzaki, H.; Kawazu, K. Nostodione A, a novel mitotic spindle poison from a blue-green alga *Nostoc commune*. *Z. Naturforschung* **1994**, *49*, 464–470. [[CrossRef](#)]
3. Yamada, S.; Ohkubo, S.; Miyashita, H.; Setoguchi, H. Genetic diversity of symbiotic cyanobacteria in *Cycas revoluta* (Cycadaceae). *FEMS Microbiol. Ecol.* **2012**, *81*, 696–706. [[CrossRef](#)] [[PubMed](#)]
4. Kaasalainen, U.; Fewer, D.; Jokela, J.; Wahlsten, M.; Sivonen, K.; Rikkinen, J. Cyanobacteria produce a high variety of hepatotoxic peptides in lichen symbiosis. *Proc. Natl. Acad. Sci. USA* **2012**, *109*, 5886–5891. [[CrossRef](#)]
5. Sand-Jensen, K. Ecophysiology of gelatinous *Nostoc* colonies: Unprecedented slow growth and survival in resource-poor and harsh environments. *Ann. Bot.* **2014**, *114*, 17–33. [[CrossRef](#)] [[PubMed](#)]
6. Hitzfeld, B.; Lampert, C.; Spaeth, N.; Mountfort, D.; Kaspar, H.; Dietrich, D. Toxin production in cyanobacterial mats from ponds on the McMurdo Ice Shelf, Antarctica. *Toxicon* **2000**, *38*, 1731–1748. [[CrossRef](#)]
7. Jones, K. Interactions between desiccation and dark nitrogen fixation in tropical *Nostoc commune*. *New Phytol.* **1989**, *113*, 1–6. [[CrossRef](#)]
8. Trnková, K.; Barták, M. Desiccation-induced changes in photochemical processes of photosynthesis and spectral reflectance in *Nostoc commune* (Cyanobacteria, Nostocales) colonies from polar regions. *Phycol. Res.* **2016**, *65*, 1.
9. Thangaraj, B.; Rajasekar, D.; Vijayaraghavan, R.; Garlapati, D.; Devanesan, A.; Lakshmanan, U.; Dharmar, P. Cytomorphological and nitrogen metabolic enzyme analysis of psychrophilic and mesophilic *Nostoc* sp.: A comparative outlook. *Biotech* **2017**, *7*, 107. [[CrossRef](#)] [[PubMed](#)]
10. Scherer, S.; Potts, M. Novel water stress protein from a desiccation-tolerant cyanobacterium: Purification and partial characterization. *J. Biol. Chem.* **1989**, *264*, 12546–12553. [[PubMed](#)]
11. Potts, M. Mechanisms of desiccation tolerance in cyanobacteria. *Eur. J. Phycol.* **1999**, *34*, 319–328. [[CrossRef](#)]
12. Sand-Jensen, K.; Raun, A.; Borum, J. Metabolism and resources of spherical colonies of *Nostoc zetterstedtii*. *Limnol. Oceanogr.* **2009**, *54*, 1282–1291. [[CrossRef](#)]
13. Scherer, S.; Chen, T.; Böger, P. A new UV-A/B protecting pigment in the terrestrial cyanobacterium *Nostoc commune*. *Plant Physiol.* **1988**, *88*, 1055–1057. [[CrossRef](#)] [[PubMed](#)]
14. Kimura, Y.; Klmura, S.; Sato, S.; Katoh, H.; Abe, T.; Aral, M.; Tomlta-Yokotani, K. Evaluation of a cyanobacterium *Nostoc* sp. HK-01, as food material for space agriculture on mars. *Biol. Sci. Space* **2015**, *29*, 24–31. [[CrossRef](#)]
15. Gao, K. Chinese studies on the edible blue-green alga, *Nostoc flagelliforme*: A review. *J. Appl. Phycol.* **1998**, *10*, 37–49. [[CrossRef](#)]
16. Johnson, H.; King, S.; Banack, S.; Webster, C.; Callanaupa, W.; Cox, P. Cyanobacteria (*Nostoc commune*) used as a dietary item in the Peruvian highlands produce the neurotoxic amino acid BMAA. *J. Ethnopharmacol.* **2008**, *118*, 159–165. [[CrossRef](#)] [[PubMed](#)]
17. Roney, B.; Renhui, L.; Banack, S.; Murch, S.; Honegger, R.; Cox, P. Consumption of *fa cai Nostoc* soup: A potential for BMAA exposure from *Nostoc* cyanobacteria in China? *Amyotroph. Lateral Scler.* **2009**, *10*, 44–49. [[CrossRef](#)]
18. Li, Z.; Guo, M. Healthy efficacy of *Nostoc commune* Vaucher. *Oncotarget* **2018**, *9*, 14669–14679. [[CrossRef](#)] [[PubMed](#)]
19. Win, T.; Barone, G.; Secundo, F.; Fu, P. Algal biofertilizers and plant growth stimulants for sustainable agriculture. *Ind. Biotechnol.* **2018**, *14*, 203–211. [[CrossRef](#)]

20. Ghazal, F.; Mahdy, E.; El-Fattah, M.; El-Sadany, A.; Doha, N. The use of cyanobacteria as biofertilizer in wheat cultivation under different nitrogen rates. *Nat. Sci.* **2018**, *16*, 30–35.
21. Moore, R. Cyclic peptides and depsipeptides from cyanobacteria: A review. *J. Ind. Microbiol.* **1996**, *16*, 134–143. [[CrossRef](#)] [[PubMed](#)]
22. El-Sheekh, M.; Osman, M.; Dyan, M.; Amer, M. Production and characterization of antimicrobial active substance from the cyanobacterium *Nostoc muscorum*. *Environ. Toxicol. Pharmacol.* **2006**, *21*, 42–50. [[CrossRef](#)] [[PubMed](#)]
23. Ploutno, A.; Carmeli, S. Nostocyclone A, a novel antimicrobial cyclophane from the cyanobacterium *Nostoc* sp. *J. Nat. Prod.* **2000**, *63*, 1524–1526. [[CrossRef](#)] [[PubMed](#)]
24. Boyd, M.; Gustafson, K.; McMahon, J.; Shoemaker, R.; O’Keefe, B.; Mori, T.; Gulakowski, R.; Wu, L.; Rivera, M.; Laurencot, C.; et al. Discovery of cyanovirin-N, a novel human immunodeficiency virus-inactivating protein that binds viral surface envelope glycoprotein gp120: Potential applications to microbicide development. *Antimicrob. Agents Chemother.* **1997**, *41*, 1521–1530. [[CrossRef](#)]
25. Botos, I.; Wlodawer, A. Cyanovirin-N: A sugar-binding antiviral protein with a new twist. *Cell. Mol. Life Sci.* **2003**, *60*, 277–287. [[CrossRef](#)]
26. Dey, B.; Lerner, D.; Lusso, P.; Boyd, M.; Elder, J.; Berger, E. Multiple antiviral activities of cyanovirin-N: Blocking of human immunodeficiency virus type 1 gp120 interaction with CD4 and coreceptor and inhibition of diverse enveloped viruses. *J. Virol.* **2000**, *74*, 4562–4569. [[CrossRef](#)]
27. Mazur-Marzec, H.; Fidor, A.; Cegłowska, M.; Wiczerzak, E.; Kropidłowska, M.; Goua, M.; Macaskill, J.; Edwards, C. Cyanopeptolins with trypsin and chymotrypsin inhibitory activity from the cyanobacterium *Nostoc edaphicum* CCNP 1411. *Mar. Drugs* **2018**, *16*, 220. [[CrossRef](#)]
28. Dittmann, E.; Neilan, B.; Börner, T. Molecular biology of peptide and polyketide biosynthesis in cyanobacteria. *Appl. Microbiol. Biotechnol.* **2001**, *57*, 467–473.
29. Dembitsky, D.; Řezanka, T. Metabolites produced by nitrogen-fixing *Nostoc* species. *Folia Microbiol.* **2005**, *50*, 363–391. [[CrossRef](#)]
30. Nowruzi, B.; Khavari-Nejad, R.; Sivonen, K.; Kazemi, B.; Najafi, F.; Nejadstattari, T. Identification and toxigenic potential of *Nostoc* sp. *Algae* **2012**, *27*, 303–313. [[CrossRef](#)]
31. Řezanka, T.; Dor, I.; Dembitsky, V. Fatty acid composition of six freshwater wild cyanobacterial species. *Folia Microbiol.* **2003**, *48*, 71–75. [[CrossRef](#)] [[PubMed](#)]
32. Welker, M.; von Döhren, H. Cyanobacterial peptides—Nature’s own combinatorial biosynthesis. *FEMS Microbiol. Rev.* **2006**, *30*, 530–563.
33. Shah, S.; Akhter, N.; Auckloo, B.; Khan, I.; Lu, Y.; Wang, K.; Wu, B.; Guo, Y.-W. Structural diversity, biological properties and applications on natural products from cyanobacteria. A review. *Mar. Drugs* **2017**, *15*, 354. [[CrossRef](#)]
34. Fosgerau, K.; Hoffmann, T. Peptide therapeutics: Current status and future directions. *Drug Discov. Today* **2015**, *20*, 122–128. [[CrossRef](#)] [[PubMed](#)]
35. Lau, J.; Dunn, M. Therapeutic peptides: Historical perspectives, current development trends, and future directions. *Bioorg. Med. Chem.* **2018**, *26*, 2700–2707. [[CrossRef](#)]
36. Golakoti, T.; Ogino, J.; Heltzel, C.; Le Husebo, T.; Jensen, C.; Larsen, L.; Patterson, G.; Moore, R.; Mooberry, S.; Corbett, T.; et al. Structure determination, conformational analysis, chemical stability studies, and antitumor evaluation of the cryptophycins. Isolation of new 18 analogs from *Nostoc* sp. strain GSV 224. *J. Am. Chem. Soc.* **1995**, *117*, 12030–12049. [[CrossRef](#)]
37. Ploutno, A.; Carmeli, S. Modified peptides from a water bloom of the cyanobacterium *Nostoc* sp. *Tetrahedron* **2002**, *58*, 9949–9957. [[CrossRef](#)]
38. Kapuščík, A.; Hrouzek, P.; Kuzma, M.; Bártoová, S.; Novák, P.; Jokela, J.; Pflüger, M.; Eger, A.; Hundsberger, H.; Kopecký, J. Novel aeruginosin-865 from *Nostoc* sp. as a potent anti-inflammatory agent. *ChemBioChem* **2013**, *14*, 2329–2337. [[CrossRef](#)]
39. Nowruzi, B.; Khavari-Nejad, R.; Sivonen, K.; Kazemi, B.; Najafi, F.; Nejadstattari, T. A gene expression study on strains of *Nostoc* (Cyanobacteria) revealing antimicrobial activity under mixotrophic conditions. *Afr. J. Biotech.* **2012**, *11*, 11296–11308. [[CrossRef](#)]
40. Karjiyama, S.-I.; Kanzaki, H.; Kawazu, K.; Kobayashi, A. Nostofungicide, an antifungal lipopeptide from the field-grown terrestrial blue-green alga *Nostoc commune*. *Tetrahedron Lett.* **1998**, *39*, 3737–3740. [[CrossRef](#)]

41. Wang, H.; Fewer, D.; Holm, L.; Rouhiainen, L.; Sivonen, K. Atlas of nonribosomal peptide and polyketide biosynthetic pathways reveals common occurrence of nonmodular enzymes. *Proc. Natl. Acad. Sci. USA* **2014**, *111*, 9259–9264. [[CrossRef](#)]
42. Finking, R.; Marahiel, M. Biosynthesis of nonribosomal peptides. *Annu. Rev. Microbiol.* **2004**, *58*, 453–488. [[CrossRef](#)]
43. Dittmann, E.; Gugger, M.; Sivonen, K.; Fewer, D. Natural product biosynthetic diversity and comparative genomics of the cyanobacteria. *Trends Microbiol.* **2015**, *23*, 642–652. [[CrossRef](#)] [[PubMed](#)]
44. Meyer, S.; Kehr, J.; Mainz, A.; Dehm, D.; Petras, D.; Süßmuth, R.; Dittmann, E. Biochemical dissection of the natural diversification of microcystin provides lessons for synthetic biology of NRPS. *Cell. Chem. Biol.* **2016**, *23*, 462–471. [[CrossRef](#)] [[PubMed](#)]
45. Kim, W.; Patel, A.; Hur, G.; Tufar, P.; Wuo, M.; McCammon, J.; Burkart, M. Mechanistic probes for the epimerization domain of nonribosomal peptide synthetases. *ChemBioChem Commun.* **2019**, *20*, 147–152. [[CrossRef](#)] [[PubMed](#)]
46. Burja, A.; Banaigs, B.; Abou-Mansour, E.; Burgess, J.; Wright, P. Marine cyanobacteria—A prolific source of natural products. *Tetrahedron* **2001**, *57*, 9347–9377. [[CrossRef](#)]
47. Schwartz, R.; Hirsch, S.; Sesin, D.; Flor, J.; Chartrain, M.; Fromtling, R.; Harris, G.; Salvatore, M.; Liesch, J.; Yudin, K. Pharmaceuticals from cultured algae. *J. Ind. Microbiol.* **1990**, *5*, 113–124. [[CrossRef](#)]
48. Eggen, M.; Georg, G. The cryptophycins: Their synthesis and anticancer activity. *Med. Res. Rev.* **2002**, *22*, 85–101. [[CrossRef](#)] [[PubMed](#)]
49. Weiss, C.; Figueras, E.; Borbely, A.; Sewald, N. Cryptophycins: Cytotoxic cyclodepsipeptides with potential for tumor targeting. *J. Pept. Sci.* **2017**, *23*, 514–531. [[CrossRef](#)] [[PubMed](#)]
50. Magarvey, N.; Beck, Z.; Golakoti, T.; Ding, Y.; Huber, U.; Hemscheidt, T.; Abelson, D.; Moore, R.; Sherman, D. Biosynthetic characterization and chemoenzymatic assembly of the cryptophycins. Potent anticancer agents from *Nostoc* cyanobionts. *ACS Chem. Biol.* **2006**, *1*, 766–779. [[CrossRef](#)]
51. Golakoti, T.; Ohtani, I.; Patterson, G.; Moore, R.; Corbett, T.; Valeriote, F.; Demchik, L. Total structures of cryptophycins, potent antitumor depsipeptides from the blue-green alga *Nostoc* sp. strain GSV 224. *J. Am. Chem. Soc.* **1994**, *116*, 4729–4737.
52. Wagner, M.; Paul, D.; Shih, C.; Jordan, M.; Wilson, L.; Williams, D. In vitro pharmacology of cryptophycin 52 (LY355703) in human tumor cell lines. *Cancer Chemother. Pharmacol.* **1999**, *43*, 115–125. [[CrossRef](#)]
53. Corbett, T.; Valeriote, F.; Demchik, L.; Lowichik, N.; Polin, L.; Panchapor, C.; Pugh, S.; White, K.; Kushner, J.; Rake, J.; et al. Discovery of cryptophycin-1 and BCN-183577: Examples of strategies and problems in the detection of antitumor activity in mice. *IND* **1997**, *15*, 207–218.
54. Smith, C.; Zhang, X.; Mooberry, S.; Patterson, G.; Moore, R. Cryptophycin: A new antimicrotubule agent active against drug-resistant cells. *Cancer Res.* **1994**, *54*, 3779–3784.
55. Boinpally, R.; Polin, L.; Zhou, S.-L.; Jasti, B.; Wiegand, R.; White, K.; Kushner, J.; Horwitz, J.; Corbett, T.; Parchment, R. Pharmacokinetics and tissue distribution of cryptophycin 52 (C-52) epoxide and cryptophycin 55 (C-55) chlorohydrin in mice with subcutaneous tumors. *Cancer Chemother. Pharmacol.* **2003**, *52*, 25–33. [[CrossRef](#)]
56. Liang, J.; Moore, R.; Moher, E.; Munroe, J.; Al-awar, R.; Hay, D.; Varie, D.; Zhang, T.; Aikins, J.; Martinelli, M.; et al. Cryptophycins-309, 249 and other cryptophycin analogs: Preclinical efficacy studies with mouse and human tumors. *Investig. New Drug* **2005**, *23*, 213–224. [[CrossRef](#)]
57. Weiss, C.; Sammet, B.; Sewald, N. Recent approaches for the synthesis of modified cryptophycins. *Nat. Prod. Rep.* **2013**, *30*, 924–940. [[CrossRef](#)]
58. Edelman, M.; Gandara, D.; Hausner, P.; Israel, V.; Thornton, D.; DeSanto, J.; Doyle, L. Phase 2 study of cryptophycin 52 (LY355703) in patients previously treated with platinum based chemotherapy for advanced non-small cell lung cancer. *Lung Cancer* **2003**, *39*, 197–199. [[CrossRef](#)]
59. D’Agostino, G.; del Campo, J.; Mellado, B.; Izquierdos, M.; Minarik, T.; Cirri, L.; Marini, L.; Perez-Gracia, J.; Scambia, G. A multicancer phase II study of the cryptophycin analog LY355703 in patients with platinum-resistant ovarian cancer. *Int. J. Gynecol. Cancer* **2006**, *16*, 71–76. [[CrossRef](#)] [[PubMed](#)]
60. Verma, V.; Pillow, T.; DePalatis, L.; Li, G.; Phillips, G.; Polson, A.; Raab, H.; Spencer, S.; Zheng, B. The Cryptophycins as potent payloads for antibody drug conjugates. *Bioorg. Med. Chem. Lett.* **2015**, *25*, 864–868. [[CrossRef](#)] [[PubMed](#)]

61. Borbély, A.; Figueras, E.; Martins, A.; Esposito, S.; Auciello, G.; Monteagudo, E.; Di Marco, A.; Summa, V.; Cordella, P.; Perego, R.; et al. Synthesis and biological evaluation of RGD-cryptophycin conjugates for targeted drug delivery. *Pharmaceutics* **2019**, *11*, 151. [[CrossRef](#)]
62. Golakoti, T.; Yoshida, W.; Chaganty, S.; Moore, R. Isolation and structure determination of nostocyclopeptides A1 and A2 from the terrestrial cyanobacterium *Nostoc* sp. ATCC53789. *J. Nat. Prod.* **2001**, *64*, 54–59. [[CrossRef](#)] [[PubMed](#)]
63. Jokela, J.; Herfindal, L.; Wahlsten, M.; Permi, P.; Selheim, F.; Vasconcelos, V.; Døskeland, S.; Sivonen, K. A novel cyanobacterial nostocyclopeptide is a potent antitoxin against *Microcystis*. *ChemBioChem* **2010**, *11*, 1594–1599. [[CrossRef](#)]
64. Enck, S.; Kopp, F.; Marahiel, M.; Geyer, A. The entropy balance of nostocyclopeptide macrocyclization analysed by NMR spectroscopy. *ChemBioChem* **2008**, *9*, 2597–2601. [[CrossRef](#)]
65. Becker, J.E.; Moore, R.E.; Moore, B.S. Cloning, sequencing, and biochemical characterization of the nostocyclopeptide biosynthetic gene cluster: Molecular basis for imine macrocyclization. *Gene* **2004**, *325*, 35–42. [[CrossRef](#)]
66. Herfindal, L.; Myhren, L.; Kleppe, R.; Krakstad, C.; Selheim, F.; Jokela, J.; Sivonen, K.; Døskeland, S. Nostocyclopeptide-M1: A potent, nontoxic inhibitor of the hepatocyte drug transporters OATP1B3 and OATP1B1. *Mol. Pharm.* **2011**, *8*, 360–367. [[CrossRef](#)]
67. Gustafson, K.; Sowder, R.; Henderson, L.; Cardellina, J.; McMahon, J.; Rajamani, U.; Pannell, L.; Boyd, M. Isolation, primary sequence determination, and disulfide bond structure of cyanovirin-N, an anti-HIV (Human Immunodeficiency Virus) protein from the cyanobacterium *Nostoc ellipsosporum*. *Biochem. Biophys. Res. Commun.* **1997**, *238*, 223–228. [[CrossRef](#)]
68. Yang, F.; Bewley, C.; Louis, J.; Gustafson, K.; Boyd, M.; Gronenborn, A.; Clore, G.; Wlodawer, A. Crystal structure of cyanovirin-N, a potent HIV-inactivating protein, shows unexpected domain swapping. *J. Mol. Biol.* **1999**, *288*, 403–412. [[CrossRef](#)]
69. Bewley, C.; Otero-Quintero, S. The potent anti-HIV cyanovirin-N contains two novel carbohydrate binding sites that selectively bind to Man₈ D1D3 and Man₉ with nanomolar affinity: Implications for binding to the HIV envelope protein gp120. *J. Am. Soc.* **2001**, *123*, 3892–3902. [[CrossRef](#)]
70. Barrientos, L.; Louis, J.; Botos, I.; Mori, T.; Han, Z.; O’Keefe, B.; Boyd, M.; Wlodawer, A.; Gronenborn, A. The domain-swapped dimer of cyanovirin-N is in a metastable folded state: Reconciliation of X-Ray and NMR structures. *Structure* **2002**, *10*, 673–686. [[CrossRef](#)]
71. Barrientos, L.; O’Keefe, B.; Bray, M.; Sanchez, A.; Gronenborn, A.; Boyd, M. Cyanovirin-N binds to the viral surface glycoprotein, GP_{1,2} and inhibits infectivity of Ebola virus. *Antivir. Res.* **2003**, *58*, 47–56. [[CrossRef](#)]
72. Barrientos, L.; Gronenborn, A. The highly specific carbohydrate-binding protein cyanovirin-N: Structure anti-HIV/Ebola activity and possibilities for therapy. *Mini Rev. Med. Chem.* **2005**, *5*, 21–31. [[CrossRef](#)]
73. Esser, M.; Mori, T.; Mondor, I.; Sattentau, Q.; Dey, B.; Berger, E.; Boyd, M.; Lifson, J. Cyanovirin-N binds to gp120 to interfere with CD4-dependent human immunodeficiency virus type 1 virion binding, fusion, and infectivity but does not affect the CD4 binding site on gp120 or soluble CD4-induced conformational changes in gp120. *J. Virol.* **1999**, *73*, 4360–4371.
74. Mori, T.; Boyd, M. Cyanovirin-N, a potent human immunodeficiency virus-inactivating protein, blocks both CD4-dependent and CD4-independent binding of soluble gp120 (sgp120) to target cells, inhibits sCD4-induced binding of sgp120 to cell-associated CXCR4, and dissociates bound sgp120 from target cells. *Antimicrob. Agents Chemother.* **2001**, *45*, 664–672. [[PubMed](#)]
75. Tsai, C.-C.; Emau, P.; Jiang, Y.; Tian, B.; Morton, W.; Gustafson, K.; Boyd, M. Cyanovirin-N gel as a topical microbicide prevents rectal transmission of SHIV89.6P in macaques. *AIDS Res. Hum. Retrovir.* **2003**, *19*, 535–541. [[CrossRef](#)]
76. Lagenaur, L.; Sanders-Bear, B.; Brichacek, B.; Pal, R.; Liu, X.; Liu, Y.; Yu, R.; Venzon, D.; Lee, P.P.; Hamer, D.H. Prevention of vaginal SHIV transmission in macaques by a live recombinant *Lactobacillus*. *Mucosal. Immunol.* **2011**, *4*, 648–657. [[CrossRef](#)]
77. Lagenaur, L.; Swedek, I.; Lee, P.; Parks, T.P. Robust vaginal colonization of Macaques with a novel vaginally disintegrating tablet containing a live biotherapeutic product to prevent HIV infection in women. *PLoS ONE* **2015**, *10*, 1–17. [[CrossRef](#)]

78. Yu, R.; Cheng, A.; Lagenaur, L.; Huang, W.; Weiss, D.; Treece, J.; Sanders-Beer, B.; Hamer, D.; Lee, P.; Xu, Q.; et al. A Chinese rhesus macaque (*Macaca mulatta*) model for vaginal *Lactobacillus* colonization and live microbicide development. *J. Med. Primatol.* **2009**, *38*, 125–136. [[CrossRef](#)]
79. Lofti, H.; Sheervalilou, R.; Zarghami, N. An update of the recombinant protein expression systems of cyanovirin-N and challenges of preclinical development. *BioImpacts* **2018**, *8*, 139–151.
80. Colleluori, D.; Tien, D.; Kang, F.; Pagliei, T.; Kuss, R.; McCormick, T.; Watson, K.; McFadden, K.; Chaiken, I.; Buckheit, R.; et al. Expression, purification, and characterization of recombinant cyanovirin-N for vaginal anti-HIV microbicide development. *Protein Expr. Purif.* **2005**, *39*, 229–236. [[CrossRef](#)] [[PubMed](#)]
81. Gao, X.; Chen, W.; Guo, C.; Qian, C.; Liu, G.; Ge, F.; Huang, Y.; Kitazato, K.; Wang, Y.; Xiong, S. Soluble cytoplasmic expression, rapid purification, and characterization of cyanovirin-N as a his-SUMO fusion. *Appl. Microbiol. Biotechnol.* **2010**, *85*, 1051–1060. [[CrossRef](#)]
82. Sexton, A.; Drake, P.; Mahmood, N.; Harman, S.; Shattock, R.; Ma, J. Transgenic plant production of cyanovirin-N, an HIV microbicide. *FASEB J.* **2006**, *20*, 356–358. [[CrossRef](#)]
83. Sexton, A.; Harman, S.; Shattock, R.; Ma, J. Design, expression, and characterization of a multivalent, combination HIV microbicide. *FASEB J.* **2009**, *23*, 3590–3600. [[CrossRef](#)]
84. Mori, T.; Shoemaker, R.; Gulakowski, R.; Krepps, B.; McMahan, J.; Gustafson, K.; Pannell, L.; Boyd, M. Analysis of sequence requirements for biological activity of cyanovirin-N, a potent HIV (Human Immunodeficiency Virus)-inactivating protein. *Biochem. Biophys. Res. Commun.* **1997**, *238*, 218–222. [[CrossRef](#)]
85. Zappe, H.; Snell, M.; Bossard, M. PEGylation of cyanovirin-N, an entry inhibitor of HIV. *Adv. Drug Deliv. Rev.* **2008**, *60*, 79–87. [[CrossRef](#)]
86. Chen, J.; Huang, D.; Chen, W.; Guo, C.; Wei, B.; Wu, C.; Peng, Z.; Fan, J.; Hou, Z.; Fang, Y.; et al. Linker-extended native cyanovirin-N facilitates PEGylation and potently inhibits HIV-1 by targeting the glycan ligand. *PLoS ONE* **2014**, *9*, 1–15. [[CrossRef](#)]
87. Fujii, K.; Sivonen, K.; Kashiwagi, T.; Hirayama, K.; Harada, K.-I. Nostophycin, a novel cyclic peptide from the toxic cyanobacterium *Nostoc* sp. 152. *J. Org. Chem.* **1999**, *64*, 5777–5782. [[CrossRef](#)]
88. Namikoshi, M.; Rinehart, K.; Sakai, R.; Sivonen, K.; Carmichael, W. Structures of three new cyclic heptapeptide hepatotoxins produced by the cyanobacterium (blue-green alga) *Nostoc* sp. strain 152. *J. Org. Chem.* **1990**, *55*, 6135–6139. [[CrossRef](#)]
89. Fenner, A.; Engene, N.; Spadafora, C.; Gerwick, W.; Balunas, M. Medusamide A, a Panamanian cyanobacterial depsipeptide with multiple β -amino acids. *Org. Lett.* **2016**, *18*, 352–355. [[CrossRef](#)]
90. Kanamori, Y.; Iwasaki, A.; Sumimoto, S.; Suenaga, K. Urumamide, a novel chymotrypsin inhibitor with a β -amino acid from a marine cyanobacterium *Okeania* sp. *Tetrahedron Lett.* **2016**, *57*, 4213–4216. [[CrossRef](#)]
91. Fewer, D.P.; Österholm, J.; Rouhiainen, L.; Jokela, J.; Wahlsten, M.; Sivonen, K. Nostophycin biosynthesis is directed by a hybrid polyketide synthase-nonribosomal peptide synthetase in the toxic cyanobacterium *Nostoc* sp. strain 152. *Appl. Environ. Microbiol.* **2011**, *77*, 8034–8040. [[CrossRef](#)]
92. Kurmayer, R. The toxic cyanobacterium *Nostoc* sp. strain 152 produces highest amounts of microcystin and nostophycin under stress conditions. *J. Phycol.* **2011**, *47*, 200–207. [[CrossRef](#)] [[PubMed](#)]
93. Golakoti, T.; Yoshida, W.; Chaganty, S.; Moore, R. Isolation and structures of nostopeptolides A1, A2 and A3 from the cyanobacterium *Nostoc* sp. GSV 224. *Tetrahedron* **2000**, *56*, 9093–9102. [[CrossRef](#)]
94. Liu, L.; Jokela, J.; Herfindal, L.; Wahlsten, M.; Sinkkonen, J.; Permi, P.; Fewer, D.; Døskeland, S.; Sivonen, K. 4-methylproline guided natural product discovery: Co-occurrence of 4-hydroxy and 4-methylprolines in nostoweipeptins and nostopeptolides. *ACS Chem. Biol.* **2014**, *9*, 2646–2655. [[CrossRef](#)] [[PubMed](#)]
95. Dehm, D.; Krumbholz, J.; Baunach, M.; Wiebach, V.; Hinrichs, K.; Guljamow, A.; Tabuchi, T.; Jenke-Kodama, H.; Süßmuth, R.; Dittmann, E. Unlocking the spatial control of secondary metabolism uncovers hidden natural product diversity in *Nostoc punctiforme*. *ACS Chem. Biol.* **2019**, *14*, 1271–1279. [[CrossRef](#)]
96. Hoffmann, D.; Hevel, J.; Moore, R.; Moore, B. Sequence analysis and biochemical characterization of the nostopeptolide A biosynthetic gene cluster from *Nostoc* sp. GSV 224. *Gene* **2003**, *311*, 171–180. [[CrossRef](#)]
97. Liu, L.; Jokela, J.; Wahlsten, M.; Nowruz, B.; Permi, P.; Zhang, Y.; Xhaard, H.; Fewer, D.; Sivonen, K. Nostosins, trypsin inhibitors isolated from the terrestrial cyanobacterium *Nostoc* sp. strain FSN. *J. Nat. Prod.* **2014**, *77*, 1784–1790. [[CrossRef](#)] [[PubMed](#)]
98. Fewer, D.; Jokela, J.; Rouhiainen, L.; Wahlsten, M.; Koskenniemi, K.; Stal, L.; Sivonen, K. The non-ribosomal assembly and frequent occurrence of the protease inhibitors spumigins in the bloom-forming cyanobacterium *Nodularia spumigena*. *Mol. Microbiol.* **2009**, *73*, 924–937. [[CrossRef](#)]

99. Ishida, K.; Okita, Y.; Matsuda, H.; Okino, T.; Murakami, M. Aeruginosins, protease inhibitors from the cyanobacterium *Microcystis aeruginosa*. *Tetrahedron* **1999**, *55*, 10971–10988. [[CrossRef](#)]
100. Murakami, M.; Sun, Q.; Ishida, K.; Matsuda, H.; Okino, T.; Yamaguchi, K. Microviridins, elastase inhibitors from the cyanobacterium *Nostoc minutum* (NIES-26). *Phytochemistry* **1997**, *45*, 1197–1202. [[CrossRef](#)]
101. Sivonen, K.; Leikoski, N.; Fewer, D.; Jokela, J. Cyanobactins—Ribosomal cyclic peptides produced by cyanobacteria. *Appl. Microbiol. Biotechnol.* **2010**, *86*, 1213–1225. [[CrossRef](#)]
102. Janssen, E. Cyanobacterial peptides beyond microcystins—A review on co-occurrence, toxicity, and challenges for risk assessment. *Water Res.* **2019**, *151*, 488–499. [[CrossRef](#)]
103. Sivonen, K.; Carmichael, W.; Namikoshi, M.; Rinehart, K.; Dahlem, A.; Niemela, S. Isolation and characterization of hepatotoxic microcystin homologs from the filamentous freshwater cyanobacterium *Nostoc* sp. strain 152. *Appl. Environ. Microbiol.* **1990**, *56*, 2650–2657.
104. Beattie, K.; Kaya, K.; Sano, T.; Codd, G. Three dehydrobutyrine-containing microcystins from *Nostoc*. *Phytochemistry* **1998**, *47*, 1289–1292. [[CrossRef](#)]
105. Laub, J.; Henriksen, P.; Brittain, S.; Wang, J.; Carmichael, W.; Rinehart, K.; Moestrup, Ø. [ADMA⁵]-microcystins in *Planktothrix agardhii* strain PH-123 (cyanobacteria)—Importance for monitoring of microcystins in the environment. *Environ. Toxicol.* **2002**, *17*, 351–357. [[CrossRef](#)]
106. Oksanen, I.; Jokela, J.; Fewer, D.; Wahlsten, M.; Rikkinen, J.; Sivonen, K. Discovery of rare and highly toxic microcystins from lichen-associated cyanobacterium *Nostoc* sp. strain IO-102-I. *Appl. Environ. Microbiol.* **2004**, *70*, 5756–5763. [[CrossRef](#)]
107. Fewer, D.; Wahlsten, M.; Österholm, J.; Jokela, J.; Rouhiainen, L.; Kaasalainen, U.; Rikkinen, J.; Sivonen, K. The genetic basis for O-acetylation of the microcystin toxin in cyanobacteria. *Chem. Biol.* **2013**, *20*, 861–869. [[CrossRef](#)]
108. Schmidt, J.; Wilhelm, S.; Boyer, G. The fate of microcystins in the environment and challenges for monitoring. *Toxins* **2014**, *6*, 3354–3387. [[CrossRef](#)]
109. Gehringer, M.; Adler, L.; Roberts, A.; Moffitt, M.; Mihali, T.; Mills, T.; Fieker, C.; Neilan, B. Nodularin, a cyanobacterial toxin, is synthesized in *planta* by symbiotic *Nostoc* sp. *ISME J.* **2012**, *6*, 1834–1847. [[CrossRef](#)]
110. Jokela, J.; Heinila, L.; Shishido, T.; Wahlsten, M.; Fewer, D.; Fiore, M.; Wang, H.; Haapaniemi, E.; Permii, P.; Sivonen, K. Production of high amounts of hepatotoxin nodularin and new protease inhibitors pseudospumigins by the Brazilian benthic *Nostoc* sp. CENA543. *Front. Microbiol.* **2017**, *8*, 1963. [[CrossRef](#)]
111. Yamaki, H.; Sitachitta, N.; Sano, T.; Kaya, K. Two new chymotrypsin inhibitors isolated from the cyanobacterium *Microcystis aeruginosa* NIES-88. *J. Nat. Prod.* **2005**, *68*, 14–18. [[CrossRef](#)]
112. Okino, T.; Qi, S.; Matsuda, H.; Murakami, M.; Yamaguchi, K. Nostopeptins A and B, elastase inhibitors from the cyanobacterium *Nostoc minutum*. *J. Nat. Prod.* **1997**, *60*, 158–161. [[CrossRef](#)]
113. Mehner, C.; Müller, D.; Kehraus, S.; Hautmann, S.; Gütschow, M.; König, G. New peptolides from the cyanobacterium *Nostoc insulare* as selective and potent inhibitors of human leukocyte elastase. *ChemBioChem* **2008**, *9*, 2692–2703. [[CrossRef](#)]
114. Kaya, K.; Sano, T.; Beattie, K.; Codd, G. Nostocyclin, a novel 3-amino-6-hydroxy-2-piperidone-containing cyclic depsipeptide from the cyanobacterium *Nostoc* sp. *Tetrahedron Lett.* **1996**, *37*, 6725–6728. [[CrossRef](#)]
115. Rouhiainen, L.; Jokela, J.; Fewer, D.; Urmann, M.; Sivonen, K. Two alternative starter modules for the Non-ribosomal biosynthesis of specific anabaenopeptin variants in *Anabaena* (cyanobacteria). *Chem. Biol.* **2010**, *17*, 265–273. [[CrossRef](#)]
116. Guljamow, A.; Kreische, M.; Ishida, K.; Liaimer, A.; Altermark, B.; Bähr, L.; Hertweck, C.; Ehwald, R.; Dittmann, E. High-density cultivation of terrestrial *Nostoc* strains leads to reprogramming of secondary metabolome. *Appl. Environ. Microbiol.* **2017**, *83*, 1–15. [[CrossRef](#)]
117. Shishido, T.; Jokela, J.; Fewer, D.; Wahlsten, M.; Fiore, M.; Sivonen, K. Simultaneous production of anabaenopeptins and namalides by the cyanobacterium *Nostoc* sp. CENA543. *ACS Chem. Biol.* **2017**, *12*, 2746–2755. [[CrossRef](#)]
118. Cheruku, P.; Plaza, A.; Lauro, G.; Keffer, J.; Lloyd, J.; Bifulco, G.; Bewley, C. Discovery and synthesis of namalide reveals a new anabaenopeptin scaffold and peptidase inhibitor. *J. Med. Chem.* **2012**, *55*, 735–742. [[CrossRef](#)]
119. Sanz, M.; Salinas, R.; Pinto, E. Namalides B and C and spumigins K-N from the cultured freshwater cyanobacterium *Sphaerospermopsis torques-reginae*. *J. Nat. Prod.* **2017**, *80*, 2492–2501. [[CrossRef](#)]

120. Murakami, M.; Suzuki, S.; Itou, Y.; Kodani, S.; Ishida, K. New anabaenopeptins, potent carboxypeptidase-A inhibitors from cyanobacterium *Aphanizomenon flos-aquae*. *J. Nat. Prod.* **2000**, *63*, 1280–1282. [[CrossRef](#)]
121. Harms, H.; Kurita, K.; Pan, L.; Wahome, P.; He, H.; Kinghorn, A.; Carter, G.; Linington, R. Discovery of anabaenopeptin 679 from freshwater algal bloom material: Insights into the structure-activity relationship of anabaenopeptin protease inhibitors. *Bioorg. Med. Chem. Lett.* **2016**, *26*, 4960–4965. [[CrossRef](#)]
122. Sano, T.; Usui, T.; Ueda, K.; Osada, H.; Kaya, K. Isolation of new protein phosphatase inhibitors from two cyanobacteria species, *Planktothrix* spp. *J. Nat. Prod.* **2001**, *64*, 1052–1055. [[CrossRef](#)]



© 2019 by the authors. Licensee MDPI, Basel, Switzerland. This article is an open access article distributed under the terms and conditions of the Creative Commons Attribution (CC BY) license (<http://creativecommons.org/licenses/by/4.0/>).

Supplementary Materials

Bioactive Peptides Produced by Cyanobacteria of the Genus *Nostoc*: a Review

Anna Fidor ¹, Robert Konkel ¹ and Hanna Mazur-Marzec ^{1,2,*}

¹ Division of Marine Biotechnology, Faculty of Oceanography and Geography, University of Gdańsk, Marszałka J. Piłsudskiego 46, PL-81378 Gdynia, Poland; anna.fidor@phdstud.ug.edu.pl (A.F.); robert.konkel@phdstud.ug.edu.pl (R.K.)

² Institute of Oceanology, Polish Academy of Sciences, Powstańców Warszawy 55, PL-81712 Sopot, Poland

* Correspondence: biohm@ug.edu.pl; Tel.: +48-58-5236621; Fax: 48-58-5236712

Table 1. Peptides produced by cyanobacteria of the genus *Nostoc* (MW molecular weight).

Peptide name	MW	Strain, habitat & place of isolation	References
Aeruginosin 865	864	<i>Nostoc</i> sp. Lukešova 30/93 Terrestrial: Forest soil, Krušné mountains, Czech Republic	38
Anabaenopeptin	807 808 827 841 843 857	<i>Nostoc</i> sp. CENA543 Saline/alkaline: Salina 67 Mil Lake, Brazil <i>Nostoc</i> sp. ASN_M Freshwater: Paddy fields, Golestan province, Iran <i>N. punctiforme</i> PCC73102 Terrestrial: Isolated from <i>Macrozamia</i> sp., Australia	117 30 115
Banyascyclamide A	537	<i>Nostoc</i> sp. TAU IL-235	37
Banyascyclamide B	521	Freshwater: Banyas stream, Jordan River, Israel	
Banyascyclamide C	555		
Banyaside A	992	<i>Nostoc</i> sp. TAU IL-235	123
Banyaside B	949	Freshwater: Banyas stream, Jordan River, Israel	
Banyasin A	713	<i>Nostoc</i> sp. TAU IL-235 Freshwater: Banyas stream, Jordan River, Israel	123
Cryptophycin-1 (A)	654	<i>Nostoc</i> sp. ATCC 53789	47
Cryptophycin-2(B)	620	Terrestrial: Lichen, Arron Island, Scotland	
Cryptophycin-3 (C)	638	<i>Nostoc</i> sp. GSV 224	36, 51
Cryptophycin-4 (D)	604	Terrestrial: India	
Cryptophycin-16	640		
Cryptophycin-17	624		
Cryptophycin-18	638		
Cryptophycin-19	624		
Cryptophycin-21	640		
Cryptophycin-23	674		
Cryptophycin-24	606		
Cryptophycin-26	638		
Cryptophycin-28	624		
Cryptophycin-29	624		
Cryptophycin-30	656		
Cryptophycin-31	688		
Cryptophycin-38	654		

Cryptophycin-40	640		
Cryptophycin-43	590		
Cryptophycin-45	658		
Cryptophycin-46	638		
Cryptophycin-49	624		
Cryptophycin-50	640		
Cryptophycin-54	654		
Cryptophycin-175	672		
Cryptophycin-176	626		
Cryptophycin-326	675		
Cryptophycin-327	655		
Cyanopeptolin 962	962	<i>N. edaphicum</i> CCNP 1411	27
Cyanopeptolin 969	969	Brackish water: Gulf of Gdańsk,	
Cyanopeptolin 978	978	Baltic Sea	
Cyanopeptolin 985	985		
Cyanopeptolin 990	990		
Cyanopeptolin 992	992		
Cyanopeptolin 999	999		
Cyanopeptolin 1006	1006		
Cyanopeptolin 1013	1013		
Cyanopeptolin 1018	1018		
Cyanopeptolin 1020	1020		
Cyanopeptolin 1027	1027		
Cyanopeptolin 1048	1048		
Cyanovirin-N	11013	<i>N. elliposporum</i>	24
Hassallidin 1	1295	<i>Nostoc</i> sp. CENA 219	124
Hassallidin 2	1293	Freshwater: Brazil	
Hassallidin 3	1279	<i>N. calcicula</i> 6 sf calc	125
Hassallidin 4	1279	Dobré Pole, Czech Republic	
Hassallidin 5	1277		
Hassallidin 7	1313		
Hassallidin 8	1269		
Hassallidin 10	1281		
Hassallidin 11	1297		
Hassallidin 12	1297		
Hassallidin 14	1297		
Hassallidin 15	1297		
Hassallidin 17	1263		
Hassallidin 19	1297		
Hassallidin 20	1263		
Hassallidin 22	1263		
Hassallidin 24	1265		
Hassallidin 26	1297		
Hassallidin 27	1263		
Insulapeptolide A	941	<i>N. insulare</i> SAG 54.79	113
Insulapeptolide B	955	Terrestrial: Soil	
Insulapeptolide C	955		
Insulapeptolide D	969		
Insulapeptolide E	1020		
Insulapeptolide F	1006		
Insulapeptolide G	991		
Insulapeptolide H	1005		

[MeAsp ³ , Adda ⁵ , Mdha ⁷] microcystin LA	908	<i>Nostoc</i> sp. BHU 001 Freshwater: Agricultural pond, India	126
[MeAsp ³ , Adda ⁵ , Mdha ⁷] microcystin AR	952	<i>Nostoc</i> sp. BHU 001 Freshwater: Agricultural pond, India	126
[Leu/Ile ² , Asp ³ , ADDA ⁵ , Mdha ⁷] microcystin	980	<i>Nostoc</i> sp. Treb K1/5 Pool no. 1 in the Collection of water a wetland plants, benthos Třeboň, Czech Republic	127
[MeAsp ³ , DMAdda ⁵ , Mdha ⁷] microcystin LR	980	<i>Nostoc</i> sp. IO-102-I Terrestrial: Isolated from lichen, Sysmä, Finland	106
		<i>Nostoc</i> sp. NR1 Freshwater: Nile River, Egypt	128
[MeAsp ³ , Adda ⁵ , Mdha ⁷] microcystin LR	995	<i>Nostoc</i> sp. BHU 001 Freshwater: Agricultural pond, India	126
[Asp ³ , ADMAdda ⁵ , Mdha ⁷] microcystin LR	1008	<i>Nostoc</i> sp. 152 Freshwater: Lake Säaskjärvi, Finland	88, 103
		<i>Nostoc</i> sp. IO-102-I Terrestrial: Isolated from lichen, Sysmä, Finland	106
[Asp ³ , ADMAdda ⁵ , Dhb ⁷] microcystin LR	1008	<i>Nostoc</i> sp. DUN 901 Brackish water: Lake, UK	104
		<i>Nostoc</i> sp. NR1 Freshwater: Nile River, Egypt	128
[MeAsp ³ , DMAdda ⁵ , Mdha ⁷] microcystin LR	1008	<i>Nostoc</i> sp. BHU 001 Freshwater: Agricultural pond, India	126
[MeAsp ³ , ADMAdda ⁵ , Mdhb ⁷] microcystin LR	1008	<i>Nostoc</i> sp. 152 Freshwater: Lake Säaskjärvi, Finland	103
[Asp ³ , Adda ⁵ , Mdha ⁷] microcystin FR	1014	<i>Nostoc</i> sp. Treb K1/5 Pool no. 1 in the Collection of water a wetland plants, benthos Třeboň, Czech Republic	127
[Asp ³ , ADMAdda ⁵ , Mdha ⁷] microcystin L-Har	1022	<i>Nostoc</i> sp. 152 Freshwater: Lake Säaskjärvi, Finland	103
[MeAsp ³ , ADMAdda ⁵ , Mdha ⁷] microcystin LR	1022	<i>Nostoc</i> sp. 152 Freshwater: Lake Säaskjärvi, Finland	88, 103
		<i>Nostoc</i> sp. IO-102-I Terrestrial: Isolated from lichen, Sysmä, Finland	106
[Asp ³ , Adda ⁵ , Mdha ⁷] microcystin YR	1030	<i>Nostoc</i> sp. Treb K1/5 Pool no. 1 in the Collection of water a wetland plants, benthos Třeboň, Czech Republic	127
[MeAsp ³ , Adda ⁵ , Dha ⁷] microcystin YR	1030	<i>Nostoc</i> sp. CENA88 Freshwater: Sao Paulo, Brazil	129
[MeAsp ³ , ADMAdda ⁵ , Mdha ⁷] microcystin L-Har	1036	<i>Nostoc</i> sp. 152 Freshwater: Lake Säaskjärvi, Finland	130
[MeAsp ³ , ADMAdda ⁵ , Mdha ⁷] microcystin XR	1036	<i>Nostoc</i> sp. IO-102-I Terrestrial: Isolated from lichen, Sysmä, Finland	106
[Asp ³ , ADMAdda ⁵ , Dhb ⁷] microcystin RR	1051	<i>Nostoc</i> sp. DUN 901 Brackish water: Lake, UK	104
[MeAsp ³ , Adda ⁵ , Mdha ⁷] microcystin WR	1067	<i>Nostoc</i> sp. BHU 001 Freshwater: Agricultural pond, India	126

[Asp ³ , ADMAdda ⁵ , Dhb ⁷] microcystin HtyR	1072	<i>Nostoc</i> sp. DUN 901 Brackish water: Lake, UK	104
[MeAsp ³ , ADMAdda ⁵ , Mdha ⁷] microcystin XR	1076	<i>Nostoc</i> sp. IO-102-I Terrestrial: Isolated from lichen, Sysmä, Finland	106
Microviridin G	1805	<i>N. minutum</i> NIES-26	100
Microviridin H	1837	Terrestrial: Ishigaki, Japan <i>N. punctiforme</i> PCC73102 Terrestrial: Isolated from <i>Macrozamia</i> sp., Australia	95
Muscoride A	512	<i>N. muscorum</i> IAM M-14 Freshwater	131
Namalide B	575	<i>Nostoc</i> sp. CENA 543	117
Namalide D	559	Saline/alkaline: Salina 67 Mil Lake, Brazil	
Namalide E	545		
Namalide F	545		
Nodularin	824	<i>Nostoc</i> sp. 65.1 Terrestrial: Cycad symbiont, Australia	109, 132
Nodularin L-Har	838	<i>Nostoc</i> sp. 73.1 Terrestrial: Cycad symbiont, Australia	
Nostamide A	841	<i>N. punctiforme</i> PCC73102 Terrestrial: Isolated from <i>Macrozamia</i> sp., Australia	115 117
Nostamide B	805	<i>Nostoc</i> sp. CENA543	
Nostamide C	777	Saline/alkaline: Salina 67 Mil Lake, Brazil	
Nostamide D	777		
Nostamide E	777		
Nostocyclamide A	490	<i>Nostoc</i> sp. 31	133, 134
Nostocyclamide M	506	Freshwater	
Nostocyclin A (1)	1116	<i>Nostoc</i> sp. DUN 901 Brackish water: Lake, UK	114
Nostocyclopeptide A1	756	<i>Nostoc</i> sp. ATCC 53789	62
Nostocyclopeptide A2	790	Terrestrial: Isolated from lichen, Arron Island, Scotland	
Nostocyclopeptide A3	804	<i>Nostoc</i> sp. ASN_M Freshwater: Paddy fields, Golestan province, Iran	30
Nostocyclopeptide M1	881	<i>Nostoc</i> sp. XSPORK 13A Seawater: Isolated from gastropod, Cape of Porkkala, Baltic Sea	63
Nostofungicide	1080	<i>N. commune</i> OK-1 Terrestrial: Okayama, Japan	40
Nostoginin BN 741	741	<i>Nostoc</i> sp. TAU IL-235	37
Nostoginin BN 578	578	Freshwater: Banyas, Jordan River, Israel	
Nostopeptolide A1	1080	<i>Nostoc</i> sp. GSV224	93
Nostopeptolide A2	1066	Terrestrial: India	
Nostopeptolide A3	1080	<i>Nostoc</i> sp. XPORK 5A	94
Nostopeptolide L1	1063	Seawater: Isolated from gastropod, Cape of Porkkala, Baltic Sea	
Nostopeptolide L2	1047	<i>Nostoc</i> sp. UK2aImI	94
Nostopeptolide L3	1049		
Nostopeptolide L4	1033	Terrestrial: Isolated from lichen	
Nostopeptin A	954	<i>N. minutum</i> Nies-26	112
Nostopeptin B	926	Terrestrial/Freshwater: Ishigaki, Japonia	

Nostopeptin BN 920	920	<i>Nostoc</i> sp. TAU IL-235 Freshwater: Banyas, Jordan River, Israel	37
Nostophyscin	888	<i>Nostoc</i> sp. 152 Freshwater: Sääksjärvi Lake, Finland	87, 92
Nostosin A	449	<i>Nostoc</i> sp. FSN	97
Nostosin B	451	Terrestrial/freshwater: Paddy fields, Golestan, Iran	
Nostoweipeptin W1	1214	<i>Nostoc</i> sp. XPORK 5A	94
Nostoweipeptin W2	1198	Brackish water: Gulf of Finland, Baltic Sea	
Nostoweipeptin W3	1198		
Nostoweipeptin W4	1200		
Nostoweipeptin W5	1200		
Nostoweipeptin W6	1200		
Nostoweipeptin W7	1172		
Schizopeptin 791	791	<i>Nostoc</i> sp. CENA543 Saline/alkaline: Salina 67 Mil Lake, Brazil	117
Tenuocyclamide A	459	<i>N. spongiaeforme</i> var. <i>tenue</i> TAU IL-184-6	135
Tenuocyclamide B	459	Terrestrial: Soil/Litophytic sample, Bet Dagan, Israel	
Tenuocyclamide C	505		
Tenuocyclamide D	521		

References

123. Ploutno, A.; Carmeli, S. Banyasin A and banyasides A and B, three novel modified peptides from a water bloom of the cyanobacterium *Nostoc* sp. *Tetrahedron* **2005**, *61*, 575–583.
124. Vestola, J.; Shishido, T.; Jokela, J.; Fewer, D.; Aitio, O.; Permi, P.; Wahlsten, M.; Wang, H.; Rouhiainen, L.; Sivonen, K. Hassallidins, antifungal glycolipopeptides, are widespread among cyanobacteria and are the end-product of a nonribosomal pathway. *Proc. Natl. Acad. Sci. USA* **2014**, *111*, 1909–1917.
125. Shishido, T.; Humisto, A.; Jokela, J.; Liu, L.; Wahlsten, M.; Tamrakar, A.; Fewer, D.; Permi, P.; Andreote, A.; Fiore, M.; et al. Antifungal compounds from cyanobacteria. *Mar. Drugs* **2015**, *13*, 2124–2140.
126. Bajpai, R.; Sharma, N.; Lawton, L.; Edwards, C.; Rai, A. Microcystin producing cyanobacterium *Nostoc* sp. BHU001 from a pond in India. *Toxicon* **2009**, *53*, 587–590.
127. Kust, A.; Urajová, P.; Hrouzek, P.; Vu, D.; Čapková, K.; Štenclová, L.; Řeháková, K.; Kozlíková-Zapomělová, E.; Lepšová-Skácelová, O.; Lukešová, A.; et al. A new microcystin producing *Nostoc* strain discovered in broad toxicological screening of non-planktic Nostocaceae (cyanobacteria). *Toxicon* **2018**, *150*, 66–73.
128. Abu-Serie, M.; Nasser, N.; El-Wahab, A.; Shehawy, R.; Pienaar, H.; Baddour, N.; Amer, R. In vivo assessment of the hepatotoxicity of a new *Nostoc* isolate from the Nile River: *Nostoc* sp. strain NR1. *Toxicon* **2018**, *143*, 81–89.
129. Genuário, D.; Silva-Stenico, M.; Welker, M.; Moraes, L.; Fiore, M. Characterization of microcystin and detection of microcystin synthetase genes from a Brazilian isolate of *Nostoc*. *Toxicon* **2010**, *55*, 846–854.
130. Sivonen, K.; Namikoshi, M.; Evans, W.; Färdig, M.; Carmichael, W.; Rinehart, K. Three new microcystins, cyclic heptapeptide hepatotoxins, from *Nostoc* sp. strain 152. *Chem. Res. Toxicol.* **1992**, *5*, 464–469.
131. Nagatsu, A.; Kajitani, H.; Sakakibara, J. Muscoride A: A new oxazole peptide alkaloid from freshwater cyanobacterium *Nostoc muscorum*. *Tetrahedron Lett.* **1995**, *36*, 4097–4100.
132. Gehringer, M.; Pengelly, J.; Cuddy, W.; Fieker, C.; Forster, P.; Neilan, B. Host selection of symbiotic cyanobacteria in 31 species of the Australian cycad genus: *Macrozamia* (Zamiaceae). *Mol. Plant. Microbe Interact.* **2010**, *23*, 811–822.

133. Todorova, A.; Jüttner, F. Nostocyclamide: A new macrocyclic, thiazole-containing allelochemical from *Nostoc* sp. 31 (cyanobacteria). *J. Org. Chem.* **1995**, *60*, 7891–7895.
134. Jüttner, F.; Todorova, A.; Walch, N.; von Philipsborn, W. Nostocyclamide M: A cyanobacterial cyclic peptide with allelopathic activity from *Nostoc* sp. 31. *Phytochem.* **2001**, *57*, 613–619.
135. Banker, R.; Carmeli, S. Tenuocyclamide A-D, cyclic hexapeptides from the cyanobacterium *Nostoc spongiaeforme* var. *tenuis*. *J. Nat. Prod.* **1998**, *61*, 1248–1251.

Statement of Co-Authorship

I, the undersigned, acknowledge the above contribution of work undertaken for the published work "Bioactive peptides produced by Cyanobacteria of the genus *Nostoc*: a review" (*Marine Drugs*, 2019, DOI:10.3390/md17100561) contributing to the dissertation "Peptides produced by Baltic cyanobacterium *Nostoc edaphicum* CCNP1411 - structure and biological activity".

All authors were equally involved in planning, discussing and writing the article.

.....
(Anna Fidor)

Statement of Co-Authorship

I, the undersigned, acknowledge the above contribution of work undertaken for the published work "Bioactive peptides produced by Cyanobacteria of the genus *Nostoc*: a review" (*Marine Drugs*, 2019, DOI:10.3390/md17100561) contributing to the dissertation "Peptides produced by Baltic cyanobacterium *Nostoc edaphicum* CCNP1411 - structure and biological activity".

All authors were equally involved in planning, discussing and writing the article.


.....
(Hanna Mazur-Marzec)

Statement of Co-Authorship

All authors were equally involved in planning, discussing and writing the article.

I, the undersigned, acknowledge the above contribution of work undertaken for the published work "Bioactive peptides produced by Cyanobacteria of the genus *Nostoc*: a review" (*Marine Drugs*, 2019, DOI:10.3390/md17100561) contributing to the dissertation "Peptides produced by Baltic cyanobacterium *Nostoc edaphicum* CCNP1411 - structure and biological activity".

The assessment of my and PhD candidate (Anna Fidor) contribution to the work is 33 % and 33 %.





.....
(Robert Konkel)

Publication 2



Article

Cyanopeptolins with Trypsin and Chymotrypsin Inhibitory Activity from the Cyanobacterium *Nostoc edaphicum* CCNP1411

Hanna Mazur-Marzec ^{1,2,*} , Anna Fidor ¹, Marta Cegłowska ², Ewa Wieczerek ³,
Magdalena Kropidłowska ³, Marie Goua ⁴ , Jenny Macaskill ⁴  and Christine Edwards ⁴

¹ Division of Marine Biotechnology, Faculty of Oceanography and Geography, University of Gdańsk, Marszałka J. Piłsudskiego 46, PL-81378 Gdynia, Poland; anna.fidor77@gmail.com

² Institute of Oceanology, Polish Academy of Sciences, Powstańców Warszawy 55, PL-81712 Sopot, Poland; mceglowska@iopan.pl

³ Department of Biomedical Chemistry, Faculty of Chemistry, University of Gdańsk, Wita Stwosza 63, PL-80308 Gdańsk, Poland; ewa.wieczerek@ug.edu.pl (E.W.); magdalena.kropidlowska@phdstud.ug.edu.pl (M.K.)

⁴ School of Pharmacy and Life Sciences, Robert Gordon University, Aberdeen AB10 7GJ, UK; m.goua@rgu.ac.uk (M.G.); j.s.macaskill@rgu.ac.uk (J.M.); c.edwards@rgu.ac.uk (C.E.)

* Correspondence: biohm@ug.edu.pl; Tel.: +48-58-5236621; Fax: 48-58-5236712

Received: 5 June 2018; Accepted: 20 June 2018; Published: 26 June 2018



Abstract: Cyanopeptolins (CPs) are one of the most frequently occurring cyanobacterial peptides, many of which are inhibitors of serine proteases. Some CP variants are also acutely toxic to aquatic organisms, especially small crustaceans. In this study, thirteen CPs, including twelve new variants, were detected in the cyanobacterium *Nostoc edaphicum* CCNP1411 isolated from the Gulf of Gdańsk (southern Baltic Sea). Structural elucidation was performed by tandem mass spectrometry with verification by NMR for CP962 and CP985. Trypsin and chymotrypsin inhibition assays confirmed the significance of the residue adjacent to 3-amino-6-hydroxy-2-piperidone (Ahp) for the activity of the peptides. Arginine-containing CPs (CPs-Arg²) inhibited trypsin at low IC₅₀ values (0.24–0.26 μM) and showed mild activity against chymotrypsin (IC₅₀ 3.1–3.8 μM), while tyrosine-containing CPs (CPs-Tyr²) were selectively and potently active against chymotrypsin (IC₅₀ 0.26 μM). No degradation of the peptides was observed during the enzyme assays. Neither of the CPs were active against thrombin, elastase or protein phosphatase 1. Two CPs (CP962 and CP985) had no cytotoxic effects on MCF-7 breast cancer cells. Strong and selective activity of the new cyanopeptolin variants makes them potential candidates for the development of drugs against metabolic disorders and other diseases.

Keywords: cyanobacteria; *Nostoc*; cyanopeptolins; protease inhibitors

1. Introduction

Cyanobacterial peptides belong to the most interesting group of natural bioactive products. Initially, they were recognized as hepatotoxic and inflammatory agents. In the late 1970s, the therapeutic potential of the compounds attracted the attention of the scientific community [1,2]. Since then, numerous and structurally diverse cyanopeptides have been identified, including potent anticancer agents such as dolastatin 10, cryptophycin 52, largazole, and apratoxin [3–7]. Cyanopeptides have also been recognized as potent inhibitors of key metabolic enzymes, targeting mainly serine proteases and protein phosphatases [7–9]. Among these compounds, cyanopeptolins (CPs), a large family of cyclic depsipeptides (peptidolactones), are commonly produced by different cyanobacterial genera, including *Microcystis*, *Planktothrix*, *Anabaena* and *Nostoc*. These nonribosomal peptides (NRPs) are composed

of a six-amino acid ring and a side chain with one or two residues. All CPs are characterized by the presence of 3-amino-6-hydroxy-2-piperidone (Ahp) in position 3 (Figures 1 and 2). In a few CP-type peptides, the occurrence of *O*-methylated Ahp (Amp) in this position has been reported [10–12]. Ahp is also present in other cyclodepsipeptides such as aeruginopeptins, micropeptins, microcystilide, nostopeptins, and oscillapeptins. Position 1 in CP-type peptides is conserved and occupied by *L*-threonine with β -hydroxy group linked by an ester bond to carboxy terminus of amino acid in position 6 (i.e., Val, Ile or *allo*-Ile). Position 2 is most variable and occupied by residues differing in structure and polarity (e.g., Arg, Leu, Gln, Tyr, Phe, MeTyr, H₄Tyr, Dhb) [13]. In position 4, Leu/Ile, Phe or Thr can be found, while in position 5, *N*-methylated aromatic amino acids, *N*-MeTyr or MePhe, or their homo-variants are usually present. In some CPs, Tyr or *N*-MeTyr were modified by chlorination [14]. The side chain is attached via the amino group on Thr. Usually, two major types of side chains were reported: with 1–2 amino acid residues (e.g., Asp, Glu) and aliphatic fatty acid of variable length or with glyceric acid directly linked to Thr or to an amino acid side chain [15–17]. Glyceric acid can be modified by sulfation or/and *O*-methylation [11,18]. In the side chain of aeruginopeptins, micropeptins or microcystilide, a hydroxyphenyl lactic acid (Hpla) was reported [19–21].

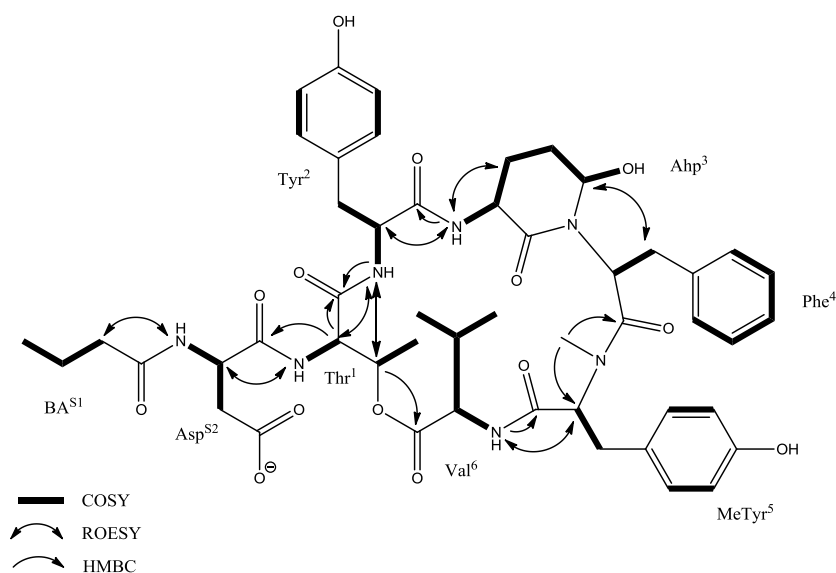


Figure 1. COSY, ROESY, and HMBC correlations in cyanopeptolin CP985.

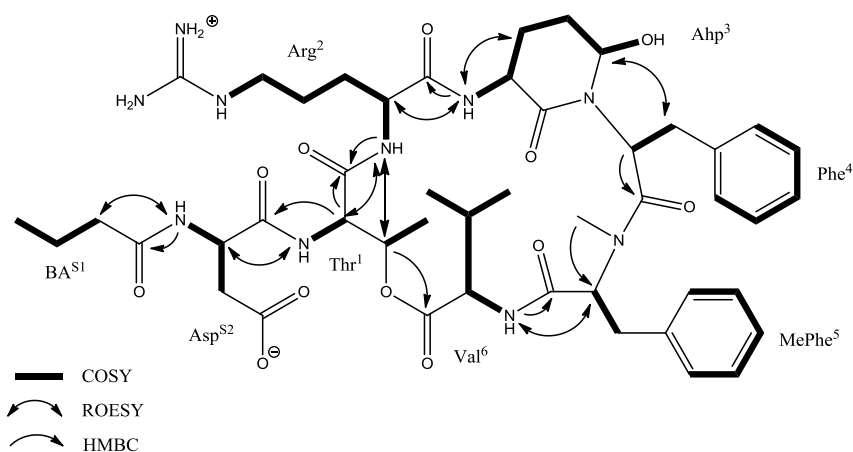


Figure 2. Key COSY, ROESY, and HMBC correlations in cyanopeptolin CP962.

Cyanopeptolins, like other nonribosomal peptides, are synthesized on large multi-enzyme complexes with modular structure. The general organization of the gene clusters encoding the enzymes in different cyanobacteria is similar, however, some differences in the specificity of adenylation domains and in the presence of tailoring domains exist [22–24]. In the CP gene cluster from *Microcystis* and *Anabaena*, a halogenase gene was present [23,24], whereas in *Planktothrix* a glyceric acid-activating domain and sulfotransferase domain occurred [22]. The modifications in gene clusters and differences in substrate specificity of adenylation domains result in intra- and interspecies diversity of CP structures.

The majority of CPs showed inhibitory activity against serine proteases, such as trypsin, chymotrypsin, thrombin, and elastase (e.g., [12,25–30]). Cyanopeptolins with one (CP S) or two sulphate groups (CP SS) also inhibited plasmin [18]. The activity of the peptides was found to be determined by the residue in position 2, however, the significance of other structural elements was also reported [12]. In ichthyopeptins, CP analogues with 2-hydroxy-3-(4'-hydroxyphenyl)lactic acid (PAA) in the side chain, strong antiviral activity against influenza A virus was observed [31]. Tests on small crustaceans revealed the harmful effects of Ahp-containing cyclic depsipeptides [16,32,33]. For CP SS, the toxicity against *Daphnia magna* was even higher than for microcystin-LR [10], the most widely studied cyanobacterial toxin.

In cyanobacterial strains from the *Nostoc* genus, typical CP variants produced by *Microcystis* have not been reported. However, several other CP-type structures, namely nostopeptins, insulapeptolides, and nostocyclins were identified (Table 1) [34–38]. Nostopeptin A and B from *N. minutum* NIES-26, with 3-hydroxy-4-methylproline (Hmp) in position 1, showed inhibitory activity against elastase and chymotrypsin, but were inactive against papain, trypsin, thrombin, and plasmin [35]. Insulapeptolides A–D from *N. insulare* are characterized by the presence of Hmp in position 1 and citrulline (Cit) in the side chain. Extracts containing these peptides potently and selectively inhibited human leukocyte elastase (HLE) [38]. Nostocyclin from *Nostoc* sp. DUN901 has D-Hpla in the side chain and two homoserine residues (Hse): one in a ring part and one in a side chain of the molecule [34]. The peptide was not toxic in mouse bioassay, but showed weak activity against protein phosphatases [34,39].

Among cyanobacterial strains from the same species, significant differences in the peptide profiles are frequently reported. In our study, the structures of CPs produced by *N. edaphicum* CCNP1411 isolated from coastal waters of the Gulf of Gdańsk, southern Baltic Sea, were elucidated. In total, thirteen CP variants were identified. They represent structures typical of CPs from *Microcystis*, but different from CP-type peptides previously found in other *Nostoc* strains. The biological activity of the peptides against serine proteases, protein phosphatase 1, and MCF-7 breast cancer cells were assessed.

Table 1. Cyanopeptolin-type peptides identified in cyanobacteria from *Nostoc* genus.

Molecular Mass	Peptide Name	Structure	Enzyme Inhibition	References
921	Nostopeptin BN920	[Thr+Leu+Ahp ¹ +Phe+MeTyr+Val]Gln+Ac ²	Chymotrypsin (IC ₅₀ 0.11 µM)	[36]
926	Nostopeptin B	[Hmp ³ +Leu+Ahp+Ile+MeTyr+Ile]Gln+Ac	Elastase (IC ₅₀ 11.0 µg/mL) Chymotrypsin (IC ₅₀ 1.6 µg/mL)	[35]
937	Nostopeptin A	[Hmp+Leu+Ahp+Ile+MeTyr+Ile]Gln+BA ⁴	Elastase (IC ₅₀ 1.3 µg/mL) Chymotrypsin (IC ₅₀ 1.4 µg/mL)	[35]
942	Insulapeptolide A	[Hmp+Leu+Ahp+Ile+MeTyr+Val]Cit ⁵ +Ac	HLE ¹⁰ (IC ₅₀ 0.14 µM) *	[38]
956	Insulapeptolide B	[Hmp+Leu+Ahp+Leu+MeTyr+Ile]Cit+Ac	HLE (IC ₅₀ 0.10 µM) *	
956	Insulapeptolide C	[Hmp+Leu+Ahp+Ile+diMeTyr ⁶ +Val]Cit+Ac	HLE (IC ₅₀ 0.090 µM) *	
970	Insulapeptolide D	[Hmp+Leu+Ahp+Ile+diMeTyr+Ile]Cit+Ac	HLE (IC ₅₀ 0.085 µM) *	
991	Insulapeptolide G	[Thr+Hph ⁷ +Ahp+Thr+MePhe+Val]Ser+Pro+BA	HLE (IC ₅₀ 3.5 µM) *	
1005	Insulapeptolide H	[Thr+Hph+Ahp+Thr+MeTyr+Ile]Ser+Pro+BA	HLE (IC ₅₀ 2.7µM) *	
1007	Insulapeptolide F	[Thr+Hph+Ahp+Thr+MeTyr+Val]Ser+Pro+BA	HLE (IC ₅₀ 1.6 µM) *	
1021	Insulapeptolide E	[Thr+Hph+Ahp+Thr+MeTyr+Ile]Ser+Pro+BA	HLE (IC ₅₀ 3.2 µM) *	
1116	Nostocyclin	[Thr+Hse ⁸ +Ahp+Phe+MeTyr+Val]Hse+Ile+Hpla ⁹	PP1 (IC ₅₀ 64.0 µM)	

* activity of extracts; ¹ Ahp 3-amino-6-hydroxy-2-piperidone; ² Ac acetic acid; ³ Hmp 3-hydroxy-4-methyl-proline; ⁴ BA butanoic acid; ⁵ Cit citrulline; ⁶ diMeTyr *N,O*-dimethyltyrosine; ⁷ Hph homophenylalanine; ⁸ Hse homoserine; ⁹ Hpla *p*-hydroxyphenyllactic acid; ¹⁰ HLE human leukocyte elastase.

2. Results

2.1. LC-MS/MS Analysis of Cyanopeptolins

Fractionation of *N. edaphicum* CCNP1411 crude extract (Figure S1) resulted in isolation of thirteen CPs. Structures were identified using a quadrupole/time of flight mass spectrometer and a triple quadrupole/linear ion trap mass spectrometer (Table 2). Structural elucidation of the peptides was based on fragmentation spectra with diagnostic ions, including immonium ions and a series of other fragment ions associated with specific residues. Depending on the residue in position 2, two types of spectra were obtained. Arg²-containing CPs (CPs-Arg²), gave pseudomolecular ions $[M + H]^+$ at m/z 1049, 1021, 1019, 1007, 979, 993, 991, and 963. The Tyr²-containing peptides (CPs-Tyr²) were detected as dehydrated protonated molecules $[M + H - H_2O]^+$ at m/z 1010, 996, 982, 968, and 952, and the Tyr-immonium ion (m/z 136) was always present in their spectra. The putative planar structures of CPs detected in *N. edaphicum* CCNP1411 and their fragmentation spectra are presented in Figures 1–4 and in supplementary information (Figures S2–S12). Amino acids at positions 1, 3, 4, 6, and 7 were found to be conserved and occupied by Thr¹, Ahp³, Phe⁴, Val⁶, and Asp⁷, respectively. The ion peak corresponding to the longest sequence of residues common to all CP variants was observed in the spectra at m/z 297 $[Asp + Thr + Val + H - H_2O]^+$ or/and at m/z 269 $[Asp + Thr + Val + H - H_2O - CO]^+$. The presence of butanoic acid (BA), hexanoic acid (HA), or octanoic acid (OA) in the side chain was mainly indicated by ion peaks formed by the cleavage of the corresponding fatty acid group (FA) and the exocyclic aspartic acid (Figures 3 and 4; Figures S2–S12). As this cleavage produced a stable cyclic part of the molecule, the ions $[M + H - (H_2O) - (FA + Asp)]^+$ usually belonged to the most abundant ones. The residue in position 5 (i.e., *N*-MePhe, *N*-MeTyr or *N*-MeHty) was identified based on immonium ion peaks at m/z 134, 150 or 164, respectively, and peaks at m/z 404, 420, and 434 corresponding to $[Ahp + Phe + (MePhe/MeTyr/MeHty) + H - H_2O]^+$. Ion peak at m/z 120, as well as peaks at 243 $[Ahp + Phe + H - H_2O]^+$ and 215 $[Ahp + Phe + H - H_2O - CO]^+$ confirmed the presence of Phe in position 4.

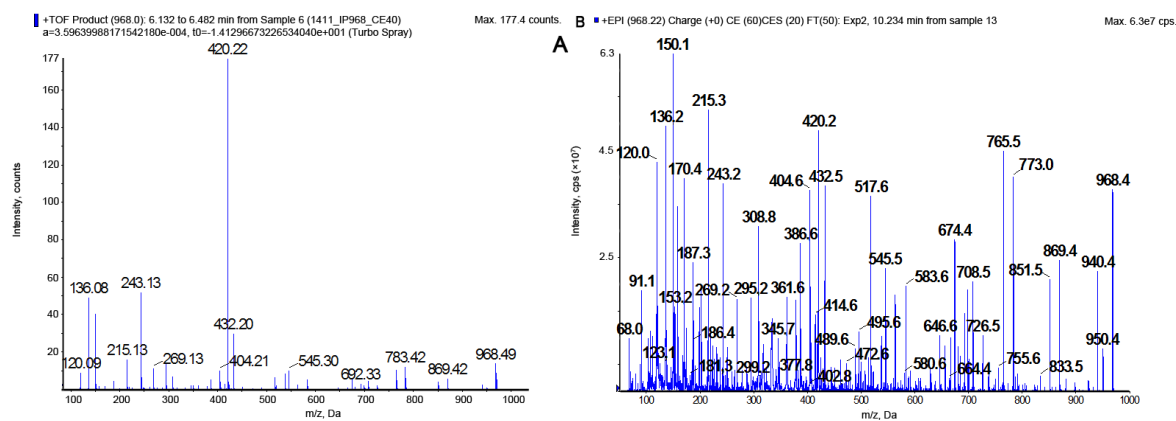


Figure 3. The product ion mass spectra of CP985 $[Thr+Tyr+Ahp+Phe+MeTyr+Val]Asp+BA$ with precursor ion $[M + H - H_2O]$ at m/z 968. The spectra were recorded with application of a hybrid quadrupole/time-of-flight mass spectrometer (QTOF) (A) and a hybrid triple quadrupole/linear ion trap mass spectrometer (QTRAP) (B). The mass signals were assigned to the following fragments: 950 $[M + H - 2H_2O]^+$, 869 $[M + H - Val - H_2O]^+$, 851 $[M + H - Val - 2H_2O]^+$, 773 $[M + 2H - (BA+Asp) - CO]^+$, 765 $[M + 2H - (BA + Asp) - 2H_2O]^+$, 692 $[M + H - (Val + MeTyr) - H_2O]^+$, 674 $[M+H-(Val+MeTyr)-2H_2O]^+$, 646 $[M + H - (Val + MeTyr) - 2H_2O - CO]^+$, 432 $[M + H - (Val + MeTyr + Phe + Ahp) - H_2O]^+$, 420 $[Ahp + Phe + MeTyr + H - H_2O]^+$, 404 $[M + H - (Val + MeTyr + Phe + Ahp) - H_2O - CO]^+$, 386 $[BA + Asp + Thr + Val + H]^+$, 308 $[Phe(-N) + MeTyr + H]^+$, 297 $[Asp + Thr + Val + H - H_2O - CO]^+$, 243 $[Ahp + Phe + H - H_2O]^+$, 215 $[Ahp + Phe + H - H_2O - CO]^+$, 150 MeTyr immonium ion, 136 Tyr immonium ion, 120 Phe immonium ion.

Table 2. Cyanopeptolins identified in *Nostoc edaphicum* CCNP 1411. The activities of the peptides were assessed in serine proteases (trypsin, chymotrypsin, elastase, and thrombin) and protein phosphatases 1 (PP 1) inhibition assays (- not active; */** small/medium activity; *m/z* of precursor ions: [M + H]⁺ for CPs-Arg² and [M + H – H₂O]⁺ for CPs-Tyr²).

Cyanopeptolin CP	<i>m/z</i>	Structure	Enzyme Inhibition (IC ₅₀ [μM])				
			Chymotrypsin	Trypsin	Elastase	Thrombin	Protein Phosphatase 1
CP 1048	1049	[Thr+Arg+Ahp+Phe+MeHty+Val]Asp+OA	*	**	-	-	-
CP 1020	1021	[Thr+Arg+Ahp+Phe+MeHty+Val Asp+HA	3.1	0.25	-	-	-
CP 1018	1019	[Thr+Arg+Ahp+Phe+MePhe+Val]Asp+ OA	-	0.24	-	-	-
CP 1006	1007	[Thr+Arg+Ahp+Phe+MeTyr+Val]Asp+HA	*	**	-	-	-
CP 992	993	[Thr+Arg+Ahp+Phe+MeHty+Val]Asp+BA	3.5	0.24	-	-	-
CP 990	991	[Thr+Arg+Ahp+Phe+MePhe+Val]Asp+HA	-	**	-	-	-
CP 978	979	[Thr+Arg+Ahp+Phe+MeTyr+Val]Asp+BA	3.8	0.26	-	-	-
CP 962	963	[Thr+Arg+Ahp+Phe+MePhe+Val]Asp+BA	-	**	-	-	-
CP 1027	1010	[Thr+Tyr+Ahp+Phe+MeHty+Val]Asp+HA	0.26	-	-	-	-
CP 1013	996	[Thr+Tyr+Ahp+Phe+MeTyr+Val]Asp+HA	**	-	-	-	-
CP 999	982	[Thr+Tyr+Ahp+Phe+MeHty+Val]Asp+BA	**	-	-	-	-
CP 985	968	[Thr+Tyr+Ahp+Phe+MeTyr+Val]Asp+BA	0.26	-	-	-	-
CP 969	952	[Thr+Tyr+Ahp+Phe+MePhe+Val]Asp+BA	**	-	-	-	-

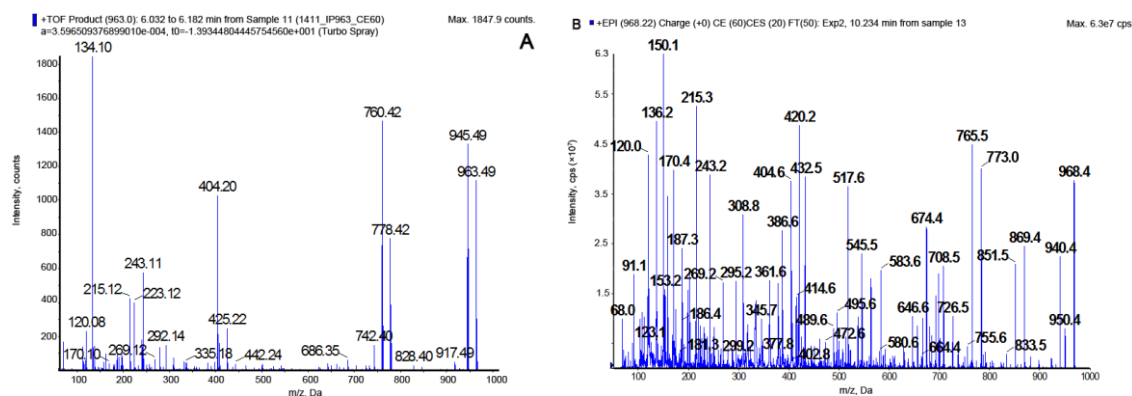


Figure 4. The product ion mass spectra of CP962 [Thr+Arg+Ahp+Phe+MePhe+Val]Asp+BA with precursor ion $[M + H]^+$ at m/z 963. The spectra were recorded with application of a hybrid quadrupole/time-of-flight mass spectrometer (QTOF) (A) and a hybrid triple quadrupole/linear ion trap mass spectrometer (QTRAP) (B). The mass signals were assigned to the following fragments: 945 $[M + H - H_2O]^+$, 917 $[M + H - H_2O - CO]^+$, 846 $[M + H - Val - H_2O]^+$, 828 $[M + H - Val - 2H_2O]^+$, 778 $[M + 2H - (BA + Asp)]^+$, 760 $[M + 2H - (BA + Asp) - H_2O]^+$, 742 $[M + 2H - (BA + Asp) - 2H_2O]^+$, 685 $[M + H - (Val + MePhe) - H_2O]^+$, 425 $[BA + Asp + Thr + Arg + H - H_2O]^+$, 404 $[Ahp + Phe + MePhe + H - H_2O]^+$, 297 $[Asp + Thr + Val + H - H_2O]^+$, 243 $[Ahp + Phe + H - H_2O]^+$, 215 $[Ahp + Phe + H - H_2O - CO]^+$, 134 MePhe immonium ion, 120 Phe immonium ion, 70-Arg.

2.2. NMR Analysis

In order to confirm the structures, two CPs (i.e., CP962 and CP985) were purified in sufficient quantities for NMR spectroscopy. For both compounds the 1H -NMR spectra displayed the typical pattern of a peptide (i.e., doublet amide protons (δ_H 6.95–8.51 ppm) and a single amide methyl group (δ_H 2.71 ppm for CP985 and 2.84 ppm for CP962). The COSY, TOCSY, and HMBC experiments allowed assignment of NMR spin systems to Asp, Thr, Tyr, Ahp (3-amino-6-hydroxypiperid-2-one), Phe, MeTyr (*N*-methyl tyrosine), Val, and butanoic acid (BA) in the case of cyanopeptolin CP985 (Table 3, Figures S13–S18b). The presence of aromatic amino acid residues was recognized by the signals occurring in the aromatic region of the spectrum (δ_H 6.5–7.5 ppm). The AA'BB' spin systems between two sets of tyrosine (Tyr-H2'/6' and Tyr-H3'/5', $J_{H,H} = 8.4$ Hz) and *N*-methyl tyrosine aromatic protons (MeTyr-H2'/6' and MeTyr-H3'/5', $J_{H,H} = 8.4$ Hz) indicated the presence of two *para*-di-substituted phenyl rings. The 1H - ^{13}C long range correlation from MeTyr-NH-CH₃ group (δ_H 2.71 ppm) to the MeTyr-C2 atom (δ_C 61.3 ppm) revealed the presence of *N*-methyl tyrosine residue. Phenylalanine was found to be the third aromatic amino acid residue based on the COSY interaction between Phe-H2'/6', Phe-H3'/5', and Phe-H4', and the HMBC correlation from two diastereotopic methylene protons Phe-3a (δ_H 2.88 ppm) and Phe-3b (δ_H 1.81 ppm) to the aromatic Phe-C2'/6' carbons. The presence of Asp, Val, and Thr was confirmed by their characteristic spin systems in the COSY spectrum (Figure S17b). The macrocyclic ring closure between threonine and valine was verified by HMBC correlation between Thr-H3 (δ_H 5.36 ppm) and Val-C1 (δ_C 172.4 ppm) (Figure S15b). The presence of Ahp residue was detected by the characteristic signal of the OH proton (δ_H 5.99 ppm) and a broad singlet (δ_H 5.06 ppm) derived from H5 proton (Figure S13). The HMBC correlations from Ahp-C1 to Ahp-H5 and Ahp-H2 confirmed the cyclic nature of this residue.

The COSY, TOCSY, and HMBC data allowed identification of amino acid residues in CP CP962 as Asp, Thr, Arg, Ahp, Phe, MePhe (*N*-methyl phenylalanine), Val, and BA, analogously to CP985 (Table 4, Figures S19–S24b). Two aromatic residues were found: phenylalanine and *N*-methyl phenylalanine. The occurrence of *N*-methyl group was established by the 1H - ^{13}C long range correlation from MePhe-NH-CH₃ group (δ_H 2.84 ppm) to the MePhe-C2 atom. The typical ^{13}C chemical shift of the guanidine quaternary carbon (δ_C 158.7 ppm) indicated the presence of Arg whose complete spin system was assigned based on TOCSY and COSY interactions (Figure S23b). The diagnostic

regions of the TOCSY, ROESY and HMBC spectra of both cyanopeptolins analyzed are presented in corresponding figures in Supplementary.

Table 3. NMR Spectroscopic data (700 MHz, DMSO-*d*₆) for cyanopeptolin CP985 [Thr+Tyr+Ahp+Phe+MeTyr+Val]Asp+BA.

Unit	Position	δ_C	δ_H (J in Hz)	ROESY	HMBC ^a		
BA	1	172.9, C	2.11, m	Asp-NH	BA-1, BA-3, BA-4 BA-1, BA-2, BA-4 BA-2		
	2	37.7, CH ₂	1.56, m				
	3	19.2, CH ₂	0.89, t (7.2, 7.2)				
	4	14.2, CH ₃					
Asp	1	171.7, C	4.58, dd (8.0, 5.0)	Thr-NH	Asp-4		
	2						
	3a					49.9, CH	2.65, m
	3b					36.1, CH ₂	2.46, m
	4					172.4, C	8.26, m
NH							
Thr ¹	1	168.9, C	4.52, d (10.0)	Tyr-NH Tyr-NH Asp-2	Thr-1, Asp-1 Val-1 Thr-2, Thr-3		
	2	54.7, CH	5.36, q (6.8, 6.9, 6.8)				
	3	72.6, CH	1.16, d (7.2)				
	4	18.0, CH ₃	7.52, d (9.3)				
	NH						
Tyr ²	1	169.9, C	4.31, m	Ahp-NH Thr-2, Thr-3	Tyr-2, Tyr-1' Tyr-1' Tyr-4' Thr-1		
	2						
	3a					54.2, CH	3.11, m
	3b					35.5, CH ₂	2.55, m
	1'					128.5, C	6.89, d (8.4)
	2'/6'					130.1, CH	6.58, d (8.4)
	3'/5'					115.5, CH	8.46, d (8.8)
	4'					156.1, C	
NH							
Ahp ³	1	169.0, C	3.62, m	Ahp-NH Phe-3a, Phe-3b Tyr-2, Ahp-3	Ahp-1, Ahp-3 Ahp-2 Ahp-1 Tyr-1		
	2						
	3					49.4, CH	2.41, m
	4					22.0, CH ₂	1.64, m
	5					21.9, CH ₂	5.06, brs
	NH					74.1, CH	7.06, d (8.8)
	OH						5.99, d (3.1)
Phe ⁴	1	170.8, C	4.76, dd (7.1, 4.6)	Ahp-5	Phe-2, Phe-1', Phe-2'/6' Phe-3a, Phe-3b, Phe-4' Phe-1' Phe C2'/6'		
	2						
	3a					50.7, CH	2.88, t (12.9, 12.9)
	3b					35.8, CH ₂	1.81, dd (10.4, 3.9)
	1'					137.2, C	6.84, d (7.0)
	2'/6'					129.9, CH	7.19, t (7.3, 7.3)
	3'/5'					128.2, CH	7.14, d (7.0)
	4'					126.7, CH	
MeTyr ⁵	1	169.4, C	4.89, dd (8.9, 2.5)	Val-NH	MeTyr-1' MeTyr-1', MeTyr-3'/5' MeTyr-2'/6', MeTyr-4' MeTyr-2, Phe-1 MeTyr-3'/5', MeTyr-4'		
	2						
	3					61.3, CH	3.10, m
	1'					33.3, CH ₂	7.00, d (8.4)
	2'/6'					128.2, C	6.78, d (8.4)
	3'/5'					130.9, CH	2.71, s
	4'					115.5, CH	9.33, s
	NCH ₃					156.7, C	
	OH					33.3, CH ₃	
Val ⁶	1	172.4, C	4.63, dd (4.9, 4.6)	MeTyr-2	Val-2, Val-3, Val-5 Val-2, Val-3, Val-4 MeTyr-1		
	2						
	3					56.3, CH	2.02, m
	4					31.4, CH	0.84, d (6.6)
	5					19.7, CH ₃	0.71, d (6.6)
	NH					17.7, CH ₃	7.39, d (9.7)

^a HMBC correlations are given from proton(s) stated to the indicated carbon atom.

Table 4. NMR Spectroscopic data (700 MHz, DMSO-d₆) for cyanopeptolin CPL962 [Thr+Arg+Ahp+Phe+MePhe+Val]Asp+BA.

Unit	Position	δ_C	δ_H (J in Hz)	ROESY	HMBC ^a
BA	1	172.2, C	2.08, m	Asp-NH	BA-1, BA-3, BA-4 BA-1, BA-2, BA-4 BA-2
	2	37.4, CH ₂	1.52, m		
	3	19.3, CH ₂	0.87, t (7.4, 7.4)		
	4	14.1, CH ₃			
Asp	1	173.7, C	4.54, m	Thr-NH	Asp-2, Asp-4 BA-1
	2	50.8, CH	2.51, m		
	3a	40.1, CH ₂	2.12, m		
	3b	175.3, C	8.00, d (8.0)		
	4				
NH					
Thr¹	1	169.9, C	4.58, d (9.0)	Arg-NH Arg-NH Asp-2	Thr-1 Thr-4, Val-1 Thr-2, Thr-3
	2	55.0, CH	5.30, q (6.8, 6.5, 6.8)		
	3	72.3, CH	1.15, d (6.5)		
	4	17.9, CH ₃	7.23, d (7.6)		
	NH				
Arg²	1	170.4, C	4.15, m	Ahp-NH Thr-2, Thr-3	Thr-1
	2	49.0, CH	1.88, m		
	3	26.4, CH ₂	1.46, m		
	4	24.5, CH ₂	2.95, m		
	5	39.8, CH ₂	8.5, d (8.7)		
	6	158.7, C			
NH					
Ahp³	1	169.6, C	3.65, m	Phe-3a, Phe-3b Arg-2, Ahp-3	Ahp-1, Ahp-3 Ahp-1 Arg-1
	2	48.6, CH	2.43, m		
	3	21.7, CH ₂	1.68, m		
	4	22.0, CH ₂	5.03, brs		
	5	74.2, CH	6.95, d (9.7)		
	NH		6.01, d (2.6)		
OH					
Phe⁴	1	170.0, C	4.74, dd (7.2, 3.5)	Ahp-5	Phe-1, Phe-3a, Phe-3b Phe-1' Phe-3a, Phe-3b, Phe-4' Phe-1' Phe-3'/5'
	2	50.6, CH			
	3a	35.6, CH ₂	2.86, m		
	3b	137.1, C	1.69, m		
	1'	129.8, CH	6.78, d (7.1)		
	2'/6'	128.2, CH	7.17, t (7.1, 7.1)		
	3'/5'	126.7, CH	7.13, d (7.8)		
	4'				
MePhe⁵	1	169.4, C	5.02, m 3.23, m 7.24, d (7.6) 7.41, t (7.7, 7.7) 7.32, d (7.5) 2.84, s	Val-NH	MePhe-1' MePhe-1' MePhe-4' MePhe-3'/5' MePhe-2
	2	60.9, CH			
	3	34.4, CH ₂			
	1'	138.4, C			
	2'/6'	130.0, CH			
	3'/5'	129.1, CH			
	4'	127.2, CH			
	NCH ₃	35.6, CH ₃			
Val⁶	1	172.6, C	4.71, dd (5.2, 4.2)	MePhe-2	Val-3 Val-2, Val-3, Val-5 Val-2, Val-3, Val-4 MePhe-1
	2	56.4, CH	2.05, m		
	3	31.6, CH	0.88, d (6.9)		
	4	19.7, CH ₃	0.76, d (6.9)		
	5	17.8, CH ₃	7.41, d (7.7)		
	NH				

^a HMBC correlations are given from proton(s) stated to the indicated carbon atom.

2.3. Bioassays

Preparative chromatography resulted in separation of several fractions containing thirteen pure cyanopeptolin variants (Table 2). These peptides were evaluated for inhibition against four serine proteases and protein phosphatase 1. In addition, their effect on MCF-7 breast cancer cells was tested. However, only six CPs were isolated from *N. edaphicum* CCNP1411 in sufficient amounts to obtain quantitative results of the assays. None of the peptides were active against thrombin, elastase, and protein phosphatase 1, even at the highest concentration used in the study (45.4 $\mu\text{g}/\text{mL}$). However, all CPs with Arg in position 2 significantly reduced the activity of trypsin. The IC_{50} values of trypsin inhibitors were comparable and in the range of 0.24–0.26 μM . The CPs-Arg² with *N*-MeTyr or *N*-MeHty in position 5 were also active against chymotrypsin, but the IC_{50} values were lower ($\text{IC}_{50} = 3.1\text{--}3.8 \mu\text{M}$). Chymotrypsin inhibition activity of CPs-Arg² was not observed when position 5 was occupied by MePhe. All CPs-Tyr² reduced activity of chymotrypsin and were inactive against other enzymes. For CP1027 and CP985, the IC_{50} was 0.26 μM . Following enzyme inhibition assays, all samples with Arg²-containing CP962 and Tyr²-containing CP985 (at 4.54 $\mu\text{g}/\text{mL}$) were analyzed by LC-MS/MS. The recovery was based on extracted mass chromatogram of parent ions. The enzymes did not cause any significant loss of the peptides; their contents were in the range from 94.6% to 97.7% of that in samples without the enzyme.

Due to limited amounts of pure peptides isolated from *N. edaphicum* CCNP1411, only Arg²-containing CP962 and Tyr²-containing CP985 were used in MTT (3-(4,5-dimethylthiazole-2-yl)-2,5-diphenyltetrazolium bromide) assay. After 24-h exposure, no cytotoxic effects on the MCF-7 cells were observed (Figure 5).

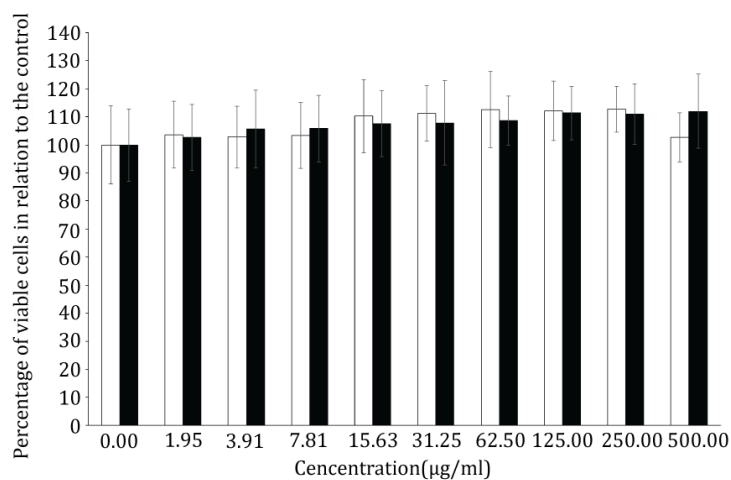


Figure 5. Viability of breast cancer cells MCF-7 treated for 24 h with Arg²-containing CP962 (white bars) and Tyr²-containing CP985 (black bars), isolated from *N. edaphicum* CCNP1411. Data are presented as percentage of the control, mean \pm s.e.m, $n = 3$.

3. Discussion

Cyanobacteria from the *Nostoc* genus, especially the symbiotic strains and those living in waters from tropical regions, are important producers of bioactive compounds with potential biotechnological or pharmaceutical application [37,40–43]. One of the most prominent examples are cryptophycins, cyclic depsipeptides isolated from *Nostoc* sp. ATCC 53789 and GSV 224. They are promising candidates for anti-cancer drug development [44,45]. Another important *Nostoc* metabolite is cyanovirin-N, a small cyanobacterial lectin which blocks the entry of the enveloped viruses such as HIV, influenza, and Ebola [46].

In this study, the structures of CPs produced by *N. edaphicum* CCNP1411 from the Baltic Sea were elucidated based on the fragmentation spectra of their pseudomolecular ions (CPs-Arg²)

(Figure 4; Figures S2–S8) or the dehydrated forms of the ions (CPs-Tyr²) (Figure 3; Figures S9–S12). The occurrence of the dehydrated pseudomolecular ion as a precursor ion in mass fragmentation spectra of Tyr²-(and Ile²)-containing aeruginopeptins has been previously reported [20,47]. It was suggested that the cleavage of an ester bond at Thr¹ and subsequent dehydration resulted in the generation of linear peptides. For the two CPs, Arg²-containing CP962 and Tyr²-containing CP985, the composition and sequences of amino acids were confirmed by NMR spectroscopy. The results of the analyses were consistent with structure elucidation performed by tandem mass spectrometry. The core structures of these peptides were more similar to those identified in *Microcystis* [13,14,28,32], compared to those reported from other *Nostoc* isolates (Table 1). For example, instead of Arg² or Tyr² present in position 2 of the CPs identified in this work, nostopeptin and insulapeptolides from *N. minutum* and *N. insulare* possess Leu² or Hph² (homophenylalanine) [35,38]. Of the CPs identified in this study, only CP1006A (*m/z* 1007) was previously reported. This peptide, along with its chlorinated derivative (CP1040A) were found in *Microcystis* bloom and culture samples [14,48].

The structural diversity of CPs, specifically the residue in position 2, was found to have significant effect on activity of the peptides against serine proteases: trypsin and chymotrypsin [28,29,32]. The CP-type peptides with potent inhibitory activity against trypsin were characterized by the presence of basic amino acid (Arg or Lys), whereas in peptides active against chymotrypsin, position 2 was occupied by hydrophobic residues (Tyr, Phe, Hty or Leu). The same structure-activity relationship was observed in this study. Eight CPs-Arg² inhibited the activity of trypsin with IC₅₀ values of 0.24–0.26 μM, and five CPs-Tyr² inhibited chymotrypsin with similar potency. In addition, the inhibitory activity of CPs produced by CCNP1411 seemed to be affected by the residue in position 5. Only those CPs-Arg² which had *N*-MeTyr⁵ or *N*-MeHty⁵ in this position were active against chymotrypsin. However, to unequivocally prove the significance of this structure-activity relationship, more CPs should be tested. The fact that some CPs-Arg², apart from strong inhibition of trypsin, are also active against chymotrypsin was previously documented by other authors [12,29,49]. The trypsin inhibition activity of CP-type peptides was suggested to be enhanced by the presence of isoleucine in position 6, instead of valine. Other modifications in the structure of Ahp-containing cyclic depsipeptides, such as the presence of chloride or sulfide groups, may also have an effect on enzyme inhibition activity [12].

Cyanobacteria produce many other Ahp-containing cyclic depsipeptides with inhibitory activity against proteases [28,29]. The majority of the peptides were active at micromolar concentrations, but some had even lower IC₅₀ values. Symplocamide A, with citrulline in position 2, showed potent activity against chymotrypsin with IC₅₀ of 0.38 μM, and was 200-times less active against trypsin (IC₅₀ 80.2 μM) [29]. Symplocamide A also had cytotoxic activity to NCI H460 lung cancer cells and neuro-2A neuroblastoma cells [29]. Chymotrypsin was most potently inhibited by the glyceric acid 3'-*O*-phosphate-containing micropeptin T20 from *M. aeruginosa*, characterized by the presence of the Thr-Phe-Ahp sequence (IC₅₀ 2.5 nM) [50]. Picomolar inhibition of trypsin was documented for CP 1020, which was also active against chymotrypsin, plasmin, human kallikrein, and factor XIa [32]. The structure of CP1020 differs from CP978 isolated in our study only in the presence of Glu in a side chain, instead of Asp. In enzymatic assays, CP978 and other CPs isolated from *N. edaphicum* CCNP1411 were less active than CP1020, but still belong to the most potent protease inhibitors among this class of compounds [12,28,29,32]. Ahp-containing depsipeptides were suggested to block the active center of trypsin or /and chymotrypsin, so the enzymes cannot cleave the peptide bonds at the carboxyl side of Arg or Tyr, respectively [25,28]. In this study, the Tyr²-containing CP985 and Arg²-containing CP962 exposed to proteases inhibited the activity of chymotrypsin or /and trypsin, but their concentrations remained almost unchanged. These results are in line with the hypothesis by Yamaki et al. [28] and confirm the blockage of the active centers of the enzymes by the peptides.

Trypsin and chymotrypsin, the two enzymes inhibited by CPs from CCNP1411, are essential for food digestion. Their deregulation can also lead to a number of human diseases such as cancer, cardiovascular and inflammatory diseases. The molecules that modify activity of these proteases, and especially those that act selectively, are widely explored as agents of significant biotechnological

and pharmaceutical potential [51]. As the new CP variants identified in *N. edaphicum* CCNP1411 inhibited the activity of trypsin or chymotrypsin at low concentrations and were inactive against the other tested enzymes and MCF-7 breast cancer cells, their possible use as therapeutic agents should be further explored.

Besides its therapeutic potential, this class of protease inhibitors was proven to be an important group of defense agents protecting cyanobacteria from grazers. Oscillapeptin J, CP SS and CP 1020 induced acute effects in small crustaceans [18,32,33]. However, CP SS was not toxic to the isolated rat hepatocytes [18], and oscillapeptin J did not induce any harmful effects in mice when administered intraperitoneally at concentrations up to 1000 µg/kg b.w. [52]. In the case of CP1020, induction of anti-inflammatory effects in human hepatoma cell line Huh7 was observed [53]. In addition, exposure of zebrafish eleuthero-embryos to CP1020 led to transcriptional alterations of genes involved in many important processes, including DNA damage recognition and repair, and circadian rhythm [54]. These findings, along with the acute toxicity of CP-type compounds observed in crustaceans suggest that their activity is not only related to the inhibition of digestive enzymes.

4. Materials and Methods

4.1. Culture Conditions

Nostoc cf. edaphicum CCNP 1411 (GenBank accession number KJ161445) was isolated in 2010 from the Gulf of Gdańsk, southern Baltic Sea, and established as monospecies culture by Dr. Justyna Kobos. Purification of the strain was carried out by multiple transfer to a liquid or/and solid (1% bacterial agar) Z8S medium [55]. To obtain a higher biomass of the cyanobacterium, the culture was grown in 5-L bottles at 22 °C ± 1 °C, at continuous light of 10–30 µE/m²/s. The collected biomass was lyophilized and kept at –20 °C until used.

4.2. Extraction and Isolation

Freeze-dried biomass of *N. edaphicum* (36 g) was extracted twice with 75% methanol (MeOH) (1 L) by vortexing for 30 min. Following centrifugation at 4,000 g, the extracts were pooled and diluted in water purified using ELGA PURELAB[®] flex (Veolia, London, UK) to adjust the concentration of MeOH to <10%. Then, the sample was loaded onto the preconditioned 120-g SNAP KP-C18-HS cartridge (Biotage Uppsala, Sweden). Sample components were eluted using an Isolera flash chromatography system (Biotage Uppsala, Sweden), with a step gradient (10–100% MeOH in water) with 3 column volumes of eluent at each step. Absorbance was monitored at 210 nm and 280 nm. The flow rate was 40 mL/min and 60-mL fractions were collected. Fraction composition was analyzed by UPLC-MS/MS. Fractions containing the same peptides were pooled, diluted with water to <10% MeOH, and concentrated on YMC C18 cartridges (20 mm ID × 2 cm; YMC, GmbH, Dinslaken, Germany).

Six pooled fractions were further purified using preparative HPLC (Biotage Parallelex Flex, Cardiff, UK) and Flex V3 software for instrument control and data acquisition. The separation was performed on XBridge Prep C18 column (5 µm CBD, 19 mm ID × 250 mm long; Waters, Elstree, UK) using a 30-min linear gradient from 15% to 80% acetonitrile in MilliQ water with 0.1% formic acid. Absorbance was monitored at 210 nm and 280 nm. The flow rate was 20 mL/min and 4-mL fractions were collected.

4.3. LC-MS/MS Analyses

At each step of the extraction and isolation procedure, the content of the collected fractions was determined by UPLC-MS/MS. The system comprised a Waters Acquity Ultra performance LC coupled to a photodiode array detector (PDA) and a Xevo quadrupole time of flight mass detector (Waters, Elstree, UK). Samples were separated on an ethylene-bridged hybrid BEH C18 column (2.1 mm ID × 100 mm; 1.7 µm, Waters) maintained at 40 °C. The mobile phase was Milli-Q water and acetonitrile (solvent B), both containing 0.1% formic acid. Separation was performed using

gradient elution (0.3 mL/min) from 20% to 70% B over 10 min, followed by a 100% B wash step and re-equilibration. Data was acquired in positive ion electrospray scanning from m/z 50 to 2000 with a scan time of 2 s and inter-scan delay of 0.1 s. The capillary and cone voltages were set at 0.7 kV and 25 V, respectively. The desolvation gas was maintained at 400 L/h at a temperature of 300 °C. The cone gas was set at 50 L/h with a source temperature of 80 °C. Instrument control, data acquisition and processing were achieved using MassLynx v4.1 (Waters, Milford, MA, USA).

Structures of cyanopeptolins were additionally characterized using Agilent 1200 HPLC (Agilent Technologies, Waldbronn, Germany) coupled to a hybrid triple quadrupole/linear ion trap mass spectrometer QTRAP5500 (Applied Biosystems MDS Sciex, Concord, ON, Canada). Peptides were separated on Zorbax Eclipse XDB-C18 column (4.6 mm ID \times 150 mm, 5 μ m; Agilent Technologies, Santa Clara, CA, USA) column. A gradient elution (0.6 mL/min) was applied with mobile phase composed of 5% acetonitrile in MilliQ water and acetonitrile (solvent B), both containing 0.1% formic acid. The gradient started at 15% B and went to 50% B within 5 min. The content of phase B was then increased to 100% within the next 3 min and kept at that level for 10 min before returning to the starting conditions. The QTRAP MS/MS system was operated in the positive mode, with turbo ion source voltage set at 5.5 kV and temperature at 550 °C. For ions within the m/z range 500–1250 and signal intensity above the threshold of 500,000 cps, fragmentation spectra were acquired within a range 50–1000 Da, at collision energy of 60 V and declustering potential set at 80 eV. Data acquisition and processing were accomplished with the Analyst[®] Software (version 1.5.1, Applied Biosystems, Concord, ON, Canada).

4.4. NMR Analyses

1D ¹H-NMR and 2D homo- and heteronuclear 2D NMR (COSY, TOCSY, ROESY, HSQC, and HMBC) were acquired on a Bruker Avance III spectrometers, 500 MHz and 700 MHz. Spectra were recorded in DMSO-*d*₆. NMR data were processed and analyzed by TopSpin (Bruker, Billerica, MA, USA) and SPARKY software (3.114, Goddard and Kneller, freeware <https://www.cgl.ucsf.edu/home/sparky>).

4.5. Enzyme Inhibition Assay

The chymotrypsin and trypsin inhibition assays were performed following the procedures of Ploutno and Carmeli [41]. The α -chymotrypsin from bovine pancreas (C4129), trypsin from porcine pancreas (T0303), aprotinin (1.5–200 μ g/mL) as enzyme inhibitor, *N*-Suc-Gly-Gly-*p*-nitroanilide and *N*- α -benzoyl-DL-arginine-*p*-nitroanilide hydrochloride (BAPNA) as chymotrypsin and trypsin substrates, respectively were used. Enzymes (0.1 mg/mL) and substrate (2 mM) were dissolved in the same buffer (50 mM Tris-HCl, 100 mM NaCl, 1 mM CaCl₂, pH 7.5). The thrombin inhibition assay was performed according to Ocampo and Bennet [56]. Thrombin (T4648) was dissolved in buffer (0.5 mg/mL; 0.2 M Tris-HCl; pH 8.0); substrate (*N*-*p*-tosyl-Gly-L-Pro-L-Lys-*p*-nitroanilide acetate salt, 0.5 mg/mL) and inhibitor (4-(2-aminoethyl)benzenesulfonyl fluoride hydrochloride (AEBSF; 60–2400 μ g/mL)) were dissolved in MilliQ water. The elastase inhibition assay was performed according to Kwan et al. [57]. The enzyme (75 μ g/mL; E0258) from porcine pancreas, substrate (2 mM; *N*-Suc-Ala-Ala-Ala-*p*-nitroanilide) and inhibitor (elastatinal; 5–125 μ g/mL) were dissolved in buffer (0.2 M Tris-HCl; pH 8.0). All enzymes, substrates and inhibitors used for proteases inhibition assays were from Sigma-Aldrich (St. Louis, MO, USA). Protein phosphatase 1 inhibition assay was performed according to the procedure described by Rapala et al. [58]. PP1 was from England Biolabs, Hitchin, UK (754S) and the substrate, *p*-nitrophenyl phosphate disodium salt hexahydrate (*p*-NPP), was from Sigma-Aldrich (Irvine, UK). Microcystin MC-LR (0.125–4.0 ng/mL) from Enzo Life Sciences, Lausen, Switzerland was used as inhibitor. The enzyme was dissolved in buffer solution A (50 mM Tris at pH 7.4, 1 mg/mL bovine serum albumin (BSA; Sigma -Aldrich, St. Louis, MO, USA), 1 mM MnCl₂, 2 mM dithiothreitol (DTT; Sigma-Aldrich, St. Louis, MO, USA)). *p*-NPP (5.5 mg/mL) was dissolved in buffer solution B (50 mM Tris, pH 8.1, 0.5 mg/mL BSA, 20 mM MgCl₂ \times 6H₂O,

200 mM $\text{MnCl}_2 \times 4\text{H}_2\text{O}$). All enzyme inhibition assays were performed in a 96 multi-well plate at 37 °C, in triplicate. The absorbance of the reaction mixtures was measured at 405 nm using a microplate reader (Molecular Devices, Sunnyvale, CA, USA). After trypsin and chymotrypsin inhibition assays, the samples with and without the enzymes and containing the highest concentration of CP962 and CP985 (45.4 $\mu\text{g}/\text{mL}$) were analyzed by LC-MS/MS. The content of the peptides was determined based of the peak area of the extracted ions.

4.6. Cytotoxicity Assay

For the test, two CPs were selected: Arg²-containing CP962 and Tyr²-containing CP985. MCF-7 breast cancer cells were seeded at 7.5×10^3 cells/100 μL in a 96-well plates and incubated at 37 °C, 5% CO_2 for 24 h. The cells were then treated for a further 24 h with CP962 and CP985 (0 to 500 $\mu\text{g}/\text{mL}$). After 24 h, sterile-filtered 3-(4,5-dimethylthiazol-2-yl)-2,5-diphenyltetrazolium bromide solution (MTT; 1 mg/mL) was added to each well. After 4 h incubation at 37 °C in the dark, the MTT solution was removed and formazan crystals solubilized in DMSO. The plates were shaken for 20 min, in the dark, at room temperature and absorbance was measured at 560 nm (Synergy/HT, BIOTEK, Wnooski, VT, USA). For each CP, three independent experiments were carried out and each treatment consisted of six replicates per plate. Bar charts were used to represent the viability of MCF-7 cells treated with CP962 and CP985, compared to the control (i.e., untreated cells) that represented 100% cell viability.

5. Conclusions

Nostoc edaphicum CCNP1411 isolated from the Gulf of Gdańsk (southern Baltic) produces at least thirteen CPs, including twelve variants reported here for the first time. The structures of the peptides are different from other Ahp-containing cyclic depsipeptides previously found in *Nostoc*. The activity of the peptides was mainly determined by the presence of Arg² or Tyr² in Ahp-adjacent position. The fact that trypsin and chymotrypsin did not degrade the tested CPs constitutes an additional evidence for enzyme inactivation by the peptides. Neither of the CP inhibited thrombin, elastase, and protein phosphatase 1; CP962 and CP985 also showed no cytotoxic effects on MCF-7 breast cancer cells. The CPs produced by *N. edaphicum* CCNP1411, as peptidic structures with selective and potent proteases inhibiting activity, are potential lead compounds in drug discovery process.

Supplementary Materials: The following are available online at <http://www.mdpi.com/1660-3397/16/7/220/s1>. Figure S1: LC-MS/MS chromatogram of cyanopeptolins (CPs) in crude extract from *Nostoc edaphicum* CCNP1411 (A) and chromatograms of isolated peptides: CP962 (B) and CP985 (C); Figure S2: Chemical structure (A) and product ion mass spectra of cyanopeptolin CP1049 [Thr+Arg+Ahp+Phe+MeHty+Val]Asp+OA with precursor ion $[M + H]^+$ at m/z 1049. The spectra were recorded with application of a hybride quadrupole/time-of-flight mass spectrometer (QTOF) (B) and a hybride triple quadrupole/linear ion trap mass spectrometer (QTRAP) (C). The mass signals were assigned to the following fragments: 1031 $[M + H - \text{H}_2\text{O}]^+$, 1003 $[M + H - \text{H}_2\text{O} - \text{CO}]^+$, 932 $[M + H - \text{Val} - \text{H}_2\text{O}]^+$, 914 $[M + H - \text{Val} - 2\text{H}_2\text{O}]^+$, 808 $[M + 2\text{H} - (\text{Asp} + \text{OA})]^+$, 790 $[M + 2\text{H} - (\text{Asp} + \text{OA}) - \text{H}_2\text{O}]^+$, 772 $[M + 2\text{H} - (\text{Asp} + \text{OA}) - 2\text{H}_2\text{O}]^+$, 741 $[M + H - (\text{Val} + \text{MeHty}) - \text{H}_2\text{O}]^+$, 673 $[M + 2\text{H} - \text{Val} - (\text{Asp} + \text{OA}) - 2\text{H}_2\text{O}]^+$, 481 $[\text{OA} + \text{Asp} + \text{Thr} + \text{Arg} + \text{H} - \text{H}_2\text{O}]^+$, 434 $[\text{Ahp} + \text{Phe} + \text{MeHty} + \text{H} - \text{H}_2\text{O}]^+$, 338 $[\text{Arg} + \text{Thr} + \text{Val} + \text{H} - \text{H}_2\text{O}]^+$, 322 $[\text{Phe}(-\text{N}) + \text{MeHty} + \text{H}]^+$, 297 $[\text{Asp} + \text{Thr} + \text{Val} + \text{H} - \text{H}_2\text{O}]^+$, 243 $[\text{Ahp} + \text{Phe} + \text{H} - \text{H}_2\text{O}]^+$, 215 $[\text{Ahp} + \text{Phe} + \text{H} - \text{H}_2\text{O} - \text{CO}]^+$, 164 MeHty immonium ion, 120 Phe immonium ion, 70-Arg; Figure S3: Chemical structure (A) and product ion mass spectra of cyanopeptolin CP1020 [Thr+Arg+Ahp+Phe+MeHty+Val]Asp+HA with precursor ion $[M + H]^+$ at m/z 1021. The spectra were recorded with application of QTOF (B) and QTRAP (C) mass spectrometers. The mass signals were assigned to the following fragments: 1003 $[M + H - \text{H}_2\text{O}]^+$, 975 $[M + H - \text{H}_2\text{O} - \text{CO}]^+$, 886 $[M + H - \text{Val} - 2\text{H}_2\text{O}]^+$, 808 $[M + 2\text{H} - (\text{Asp} + \text{HA})]^+$, 790 $[M + 2\text{H} - (\text{Asp} + \text{HA}) - \text{H}_2\text{O}]^+$, 772 $[M + 2\text{H} - (\text{Asp} + \text{OA}) - 2\text{H}_2\text{O}]^+$, 713 $[M + H - (\text{Val} + \text{MeHty}) - \text{H}_2\text{O}]^+$, 691 $[M + 2\text{H} - \text{Val} - (\text{Asp} + \text{HA}) - \text{H}_2\text{O}]^+$, 673 $[M + 2\text{H} - \text{Val} - (\text{Asp} + \text{HA}) - 2\text{H}_2\text{O}]^+$, 453 $[\text{HA} + \text{Asp} + \text{Thr} + \text{Arg} + \text{H} - \text{H}_2\text{O}]^+$, 434 $[\text{Ahp} + \text{Phe} + \text{MeHty} + \text{H} - \text{H}_2\text{O}]^+$, 338 $[\text{Arg} + \text{Thr} + \text{Val} + \text{H} - \text{H}_2\text{O}]^+$, 322 $[\text{Phe}(-\text{N}) + \text{MeHty} + \text{H}]^+$, 297 $[\text{Asp} + \text{Thr} + \text{Val} + \text{H} - \text{H}_2\text{O}]^+$, 243 $[\text{Ahp} + \text{Phe} + \text{H} - \text{H}_2\text{O}]^+$, 215 $[\text{Ahp} + \text{Phe} + \text{H} - \text{H}_2\text{O} - \text{CO}]^+$, 164 MeHty immonium ion, 120 Phe immonium ion, 70-Arg; Figure S4: Chemical structure (A) and product ion mass spectra of cyanopeptolin CP1018 [Thr+Arg+Ahp+Phe+MePhe+Val]Asp+OA with precursor ion $[M + H]^+$ at m/z 1019. The spectra were recorded with application of QTOF (B) and QTRAP (C) mass spectrometers. The mass signals were assigned to the following fragments: 1001 $[M + H - \text{H}_2\text{O}]^+$, 983 $[M + H - 2\text{H}_2\text{O}]^+$, 973 $[M + H - \text{H}_2\text{O} - \text{CO}]^+$, 902 $[M + H - \text{Val} - \text{H}_2\text{O}]^+$, 884 $[M + H - \text{Val} - 2\text{H}_2\text{O}]^+$, 778 $[M + 2\text{H} - (\text{Asp} + \text{OA})]^+$, 760 $[M + 2\text{H} - (\text{Asp} + \text{OA}) - \text{H}_2\text{O}]^+$, 742 $[M + 2\text{H} - (\text{Asp} + \text{OA}) - 2\text{H}_2\text{O}]^+$, 661 $[M + 2\text{H} - \text{Val} - (\text{Asp} + \text{OA}) - \text{H}_2\text{O}]^+$, 643 $[M + 2\text{H} - \text{Val} - (\text{Asp} + \text{OA}) - 2\text{H}_2\text{O}]^+$, 481 $[\text{OA} + \text{Asp} + \text{Thr} + \text{Arg} + \text{H} - \text{H}_2\text{O}]^+$,

404 [Ahp + Phe + MePhe + H - H₂O]⁺, 338 [Arg + Thr + Val + H - H₂O]⁺, 308 [Phe(-N) + MeTyr + H]⁺, 297 [Asp + Thr + Val + H - H₂O]⁺, 243 [Ahp + Phe + H - H₂O]⁺, 215 [Ahp + Phe + H - H₂O - CO]⁺, 134 MePhe immonium ion, 120 Phe immonium ion, 70-Arg; Figure S5: Chemical structure (A) and product ion mass spectra of cyanopeptolin CP1006 [Thr+Arg+Ahp+Phe+MeTyr+Val]Asp+HA with precursor ion [M + H]⁺ at *m/z* 1007. The spectra were recorded with application of QTOF (B) and QTRAP (A) mass spectrometers. The mass signals were assigned to the following fragments: 989 [M + H - H₂O]⁺, 961 [M + H - H₂O - CO]⁺, 872 [M + H - Val - 2H₂O]⁺, 794 [M + 2H - (Asp + HA)]⁺, 776 [M + 2H - (Asp + HA) - H₂O]⁺, 766 [M + 2H - (Asp + HA) - CO]⁺, 758 [M + 2H - (Asp + HA) - 2H₂O]⁺, 713 [M + H - (Val + MeHTyr) - H₂O]⁺, 659 [M + 2H - Val - (Asp + HA) - 2H₂O]⁺, 453 [HA + Asp + Thr + Arg + H - H₂O]⁺, 420 [Ahp + Phe + MeTyr + H - H₂O]⁺, 338 [Arg + Thr + Val + H - H₂O]⁺, 308 [Phe(-N) + MeTyr + H]⁺, 297 [Asp + Thr + Val + H - H₂O]⁺, 243 [Ahp + Phe + H - H₂O]⁺, 215 [Ahp + Phe + H - H₂O - CO]⁺, 150 MeTyr immonium ion, 120 Phe immonium ion, 70-Arg; Figure S6: Chemical structure (A) and product ion mass spectra of cyanopeptolin CP992 [Thr+Arg+Ahp+Phe+MeHTy+Val]Asp+BA with precursor ion [M + H]⁺ at *m/z* 993. The spectra were recorded with application of QTOF (B) and QTRAP (C) mass spectrometers. The mass signals were assigned to the following fragments: 975 [M + H - H₂O]⁺, 947 [M + H - H₂O - CO]⁺, 858 [M + H - Val - 2H₂O]⁺, 808 [M + 2H - (Asp + BA)]⁺, 790 [M + 2H - (Asp + BA) - H₂O]⁺, 772 [M + 2H - (Asp + BA) - 2H₂O]⁺, 673 [M + 2H - Val - (Asp + BA) - 2H₂O]⁺, 434 [Ahp + Phe + MeHTy + H - H₂O]⁺, 425 [BA + Asp + Thr + Arg + H - H₂O]⁺, 338 [Arg + Thr + Val + H - H₂O]⁺, 322 [Phe(-N) + MeHTy + H]⁺, 243 [Ahp + Ph + H - H₂O]⁺, 215 [Ahp + Phe + H - H₂O - CO]⁺, 164 MeHTy immonium ion, 120 Phe immonium ion, 70-Arg; Figure S7: Chemical structure (A) and product ion mass spectra of cyanopeptolin CP990 [Thr+Arg+Ahp+Phe+MePhe+Val]Asp+HA with precursor ion [M + H]⁺ at *m/z* 991. The spectra were recorded with application of QTOF (B) and QTRAP (C) mass spectrometers. The mass signals were assigned to the following fragments: 973 [M + H - H₂O]⁺, 945 [M + H - H₂O - CO]⁺, 856 [M + H - Val - 2H₂O]⁺, 778 [M + 2H - (Asp + HA)]⁺, 760 [M + 2H - (Asp + HA) - H₂O]⁺, 750 [M + 2H - (Asp + HA) - CO]⁺, 742 [M + 2H - (Asp + HA) - 2H₂O]⁺, 643 [M + 2H - Val - (Asp + HA) - 2H₂O]⁺, 453 [HA + Asp + Thr + Arg + H - H₂O]⁺, 404 [Ahp + Phe + MePhe + H - H₂O]⁺, 338 [Arg + Thr + Val + H - H₂O]⁺, 297 [Asp + Thr + Val + H - H₂O]⁺, 243 [Ahp+Phe+H-H₂O]⁺, 215 [Ahp+Phe+H-H₂O-CO]⁺, 134 MePhe immonium ion, 120 Phe immonium ion, 70-Arg; Figure S8: Chemical structure (A) and product ion mass spectra of cyanopeptolin CP978 [Thr+Arg+Ahp+Phe+MeTyr+Val]Asp+BA with precursor ion [M+H]⁺ at *m/z* 979. The spectra were recorded with application of QTOF (B) and QTRAP (C) mass spectrometers. The mass signals were assigned to the following fragments: 961 [M + H - H₂O]⁺, 933 [M + H - H₂O - CO]⁺, 844 [M + H - Val - 2H₂O]⁺, 794 [M + 2H - (Asp + BA)]⁺, 776 [M + 2H - (Asp + BA) - H₂O]⁺, 758 [M + 2H - (Asp + BA) - 2H₂O]⁺, 659 [M + 2H - Val - (Asp + BA) - 2H₂O]⁺, 425 [BA + Asp + Thr + Arg + H - H₂O]⁺, 420 [Ahp + Phe + MeTyr + H - H₂O]⁺, 338 [Arg + Thr + Val + H - H₂O]⁺, 308 [Phe(-N) + MeTyr + H]⁺, 243 [Ahp + Phe + H - H₂O]⁺, 215 [Ahp + Phe + H - H₂O - CO]⁺, 150 MeTyr immonium ion, 120 Phe immonium ion, 70-Arg; Figure S9: Chemical structure (A) and product ion mass spectra of cyanopeptolin CP1027 [Thr+Tyr+Ahp+Phe+MeHTy+Val]Asp+HA with precursor ion [M+H-H₂O]⁺ at *m/z* 1010. The spectra were recorded with application of QTOF (B) and QTRAP (C) mass spectrometers. The mass signals were assigned to the following fragments: 992 [M + H - 2H₂O]⁺, 982 [M + H - H₂O - CO]⁺, 964 [M + H - 2H₂O - CO]⁺, 911 [M + H - Val - H₂O]⁺, 893 [M + H - Val - 2H₂O]⁺, 819 [M + H - MeHTy - H₂O]⁺, 797 [M + 2H - (Asp + HA) - H₂O]⁺, 779 [M + 2H - (Asp + HA) - 2H₂O]⁺, 751 [M + 2H - (Asp + HA) - 2H₂O - CO]⁺, 702 [M + H - (Val + MeHTy) - H₂O]⁺, 674 [M + H - (Val + MeHTy) - H₂O - CO]⁺, 460 [M + H - (Val + MeHTy + Phe + Ahp) - H₂O]⁺, 442 [M + H - (Val + MeHTy + Phe + Ahp) - 2H₂O]⁺, 434 [Ahp + Phe + MeHTy + H - H₂O]⁺, 322 [Phe(-N) + MeHTy + H]⁺, 297 [Asp + Thr + Val + H - H₂O]⁺, 243 [Ahp + Phe + H - H₂O]⁺, 215 [Ahp + Phe + H - H₂O - CO]⁺, 164 MeHTy immonium ion, 136 Tyr immonium ion, 120 Phe immonium ion; Figure S10: Chemical structure (A) and product ion mass spectra of cyanopeptolin CP1013 [Thr+Tyr+Ahp+Phe+MeTyr+Val]Asp+HA with precursor ion [M+H-H₂O]⁺ at *m/z* 996. The spectra were recorded with application of QTOF (B) and QTRAP (C) mass spectrometers. The mass signals were assigned to the following fragments: 978 [M + H - 2H₂O]⁺, 968 [M + H - H₂O - CO]⁺, 897 [M + H - Val - H₂O]⁺, 879 [M + H - Val - 2H₂O]⁺, 819 [M + H - MeTyr - H₂O]⁺, 783 [M + 2H - (Asp + HA) - H₂O]⁺, 765 [M + 2H - (Asp + HA) - 2H₂O]⁺, 736 [M + H - (Asp + HA) - 2H₂O - CO]⁺, 720 [M + H - (Val + MeTyr) - H₂O]⁺, 702 [M + H - (Val + MeTyr) - 2H₂O]⁺, 666 [M + 2H - Val - (Asp + HA) - 2H₂O]⁺, 460 [M + H - (Val + MeTyr + Phe + Ahp) - H₂O]⁺, 420 [Ahp + Phe + MeTyr + H - H₂O]⁺, 432 [M + H - (Val + MeTyr + Phe + Ahp) - H₂O - CO]⁺, 414 [HA + Asp + Thr + Val + H]⁺, 297 [Asp + Thr + Val + H - H₂O]⁺, 243 [Ahp + Phe + H - H₂O]⁺, 215 [Ahp + Phe + H - H₂O - CO]⁺, 150 MeTyr immonium ion, 136 Tyr immonium ion, 120 Phe immonium ion; Figure S11. Chemical structure (A) and product ion mass spectra of cyanopeptolin CP999 [Thr+Tyr+Ahp+Phe+MeHTy+Val]Asp+BA with precursor ion [M+H-H₂O]⁺ at *m/z* 982. The spectra were recorded with application of QTOF (B) and QTRAP (C) mass spectrometers. The mass signals were assigned to the following fragments: 964 [M + H - 2H₂O]⁺, 954 [M + H - H₂O - CO]⁺, 883 [M + H - Val - H₂O]⁺, 865 [M + H - Val - 2H₂O]⁺, 797 [M + 2H - (Asp + BA) - H₂O]⁺, 779 [M + 2H - (Asp + BA) - 2H₂O]⁺, 751 [M + 2H - (Asp + BA) - 2H₂O - CO]⁺, 692 [M + H - (Val + MeHTy) - H₂O]⁺, 674 [M + H - (Val + MeHTy) - 2H₂O]⁺, 698 [M + 2H - Val - (Asp + BA) - H₂O]⁺, 680 [M + 2H - Val - (Asp + BA) - 2H₂O]⁺, 646 [M + H - (Val + MeHTy) - 2H₂O - CO]⁺, 434 [Ahp + Phe + MeHTy + H - H₂O]⁺, 432 [M + H - (Val + MeHTy + Phe + Ahp) - H₂O]⁺, 386 [BA + Asp + Thr + Val + H]⁺, 322 [Phe(-N) + MeHTy + H]⁺, 269 [Asp + Thr + Val + H - H₂O - CO]⁺, 243 [Ahp + Phe + H - H₂O]⁺, 215 [Ahp + Phe + H - H₂O - CO]⁺, 164 MeHTy immonium ion, 136 Tyr immonium ion, 120 Phe immonium ion; Figure S12. Chemical structure (A) and product ion mass spectra of cyanopeptolin CP969 [Thr+Tyr+Ahp+Phe+MePhe+Val]Asp+BA with precursor ion [M + H - H₂O]⁺ at *m/z* 952. The spectra were recorded with application of QTOF (B) and QTRAP (C) mass spectrometers. The mass signals were assigned to the following fragments: 934 [M + H - 2H₂O]⁺, 924 [M + H - H₂O - CO]⁺, 853 [M + H - Val - H₂O]⁺, 835 [M + H - Val - 2H₂O]⁺, 791 [M + H -

MePhe – H₂O]⁺, 767 [M + 2H – (Asp + BA) – H₂O]⁺, 749 [M + 2H – (Asp + BA) – 2H₂O]⁺, 692 [M + H – (Val + MePhe) – H₂O]⁺, 674 [M + H – (Val + MePhe) – 2H₂O]⁺, 432 [M + H – (Val + MePhe + Phe + Ahp) – H₂O]⁺, 414 [M + H – (Val + MePhe + Phe + Ahp) – 2H₂O]⁺, 404 [Ahp + Phe + MePhe + H – H₂O]⁺, 386 [BA + Asp + Thr + Val + H]⁺, 297 [Asp + Thr + Val + H – H₂O]⁺, 243 [Ahp + Phe + H – H₂O]⁺, 215 [Ahp + Phe + H – H₂O – CO]⁺, 134 MePhe immonium ion, 136 Tyr immonium ion, 120 Phe immonium ion; Figure S13. ¹H-NMR Spectrum of cyanopeptolin CP985 in DMSO-d₆; Figure S14. HSQC Spectrum of cyanopeptolin CP985 in DMSO-d₆; Figure S15a. HMBC Spectrum of cyanopeptolin CP985 in DMSO-d₆; Figure S15b. Detailed NH–C=O region of the HMBC spectrum of cyanopeptolin CP985; Figure S15c. Detailed aromatic region of the HMBC spectrum of cyanopeptolin CP985; Figure S16. COSY Spectrum of cyanopeptolin CP985 in DMSO-d₆; Figure S17a. TOCSY Spectrum of cyanopeptolin CP985 in DMSO-d₆; Figure S17b. Amino acid spin systems in the diagnostic region of the TOCSY spectrum of cyanopeptolin CP985; Figure S18a. ROESY Spectrum of cyanopeptolin CP985 in DMSO-d₆; Figure S18b. Overlaid fragments of TOCSY (green) and ROESY (red) spectra of cyanopeptolin CP985; Figure S19. ¹H-NMR Spectrum of cyanopeptolin CP962 in DMSO-d₆; Figure S20. HSQC Spectrum of cyanopeptolin CP962 in DMSO-d₆; Figure S21a. HMBC Spectrum of cyanopeptolin CP962 in DMSO-d₆; Figure S21b. Detailed NH–C=O region of the HMBC spectrum of cyanopeptolin CP962; Figure S21c. Detailed aromatic region of the HMBC spectrum of cyanopeptolin CP962; Figure S22. COSY Spectrum of cyanopeptolin CP962 in DMSO-d₆; Figure S23a. TOCSY Spectrum of cyanopeptolin CP962 in DMSO-d₆; Figure S23b. Amino acid spin systems in the diagnostic region of the TOCSY spectrum of cyanopeptolin CP962; Figure S24a. ROESY Spectrum of cyanopeptolin CP962 in DMSO-d₆; Figure S24b. Overlaid fragments of TOCSY (green) and ROESY (red) spectra of cyanopeptolin CP962.

Author Contributions: H.M.-M. and C.E. designed the study and performed the extraction, fractionation, and isolation of CPs. H.M.-M., C.E., A.F., and M.C. participated in LC-MS/MS analyses, and in acquisition and interpretation of data and manuscript preparation. A.F. and M.C. performed the enzyme inhibition assays; M.G. and J.M. performed MTT assay. NMR analyses were done by E.W. and M.K. All authors discussed the results and contributed to the work on the manuscript.

Acknowledgments: The work was supported by the National Science Centre in Poland 2016/21/B/NZ9/02304 to Hanna Mazur-Marzec and 2014/15/B/NZ7/01014 to Elżbieta Jankowska. COST action ES1105 “CYANOCOST—Cyanobacterial blooms and toxins in water resources: Occurrence, impacts and management” is acknowledged for adding value to this study through networking and knowledge sharing with European experts.

Conflicts of Interest: The authors declare no conflicts of interest.

References

- Moore, R.E. Cyclic peptides and depsipeptides from cyanobacteria: A review. *J. Ind. Microbiol.* **1996**, *16*, 134–143. [[CrossRef](#)] [[PubMed](#)]
- Gerwick, L.; Gerwick, W.H.; Coates, R.C.; Engene, N.; Grindberg, R.V.; Jones, A.C.; Sorrels, C.M. Giant marine cyanobacteria produce exciting potential pharmaceuticals. *Microbe* **2008**, *3*, 277–284. [[CrossRef](#)]
- Nagarajan, M.; Maruthanayagam, V.; Sundararaman, M. A review of pharmacological and toxicological potentials of marine cyanobacterial metabolites. *J. Appl. Toxicol.* **2011**, *33*, 153–185. [[CrossRef](#)] [[PubMed](#)]
- Sainis, I.; Fokas, D.; Vareli, K.; Tzakos, A.G.; Kounnis, V.; Briasoulis, E. Cyanobacterial cyclopeptides as lead compounds to novel targeted cancer drugs. *Mar. Drugs* **2010**, *8*, 629–657. [[CrossRef](#)] [[PubMed](#)]
- Costa, M.; Costa-Rodrigues, J.; Fernandes, M.H.; Barros, P.; Vasconcelos, V.; Martins, R. Marine cyanobacteria compounds with anticancer properties: A Review on the implication of apoptosis. *Mar. Drugs* **2012**, *10*, 2181–2207. [[CrossRef](#)] [[PubMed](#)]
- Hong, J.; Luesch, H. Largazole: From discovery to broad-spectrum therapy. *Nat. Prod. Rep.* **2012**, *29*, 449–456. [[CrossRef](#)] [[PubMed](#)]
- Salvador-Reyes, L.A.; Luesch, H. Biological targets and mechanisms of action of natural products from marine cyanobacteria. *Nat. Prod. Rep.* **2015**, *32*, 478–503. [[CrossRef](#)] [[PubMed](#)]
- Ersmark, K.; Del Valle, J.R.; Hanessian, S. Chemistry and biology of the aeruginosin family of serine protease inhibitors. *Angew. Chem. Int. Ed. Engl.* **2008**, *47*, 1202–1223. [[CrossRef](#)] [[PubMed](#)]
- Chlipala, G.; Mo, S.; Orjala, J. Chemodiversity in freshwater and terrestrial cyanobacteria—A source for drug discovery. *Curr. Drug Targets* **2011**, *12*, 1654–1673. [[CrossRef](#)] [[PubMed](#)]
- Elkobi-Peer, S.; Carmeli, S. New prenylated aeruginosin, microphycin, anabaenopeptin and micropeptin analogues from microcystis bloom material collected in Kibbutz Kfar Blum, Israel. *Mar. drugs* **2015**, *13*, 2347–2375. [[CrossRef](#)] [[PubMed](#)]
- Itou, Y.; Ishida, K.; Shin, H.; Murakami, M. Oscillapeptins A to F, serine protease inhibitors from the three strains of *Oscillatoria agardhii*. *Tetrahedron* **1999**, *55*, 6871–6882. [[CrossRef](#)]

12. Gesner-Apter, S.; Carmeli, S. Protease inhibitors from a water bloom of the cyanobacterium *Microcystis aeruginosa*. *J. Nat. Prod.* **2009**, *72*, 1429–1436. [[CrossRef](#)] [[PubMed](#)]
13. Welker, M.; von Döhren, H. Cyanobacterial peptides—Nature’s own combinatorial biosynthesis. *FEMS Microbiol. Rev.* **2006**, *30*, 530–563. [[CrossRef](#)] [[PubMed](#)]
14. Cadel-Six, S.; Dauga, C.; Castests, A.; Rippka, R.; Bouchier, C.; Tandeau de Marsac, N.; Welker, M. Halogenase genes in nonribosomal peptide synthetase gene clusters of *Microcystis* (Cyanobacteria): Sporadic distribution and evolution. *Mol. Biol. Evol.* **2008**, *25*, 2031–2041. [[CrossRef](#)] [[PubMed](#)]
15. Martin, C.; Oberer, L.; Ino, T.; König, W.; Busch, M.; Weckesser, J. Cyanopeptolins, new depsipeptides from the cyanobacterium *Microcystis* sp. PCC 7806. *J. Antibiot.* **1993**, *46*, 1550–1556. [[CrossRef](#)] [[PubMed](#)]
16. Czarnecki, O.; Henning, M.; Lippert, I.; Welker, M. Identification of peptide metabolites of *Microcystis* (Cyanobacteria) that inhibit trypsin-like activity in planktonic herbivorous *Daphnia* (Cladocera). *Environ. Microbiol.* **2006**, *8*, 77–87. [[CrossRef](#)] [[PubMed](#)]
17. Welker, M.; Brunke, M.; Preussel, K.; Lippert, I.; von Döhren, H. Diversity and distribution of *Microcystis* (Cyanobacteria) oligopeptide chemotypes from natural communities studied by single-colony mass spectrometry. *Microbiology* **2004**, *150*, 1785–1796. [[CrossRef](#)] [[PubMed](#)]
18. Jakobi, C.; Rinehart, K.; Neuber, R.; Mez, K.; Weckesser, J. Cyanopeptolin SS, a disulphated depsipeptide from a water bloom: Structural elucidation and biological activities. *Phycologia* **1996**, *35*, 111–116. [[CrossRef](#)]
19. Tsukamoto, S.; Painuly, P.; Young, K.; Yang, X.; Shimizu, Y. Microcystilide A: A novel cell-differentiation-promoting depsipeptide from *Microcystis aeruginosa* NO-15-1840. *J. Am. Chem. Soc.* **1993**, *115*, 11046–11047. [[CrossRef](#)]
20. Harada, K.; Mayumi, T.; Shimada, T.; Fuji, K.; Kondo, F.; Park, H.; Watanabe, M. Co-production of microcystins and aeruginopeptins by natural cyanobacterial bloom. *Environ. Toxicol.* **2001**, *16*, 298–305. [[CrossRef](#)] [[PubMed](#)]
21. Adiv, S.; Aharonv-Nadborny, R.; Carmeli, S. Micropeptins from *Microcystis aeruginosa* collected in Dalton reservoir, Israel. *Tetrahedron* **2010**, *66*, 7429–7436. [[CrossRef](#)]
22. Rounge, T.; Rohrlack, T.; Tooming-Klunderud, A.; Kristensen, T.; Jakobsen, K. Comparison of cyanopeptolin genes in *Planktothrix*, *Microcystis* and *Anabaena* strains: Evidence for independent evolution within each genus. *Appl. Environ. Microbiol.* **2007**, *73*, 7322–7330. [[CrossRef](#)] [[PubMed](#)]
23. Tooming-Klunderud, A.; Rohrlack, T.; Shalchian-Tabrizi, K.; Kristensen, T.; Jakobsen, K. Structural analysis of non-ribosomal halogenated cyclic peptide and its putative operon from *Microcystis*: Implications for evolution of cyanopeptolins. *Microbiol.* **2007**, *153*, 1382–1393. [[CrossRef](#)] [[PubMed](#)]
24. Rouhiainen, L.; Paulin, L.; Suomalainen, S.; Hyttiäinen, H.; Buikema, W.; Haselkorn, R.; Sivonen, K. Genes encoding synthetases of cyclic depsipeptides, anabaenopeptilides, in *Anabaena* strain 90. *Mol. Microbiol.* **2000**, *37*, 156–167. [[CrossRef](#)] [[PubMed](#)]
25. Weckesser, J.; Martin, C.; Jakobi, C. Cyanopeptolins, depsipeptides from cyanobacteria. *System. Appl. Microbiol.* **1996**, *19*, 133–138. [[CrossRef](#)]
26. Namikoshi, M.; Rinehart, K. Bioactive compounds produced by cyanobacteria. *J. Ind. Microbiol. Biotechnol.* **1996**, *17*, 373–384. [[CrossRef](#)]
27. Bister, B.; Keller, S.; Baumann, H.; Nicholson, G.; Weist, S.; Jung, G.; Süßmuth, R.; Jüttner, F. Cyanopeptolin 963 A, a chymotrypsin inhibitor of *Microcystis* PCC 7806. *J. Nat. Prod.* **2004**, *67*, 1755–1757. [[CrossRef](#)] [[PubMed](#)]
28. Yamaki, H.; Sitachitta, N.; Sano, T.; Kaya, K. Two new chymotrypsin inhibitors isolated from the cyanobacterium *Microcystis aeruginosa* NIES-88. *J. Nat. Prod.* **2005**, *68*, 14–18. [[CrossRef](#)] [[PubMed](#)]
29. Linington, R.; Edwards, D.; Shuman, C.; McPhail, K.; Matainaho, T.; Gerwick, W. Symplocamide A, a potent cytotoxin and chymotrypsin inhibitor from the marine cyanobacterium *Symploca* sp. *J. Nat. Prod.* **2008**, *71*, 22–27. [[CrossRef](#)] [[PubMed](#)]
30. Okumura, H.; Philmus, B.; Portmann, C.; Hemscheidt, T. Homotyrosine-containing cyanopeptolins 880 & 960 and anabaenopeptins 908 & 915 from *Planktothrix agardhii* CYA 126/8. *J. Nat. Prod.* **2009**, *72*, 172–176. [[CrossRef](#)] [[PubMed](#)]
31. Zainuddin, E.; Mentel, R.; Wray, V.; Jansen, R.; Nimtz, M.; Lalk, M.; Mundt, S. Cyclic depsipeptides, ichthyopeptins A and B, from *Microcystis ichthyoblabe*. *J. Nat. Prod.* **2007**, *70*, 1084–1088. [[CrossRef](#)] [[PubMed](#)]

32. Gademann, K.; Portmann, C.; Blom, J.; Zeder, M.; Jüttner, F. Multiple toxin production in the cyanobacterium *Microcystis*: Isolation of the toxic protease inhibitor cyanopeptolin 1020. *J. Nat. Prod.* **2010**, *73*, 980–984. [[CrossRef](#)] [[PubMed](#)]
33. Blom, J.; Bister, B.; Bischoff, D.; Nicholson, G.; Jung, G.; Süßmuth, R.; Jüttner, F. Oscillapeptin J, a new grazer toxin of the freshwater cyanobacterium *Planktothrix rubescens*. *J. Nat. Prod.* **2003**, *66*, 431–434. [[CrossRef](#)] [[PubMed](#)]
34. Kaya, K.; Sano, T.; Beattie, K.; Codd, G. Nostocyclin, a novel 3-amino-6-hydroxy-2-piperidone-containing cyclic depsipeptide from the cyanobacterium *Nostoc* sp. *Tetrahedron Lett.* **1996**, *37*, 6725–6728. [[CrossRef](#)]
35. Okino, T.; Qi, S.; Matsua, H.; Murakami, M.; Yamaguchi, K. Nostopeptins A and B, elastase inhibitors from the cyanobacterium *Nostoc minutum*. *J. Nat. Prod.* **1997**, *60*, 158–161. [[CrossRef](#)]
36. Ploutno, A.; Carmeli, S. Modified peptides from a water bloom of the cyanobacterium *Nostoc* sp. *Tetrahedron* **2002**, *58*, 9949–9957. [[CrossRef](#)]
37. Dembitsky, V.; Řezanka, T. Metabolites produced by nitrogen-fixing *Nostoc* species. *Folia Microbiol.* **2005**, *50*, 363–391. [[CrossRef](#)]
38. Mehner, C.; Müller, D.; Kehraus, S.; Hautmann, S.; Gütschow, M.; König, G. New peptolides from the cyanobacterium *Nostoc insulare* as selective and potent inhibitors of human leukocyte elastase. *ChemBioChem* **2008**, *9*, 2692–2703. [[CrossRef](#)] [[PubMed](#)]
39. Hastie, J.; Borthwick, E.; Morrison, L.; Codd, G.; Cohen, P. Inhibition of several protein phosphatases by a non-covalently interacting microcystin and a novel cyanobacterial peptide, nostocyclin. *BBA* **2005**, *1726*, 187–193. [[CrossRef](#)] [[PubMed](#)]
40. Piccardi, R.; Frosini, A.; Tredici, M.; Margheri, M. Bioactivity in free-living and symbiotic cyanobacteria of the genus *Nostoc*. *J. Appl. Phycol.* **2000**, *12*, 543–547. [[CrossRef](#)]
41. Ploutno, A.; Carmeli, S. Banyasin A and banyasides A and B, three novel modified peptides from water bloom of the cyanobacterium *Nostoc* sp. *Tetrahedron* **2005**, *61*, 575–583. [[CrossRef](#)]
42. Tidgewell, K.; Clark, B.; Gerwick, W. *The Natural Products Chemistry of Cyanobacteria*; University of California San Diego: La Jolla, CA, USA, 2010; pp. 142–187.
43. Liu, L.; Jokela, J.; Herfindal, L.; Wahlsten, M.; Sinkkonen, J.; Permi, P.; Fewer, D.; Ove Døskeland, S.; Sivonen, K. 4-methylproline guided natural product discovery: Co-occurrence of 4-hydroxy- and 4-methylprolines in nostoweipeptins and nostopeptolides. *ACS Chem. Biol.* **2014**, *9*, 2646–2655. [[CrossRef](#)] [[PubMed](#)]
44. Trimurtulu, G.; Patterson, G.; Corbett, T.; Ohtani, I.; Moore, R.; Valeriote, F. Total structures of cryptophycins, potent antitumor depsipeptides from the blue-green alga *Nostoc* sp. GSV 224. *J. Am. Chem. Soc.* **1994**, *116*, 4729–4737. [[CrossRef](#)]
45. Weiss, C.; Figueras, E.; Borbely, A.; Sewald, N. Cryptophycins: Cytotoxic cyclodepsipeptides with potential for tumor targeting. *J. Pept. Sci.* **2017**, *23*, 514–531. [[CrossRef](#)] [[PubMed](#)]
46. Dey, B.; Lerner, D.; Lusso, P.; Boyd, M.; Elder, J.; Berger, E. Multiple antiviral activities of cyanovirin-N: Blocking of human immunodeficiency virus type 1 gp120 interaction with CD4 and coreceptor and inhibition of diverse enveloped viruses. *J. Virol.* **2000**, *74*, 4562–4569. [[CrossRef](#)] [[PubMed](#)]
47. Mayumi, T.; Kato, H.; Kawasaki, Y.; Harada, K. Formation of diagnostic product ions from cyanobacterial cyclic peptides by the two-bond fission mechanism using ion trap liquid chromatography/multi-stage mass spectrometry. *Rapid Commun. Mass Spectrom.* **2007**, *21*, 1025–1033. [[CrossRef](#)] [[PubMed](#)]
48. Welker, M.; Christiansen, G.; von Döhren, H. Diversity of coexisting *Planktothrix* (Cyanobacteria) chemotypes deduced by mass spectral analysis of microcystins and other oligopeptides. *Arch. Microbiol.* **2004**, *182*, 288–298. [[CrossRef](#)] [[PubMed](#)]
49. Choi, H.; Oh, S.; Yih, W.; Chin, J.; Kang, H.; Rho, J. Cyanopeptoline CB071: A cyclic depsipeptide isolated from the freshwater cyanobacterium *Aphanocapsa* sp. *Chem. Pharm. Bull.* **2008**, *56*, 1191–1193. [[CrossRef](#)] [[PubMed](#)]
50. Okano, T.; Sano, T.; Kaya, K. Micropeptin T-20, a novel phosphate-containing cyclic depsipeptide from the cyanobacterium *Microcystis aeruginosa*. *Tetrahedron Lett.* **1999**, *40*, 2379–2382. [[CrossRef](#)]
51. Srikanth, S.; Chen, Z. Plant protease inhibitors in therapeutics-focus on cancer therapy. *Front. Pharmacol.* **2016**, *7*, 1–19. [[CrossRef](#)] [[PubMed](#)]
52. Blom, J.; Baumann, H.; Codd, G.; Jüttner, F. Sensitivity and adaptation of aquatic organisms to oscillapeptin J and [D-Asp³, (E)-Dhb⁷] microcystin-RR. *Arch. Hydrobiol.* **2006**, *167*, 547–559. [[CrossRef](#)]

53. Faltermann, S.; Hutter, S.; Christen, V.; Hettich, T.; Fent, K. Anti-inflammatory activity of cyanobacterial serine protease inhibitors aeruginosin 828A and cyanopeptolin 1020 in human hepatoma cell line Huh7 and effects in Zebrafish (*Danio rerio*). *Toxins* **2016**, *8*, 219. [[CrossRef](#)] [[PubMed](#)]
54. Faltermann, S.; Zucchi, S.; Kohler, E.; Blom, J.; Pernthaler, J.; Fent, K. Molecular effects of the cyanobacterial toxin cyanopeptolin (CP1020) occurring in algal blooms: Global transcriptome analysis in zebrafish embryos. *Aquat. Toxicol.* **2014**, *149*, 33–39. [[CrossRef](#)] [[PubMed](#)]
55. Kotai, J. *Introduction for Preparation of Modified Nutrient Solution Z8 for Algae*; Norwegian Institute for Water Research Publication B-117669: Oslo, Norway, 1972; 5p.
56. Ocampo Bennet, X. *Peptide au Seiner Cyanobakterien Wasserblüte (1998) aus dem Wannsee/Berli: Strukturen and Biologische Wirksamkeit*; University of Freiburg: Freiburg, Germany, 2007; 28p.
57. Kwan, J.; Taori, K.; Paul, V.; Luesch, H. Lyngbyastatins 8–10, elastase inhibitors with cyclic depsipeptide scaffolds isolated from the marine cyanobacterium *Lyngbya semiplena*. *Mar. Drugs* **2009**, *7*, 528–538. [[CrossRef](#)] [[PubMed](#)]
58. Rapala, J.; Erkomaa, K.; Kukkonen, J.; Sivonen, K.; Lahti, K. Detection of microcystins with protein phosphatase inhibition assay, high-performance liquid chromatography–UV detection and enzyme-linked immunosorbent assay. Comparison of methods. *Anal. Chim. Acta* **2002**, *466*, 213–231. [[CrossRef](#)]



© 2018 by the authors. Licensee MDPI, Basel, Switzerland. This article is an open access article distributed under the terms and conditions of the Creative Commons Attribution (CC BY) license (<http://creativecommons.org/licenses/by/4.0/>).

Supplementary Material: Cyanopeptolins with trypsin and chymotrypsin inhibitory activity from the cyanobacterium *Nostoc edaphicum* CCNP1411

Hanna Mazur-Marzec^{1,2*}, Anna Fidor¹, Marta Ceglowska², Ewa Wiczerzak³, Magdalena Kropidłowska³, Marie Goua⁴, Jenny Macaskill⁴, Christine Edwards⁴

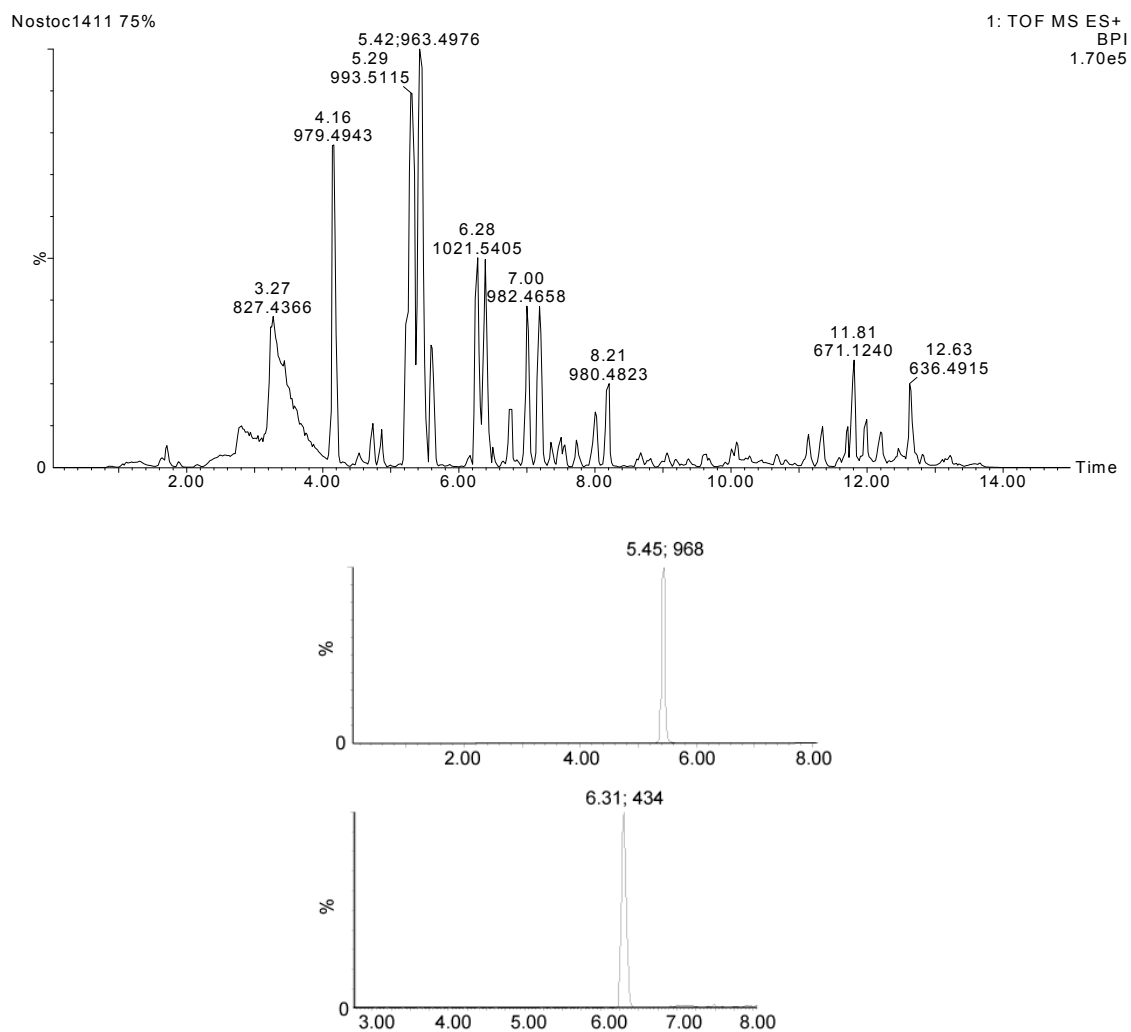


Figure S1. LC-MS/MS chromatogram of cyanopeptolins (CPs) in crude extract from *Nostoc edaphicum* CCNP1411 (A) and chromatograms of isolated peptides: CP962 (B) and CP985 (C).

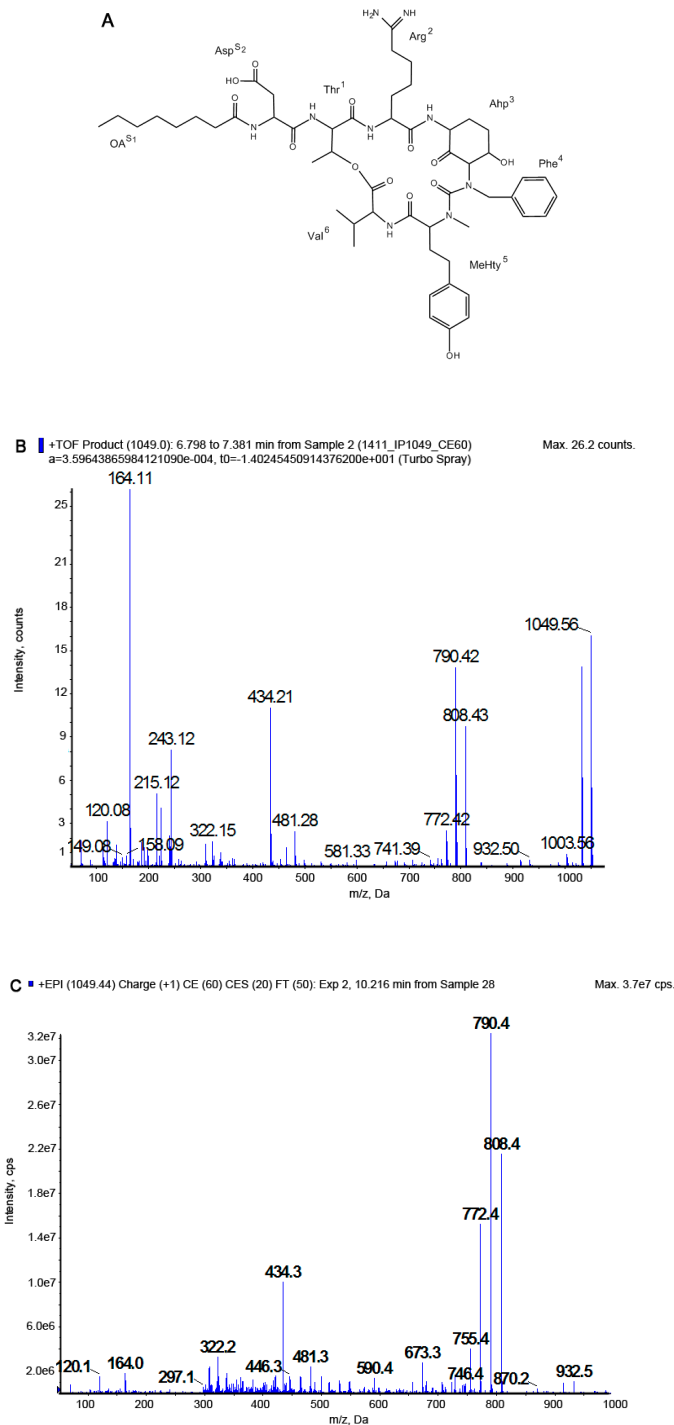


Figure S2. Chemical structure (A) and product ion mass spectra of cyanopeptolin CP1049 [Thr+Arg+Ahp+Phe+MeHty+Val]Asp+OA with precursor ion $[M + H]^+$ at m/z 1049. The spectra were recorded with application of a hybrid quadrupole/time-of-flight mass spectrometer (QTOF) (B) and a hybrid triple quadrupole/linear ion trap mass spectrometer (QTRAP) (C). The mass signals were assigned to the following fragments: 1031 $[M + H - H_2O]^+$, 1003 $[M + H - H_2O - CO]^+$, 932 $[M + H - Val - H_2O]^+$, 914 $[M + H - Val - 2H_2O]^+$, 808 $[M + 2H - (Asp + OA)]^+$, 790 $[M + 2H - (Asp + OA) - H_2O]^+$, 772 $[M + 2H - (Asp + OA) - 2H_2O]^+$, 741 $[M + H - (Val + MeHty) - H_2O]^+$, 673 $[M + 2H - Val - (Asp + OA) - 2H_2O]^+$, 481 $[OA + Asp + Thr + Arg + H - H_2O]^+$, 434 $[Ahp + Phe + MeHty + H - H_2O]^+$, 338 $[Arg + Thr + Val + H - H_2O]^+$, 322 $[Phe(-N) + MeHty + H]^+$, 297 $[Asp + Thr + Val + H - H_2O]^+$, 243 $[Ahp + Phe + H - H_2O]^+$, 215 $[Ahp + Phe + H - H_2O - CO]^+$, 164 MeHty immonium ion, 120 Phe immonium ion, 70-Arg.

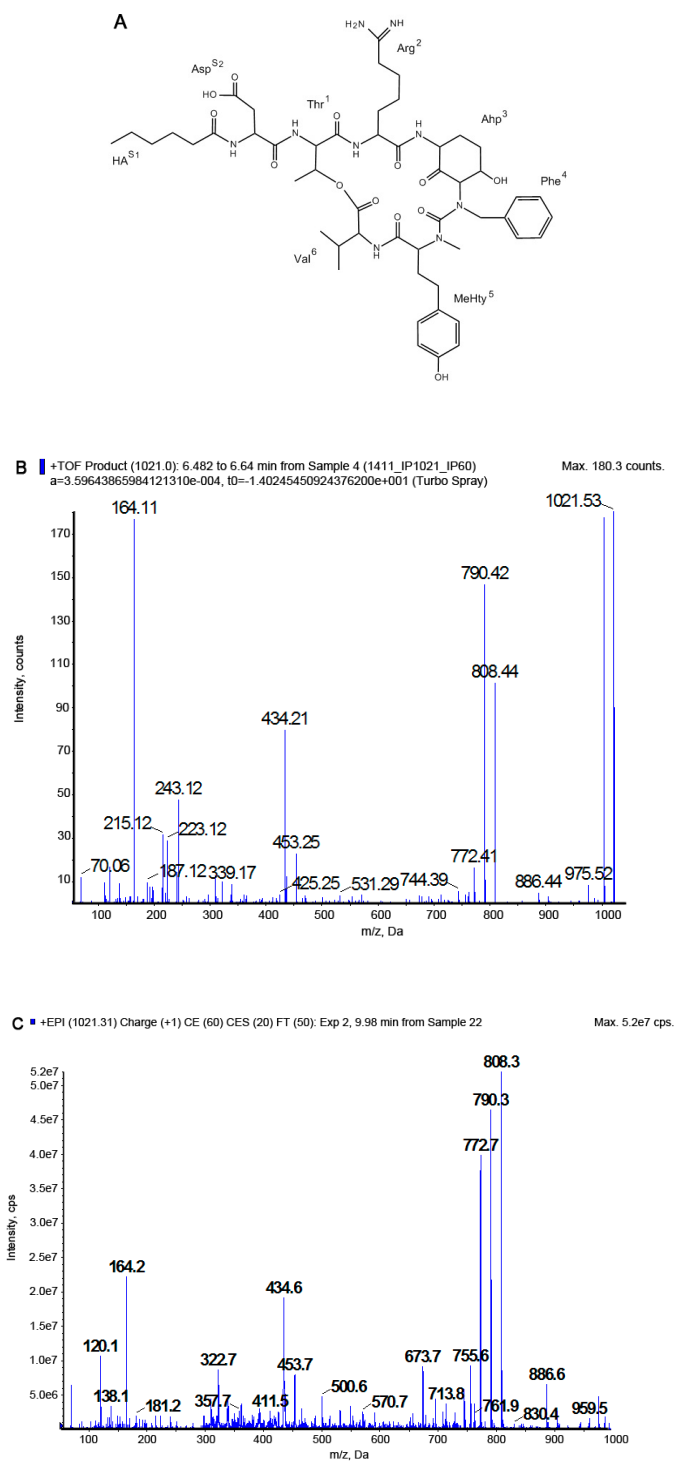


Figure S3. Chemical structure (A) and product ion mass spectra of cyanopeptolin CP1020 [Thr+Arg+Ahp+Phe+MeHty+Val]Asp+HA with precursor ion $[M+H]^+$ at m/z 1021. The spectra were recorded with application of QTOF (B) and QTRAP (C) mass spectrometers. The mass signals were assigned to the following fragments: 1003 $[M+H-H_2O]^+$, 975 $[M+H-H_2O-CO]^+$, 886 $[M+H-Val-2H_2O]^+$, 808 $[M+2H-(Asp+HA)]^+$, 790 $[M+2H-(Asp+HA)-H_2O]^+$, 772 $[M+2H-(Asp+OA)-2H_2O]^+$, 713 $[M+H-(Val+MeHty)-H_2O]^+$, 691 $[M+2H-Val-(Asp+HA)-H_2O]^+$, 673 $[M+2H-Val-(Asp+HA)-2H_2O]^+$, 453 $[HA+Asp+Thr+Arg+H-H_2O]^+$, 434 $[Ahp+Phe+MeHty+H-H_2O]^+$, 338 $[Arg+Thr+Val+H-H_2O]^+$, 322 $[Phe(-N)+MeHty+H]^+$, 297 $[Asp+Thr+Val+H-H_2O]^+$, 243 $[Ahp+Phe+H-H_2O]^+$, 215 $[Ahp+Phe+H-H_2O-CO]^+$, 164 MeHty immonium ion, 120 Phe immonium ion, 70-Arg.

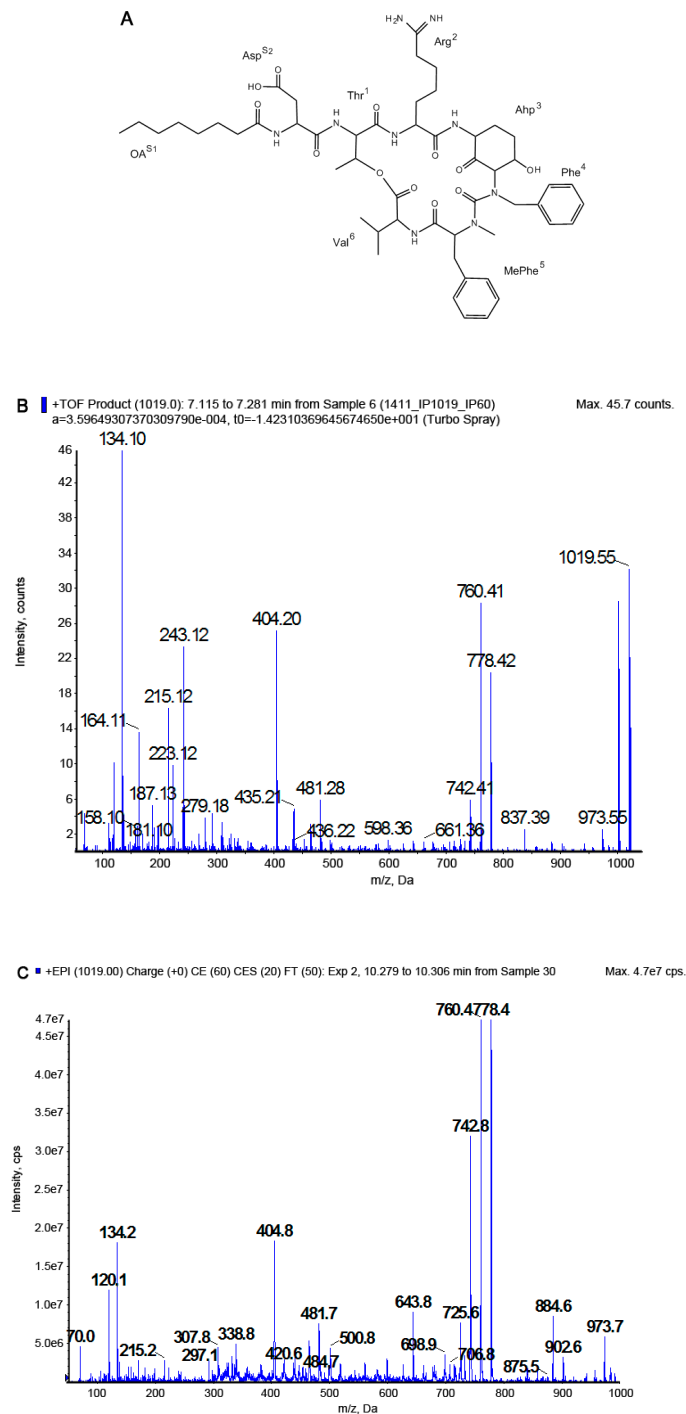


Figure S4. Chemical structure (A) and product ion mass spectra of cyanopeptolin CP1018 [Thr+Arg+Ahp+Phe+MePhe+Val]Asp+OA with precursor ion $[M+H]^+$ at m/z 1019. The spectra were recorded with application of QTOF (B) and QTRAP (C) mass spectrometers. The mass signals were assigned to the following fragments: 1001 $[M + H - H_2O]^+$, 983 $[M + H - 2H_2O]^+$, 973 $[M + H - H_2O - CO]^+$, 902 $[M + H - Val - H_2O]^+$, 884 $[M + H - Val - 2H_2O]^+$, 778 $[M + 2H - (Asp + OA)]^+$, 760 $[M + 2H - (Asp + OA) - H_2O]^+$, 742 $[M + 2H - (Asp + OA) - 2H_2O]^+$, 661 $[M + 2H - Val - (Asp+OA) - H_2O]^+$, 643 $[M + 2H - Val - (Asp + OA) - 2H_2O]^+$, 481 $[OA + Asp + Thr + Arg + H - H_2O]^+$, 404 $[Ahp + Phe + MePhe + H - H_2O]^+$, 338 $[Arg + Thr + Val + H - H_2O]^+$, 308 $[Phe(-N) + MeTyr + H]^+$, 297 $[Asp + Thr + Val + H - H_2O]^+$, 243 $[Ahp + Phe + H - H_2O]^+$, 215 $[Ahp + Phe + H - H_2O - CO]^+$, 134 MePhe immonium ion, 120 Phe immonium ion, 70-Arg.

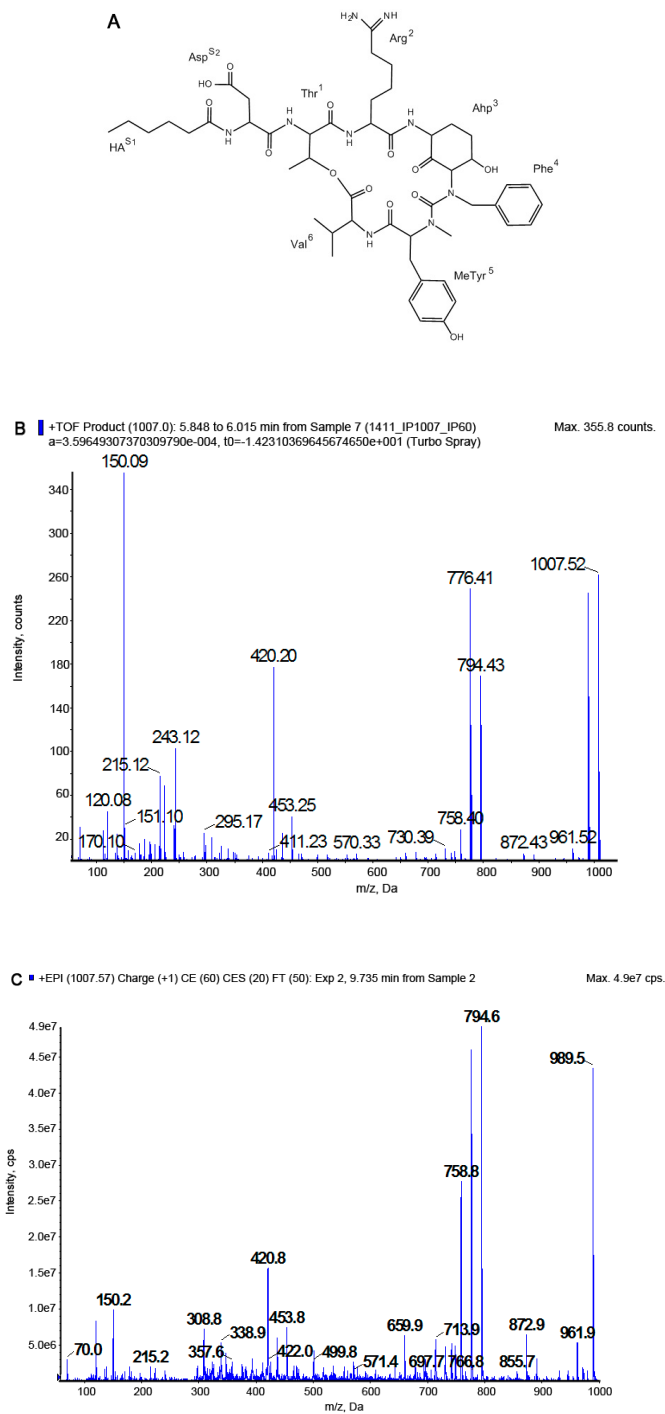


Figure S5. Chemical structure (A) and product ion mass spectra of cyanopeptolin CP1006 [Thr+Arg+Ahp+Phe+MeTyr+Val]Asp+HA with precursor ion $[M + H]^+$ at m/z 1007. The spectra were recorded with application of QTOF (B) and QTRAP (A) mass spectrometers. The mass signals were assigned to the following fragments: 989 $[M + H - H_2O]^+$, 961 $[M + H - H_2O - CO]^+$, 872 $[M + H - Val - 2H_2O]^+$, 794 $[M + 2H - (Asp + HA)]^+$, 776 $[M + 2H - (Asp + HA) - H_2O]^+$, 766 $[M + 2H - (Asp + HA) - CO]^+$, 758 $[M + 2H - (Asp + HA) - 2H_2O]^+$, 713 $[M + H - (Val + MeHTyr) - H_2O]^+$, 659 $[M + 2H - Val - (Asp + HA) - 2H_2O]^+$, 453 $[HA + Asp + Thr + Arg + H - H_2O]^+$, 420 $[Ahp + Phe + MeTyr + H - H_2O]^+$, 338 $[Arg + Thr + Val + H - H_2O]^+$, 308 $[Phe(-N) + MeTyr + H]^+$, 297 $[Asp + Thr + Val + H - H_2O]^+$, 243 $[Ahp + Phe + H - H_2O]^+$, 215 $[Ahp + Phe + H - H_2O - CO]^+$, 150 MeTyr immonium ion, 70-Arg.

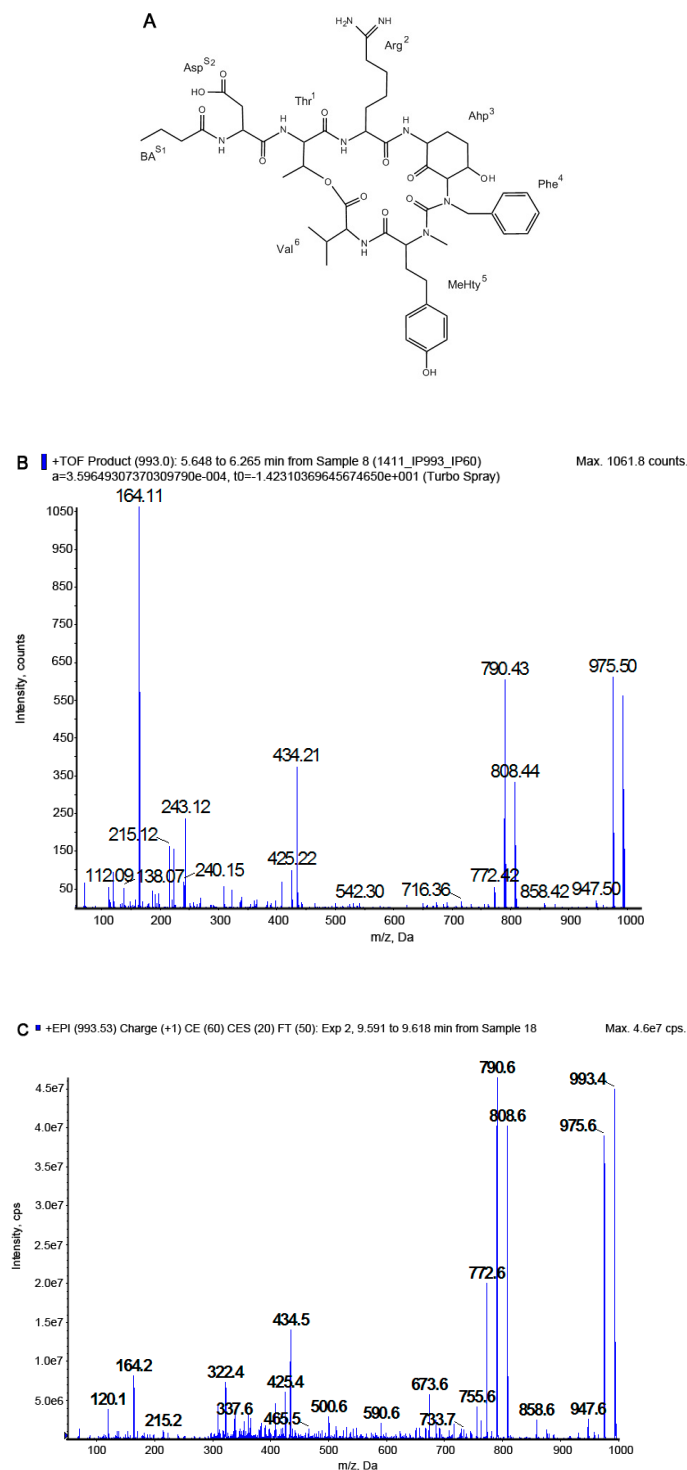


Figure S6. Chemical structure (A) and product ion mass spectra of cyanopeptolin CP992 [Thr+Arg+Ahp+Phe+MeHty+Val]Asp+BA with precursor ion $[M + H]^+$ at m/z 993. The spectra were recorded with application of QTOF (B) and QTRAP (C) mass spectrometers. The mass signals were assigned to the following fragments: 975 $[M + H - H_2O]^+$, 947 $[M + H - H_2O - CO]^+$, 858 $[M + H - Val - 2H_2O]^+$, 808 $[M + 2H - (Asp + BA)]^+$, 790 $[M + 2H - (Asp + BA) - H_2O]^+$, 772 $[M + 2H - (Asp + BA) - 2H_2O]^+$, 673 $[M + 2H - Val - (Asp + BA) - 2H_2O]^+$, 434 $[Ahp + Phe + MeHty + H - H_2O]^+$, 425 $[BA + Asp + Thr + Arg + H - H_2O]^+$, 338 $[Arg + Thr + Val + H - H_2O]^+$, 322 $[Phe(-N) + MeHty + H]^+$, 243 $[Ahp + Ph + H - H_2O]^+$, 215 $[Ahp + Phe + H - H_2O - CO]^+$, 164 MeHty immonium ion, 120 Phe immonium ion, 70-Arg.

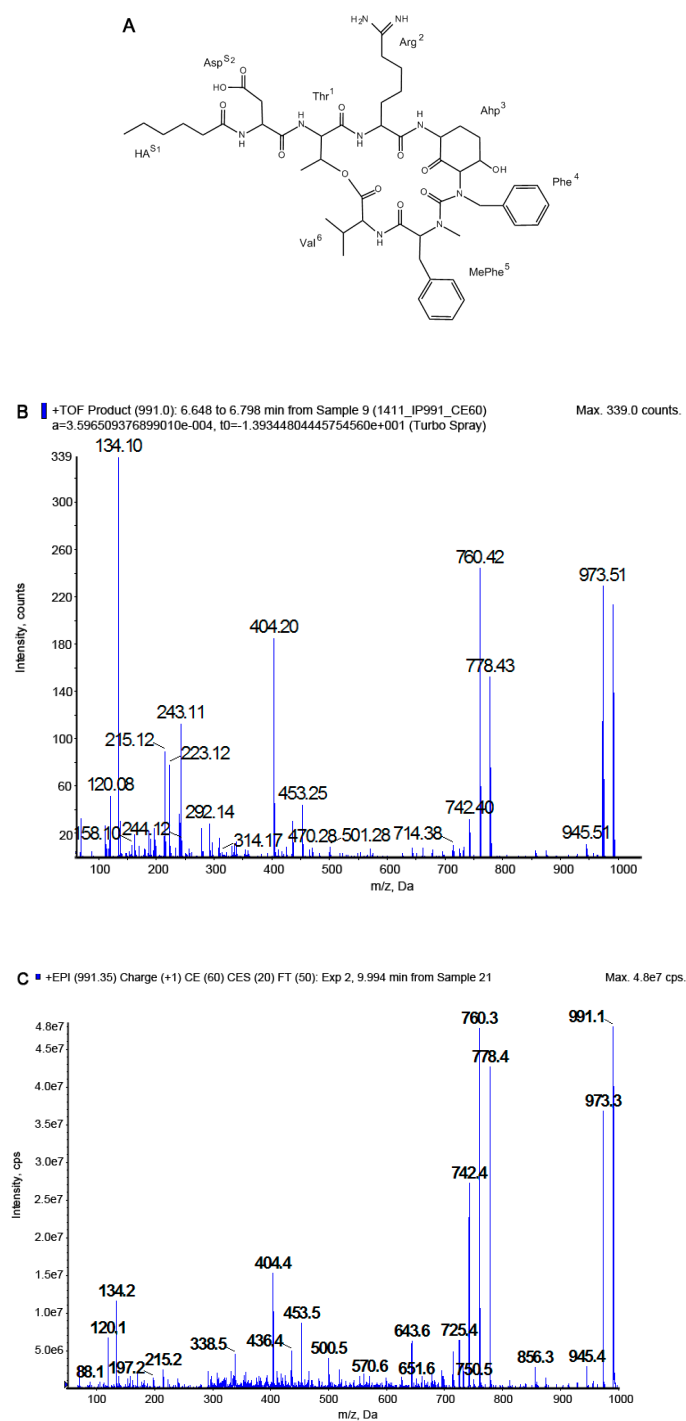


Figure S7. Chemical structure (A) and product ion mass spectra of cyanopeptolin CP990 [Thr+Arg+Ahp+Phe+MePhe+Val]Asp+HA with precursor ion $[M + H]^+$ at m/z 991. The spectra were recorded with application of QTOF (B) and QTRAP (C) mass spectrometers. The mass signals were assigned to the following fragments: 973 $[M + H - H_2O]^+$, 945 $[M + H - H_2O - CO]^+$, 856 $[M + H - Val - 2H_2O]^+$, 778 $[M + 2H - (Asp + HA)]^+$, 760 $[M + 2H - (Asp + HA) - H_2O]^+$, 750 $[M + 2H - (Asp + HA) - CO]^+$, 742 $[M + 2H - (Asp + HA) - 2H_2O]^+$, 643 $[M + 2H - Val - (Asp + HA) - 2H_2O]^+$, 453 $[HA + Asp + Thr + Arg + H - H_2O]^+$, 404 $[Ahp + Phe + MePhe + H - H_2O]^+$, 338 $[Arg + Thr + Val + H - H_2O]^+$, 297 $[Asp + Thr + Val + H - H_2O]^+$, 243 $[Ahp+Phe+H-H_2O]^+$, 215 $[Ahp+Phe+H-H_2O-CO]^+$, 134 MePhe immonium ion, 120 Phe immonium ion, 70-Arg.

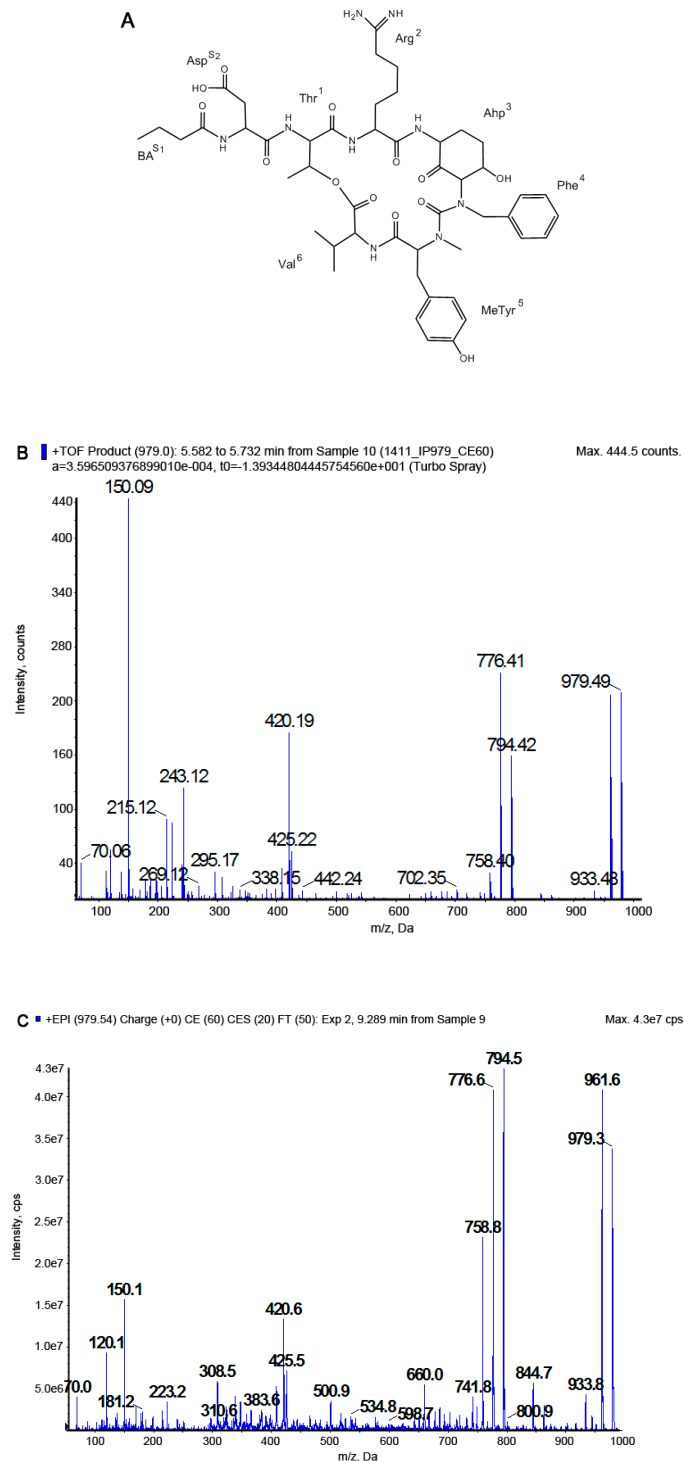


Figure S8. Chemical structure (A) and product ion mass spectra of cyanopeptolin CP978 [Thr+Arg+Ahp+Phe+MeTyr+Val]Asp+BA with precursor ion $[M+H]^+$ at m/z 979. The spectra were recorded with application of QTOF (B) and QTRAP (C) mass spectrometers. The mass signals were assigned to the following fragments: 961 $[M + H - H_2O]^+$, 933 $[M + H - H_2O - CO]^+$, 844 $[M + H - Val - 2H_2O]^+$, 794 $[M + 2H - (Asp + BA)]^+$, 776 $[M + 2H - (Asp + BA) - H_2O]^+$, 758 $[M + 2H - (Asp + BA) - 2H_2O]^+$, 659 $[M + 2H - Val - (Asp + BA) - 2H_2O]^+$, 425 $[BA + Asp + Thr + Arg + H - H_2O]^+$, 420 $[Ahp + Phe + MeTyr + H - H_2O]^+$, 338 $[Arg + Thr + Val + H - H_2O]^+$, 308 $[Phe(-N) + MeTyr + H]^+$, 243 $[Ahp + Phe + H - H_2O]^+$, 215 $[Ahp + Phe + H - H_2O - CO]^+$, 150 MeTyr immonium ion, 120 Phe immonium ion, 70-Arg.

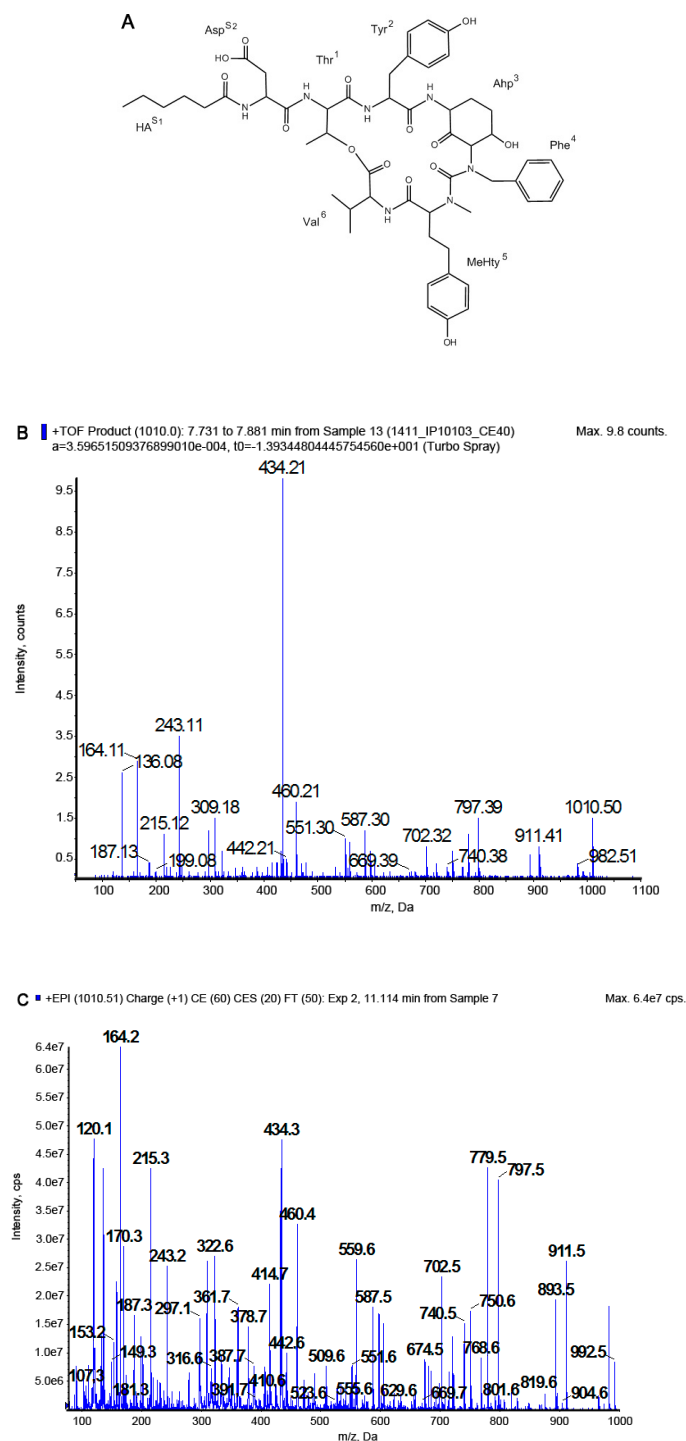


Figure S9. Chemical structure (A) and product ion mass spectra of cyanopeptolin CP1027 [Thr+Tyr+Ahp+Phe+MeHty+Val]Asp+HA with precursor ion $[M+H-H_2O]^+$ at m/z 1010. The spectra were recorded with application of QTOF (B) and QTRAP (C) mass spectrometers. The mass signals were assigned to the following fragments: 992 $[M+H-2H_2O]^+$, 982 $[M+H-H_2O-CO]^+$, 964 $[M+H-2H_2O-CO]^+$, 911 $[M+H-Val-H_2O]^+$, 893 $[M+H-Val-2H_2O]^+$, 819 $[M+H-MeHty-H_2O]^+$, 797 $[M+2H-(Asp+HA)-H_2O]^+$, 779 $[M+2H-(Asp+HA)-2H_2O]^+$, 751 $[M+2H-(Asp+HA)-2H_2O-CO]^+$, 702 $[M+H-(Val+MeHty)-H_2O]^+$, 674 $[M+H-(Val+MeHty)-H_2O-CO]^+$, 460 $[M+H-(Val+MeHty+Phe+Ahp)-H_2O]^+$, 442 $[M+H-(Val+MeHty+Phe+Ahp)-2H_2O]^+$, 434 $[Ahp+Phe+MeHty+H-H_2O]^+$, 322 $[Phe(-N)+MeHty+H]^+$, 297 $[Asp+Thr+Val+H-H_2O]^+$, 243 $[Ahp+Phe+H-H_2O]^+$, 215 $[Ahp+Phe+H-H_2O-CO]^+$, 164 MeHty immonium ion, 136 Tyr immonium ion, 120 Phe immonium ion.

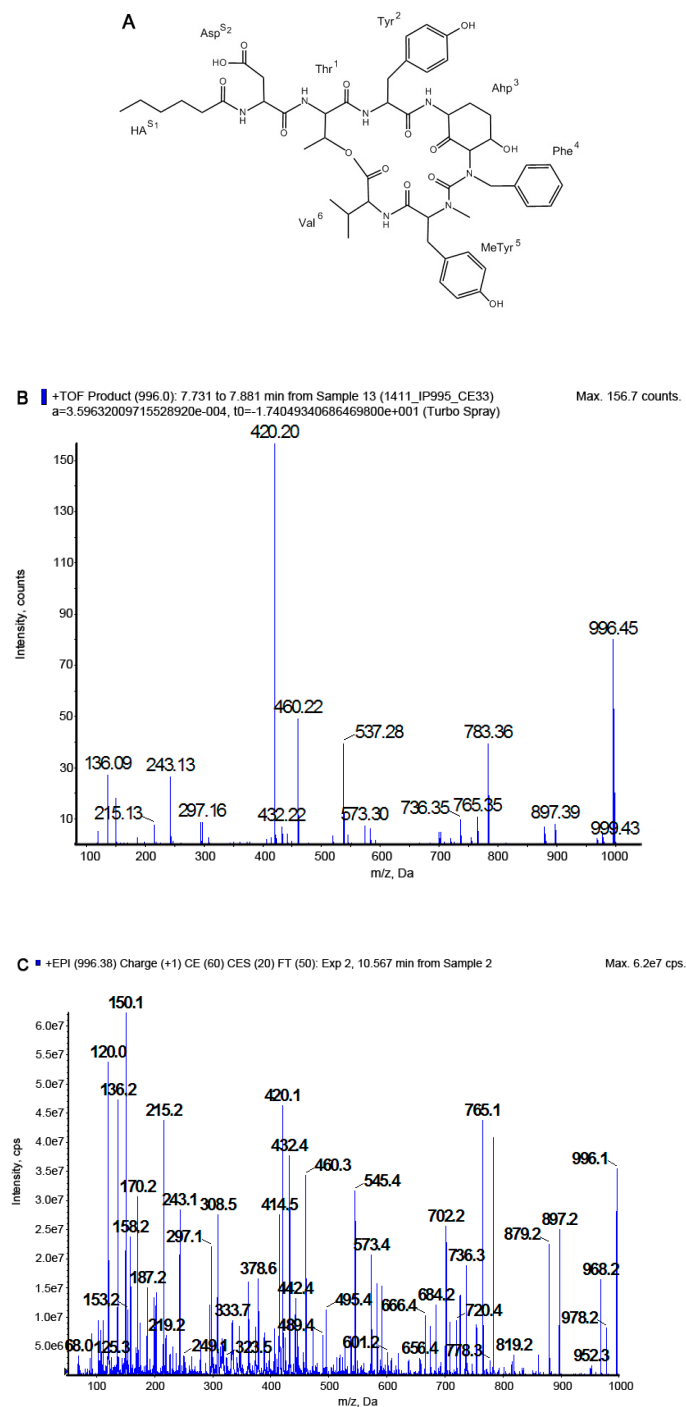


Figure S10. Chemical structure (A) and product ion mass spectra of cyanopeptolin CP1013 [Thr+Tyr+Ahp+Phe+MeTyr+Val]Asp+HA with precursor ion $[M+H-H_2O]^+$ at m/z 996. The spectra were recorded with application of QTOF (B) and QTRAP (C) mass spectrometers. The mass signals were assigned to the following fragments: 978 $[M+H-2H_2O]^+$, 968 $[M+H-H_2O-CO]^+$, 897 $[M+H-Val-H_2O]^+$, 879 $[M+H-Val-2H_2O]^+$, 819 $[M+H-MeTyr-H_2O]^+$, 783 $[M+2H-(Asp+HA)-H_2O]^+$, 765 $[M+2H-(Asp+HA)-2H_2O]^+$, 736 $[M+H-(Asp+HA)-2H_2O-CO]^+$, 720 $[M+H-(Val+MeTyr)-H_2O]^+$, 702 $[M+H-(Val+MeTyr)-2H_2O]^+$, 666 $[M+2H-Val-(Asp+HA)-2H_2O]^+$, 460 $[M+H-(Val+MeTyr+Phe+Ahp)-H_2O]^+$, 420 $[Ahp+Phe+MeTyr+H-H_2O]^+$, 432 $[M+H-(Val+MeTyr+Phe+Ahp)-H_2O-CO]^+$, 414 $[HA+Asp+Thr+Val+H]^+$, 297 $[Asp+Thr+Val+H-H_2O]^+$, 243 $[Ahp+Phe+H-H_2O]^+$, 215 $[Ahp+Phe+H-H_2O-CO]^+$, 150 MeTyr immonium ion, 136 Tyr immonium ion, 120 Phe immonium ion.

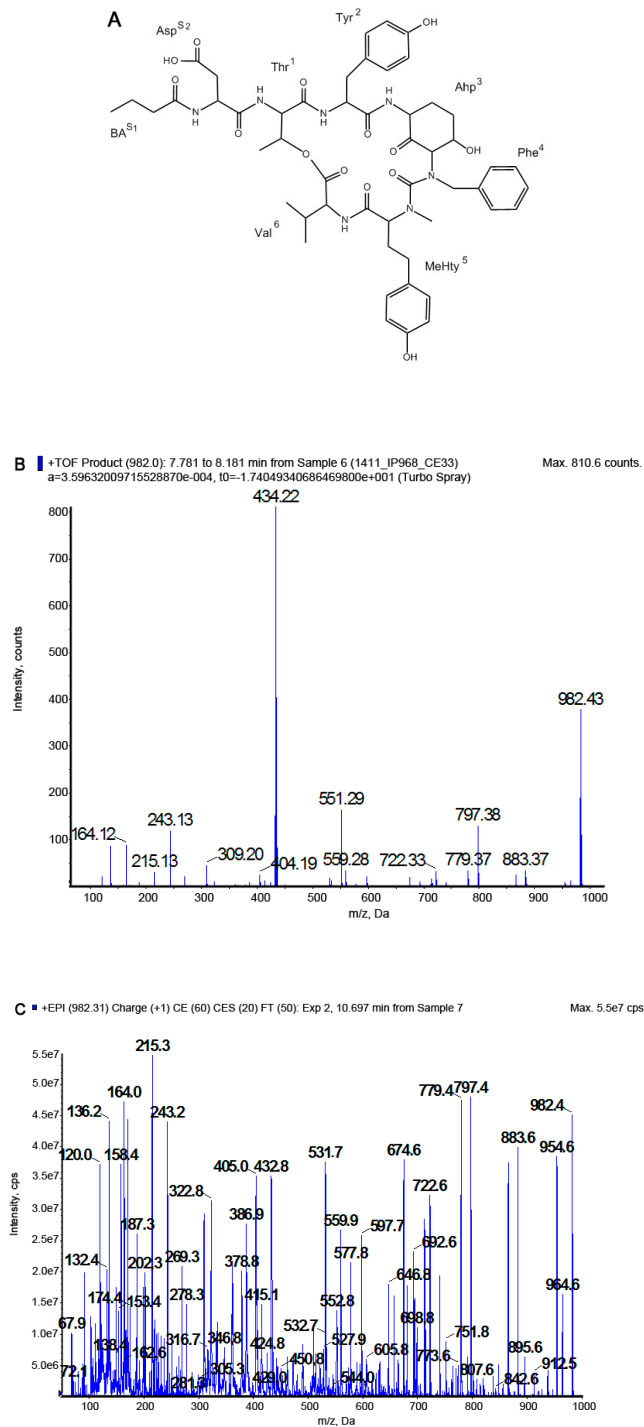


Figure S11. Chemical structure (A) and product ion mass spectra of cyanopeptolin CP999 [Thr+Tyr+Ahp+Phe+MeHty+Val]Asp+BA with precursor ion $[M+H-H_2O]^+$ at m/z 982. The spectra were recorded with application of QTOF (B) and QTRAP (C) mass spectrometers. The mass signals were assigned to the following fragments: 964 $[M+H-2H_2O]^+$, 954 $[M+H-H_2O-CO]^+$, 883 $[M+H-Val-H_2O]^+$, 865 $[M+H-Val-2H_2O]^+$, 797 $[M+2H-(Asp+BA)-H_2O]^+$, 779 $[M+2H-(Asp+BA)-2H_2O]^+$, 751 $[M+2H-(Asp+BA)-2H_2O-CO]^+$, 692 $[M+H-(Val+MeHty)-H_2O]^+$, 674 $[M+H-(Val+MeHty)-2H_2O]^+$, 698 $[M+2H-Val-(Asp+BA)-H_2O]^+$, 680 $[M+2H-Val-(Asp+BA)-2H_2O]^+$, 646 $[M+H-(Val+MeHty)-2H_2O-CO]^+$, 434 $[Ahp+Phe+MeHty+H-H_2O]^+$, 432 $[M+H-(Val+MeHty+Phe+Ahp)-H_2O]^+$, 386 $[BA+Asp+Thr+Val+H]^+$, 322 $[Phe(-N)+MeHty+H]^+$, 269 $[Asp+Thr+Val+H-H_2O-CO]^+$, 243 $[Ahp+Phe+H-$

H_2O^+ , 215 [Ahp + Phe + H - H_2O - CO] $^+$, 164 MeTyr immonium ion, 136 Tyr immonium ion, 120 Phe immonium ion.

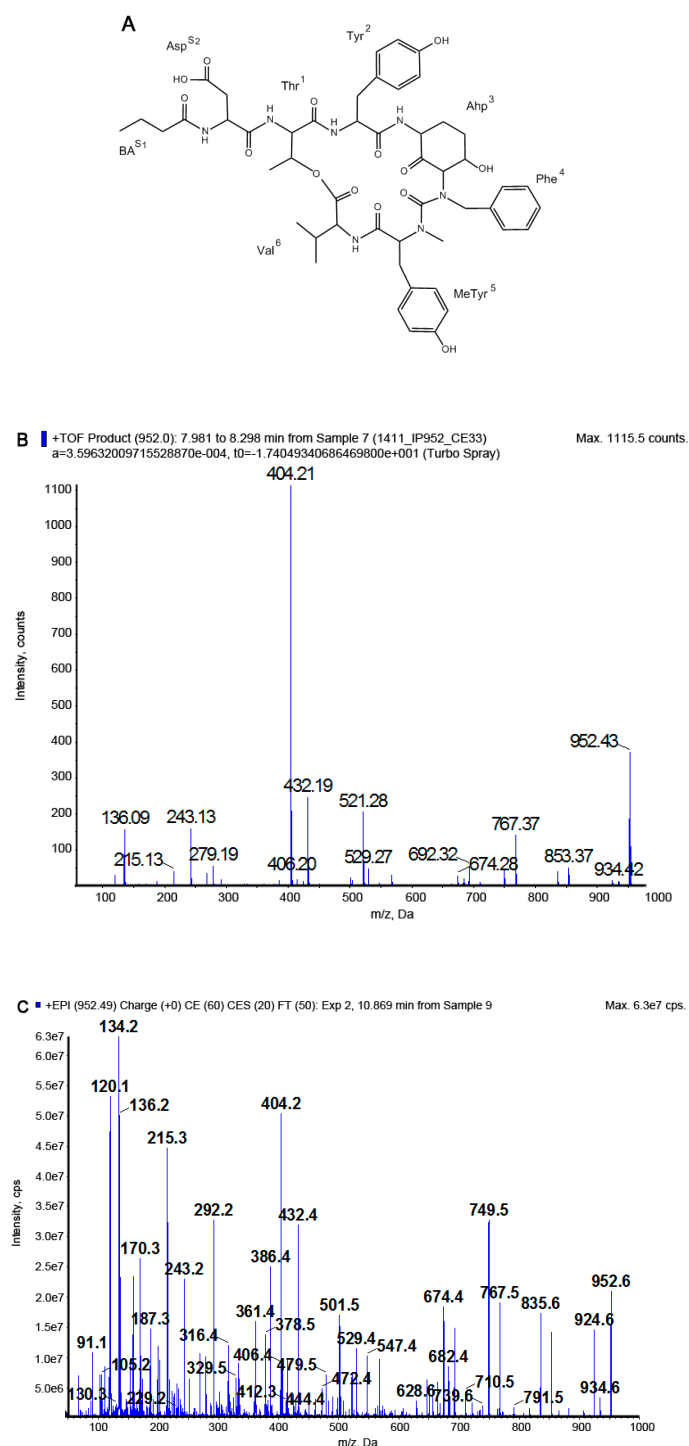


Figure S12. Chemical structure (A) and product ion mass spectra of cyanopeptolin CP969 [Thr+Tyr+Ahp+Phe+MePhe+Val]Asp+BA with precursor ion $[\text{M} + \text{H} - \text{H}_2\text{O}]^+$ at m/z 952. The spectra were recorded with application of QTOF (B) and QTRAP (C) mass spectrometers. The mass signals were assigned to the following fragments: 934 $[\text{M} + \text{H} - 2\text{H}_2\text{O}]^+$, 924 $[\text{M} + \text{H} - \text{H}_2\text{O} - \text{CO}]^+$, 853 $[\text{M} + \text{H} - \text{Val} - \text{H}_2\text{O}]^+$, 835 $[\text{M} + \text{H} - \text{Val} - 2\text{H}_2\text{O}]^+$, 791 $[\text{M} + \text{H} - \text{MePhe} - \text{H}_2\text{O}]^+$, 767 $[\text{M} + 2\text{H} - (\text{Asp} + \text{BA}) - \text{H}_2\text{O}]^+$, 749 $[\text{M} + 2\text{H} - (\text{Asp} + \text{BA}) - 2\text{H}_2\text{O}]^+$, 692 $[\text{M} + \text{H} - (\text{Val} + \text{MePhe}) - \text{H}_2\text{O}]^+$, 674 $[\text{M} + \text{H} - (\text{Val} + \text{MePhe}) - 2\text{H}_2\text{O}]^+$, 432 $[\text{M} + \text{H} - (\text{Val} + \text{MePhe} + \text{Phe} + \text{Ahp}) - \text{H}_2\text{O}]^+$, 414 $[\text{M} + \text{H} - (\text{Val} + \text{MePhe} + \text{Phe} + \text{Ahp}) - 2\text{H}_2\text{O}]^+$, 404 $[\text{Ahp} + \text{Phe} + \text{MePhe} + \text{H} - \text{H}_2\text{O}]^+$,

386 [BA + Asp + Thr + Val + H]⁺, 297 [Asp + Thr + Val + H - H₂O]⁺, 243 [Ahp + Phe + H - H₂O]⁺, 215 [Ahp + Phe + H - H₂O - CO]⁺, 134 MePhe immonium ion, 136 Tyr immonium ion, 120 Phe immonium ion.

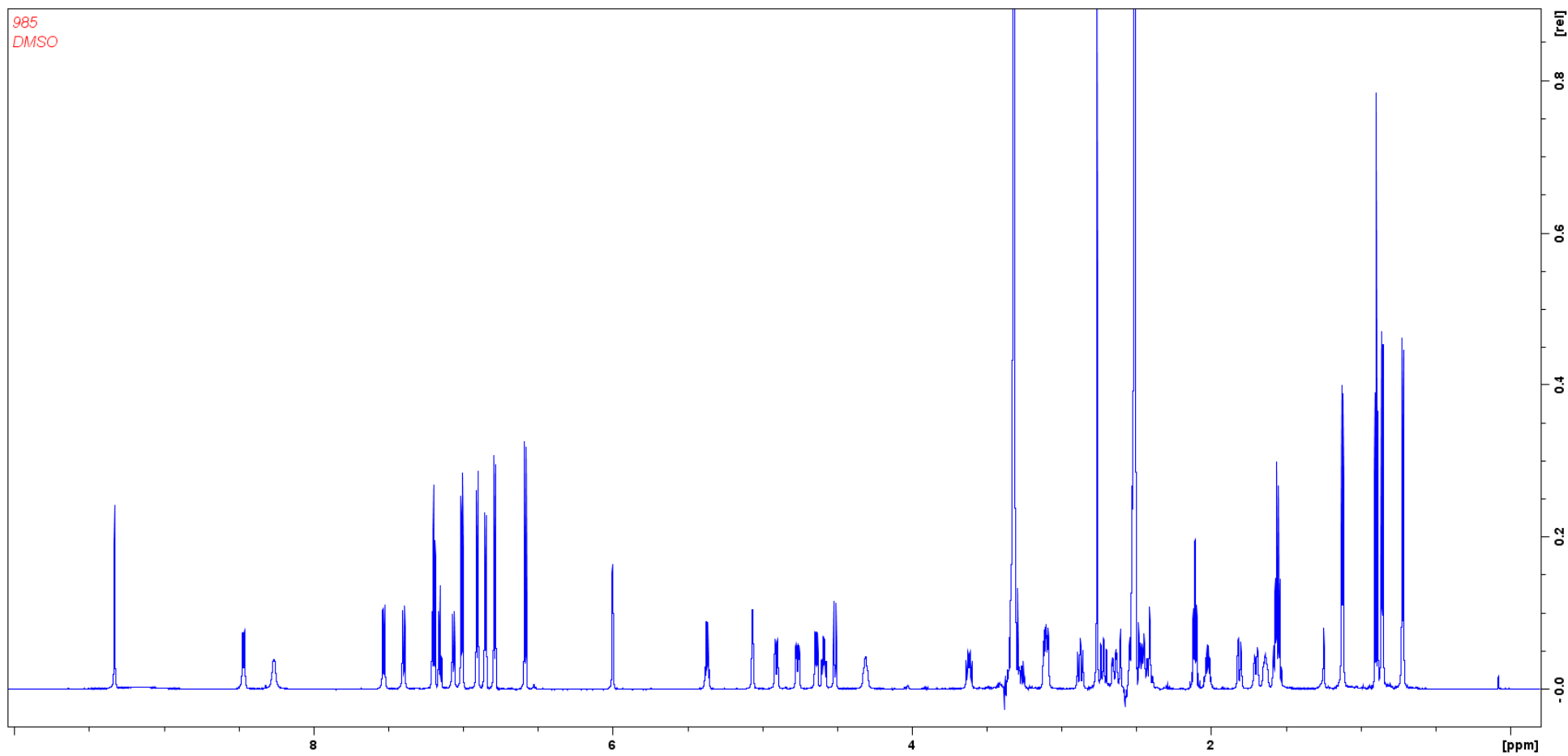


Figure S13. ^1H NMR Spectrum of cyanopeptolin CP985 in DMSO- d_6 .

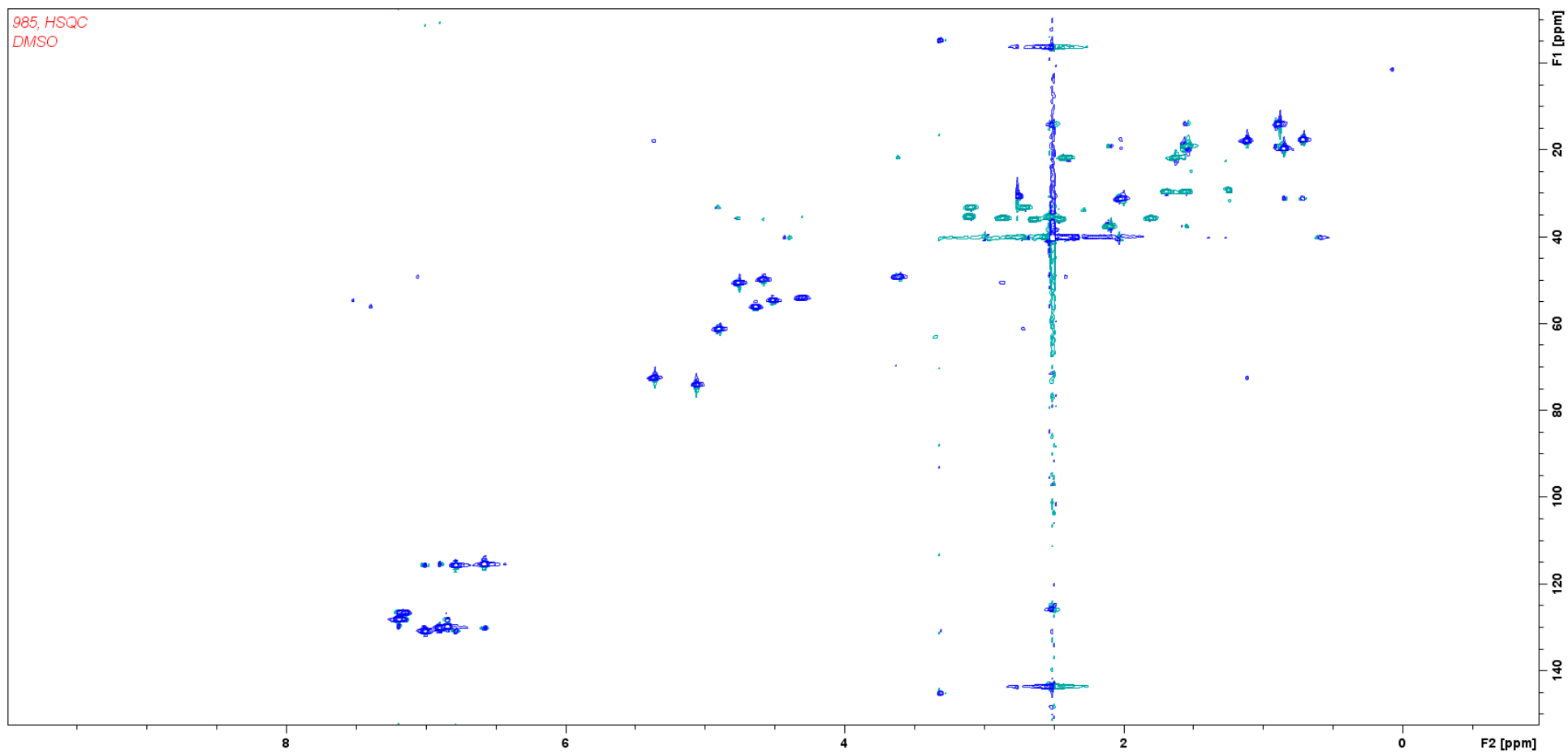


Figure S14. HSQC Spectrum of cyanopeptolin CP985 in DMSO- d_6 .

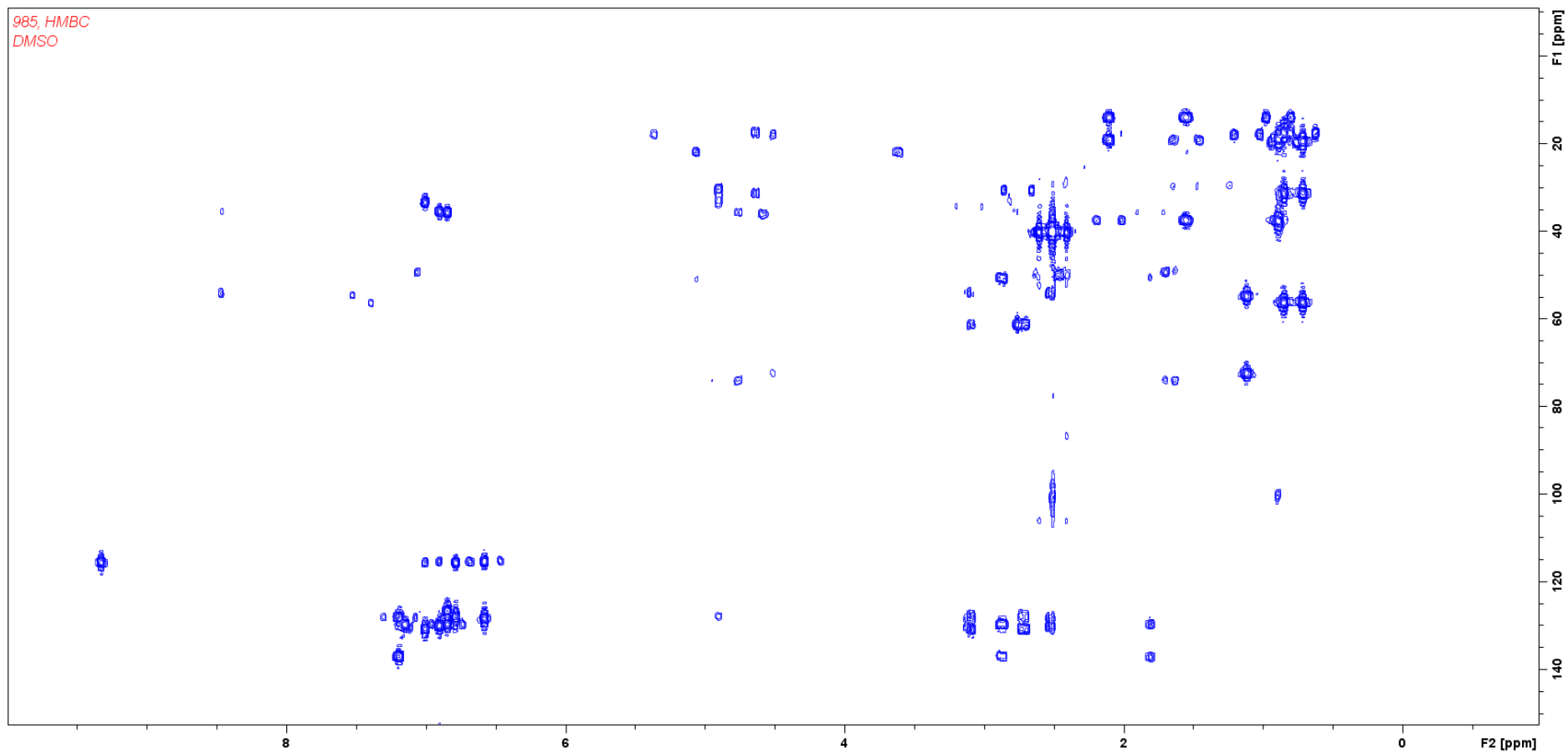


Figure S15a. HMBC Spectrum of cyanopeptolin CP985 in DMSO-d₆.

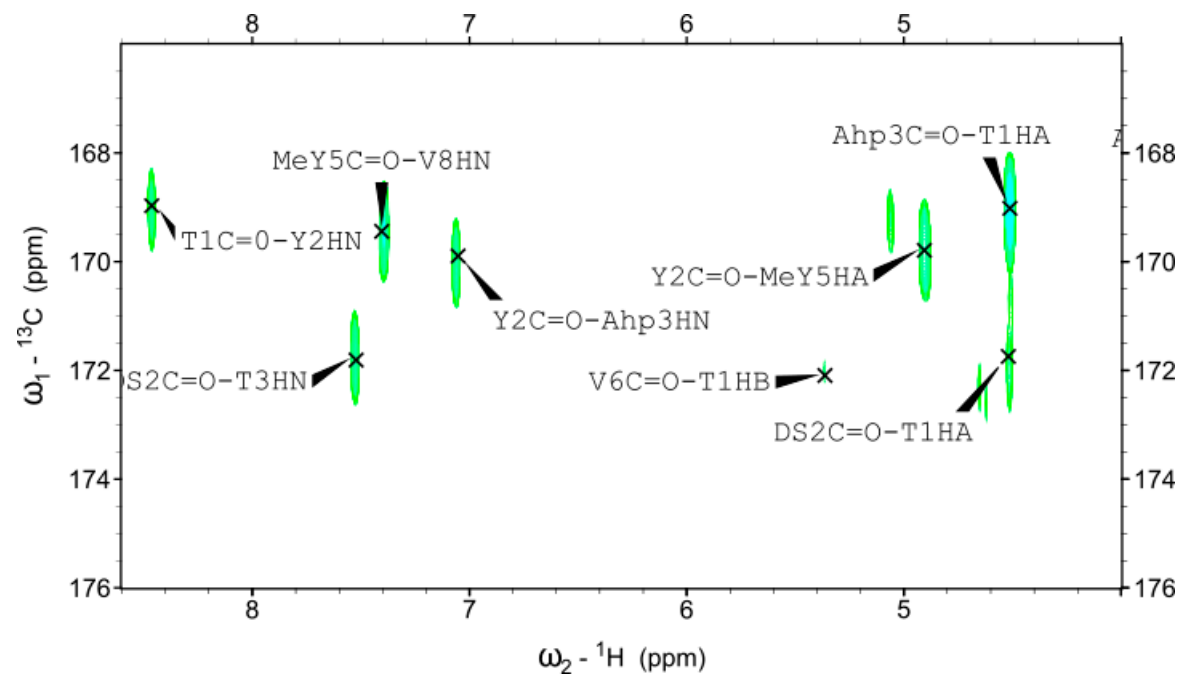


Figure S15b. Detailed NH – C=O region of the HMBC spectrum of cyanopeptolin CP985.

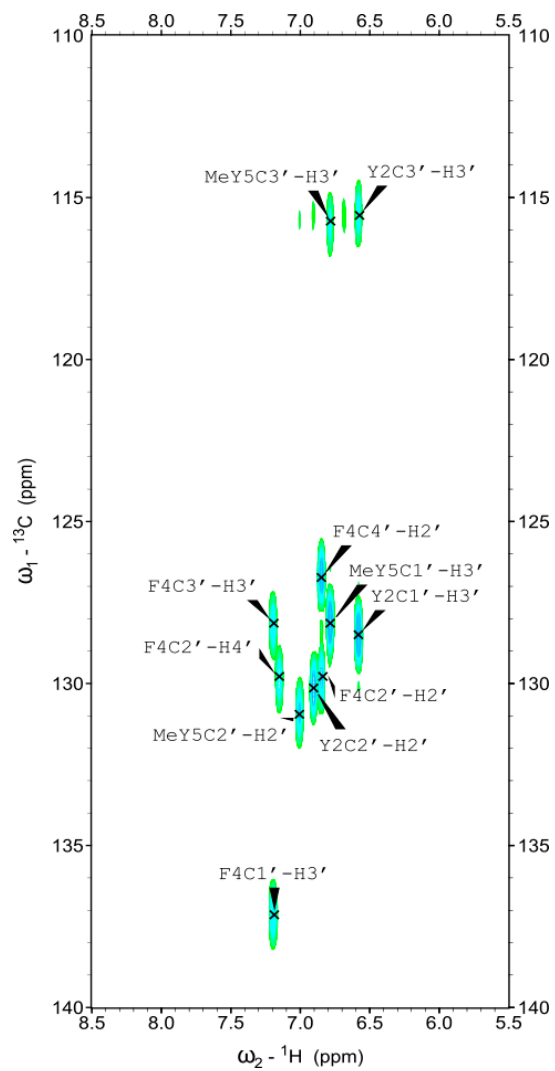


Figure S15c. Detailed aromatic region of the HMBC spectrum of cyanopeptolin CP985.

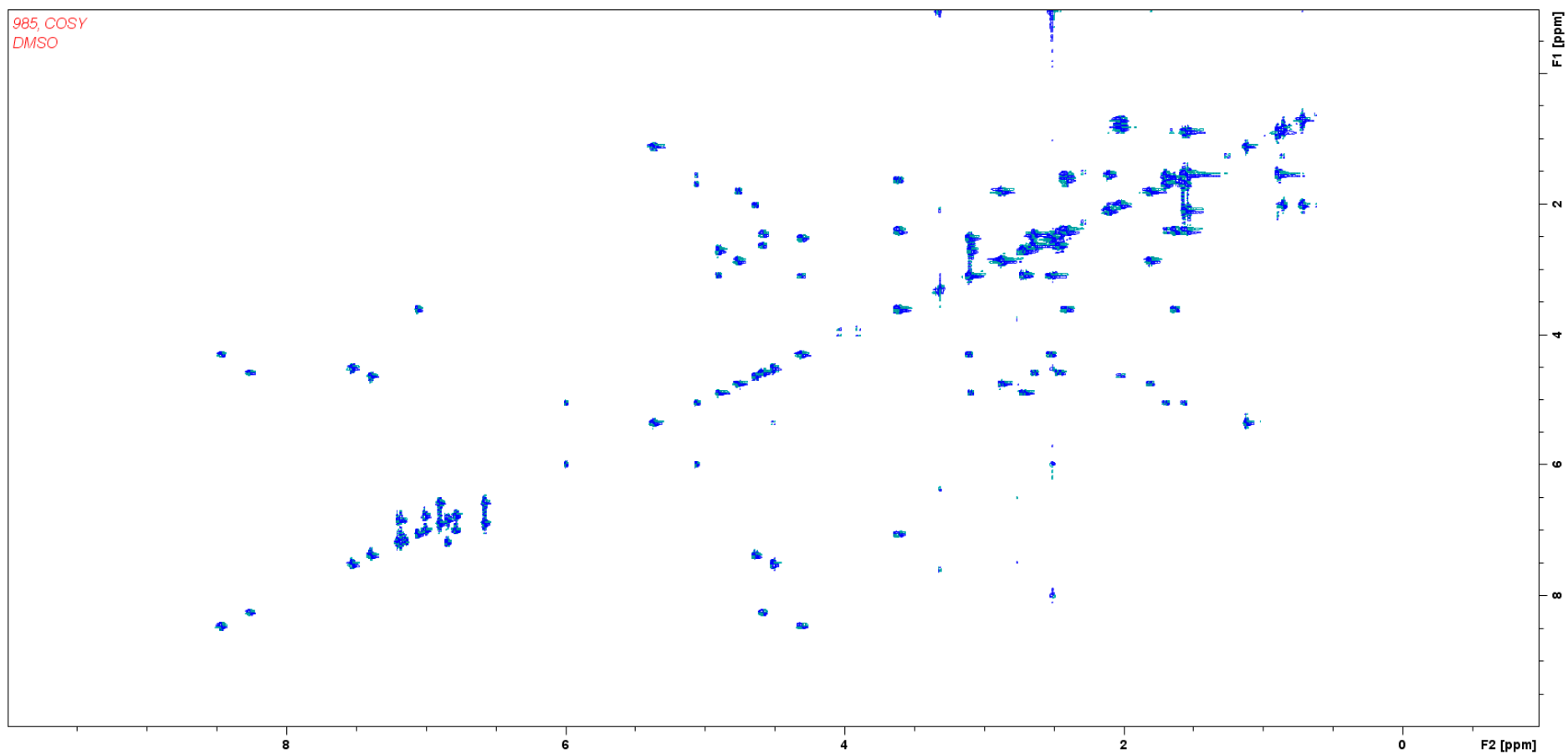


Figure S16. COSY Spectrum of cyanopeptolin CP985 in DMSO-d₆.

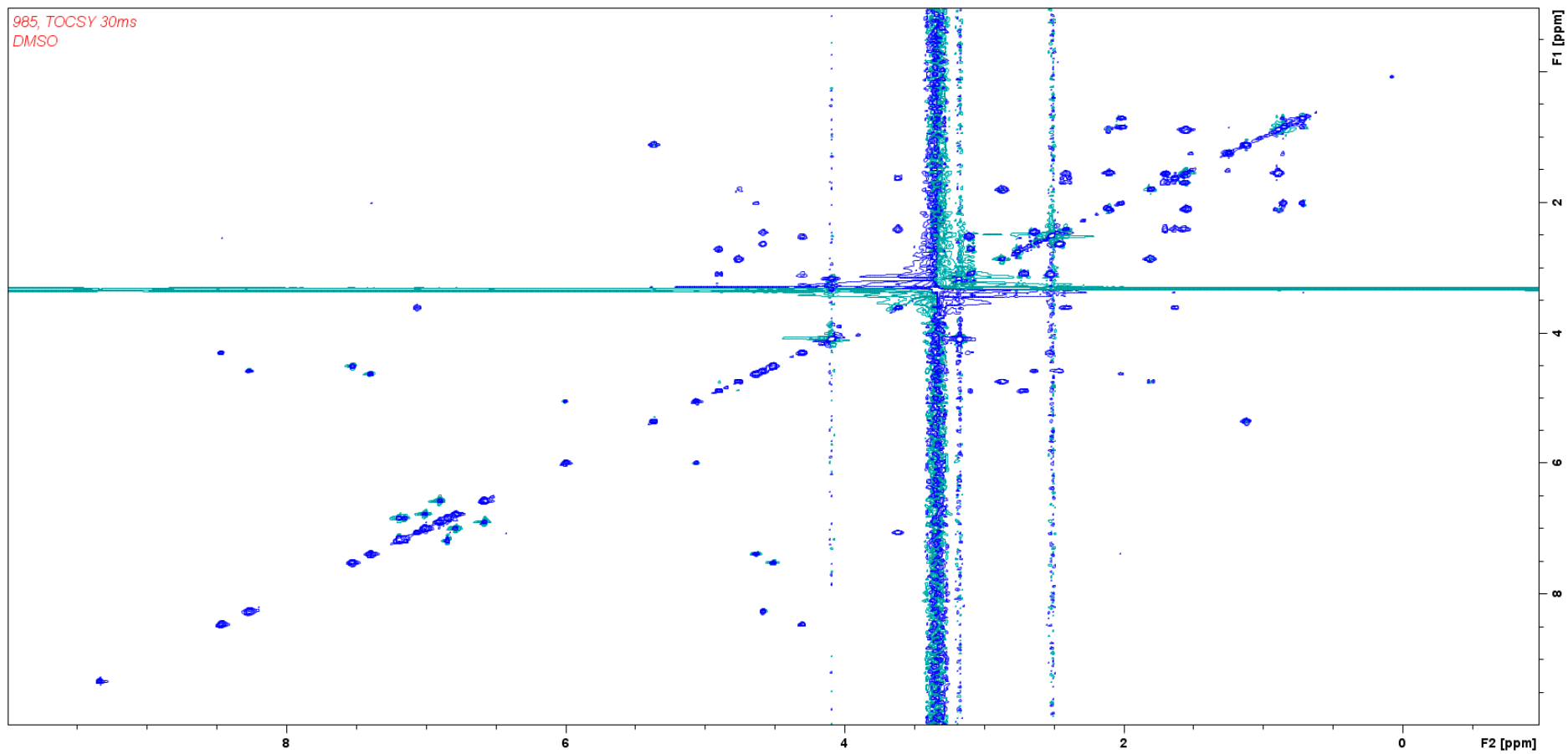


Figure S17a. TOCSY Spectrum of cyanopeptolin CP985 in DMSO-d₆.

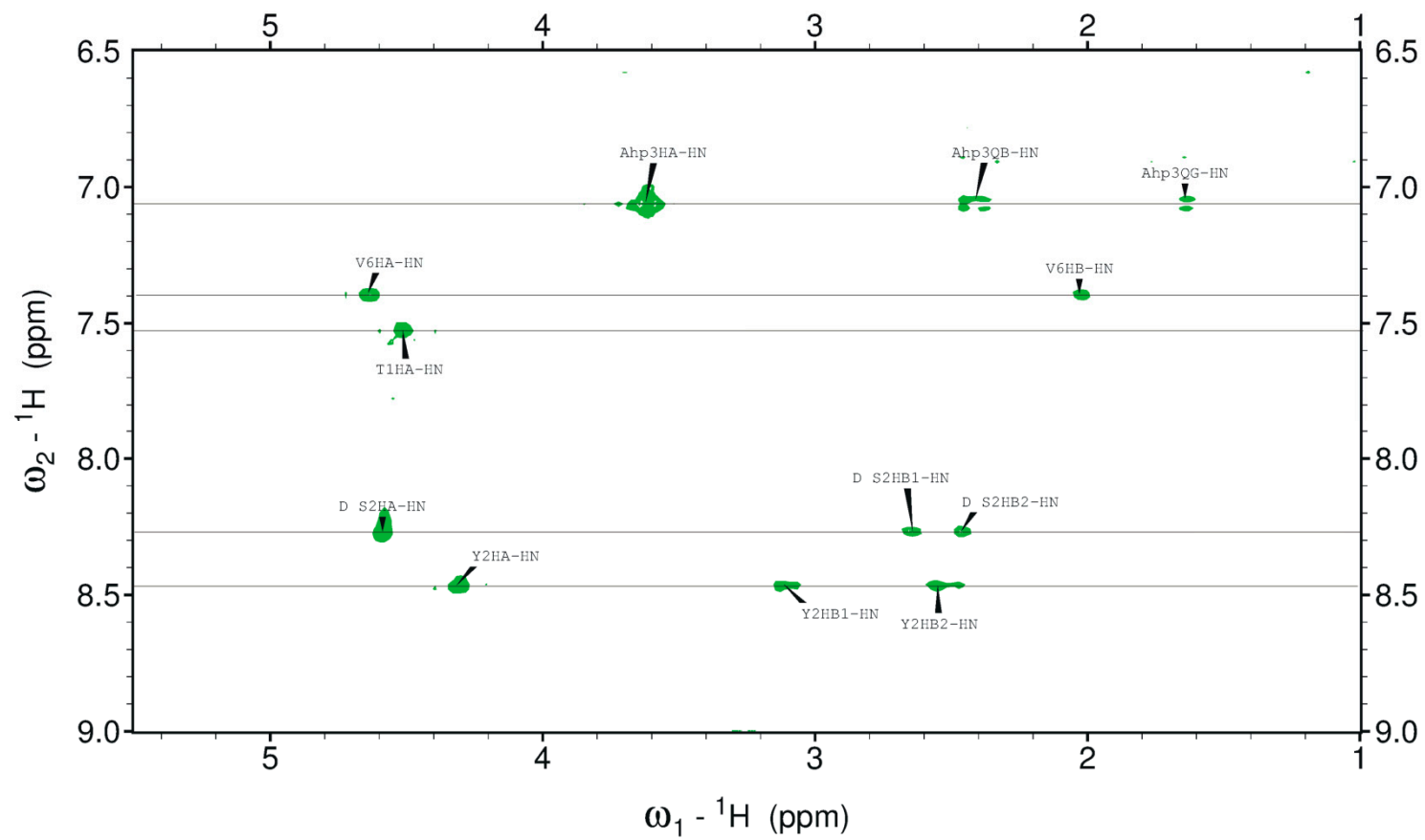


Figure S17b. Amino acid spin systems in the diagnostic region of the TOCSY spectrum of cyanopeptolin CP985.

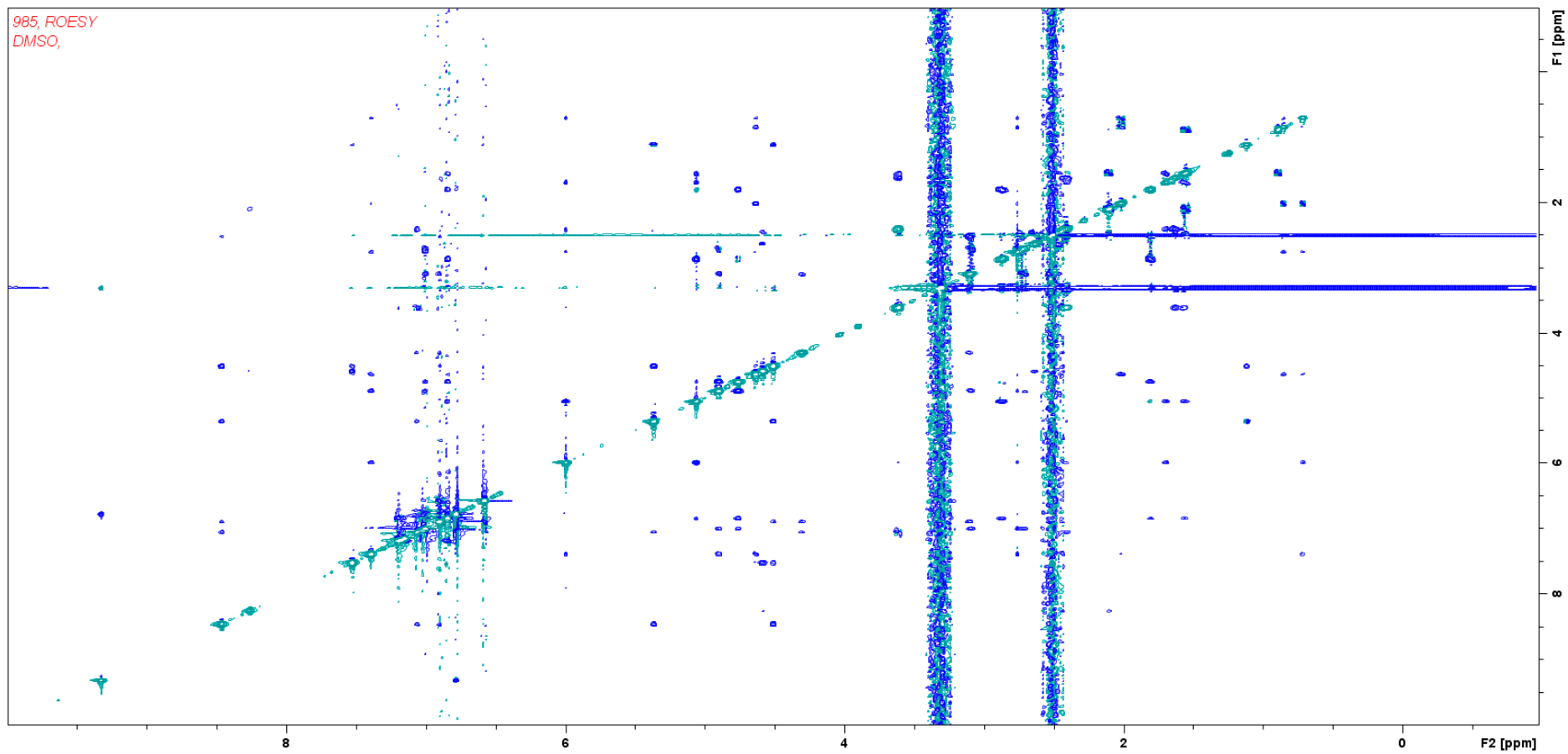


Figure S18a. ROESY Spectrum of cyanopeptolin CP985 in DMSO-d₆.

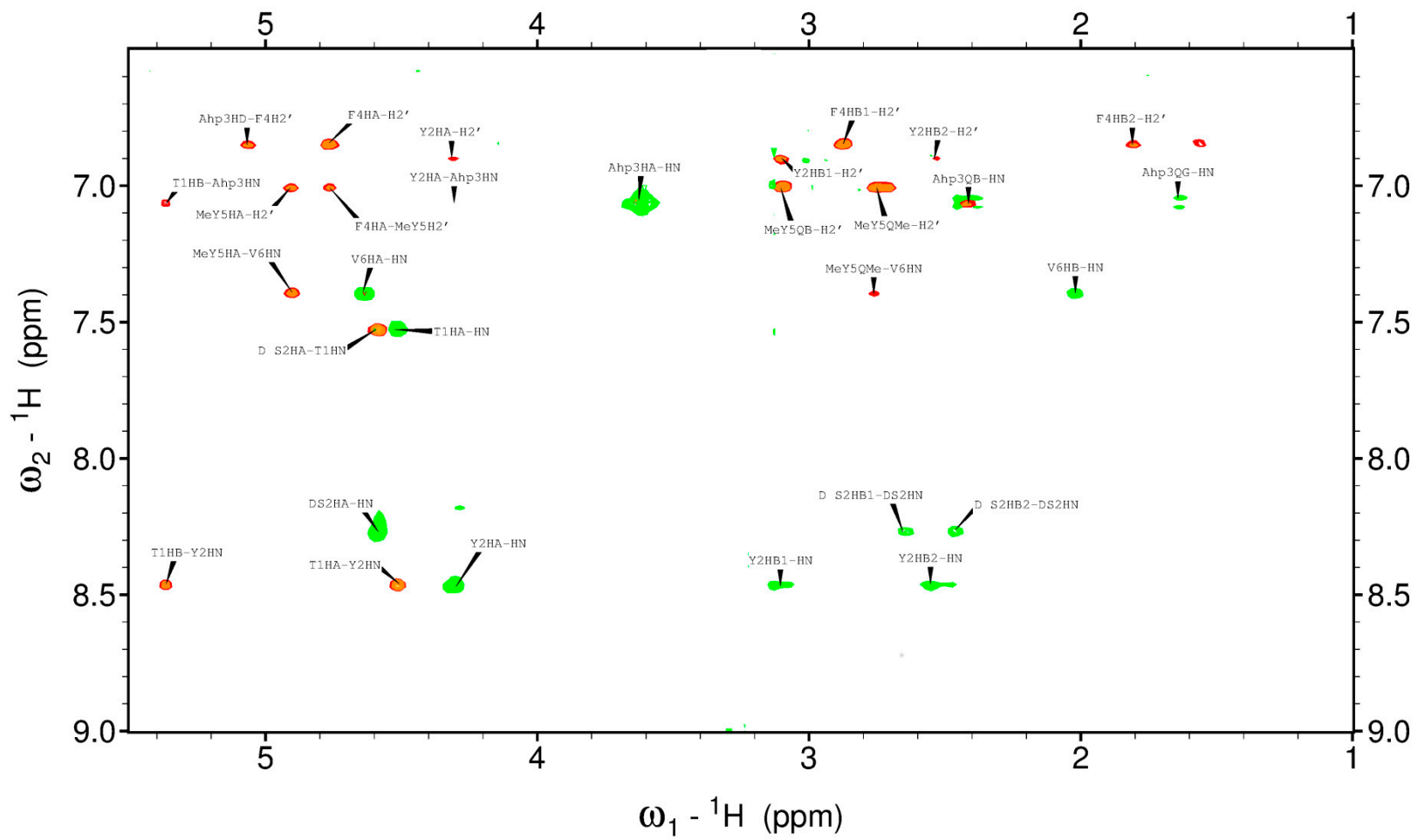


Figure S18b. Overlaid fragments of TOCSY (green) and ROESY (red) spectra of cyanopeptolin CP985.

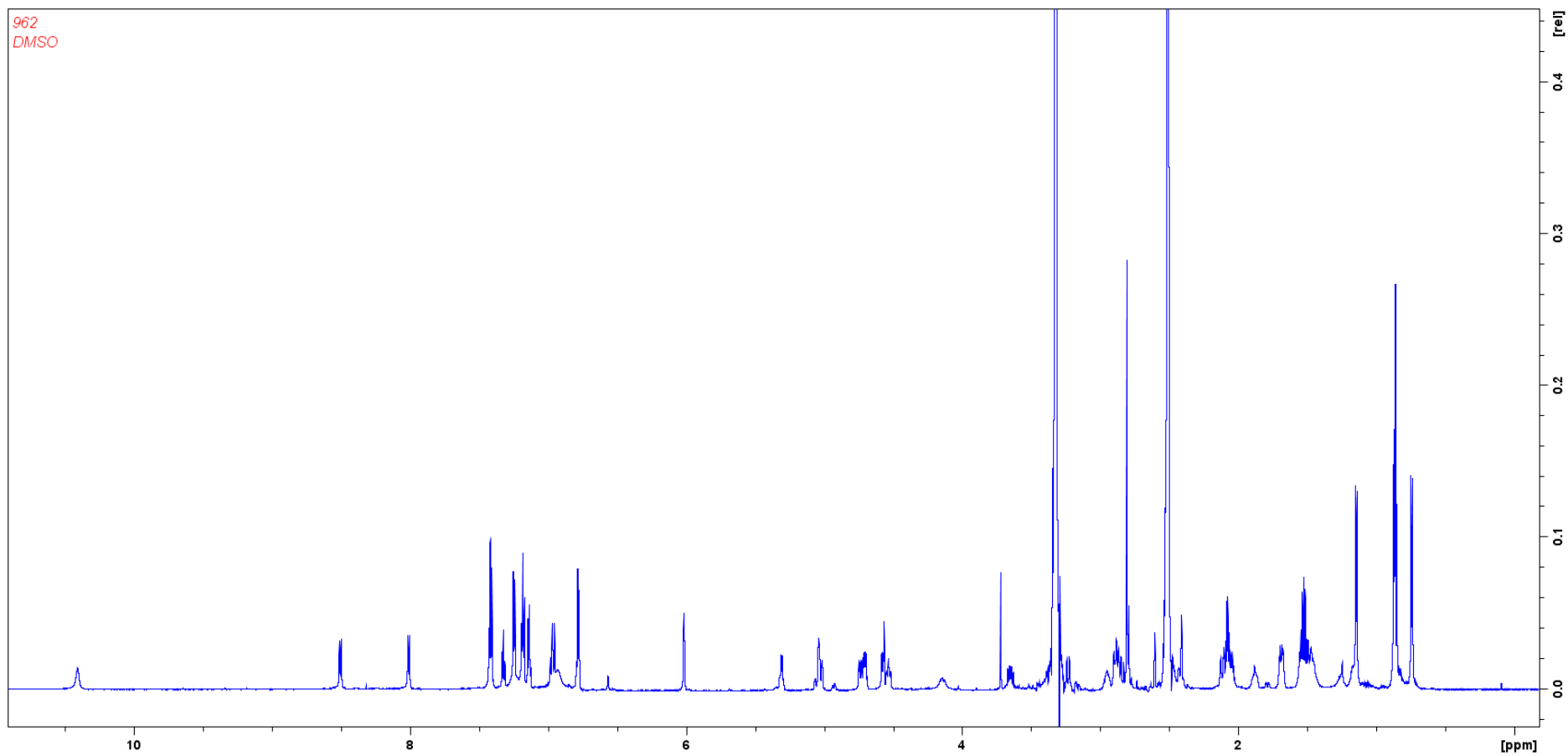


Figure S19. ^1H NMR Spectrum of cyanopeptolin CP962 in DMSO-d_6 .

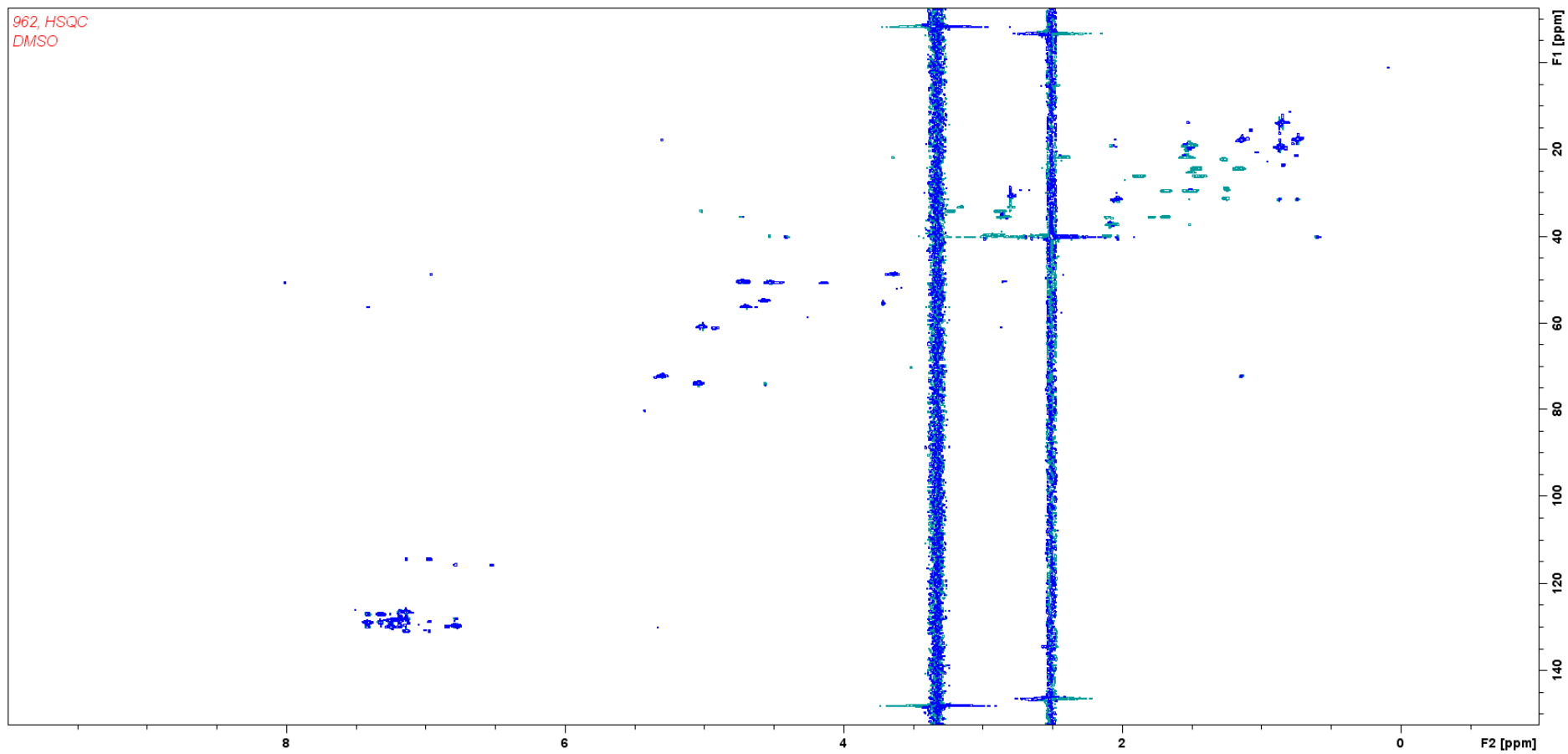


Figure S20. HSQC Spectrum of cyanopeptolin CP962 in DMSO-d₆.

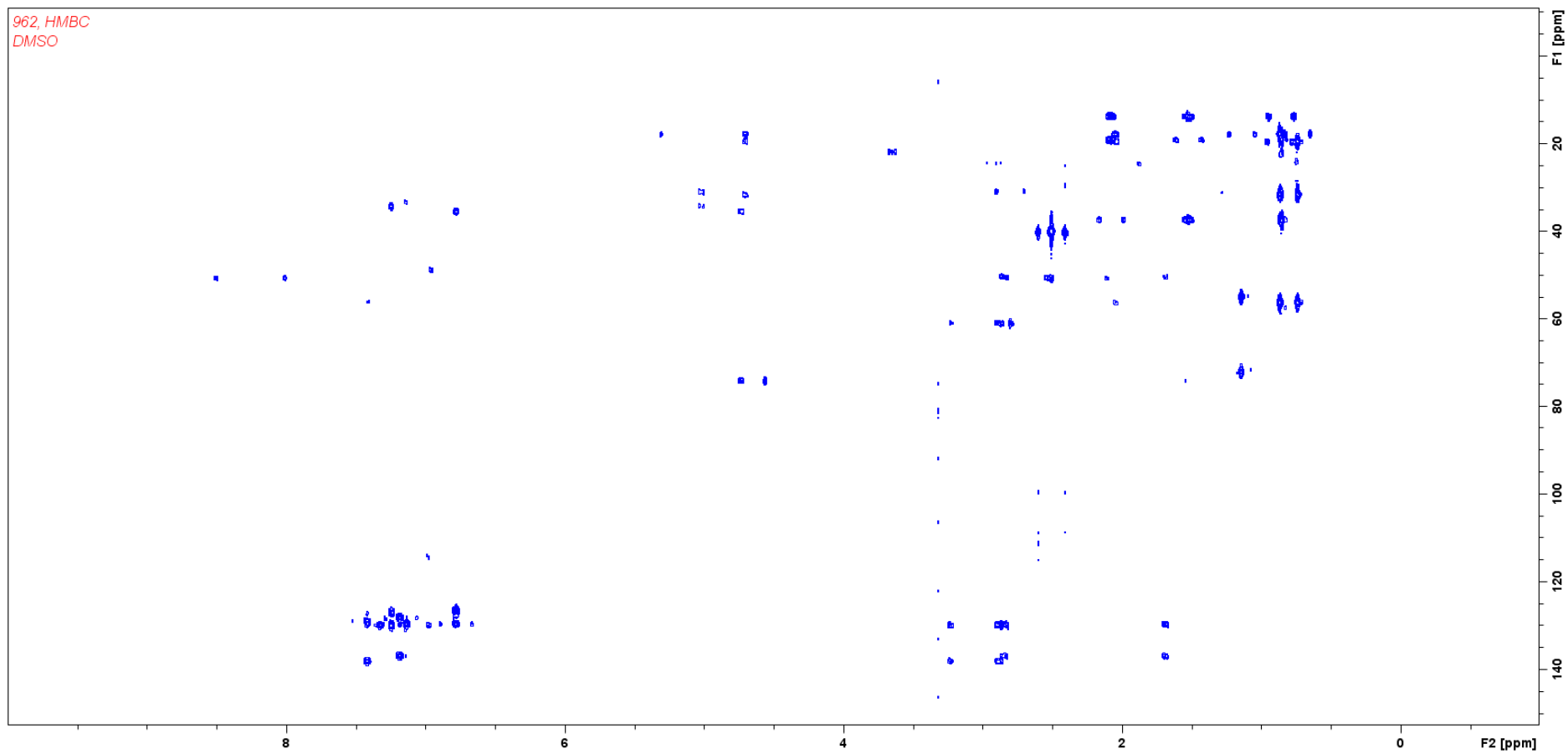


Figure S21a. HMBC Spectrum of cyanopeptolin CP962 in DMSO-d₆.

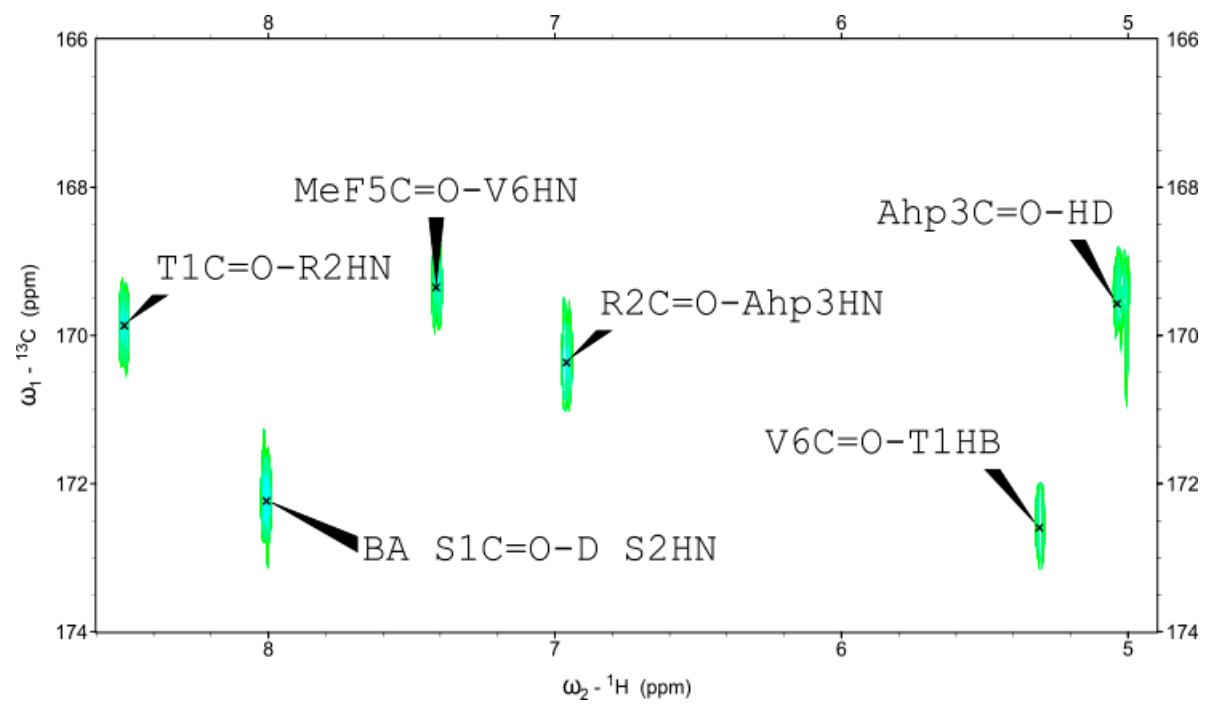


Figure S21b. Detailed NH - C=O region of the HMBC spectrum of cyanopeptolin CP962.

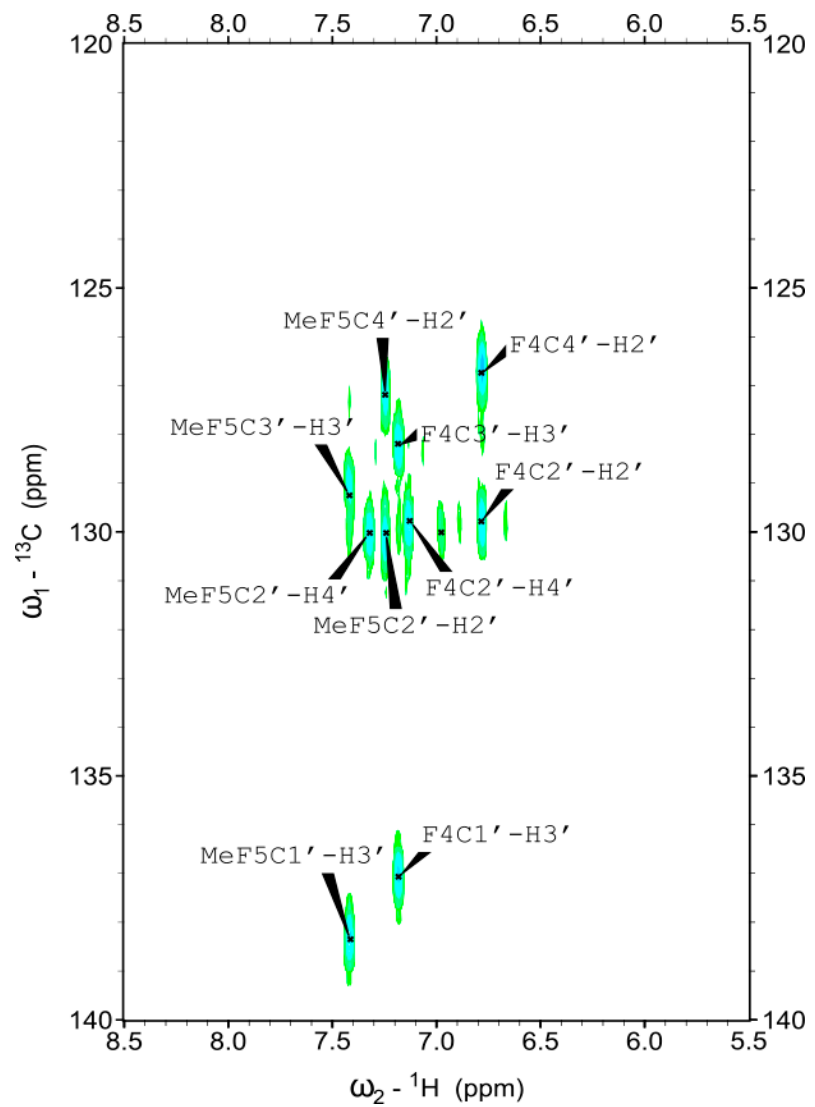


Figure S21c. Detailed aromatic region of the HMBC spectrum of cyanopeptolin CP962.

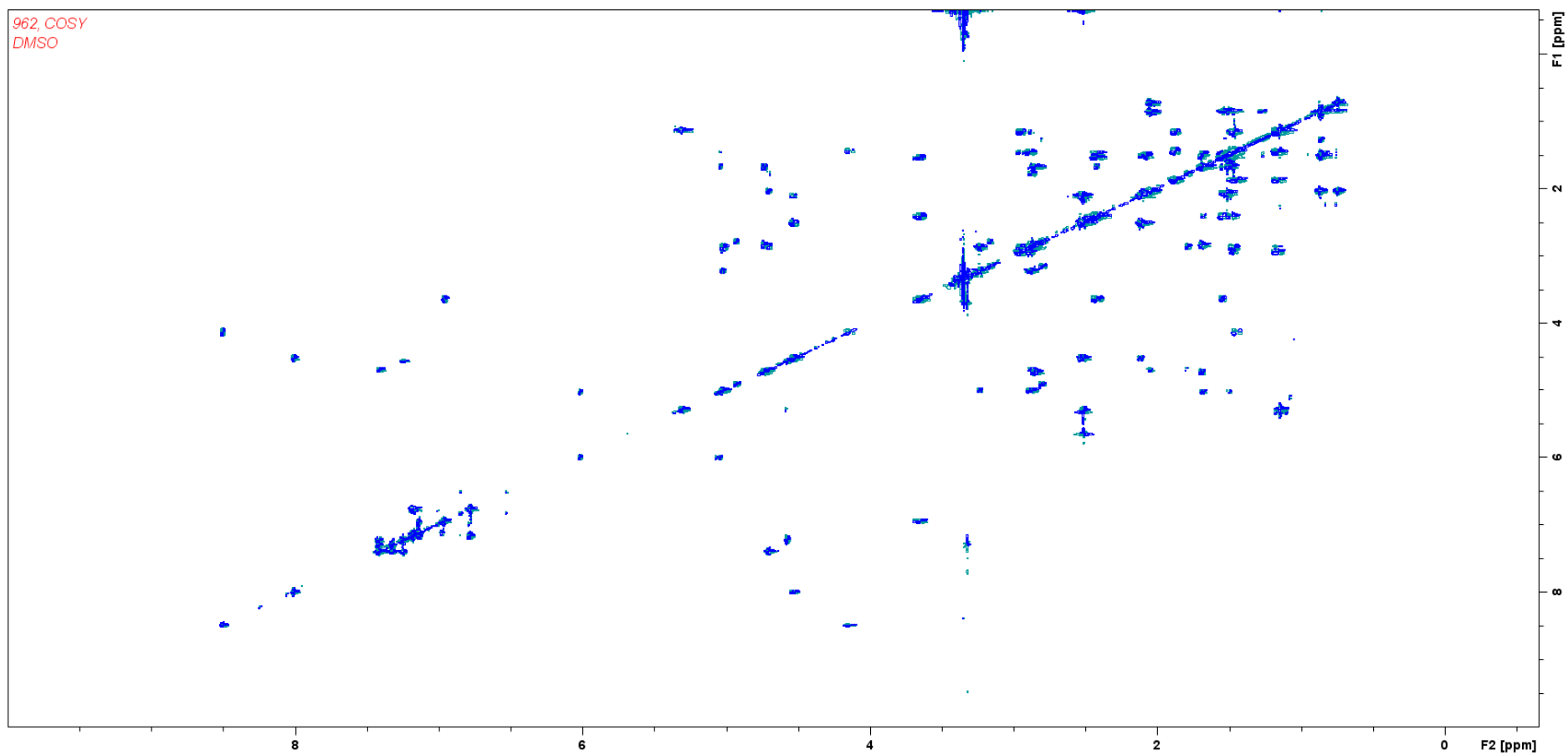


Figure S22. COSY Spectrum of cyanopeptolin CP962 in DMSO-d₆.

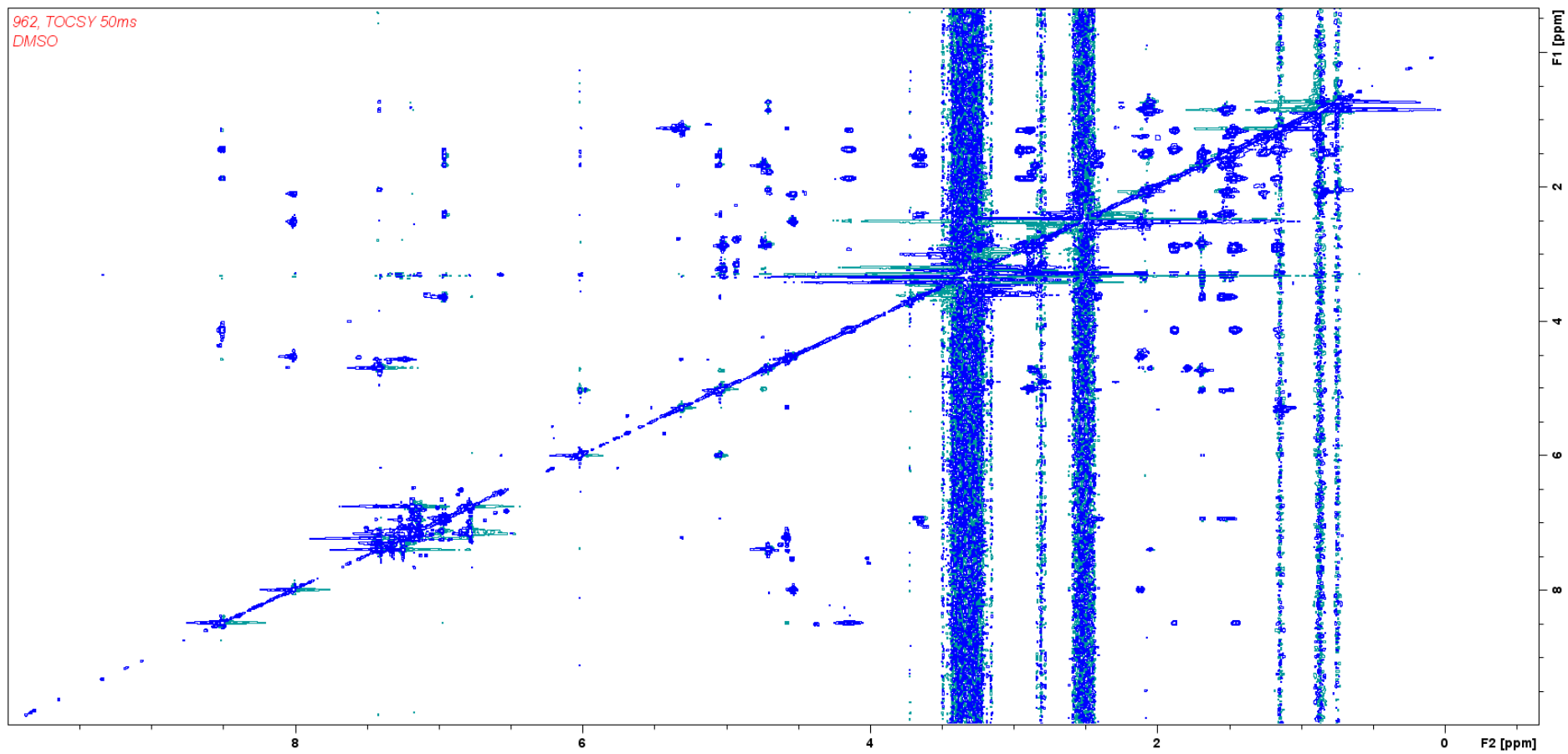


Figure S23a. TOCSY Spectrum of cyanopeptolin CP962 in DMSO-d₆.

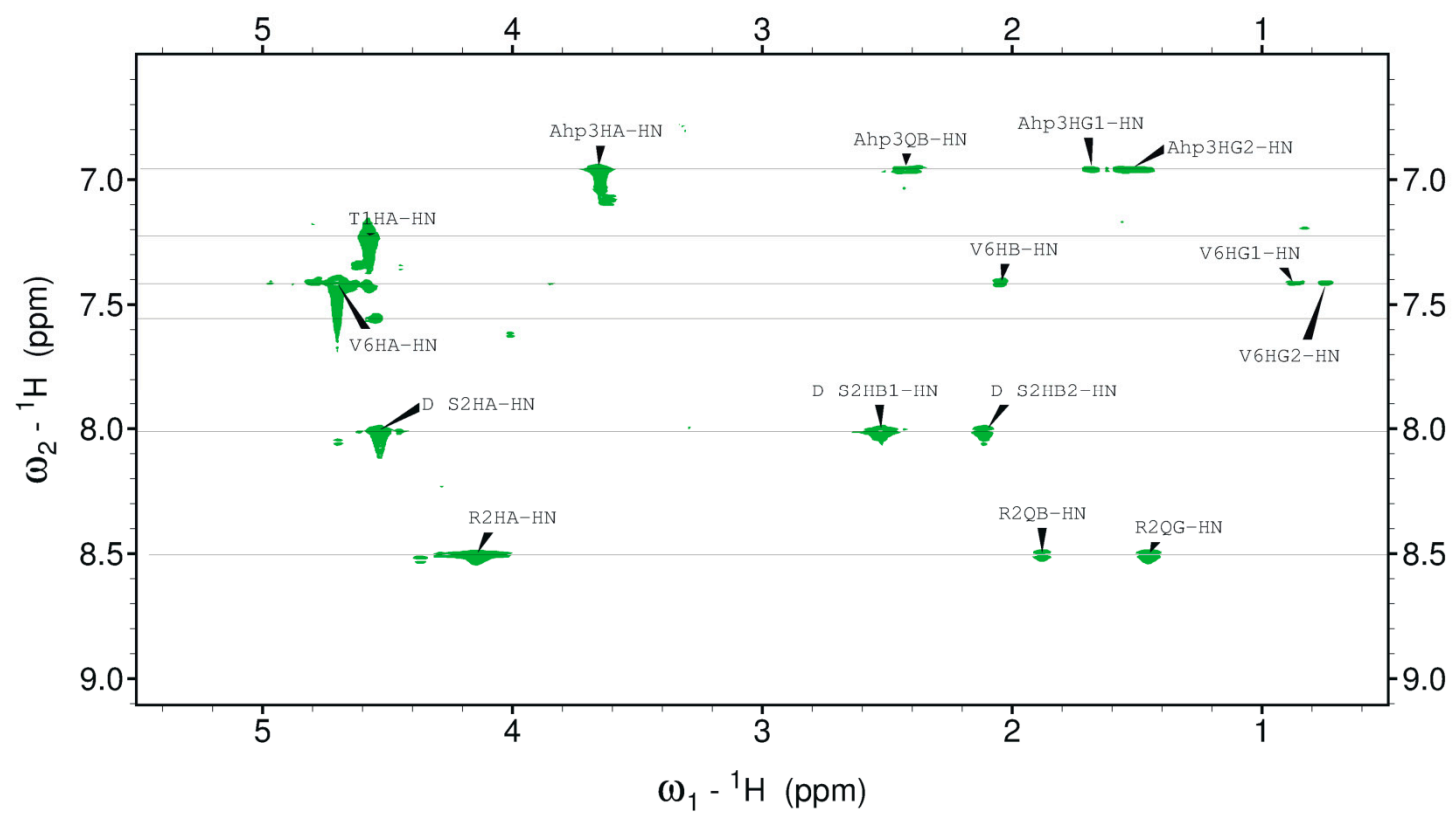


Figure S23b. Amino acid spin systems in the diagnostic region of the TOCSY spectrum of cyanopeptolin CP962.

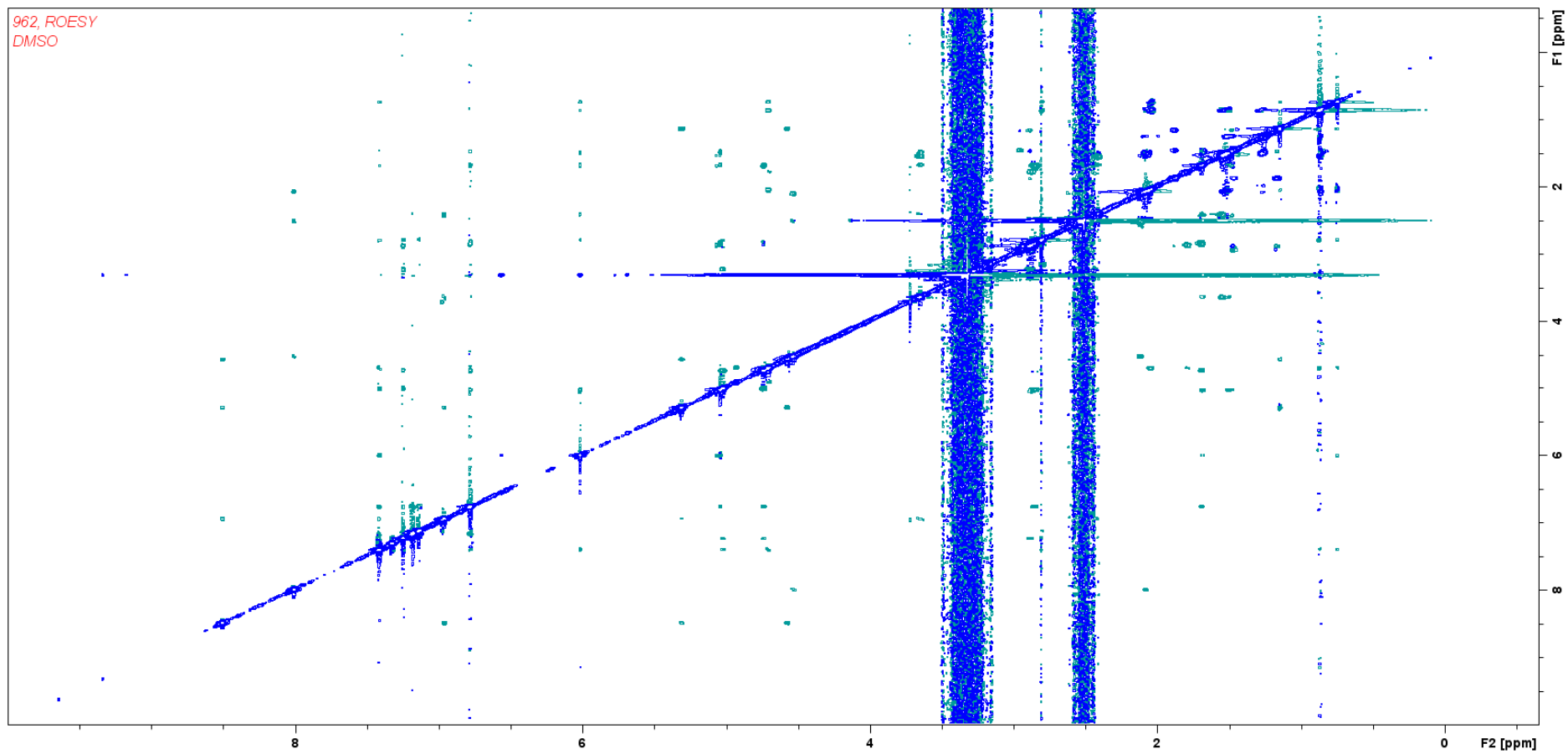


Figure S24a. ROESY Spectrum of cyanopeptolin CP962 in DMSO-d₆.

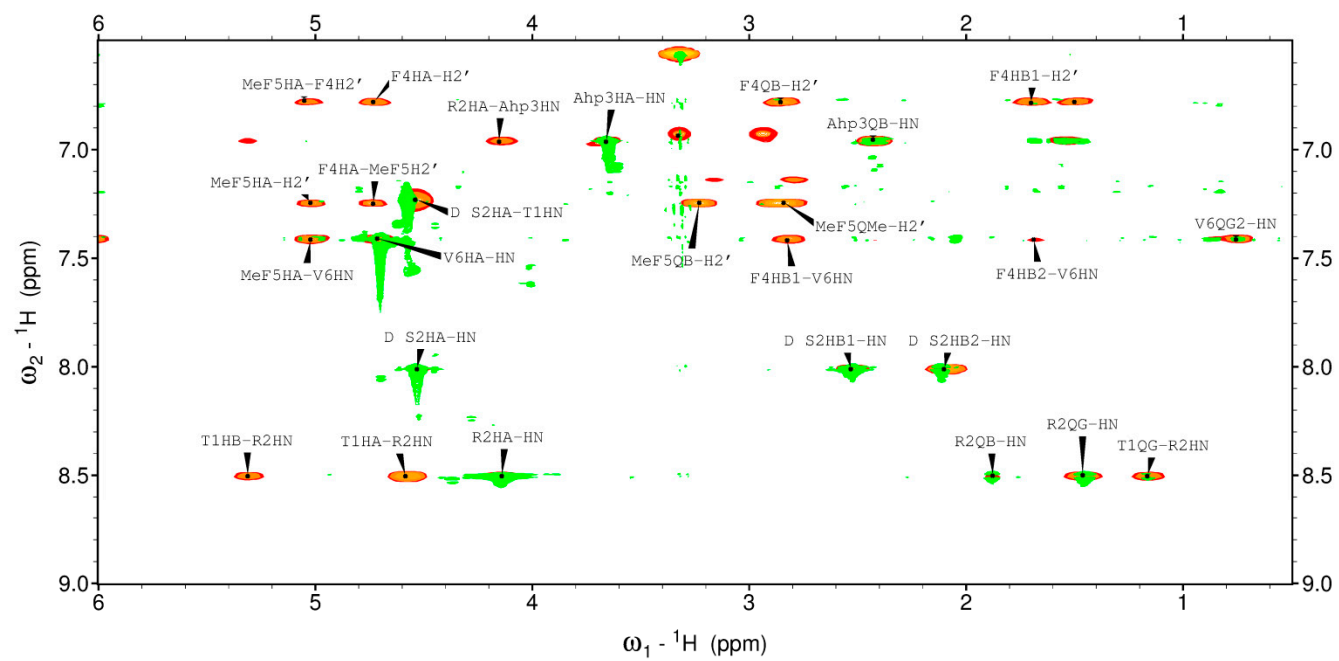


Figure S24b. Overlaid fragments of TOCSY (green) and ROESY (red) spectra of cyanopeptolin CP962.

Statement of Co-Authorship

Study design, biomass cultivation, extraction, fractionation and isolation: Hanna Mazur-Marzec, Christine Edwards
LC-MS/MS analysis, integration of data, manuscript preparation: Hanna Mazur-Marzec, Anna Fidor, Marta Ceglowska, Christine Edwards
Enzyme inhibition assays: Anna Fidor, Marta Ceglowska
MTT assays: Marie Goua, Jenny Macaskill
NMR analysis: Ewa Wieczerek, Magdalena Kropidowska

I, the undersigned, acknowledge the above contribution of work undertaken for the published work "Cyanopeptolins with trypsin and chymotrypsin inhibitory activity from the cyanobacterium *Nostoc edaphicum* CCNP1411" (*Marine Drugs*, 2018, DOI:10.3390/md16070220) contributing to the dissertation "Peptides produced by the Baltic cyanobacterium *Nostoc edaphicum* CCNP1411 – structure and biological activity".

The contribution to the work was: LC-MS/MS analyses, interpretation of data, edition of the manuscript and enzyme inhibition assays.

.....

(Anna Fidor)

Statement of Co-Authorship

Study design, biomass cultivation, extraction, fractionation and isolation: Hanna Mazur-Marzec, Christine Edwards
LC-MS/MS analysis, integration of data, manuscript preparation: Hanna Mazur-Marzec, Anna Fidor, Marta Ceglowska, Christine Edwards
Enzyme inhibition assays: Anna Fidor, Marta Ceglowska
MTT assays: Marie Goua, Jenny Macaskill
NMR analysis: Ewa Wieczerek, Magdalena Kropidowska

I, the undersigned, acknowledge the above contribution of work undertaken for the published work "Cyanopeptolins with trypsin and chymotrypsin inhibitory activity from the cyanobacterium *Nostoc edaphicum* CCNP1411" (*Marine Drugs*, 2018, DOI:10.3390/md16070220) contributing to the dissertation "Peptides produced by Baltic cyanobacterium *Nostoc edaphicum* CCNP1411 - structure and biological activity".

The contribution to the work was methodology development, compounds isolation, LC-MS/MS analyses, interpretation of data and writing the manuscript.


.....

(Hanna Mazur-Marzec)

Statement of Co-Authorship

Study design, biomass cultivation, extraction, fractionation and isolation: Hanna Mazur-Marzec, Christine Edwards
LC-MS/MS analysis, integration of data, manuscript preparation: Hanna Mazur-Marzec, Anna Fidor, Marta Ceglowska, Christine Edwards
Enzyme inhibition assays: Anna Fidor, Marta Ceglowska
MTT assays: Marie Goua, Jenny Macaskill
NMR analysis: Ewa Wieczerek, Magdalena Kropidowska

I, the undersigned, acknowledge the above contribution of work undertaken for the published work "Cyanopeptolins with trypsin and chymotrypsin inhibitory activity from the cyanobacterium *Nostoc edaphicum* CCNP1411" (*Marine Drugs*, 2018, DOI:10.3390/md16070220) contributing to the dissertation "Peptides produced by Baltic cyanobacterium *Nostoc edaphicum* CCNP1411 - structure and biological activity".

The assessment of my and PhD candidate (Anna Fidor) contribution to the work is 6 % and 34 %.


.....

(Marta Ceglowska)

Statement of Co-Authorship

Study design, biomass cultivation, extraction, fractionation and isolation: Hanna Mazur-Marzec, Christine Edwards
LC-MS/MS analysis, integration of data, manuscript preparation: Hanna Mazur-Marzec, Anna Fidor, Marta Cegłowska, Christine Edwards
Enzyme inhibition assays: Anna Fidor, Marta Cegłowska
MTT assays: Marie Goua, Jenny Macaskill
NMR analysis: Ewa Wieczerzak, Magdalena Kropidłowska

I, the undersigned, acknowledge the above contribution of work undertaken for the published work "Cyanopeptolins with trypsin and chymotrypsin inhibitory activity from the cyanobacterium *Nostoc edaphicum* CCNP1411" (*Marine Drugs*, 2018, DOI:10.3390/md16070220) contributing to the dissertation "Peptides produced by Baltic cyanobacterium *Nostoc edaphicum* CCNP1411 - structure and biological activity".

The assessment of my and PhD candidate (Anna Fidor) contribution to the work is 5 % and 34 %.



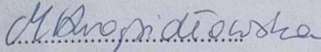
(Ewa Wieczerzak)

Statement of Co-Authorship

Study design, biomass cultivation, extraction, fractionation and isolation: Hanna Mazur-Marzec, Christine Edwards
LC-MS/MS analysis, integration of data, manuscript preparation: Hanna Mazur-Marzec, Anna Fidor, Marta Cegłowska, Christine Edwards
Enzyme inhibition assays: Anna Fidor, Marta Cegłowska
MTT assays: Marie Goua, Jenny Macaskill
NMR analysis: Ewa Wieczerzak, Magdalena Kropidłowska

I, the undersigned, acknowledge the above contribution of work undertaken for the published work "Cyanopeptolins with trypsin and chymotrypsin inhibitory activity from the cyanobacterium *Nostoc edaphicum* CCNP1411" (*Marine Drugs*, 2018, DOI:10.3390/md16070220) contributing to the dissertation "Peptides produced by Baltic cyanobacterium *Nostoc edaphicum* CCNP1411 - structure and biological activity".

The assessment of my and PhD candidate (Anna Fidor) contribution to the work is 5 % and 34 %.




(Magdalena Kropidłowska)

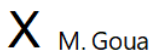
Statement of Co-Authorship

Study design, biomass cultivation, extraction, fractionation and isolation: Hanna Mazur-Marzec, Christine Edwards
LC-MS/MS analysis, integration of data, manuscript preparation: Hanna Mazur-Marzec, Anna Fidor, Marta Cegłowska, Christine Edwards
Enzyme inhibition assays: Anna Fidor, Marta Cegłowska
MTT assays: Marie Goua, Jenny Macaskill
NMR analysis: Ewa Wieczerzak, Magdalena Kropidłowska

I, the undersigned, acknowledge the above contribution of work undertaken for the published work "Cyanopeptolins with trypsin and chymotrypsin inhibitory activity from the cyanobacterium *Nostoc edaphicum* CCNP1411" (*Marine Drugs*, 2018, DOI:10.3390/md16070220) contributing to the dissertation "Peptides produced by Baltic cyanobacterium *Nostoc edaphicum* CCNP1411 - structure and biological activity".

The assessment of my and PhD candidate (Anna Fidor) contribution to the work is 5 % and 34 %.

 Odwracalny podpis



Dr Marie Goua

Co-author

Podpisany przez: Marie Goua

(Marie Goua)

Statement of Co-Authorship

Study design, biomass cultivation, extraction, fractionation and isolation: Hanna Mazur-Marzec, Christine Edwards

LC-MS/MS analysis, integration of data, manuscript preparation: Hanna Mazur-Marzec, Anna Fidor, Marta Ceglowska, Christine Edwards

Enzyme inhibition assays: Anna Fidor, Marta Ceglowska

MTT assays: Marie Goua, Jenny Macaskill

NMR analysis: Ewa Wieczerzak, Magdalena Kropidłowska

I, the undersigned, acknowledge the above contribution of work undertaken for the published work "Cyanopeptolins with trypsin and chymotrypsin inhibitory activity from the cyanobacterium *Nostoc edaphicum* CCNP1411" (*Marine Drugs*, 2018, DOI:10.3390/md16070220) contributing to the dissertation "Peptides produced by Baltic cyanobacterium *Nostoc edaphicum* CCNP1411 - structure and biological activity".

The assessment of my and PhD candidate (Anna Fidor) contribution to the work is 5 % and 34 %.



(Jenny Macaskill)

Statement of Co-Authorship

Study design, biomass cultivation, extraction, fractionation and isolation: Hanna Mazur-Marzec, Christine Edwards

LC-MS/MS analysis, integration of data, manuscript preparation: Hanna Mazur-Marzec, Anna Fidor, Marta Ceglowska, Christine Edwards

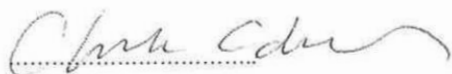
Enzyme inhibition assays: Anna Fidor, Marta Ceglowska

MTT assays: Marie Goua, Jenny Macaskill

NMR analysis: Ewa Wieczerzak, Magdalena Kropidłowska

I, the undersigned, acknowledge the above contribution of work undertaken for the published work "Cyanopeptolins with trypsin and chymotrypsin inhibitory activity from the cyanobacterium *Nostoc edaphicum* CCNP1411" (*Marine Drugs*, 2018, DOI:10.3390/md16070220) contributing to the dissertation "Peptides produced by Baltic cyanobacterium *Nostoc edaphicum* CCNP1411 - structure and biological activity".

The assessment of my and PhD candidate (Anna Fidor) contribution to the work is 6 % and 34 %.







(Christine Edwards)

Publication 3



Article

Nostoc edaphicum CCNP1411 from the Baltic Sea—A New Producer of Nostocyclopeptides

Anna Fidor ¹, Michał Grabski ², Jan Gawor ³, Robert Gromadka ³, Grzegorz Węgrzyn ²
and Hanna Mazur-Marzec ^{1,*}

¹ Division of Marine Biotechnology, Faculty of Oceanography and Geography, University of Gdańsk, Marszałka J. Piłsudskiego 46, PL-81378 Gdynia, Poland; anna.fidor@phdstud.ug.edu.pl

² Department of Molecular Biology, University of Gdansk, Wita Stwosza 59, 80-308 Gdansk, Poland; michal.grabski@phdstud.ug.edu.pl (M.G.); grzegorz.wegrzyn@biol.ug.edu.pl (G.W.)

³ DNA Sequencing and Oligonucleotide Synthesis Laboratory, Polish Academy of Sciences, Institute of Biochemistry and Biophysics, 02-106 Warsaw, Poland; gaworj@ibb.waw.pl (J.G.); robert@ibb.waw.pl (R.G.)

* Correspondence: hanna.mazur-marzec@ug.edu.pl; Tel.: +48-58-523-66-21 or +48-609-419-132

Received: 31 July 2020; Accepted: 25 August 2020; Published: 26 August 2020



Abstract: Nostocyclopeptides (Ncps) constitute a small class of nonribosomal peptides, exclusively produced by cyanobacteria of the genus *Nostoc*. The peptides inhibit the organic anion transporters, OATP1B3 and OATP1B1, and prevent the transport of the toxic microcystins and nodularin into hepatocytes. So far, only three structural analogues, Ncp-A1, Ncp-A2 and Ncp-M1, and their linear forms were identified in *Nostoc* strains as naturally produced cyanometabolites. In the current work, the whole genome sequence of the new Ncps producer, *N. edaphicum* CCNP1411 from the Baltic Sea, has been determined. The genome consists of the circular chromosome (7,733,505 bps) and five circular plasmids (from 44.5 kb to 264.8 kb). The nostocyclopeptide biosynthetic gene cluster (located between positions 7,609,981–7,643,289 bps of the chromosome) has been identified and characterized *in silico*. The LC-MS/MS analyzes of *N. edaphicum* CCNP1411 cell extracts prepared in aqueous methanol revealed several products of the genes. Besides the known peptides, Ncp-A1 and Ncp-A2, six other compounds putatively characterized as new nostocyclopeptide analogues were detected. This includes Ncp-E1 and E2 and their linear forms (Ncp-E1-L and E2-L), a cyclic Ncp-E3 and a linear Ncp-E4-L. Regardless of the extraction conditions, the cell contents of the linear nostocyclopeptides were found to be higher than the cyclic ones, suggesting a slow rate of the macrocyclization process.

Keywords: cyanobacteria; nostocyclopeptides; *Nostoc*; *ncp* gene cluster; nonribosomal peptide synthetase

1. Introduction

Secondary metabolites produced by cyanobacteria of the genus *Nostoc* (Nostocales) are characterized by a high variety of structures and biological activities [1–6]. On the basis of chemical structure, these compounds are mainly classified to peptides, polyketides, lipids, polysaccharides and alkaloids [7]. Abundantly produced cyanopeptides with anticancer, antimicrobial, antiviral and enzyme-inhibiting activity, have attracted attention of many research groups [6,8–12]. Some of the metabolites, such as nostocyclopeptides (Ncps) or cryptophycins are exclusively produced by the cyanobacteria of the genus *Nostoc* (Figure 1A). Ncps constitute a small class of nonribosomal peptides. Thus far, only three analogues of the compounds and their linear forms have been discovered. This includes Ncp-A1 and Ncp-A2 detected in *Nostoc* sp. ATCC53789 isolated from a lichen collected at Arron Island in Scotland [13]. The same peptides were detected in *Nostoc* sp. ASN_M, isolated

from soil samples of paddy fields in the Golestan province in Iran [14] and in *Nostoc* strains from liverwort *Blasia pusilla* L. collected in Northern Norway [15]. A different analogue, Ncp-M1, was found in *Nostoc* sp. XSPORK 13A, the cyanobacterium living in symbiosis with gastropod from shallow seawaters at the Cape of Porkkala (Baltic Sea) [16].

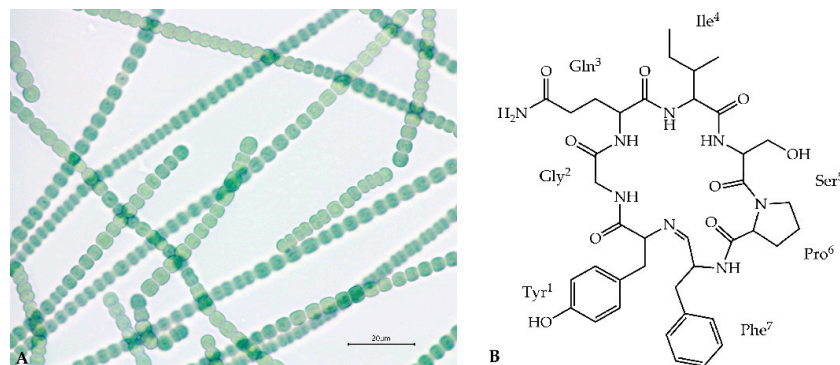


Figure 1. *Nostoc edaphicum* CCNP1411 (A) and the proposed chemical structure of Ncp-E1 (B).

Ncps are composed of seven residues and a unique imino linkage formed between C-terminal aldehyde and an *N*-terminal amine group of the conserved Tyr¹ (Figure 1B) [13,16]. The presence of modified amino acid residues, e.g., 4-methylproline, homoserine and *D*-configured glutamine, indicated the nonribosomal biosynthetic pathway of the molecules. Genetic analysis of *Nostoc* sp. ATCC53789 revealed the presence of the 33-kb Ncp gene cluster composed of two genes, *ncpA* and *ncpB*, encoding NcpA1-A3 and NcpB1-B4 modules. These proteins catalyze the activation and incorporation of Tyr, Gly, Gln, Ile and Ser into the Ncp structure [17]. They show high similarity to NosE and NosF which take part in the biosynthesis of nostopeptolides in *Nostoc* sp. GSV224 [18]. The *ncpFGCDE* fragment of the Ncp gene cluster is involved in the synthesis of MePro (*ncpCDE*), transport (*ncpF*) and proteolysis (*ncpG*) of the peptides. The characteristic features of the Ncp enzymatic complex in *Nostoc* sp. ATCC53789 is the presence of the epimerase domain (NcpA3) responsible for *D*-configuration of glutamine, and the unique reductase domain at C-terminal end of NcpB which catalyze the reductive release of a linear peptide aldehyde [19,20].

The activity of Ncps have been explored [13] and their potential as antitoxins, inhibiting the transport of hepatotoxic microcystin-LR and nodularin into the rat hepatocytes through the organic anion transporter polypeptides OATP1B1/1B3 was revealed [21]. As OATP1B3 is overexpressed in some malignant tumors (e.g., colon carcinomas) [22], Ncps, as inhibitors of this transporter protein, are suggested to be promising lead compounds for new drug development.

In our previous studies, *Nostoc edaphicum* CCNP1411 (Figure 1A) from the Baltic Sea was found to be a rich source of cyanopeptolins, the nonribosomal peptides with potent inhibitory activity against serine proteases [6]. In the current work, the potential of the strain to produce other bioactive metabolites was explored. The whole-genome sequence of *N. edaphicum* CCNP1411 has been determined, and the nostocyclopeptide biosynthetic gene cluster has been identified in the strain and characterized in silico for the first time. Furthermore, the new products of the Ncp gene cluster have been detected and their structures have been characterized by LC-MS/MS.

2. Results and Discussion

2.1. Analysis of *N. edaphicum* CCNP1411 Genome

Total DNA has been isolated from *N. edaphicum* CCNP1411, and the whole genome sequence has been determined. Identified replicons of *N. edaphicum* CCNP1411 genome consist of the circular chromosome of 7,733,505 bps, and five circular plasmids (Table 1). Within the total size of 8,316,316 bps genome (chromosome and plasmids, Figure 2), we have distinguished, according to annotation,

the total number of 6957 genes from which 6458 potentially code for proteins (CDSs), 415 are classified as pseudo-genes and 84 are coding for non-translatable RNA molecules. Pseudo-genes can be divided into subcategories due to the shift in the coding frame (180), internal stop codons (77), incomplete sequence (228), or occurrence of multiple problems (63). Genes coding for functional RNAs consist of those encoding ribosomal (rRNA) (9), transporting (tRNA) (71) and regulatory noncoding (ncRNA) (4), all embedded on the chromosome. Out of total coding and pseudo-genes sequences (6873), the vast majority (5846) initiates with the ATG start codon, while GTG and TTG occur less frequently (561 and 217 times, respectively). The frequencies of stop codons were set out as follows: TAA (3455), TAG (1750), TGA (1526). Coding and pseudo-genes sequences are distributed almost equally on the leading and complementary strand, including 3408 and 3465 sequences, respectively.

Table 1. Composition and coverage of *N. edaphicum* CCNP1411 genome.

Replicon	Accession Number	Length (bp)	Topology	G+C Content (%)	Coverage (x) Nanopore Data	Coverage (x) Illumina Data
pNe_1	CP054693.1	44,503	Circular	42.3	115.5	244.8
pNe_2	CP054694.1	99,098	Circular	40.2	168.4	135.3
pNe_3	CP054695.1	120,515	Circular	41.3	256.4	177.1
pNe_4	CP054696.1	53,840	Circular	41.6	102.4	211.5
pNe_5	CP054697.1	264,855	Circular	41.0	226.3	160.7
chr	CP054698.1	7,733,505	Circular	41.6	160.7	116.9

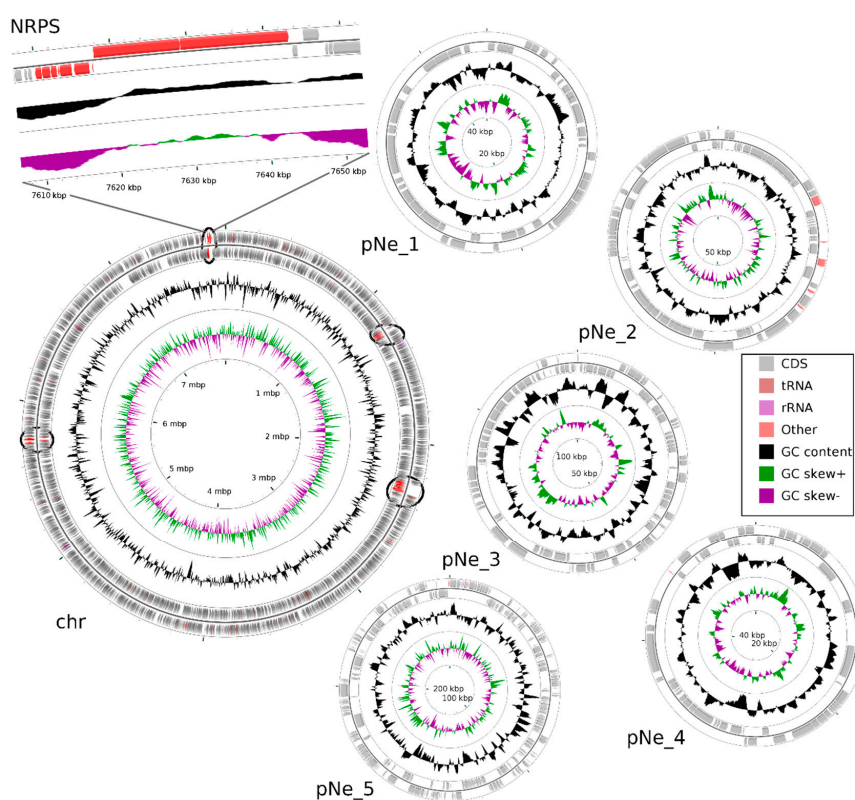


Figure 2. Map of the *N. edaphicum* CCNP1411 genome where chromosome (chr) and five plasmids (pNe_1–5) are presented. The ORFs are indicated with grey arrows split into two rings outermost showing ORFs on direct strand and inner showing complementary strand ORFs. The middle circle shows GC content (black) and the innermost circle shows GC skew (green and purple). Genes for putative NRPS/PKS are marked on the chromosome in their proper position (red within a black circle), with closeup on NRPS in position 7,609,981–7,643,289 putatively coding for Ncp biosynthetic gene cluster.

2.2. Non-Ribosomal Peptide Synthetase (NRPS) Gene Cluster of Nostocyclopeptides

Having the whole genome sequence of *N. edaphicum* CCNP1411, we have analyzed in detail the non-ribosomal peptide synthetase (NRPS) cluster, containing potential genes coding for enzymes involved in the synthesis of nostocyclopeptides. To establish correct spans for non-ribosomal peptide synthetases, 35 complete nucleotide sequence clusters derived from *Cyanobacteria* phylum were aligned resulting in hits scattered around positions 2,287,143–2,323,617 and 7,609,981–7,643,289 within the *N. edaphicum* CCNP1411 chromosome (7.7 Mbp) (Figure 2). This method of characterization presented the overall similarity of selected spans to micropeptin (cyanopeptolin) biosynthetic gene cluster [23] and nostocyclopeptide biosynthetic gene cluster [17], respectively. To confirm these results, the antiSMASH analysis was employed resulting in confirmation of previously defined NRPS spans and adding two more regions 1,213,069–1,258,319 and 5,735,625–5,780,238, to small extent (12% and 30%, respectively) similar to anabaenopeptin gene cluster [24]. For the purpose of this study, we focused on putative nostocyclopeptide producing non-ribosomal peptide synthetase. Annotation of the selected region revealed nine putative open reading frames (ORFs), transcribed in reverse (7) and forward (2) direction. The identified cluster was arranged in a similar fashion to AY167420.1 (nostocyclopeptide biosynthetic gene cluster from *Nostoc* sp. ATCC 53789), with the exception of two ORFs (>170 bp), intersecting operon (*ncpFGCDE*) putatively encoding proteins involved in MePro assembly, efflux and hydrolysis of products of the second putative operon *ncpAB* (Figure 3).

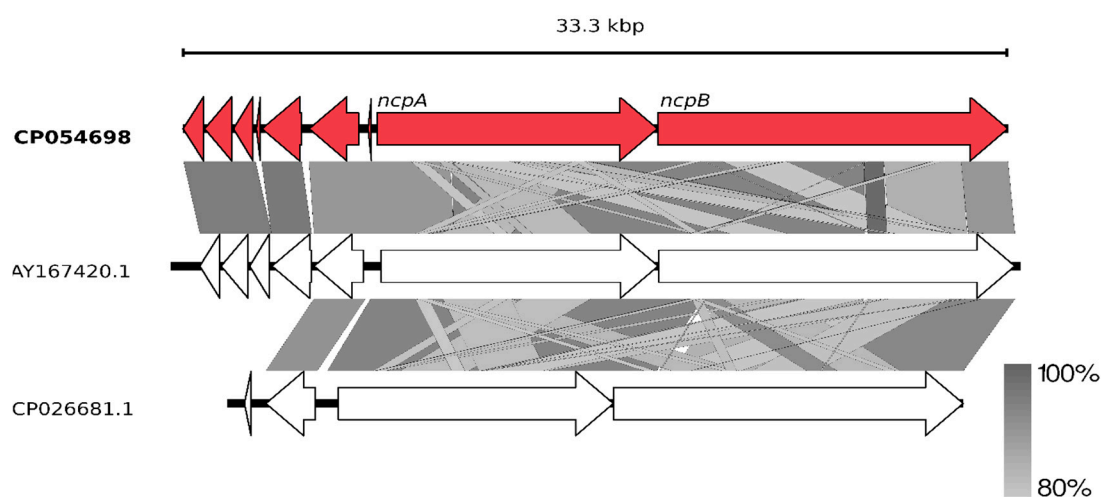


Figure 3. Schematic alignment of genes coding for putative non-ribosomal peptide synthetase from *N. edaphicum* CCNP1411 (red) and two related Ncp-producing synthetases AY167420.1 and CP026681.1 (white). The grey bar in the lower right corner shows the identity percentage associated with color of the bars connecting homologous regions. The analysis was conducted at the nucleotide level.

Two sequences ORF1 (HUN01_34350) (837 bp) and ORF2 (HUN01_34355) (1107 bp) embedded on 3' end of nostocyclopeptide gene cluster resemble *nosF* and *nosE* genes, found in the nostopeptolide (*nos*) gene cluster [18] with 96% nucleotide sequence identities in both instances, putatively encoding for zinc-dependent long-chain dehydrogenase and a Δ^1 -pyrroline-5-carboxylic acid reductase. Further upstream, there is an ORF3 (HUN01_34360) (798 bp) of 98% homology to unknown gene from AF204805.2 gene cluster, suggested previously to be involved in 4-methylproline biosynthesis [17,25], due to close proximity of downstream genes encompassing this reaction, but no experimental evidence was presented. Alignment of the sequence of this putative protein have shown a sequence homology, to some extent, to 4'-phosphopantetheinyl transferase, crucial for PCP aminoacyl substrate binding (Figure 4) [26]. Moreover, partially present adenylate-forming domain within ORF4 (HUN01_34365) (165 bp) belongs to the acyl- and aryl- CoA ligases family, and may putatively engage substrate for post-translational modification of the PCP domain. Facing the same direction, an ORF5 (HUN01_34370)

(1605 bp)-bearing putative domain classified as transpeptidase superfamily DD-carboxypeptidase and ORF6 (HUN01_34375) (2010 bp) homologous to ABC transporter ATP-binding protein/permease may be engaged in *ncpAB* peptide product transport [27]. Neither the ORF7 (HUN01_34780) Shine–Delgarno (SD) sequence upfront translation start codon could be assigned nor the TA-like signal ~12 nucleotides upstream could be found.

```

WP_000986023.1   1  -----MA[LGLGTDIVEIART]-----EAVIAR[S]GDR[L]ARV--LSDN
ORF3              61 DCYQNVNPK[ER]IGITVFEYN[R]SKAA YFOAVERTTKLRDCI[M]A[S]FNPL[ER]L[MV]KIREC

WP_000986023.1   36 EWA[I]WKTHH[Q]P[V]-----RF[L]AKRF[A]VKE[A]AAKAF[G]G[I]RNG[F]AFN[Q]F[E]V[F]
ORF3             121 TGATVRIASE[P]LYGSYYAGLIRKIEQGTQ[H]IDY[A]PLE[Q]SKWEI[G]V[Y]YQ-[S]WNL[Y]LKE

WP_000986023.1   81 N-DEL[G]KPR[L]--RLW--GEALKLAEKLCVANMHVTLADE---RH[V]ACATV[I]ES-----
ORF3             180 SPNNH[G]QTR[I]YDR[Q]WQP[C]DDQYKLD[SY]G[VD]TVIADADAIAFQ[P]V[GD]V[F]F[N]TRNFHIV

```

Figure 4. Structure-based sequence alignment of 4'-phosphopantetheinyl transferase and partial ORF3. Amino-acids highlighted in black color indicate conserved residues, whereas those in grey color indicate conservative mutations.

The main part of the *Ncp* biosynthetic gene cluster is located on the forward strand comprising two large genes which nucleotide sequences are homologous over 80% to *ncpA* and *ncpB* subunits of the *ncp* cluster in *Nostoc* sp. ATCC53789 [17]. Both these genes code for proteins consisting of repetitive modules incorporating single residue into elongating peptide. ORF 8 (HUN01_34785) (11,334 bp) encompasses three of these modules, whereas ORF 9 (HUN01_34380) (14,157 bp) encodes four modules. The core of one NRPS module consists of three succeeding domains: condensation (C), adenylation (A) and peptidyl carrier protein (PCP). Moreover, adjacent to coding spans of extreme modules, two tailoring domains were found within ORF8 and ORF9 genes (Figure 5).

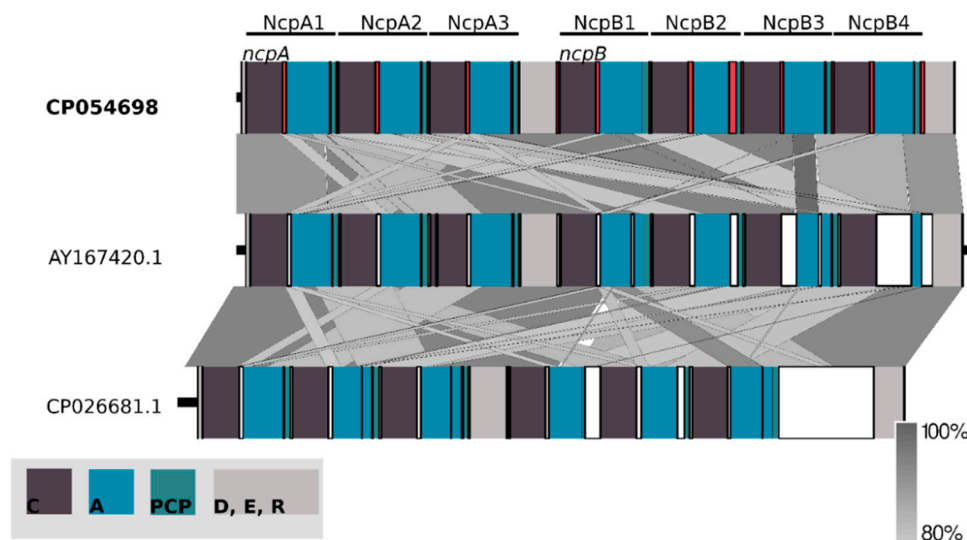


Figure 5. Schematic representation of conserved domains within *ncpA* and *ncpB* coding nucleotide sequences. They are composed of repetitive modules condensation (C), adenylation (A) and peptidyl carrier protein (PCP) domains adjacent to delineating docking, epimerization and reductase domains aligned with two related synthetases AY167420.1 and CP026681.1. The analysis was conducted at the nucleotide level.

Alignment of nucleotide sequences to the *ncpAB* operon revealed major differences in consecutive NcpB3 and NcpB4 modules. Utilizing the selected spans conjoined with conserved domain search allowed us to distinguish and compare C, A and PCP amino-acid sequences (Figure 6). Intrinsic modules of NRPS, with an exception of NcpB3 adenylation domain sequence, were found homologous

above 91%, whereas extremes have shown the biggest composition differences ranging from 13–15% to 24% in the NcpB4 adenylation domain (Figure 6).

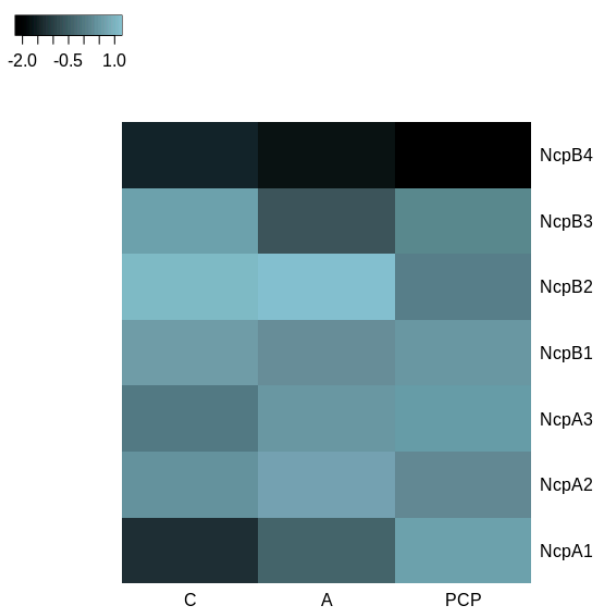


Figure 6. Heatmap of the highest (light blue) and lowest (black) percentage of similarities between NcpA and NcpB domains in *N. edaphicum* CCNP1411 and ATCC53789; values scaled by rows. The analysis was conducted at the amino acid level.

The determination of the whole genome sequence of *N. edaphicum* CCNP1411 allowed us to perform analyses of genes coding for enzymes involved in the synthesis of nostocyclopeptides. The general analysis demonstrated homology of the NRPS/PKS clusters of *N. edaphicum* CCNP1411 to systems occurring in other cyanobacteria, however, with some differences. The non-ribosomal consensus code [28,29] allowed to recognize and predict the substrate specificities of NRPS adenylation domains: tyrosine (NcpA1), glycine (NcpA2), glutamine (NcpA3) for NcpA and isoleucine/valine (NcpB1) serine (NcpB2) 4-methylproline/proline (NcpB3) phenylalanine/leucin/tyrosine (NcpB4) for NcpB (Table 2). This prediction was found to be in line with the structures of the Ncps detected in *N. edaphicum* CCNP1411.

Table 2. Characterization of substrate binding pocket amino acid residues adenylation domains of NcpA and NcpB modules based on gramicidin S synthetase (GrsA) phenylalanine activating domain. Residues in brackets mark inconsistency with AY167420.1 residues.

NRPS Module	Adenylation Domain Residue Position									Proposed Substrate
	235	236	239	278	299	301	322	330	331	
NcpA1	D	A	S	T	[I]	A	A	V	C	Tyr
NcpA2	D	I	L	Q	L	G	L	I	W	Gly
NcpA3	D	A	W	Q	F	G	L	I	D	Gln
NcpB1	D	A	F	F	L	G	V	T	F	Ile/Val
NcpB2	D	V	W	H	I	S	L	I	D	Ser
NcpB3	D	V	Q	[F]	I	A	H	V	A	Pro/MePro
NcpB4	D	A	W	[T]	I	G	[A]	V	C	Phe/Tyr/Leu

To devolve elongating product onto subsequent condensation domain, the studied synthetase utilizes PCP domains, subunits responsible for thiolation of nascent peptide intermediates, where post-transcriptional modification of conserved serine residue shifts the state of the domain from inactive *holo* to active *apo*. Modification of this residue is related to PPTase which transfers

a covalently-bound 4'-phosphopantetheine arm of CoA onto the PCP active site, enabling peptide intermediates to bind as reactive thioesters. Case residue which undergoes a nucleophilic attack by the hydroxyl group was conserved in every module within the PCP domain predicted at the front of the second helix [30].

The stand-alone docking domain (D) (7,617,812–7,617,964 bp) found on N-terminus of NcpA may be an essential component mediating interactions, recognition and specific association within NRPS subunits. The potential acceptor domain, based on sequence homology of conserved residues to C-terminal communication-mediating donor domains (COM), was found at the NcpB4 PCP domain second helix, encompassing conserved serine residue within potential binding sequence [31]. Moreover, this communication-mediating domain may putatively bind to C-terminus of NcpB3 and NcpB4 condensation (C) domains based on conserved motif LLEGIV, found by sequence homology to last five amino-acids of C-terminal docking domains residues, key for their interactions [32]. Within the same β -hairpin, a group of charged residues (ExxxxxKxR) putatively determines the binding affinity of the N-terminal domain [33].

Two tailoring domains encoded at the 5' ends of *ncpA* and *ncpB* genes were classified as epimerization (E) (7,627,742–7,629,043 bp) domain and reductase (R) (7,642,183–7,643,238 bp) domain, accordingly. Epimerization domain catalyzes the conversion of L-amino acids to D-amino acids, a reaction coherent with D-stereochemistry of the peptide glutamine residue, where His of the conserved HHxxxDG motif and Glu from the upstream EHGRE motif raceB comprise an epimerisation reaction active site [34]. Homologous HHxxxDG conserved motif sequence is found in condensation domains (C), where a similar reaction is catalyzed within peptide bond formation, putatively by the second His residue [35]. As in *ncp* cluster [17], module NcpA1 motif includes degenerate sequences in two positions HQIVGDL with leucine instead of phenylalanine residue at the start of the helix. The second histidine site-directed mutagenesis abolished enzymatic activity which might suggest that NcpA1 condensation domain is inactive [36].

Reductase domain (R) found at the C-terminus of NRPS was classified as oxidoreductase. Despite 15% discrepancy in domain composition compared to NcpB core catalytic triad Thr-Tyr-Lys and Rossmann-fold, a NAD (P) H nucleotide-binding motif GxxGxxG positions were not affected. The mechanism driving this chain release utilizes NAD (P) H cofactor for redox reaction of the final moiety of the nascent peptide to aldehyde or alcohol [37,38].

2.3. Structure Characterization of Ncps Produced by *N. edaphicum* CCNP1411

Thus far, only three Ncps, Ncp-A1, A2 and M1, and their linear aldehydes were isolated as pure natural products of *Nostoc* strains [13,16]. Ncp-A3, with MePhe in the C-terminal position, was obtained through aberrant biosynthesis in the *Nostoc* sp. ATCC53789 culture supplemented with MePhe [13]. The linear aldehydes of Ncp-A1 and Ncp-A2, with Pro instead of MePro, were chemically synthesized and used to study the Ncps epimerization and macrocyclization equilibria [19,20]. In our work, ten Ncps, differing mainly in position 4 and 7, were detected by LC-MS/MS in the *N. edaphicum* CCNP1411 cell extract (Table 3, Figure 1, Figure 7, Figure 8 and Figure S1–S7). These include five cyclic structures, four linear Ncp aldehydes, and one linear hexapeptide Ncp. The putative structures of the six peptides, which were found to be naturally produced by *Nostoc* for the first time, are marked in Table 3 in bold (Ncp-E1, Ncp-E1-L, Ncp-E2, Ncp-E2-L, Ncp-E3 and Ncp-E4-L).

Table 3. The putative structures of nostocyclopeptides (Ncps) detected in the crude extract of *N. edaphicum* CCNP1411 and the structure of Ncp-M1 identified in *Nostoc* sp. XSPORK 13 A [16]. The new analogues are marked in bold and the peptides detected in trace amounts are marked with [T]. The variable residues in position 4 and 7 are marked in blue.

Compound	Structure	m/z [M+H] ⁺		Retention Time [min]
		Cyclic	Linear-COH	
Ncp-A1	cyclo[Tyr+Gly+Gln+Ile+Ser+MePro+Leu]	757		7.1
Ncp-A1-L	Tyr+Gly+Gln+Ile+Ser+MePro+Leu		775	5.8
Ncp-A2	cyclo[Tyr+Gly+Gln+Ile+Ser+MePro+Phe]	791		6.0
Ncp-A2-L	Tyr+Gly+Gln+Ile+Ser+MePro+Phe		809	5.6
Ncp-E1	cyclo[Tyr+Gly+Gln+Ile+Ser+Pro+Phe]	777 [T]		7.2
Ncp-E1-L	Tyr+Gly+Gln+Ile+Ser+Pro+Phe		795	5.7
Ncp-E2	cyclo[Tyr+Gly+Gln+Ile+Ser+Pro+Leu]	743 [T]		6.3
Ncp-E2-L	Tyr+Gly+Gln+Ile+Ser+Pro+Leu		761	5.1
Ncp-E3	cyclo[Tyr+Gly+Gln+Val+Ser+MePro+Leu]	743 [T]		7.0
* Ncp-E4-L	[Tyr+Gly+Gln+Ile+Ser+MePro]		677 [T]	6.0
** Ncp-M1	cyclo[Tyr+Tyr+HSe+Pro+Val+MePro+Tyr]		882	27.5

* Ncp-E4-L is the only linear Ncps analogue with carboxyl group in C-terminus. ** Identified in *Nostoc* sp. XSPORK [16].

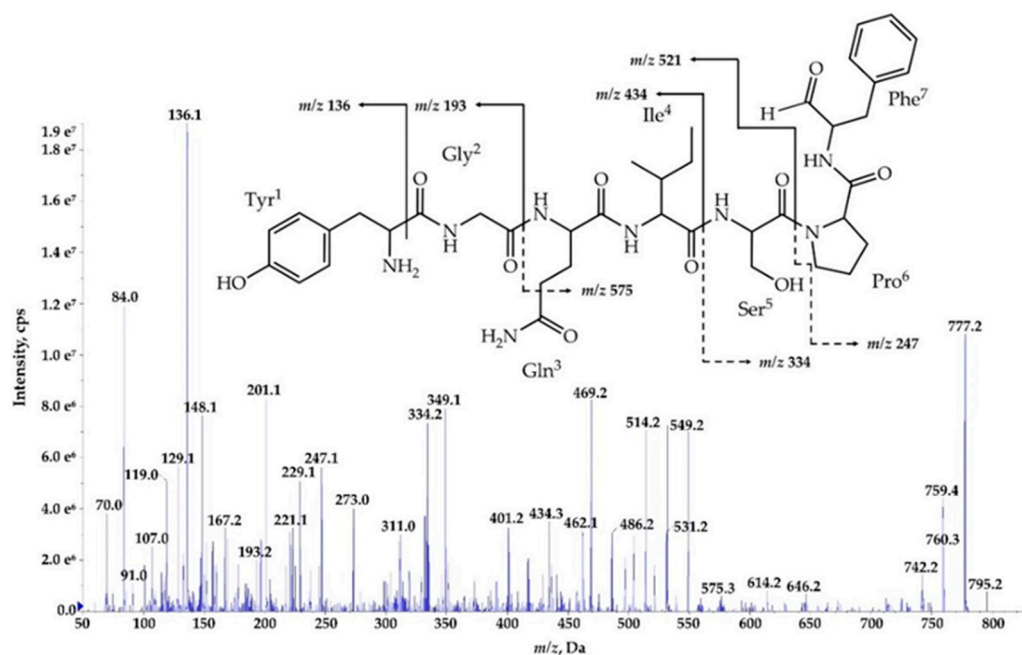


Figure 7. Postulated structure and enhanced product ion mass spectrum of the linear aldehyde nostocyclopeptide **Ncp-E1-L**; Tyr+Gly+Gln+Ile+Ser+Pro+Phe characterized based on the following fragment ions: m/z 795 [M+H]; 777 [M+H-H₂O]; 759 [M+H-2H₂O]; 646 [M+H - Phe]; 614 [M+H - Tyr-H₂O]; 575 [M+H-(Tyr+Gly)]; 549 [Tyr+Gly+Gln+Ile+Ser+H]; 531 [Tyr+Gly+Gln+Ile+Ser+H-H₂O]; 462 [Tyr+Gly+Gln+Ile+H]; 349 [Tyr+Gly+Gln+H]; 334 [Ser+Pro+Phe+2H]; 247 [Phe+Pro+H]; 229 [Phe+Pro+H]; 201 [Phe+Pro+H - CO]; 148 [Tyr-NH₂]; 136 Tyr immonium; 129, 101 (immonium), 84 Gln; 70 Pro immonium.

The process of *de novo* structure elucidation was performed manually, based mainly on a series of b and y fragment ions produced by a cleavage of the peptide bonds (Figures 7–9, Figures S1–S7), and on the presence of immonium ions (e.g., m/z 70 for Pro, 84 for MePro, 136 for Tyr) in the product ion mass spectra of the peptides. The process of structure characterization was additionally supported by the previously published MS/MS spectra of Ncps [14]. The fragment ions that derived from the two amino acids in C-terminus usually belonged to the most intensive ions in the spectra and in this study they facilitated the structure characterization. For example, in the product ion mass spectrum of Ncp-A1

(Figure S1) and Ncp-E3 (Figure S7), ions at m/z 209 [MePro+Leu+H] and m/z 181 [MePro+Leu+H-CO] were present, while in the spectrum of Ncp-E2 (Figure S5) with Pro (instead MePro), the corresponding ions at 14 unit lower m/z values, i.e., 195 and 167 were observed. The spectra of the linear Ncps contained the intensive Tyr immonium ion at m/z 136. Based on the previously determined structures of Ncp-A1 and Ncp-A2 [13], we assumed that in Ncp-E2, the amino acids in position 4 and 7, are Ile and Leu, respectively (Table 3; Figure S5). These two amino acids are difficult to distinguish by MS. Definitely, the NMR analyses are required to confirm the structures of the Ncps. The presence of Val in position 4, instead of Ile, distinguishes the Ncp-E3 from other Ncps produced by *N. edaphicum* CCNP1411. As it was previously reported [17], and also confirmed in this study, the predicted substrates of the NcpB1 protein encoded by *nepB* and involved in the incorporation of the residue in position 4 are Ile/Leu and Val. However, the domain preferentially activates Ile, which explains why only traces of Val-containing Ncps were detected in *N. edaphicum* CCNP1411 (Table 3).

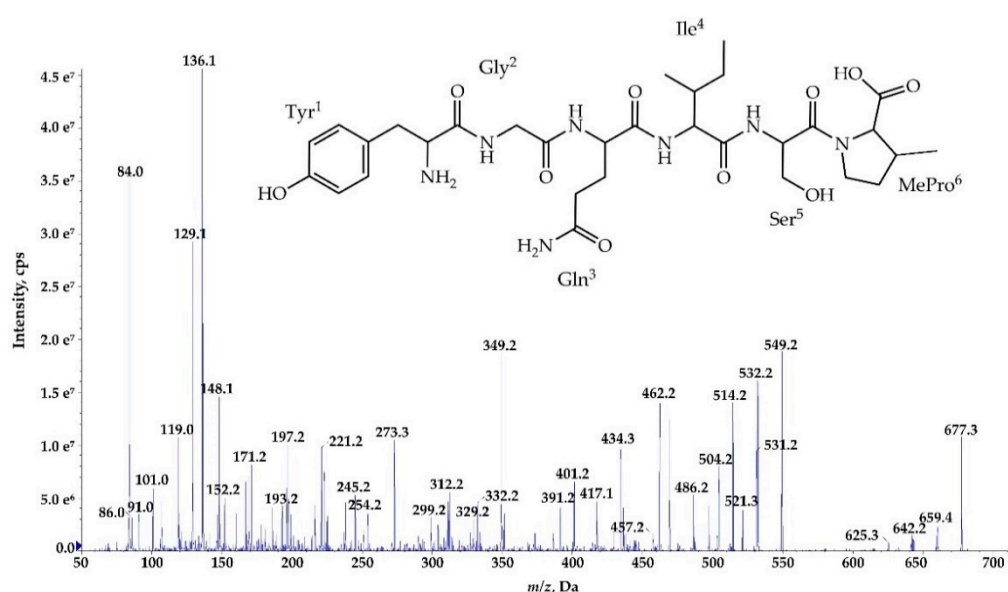


Figure 8. Postulated structure and enhanced product ion mass spectrum of a linear nostocyclopeptide **Ncp-E4-L** [Tyr+Gly+Gln+Ile+Ser+MePro] characterized based on the following fragment ions: m/z 677 [M+H]; 659 [M+H-H₂O]; 642 [M+H-H₂O-NH₃]; 549 [Tyr+Gly+Gln+Ile+Ser+H]; 531 [Tyr+Gly+Gln+Ile+Ser+H-H₂O]; 521 [Tyr+Gly+Gln+Ile+Ser+H-CO]; 462 [Tyr+Gly+Gln+Ile+H]; 434 [Tyr+Gly+Gln+Ile+H-CO]; 349 [Tyr+Gly+Gln+H]; 329 [Gln+Ile+Ser+H]; 312 [Ile+Ser+MePro+H]; 221 [Tyr+Gly+H]; 193 [Tyr+Gly+H-CO]; 148 [Tyr-NH₂]; 136 Tyr immonium; 86 Ile immonium; 84, 101 (immonium), 129 Gln; 84 MePro immonium.

Methylated Pro (MePro) in position 6 is quite conserved. MePro is a rare non-proteinogenic amino acid biosynthesized from Leu through the activity of the zinc-dependent long chain dehydrogenases and Δ^1 -pyrroline-5-carboxylic acid (P5C) reductase homologue encoded by the gene cassette *nepCDE* [17,18,25]. The genes involved in the biosynthesis of MePro were found in 30 of the 116 tested cyanobacterial strains, majority (80%) of which belonged to the genus *Nostoc* [39]. The new Ncp-E1 and Ncp-E2, detected at trace amounts, are the only Ncps produced by *N. edaphicum* CCNP1411 which contain Pro (Table 3). The presence of m/z 84 ion in the fragmentation spectra of the two Ncps complicated the process of *de novo* structure elucidation. This ion corresponds to the immonium ion of MePro and could indicate the presence of this residue. However, the two ions m/z 101 and 129, which together with ion at m/z 84, are characteristic of Gln, suggested the presence of this amino acid in Ncp-E1 and Ncp-E2. The detailed characterization of Ncp fragmentation pathways is presented in Figures 7–9 and in Supplementary Materials (Figures S1–S7).

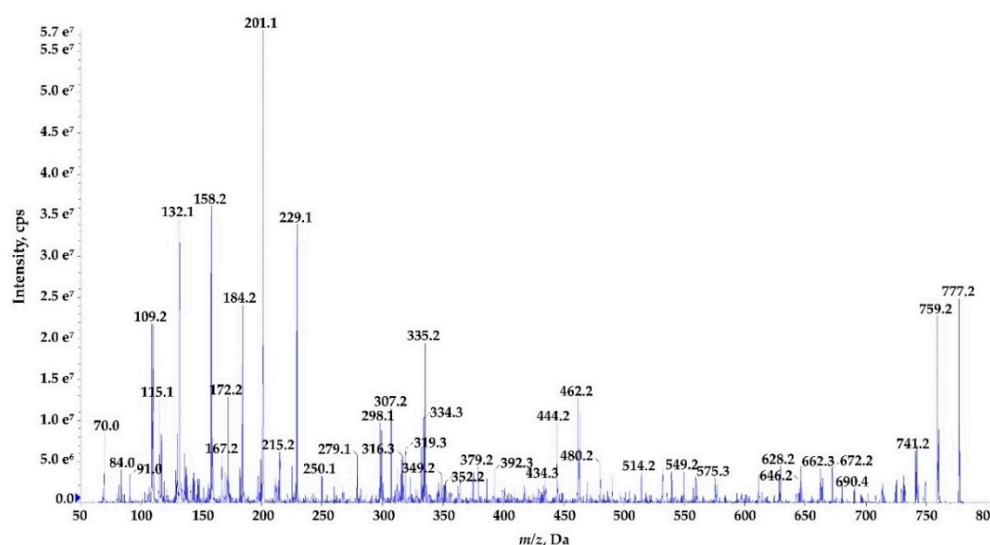


Figure 9. Enhanced product ion mass spectrum of the cyclic nostocyclopeptide **Ncp-E1** with putative structure cyclo[Tyr+Gly+Gln+Ile+Ser+Pro+Phe] characterised based on the following fragment ions: m/z 777 [M+H]; 759 [M+H-H₂O]; 741 [M+H-2H₂O]; 690 [M+H-Ser]; 672 [M+H-Ser-H₂O]; 662 [M+H-Pro-H₂O]; 646 [M+H-Phe]; 628 [M+H-Phe-H₂O]; 575 [M+H-(Ser+Pro)-H₂O]; 549 [Tyr+Gly+Glu+Ile+Ser+H]; 480 [Phe+Tyr+Gly+Gln+H]; 462 [Tyr+Gly+Gln+Ile+H]; 444 [Tyr+Gly+Gln+Ile+H-H₂O]; 434 [Tyr+Gly+Gln+Ile+H-CO]; 392 [Pro+Phe+Tyr+H]; 352 [Phe+Tyr+Gly+H]; 335 [Phe+Tyr+Gly+H-H₂O]; 316 [Ser+Pro+Phe+H]; 307 [Phe+Tyr+Gly+H-H₂O-CO]; 298 [Ile+Ser+Pro+H]; 229 [Phe+Pro+H]; 201 [Phe+Pro+H-CO]; 158 [Gly+Gln+H-CO]; 132 Phe; 70 Pro immonium. Structure of the peptide is presented in Figure 1.

In addition to the heptapeptide Ncps, *N. edaphicum* CCNP1411 produces a small amount of the linear hexapeptide, Ncp-E4-L, whose putative structure is Tyr+Gly+Gln+Ile+Ser+MePro (Table 3, Figure 9). This Ncp was detected only when higher biomass of *Nostoc* was extracted. As the proposed amino acids sequence in this molecule is the same as the sequence of the first six residues in Ncp-A1 and Ncp-A2, the hexapeptide can be a precursor of the two Ncps. The other option is that the cell concentration of the Ncps is self-regulated and the Ncp-E4-L is released through proteolytic cleavage of the final products. This hypothesis could be verified when the role of the Ncps for the producer is discovered. In the *ncp* gene cluster, the presence of *ncpG* encoding the NcpG peptidase, with high homology to enzymes hydrolyzing D-amino acid-containing peptides was revealed by Becker et al. [17] and also confirmed in this study. Therefore, the in-cell degradation of Ncps by the NcpG peptidase is possible, but it probably proceeds at D-Gln and gives other products than Ncp-E4-L.

2.4. Production of Ncps by *N. edaphicum* CCNP1411

Apart from the structural analysis, we also made attempts to determine the relative amounts of the individual Ncps produced by *N. edaphicum* CCNP1411. To exclude the effect of the extraction procedure on the amounts of the detected peptides, different solvents and pH were applied. As the process of Ncp linearization during long storage of the freeze-dried material was suggested [16], both the fresh and lyophilized biomasses were analyzed. Regardless of the extraction procedure, Ncp-A2-L with Phe in C-terminus was always found to be the main Ncp analogue (Figure 10A–D). In addition, when MePro and Pro-containing peptide were compared separately, the peak intensity of the linear Ncps with Phe in C-terminus (i.e., Ncp-A2-L and Ncp-E1-L) was higher than the Ncps with Leu. These results might indicate preferential incorporation of Phe into the synthesized peptide chain.

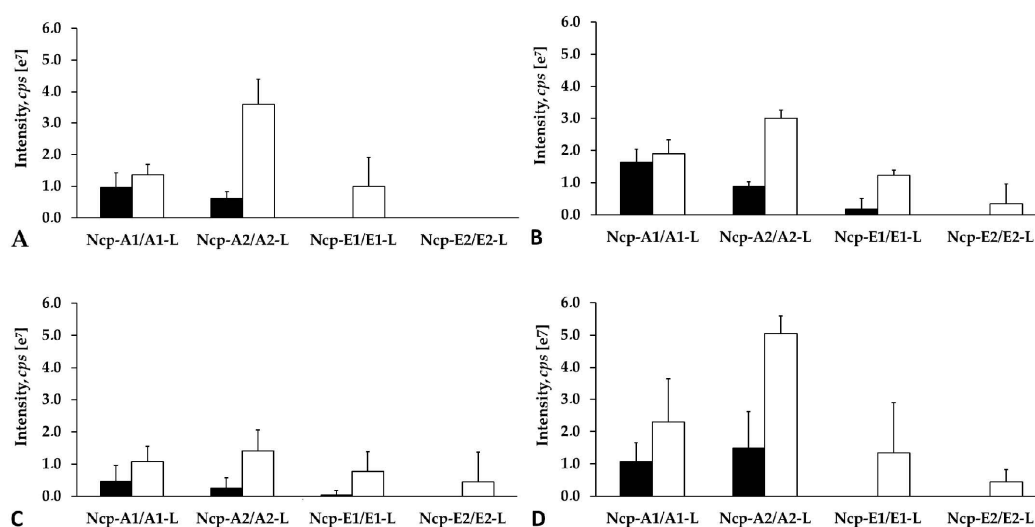


Figure 10. Relative cell contents of nostocyclopeptides extracted from 10 mg of lyophilized (A,B,D) or 500 mg fresh (C) biomass of *N. edaphicum* CCNP1411 with MilliQ water (A), 50% methanol in water (B), and 20% methanol in water (C,D). The cell content was expressed as peak intensity in LC-MS/MS chromatogram.

The study also showed that the cell contents of the linear Ncps are higher than the cyclic ones. (Figure 10A–D and Figure S8). The release of Ncps from the synthetase as linear aldehydes is catalyzed by a reductase domain, located in the C-terminal part of the NcpB [17]. This reductive release triggers the spontaneous, and enzyme independent, macrocyclization of the linear peptide [19,20]. The reaction leads to the formation of a stable imino bond between the C-terminal aldehyde and the N-terminal amine group of Tyr [19,20]. In *N. edaphicum* CCNP1411 cells, depending on the Ncp analogue, the analyzed material (fresh or lyophilized) and extraction solvent, the cyclic Ncps constituted from even less than 10% (Ncp-A2, fresh biomass) to over 90% of the linear peptide (Figure 10A–D and Figure S8). In case of Ncp-A1, with MePro-Leu in C-terminus, the contribution of the cyclic form was always most significant, and at pH 8 it reached up to 91.7% of the linear peptide aldehyde (Ncp-A1-L) (Figure 10A–D and Figure S8). The cyclic analogues, Ncp-E1 and Ncp-E3 were produced in trace amounts and their spectra were sporadically recorded. It was proven that the macrocyclization process of Ncps is determined by the geometry of the linear peptide aldehyde and the conformation of D-Gln and Gly is crucial for the folding and formation of the imino bond [19]. As these two residues are present in all detected Ncps, then, probably other elements of the structure affect the cyclization process, as well. We hypothesize that due to the steric hindrances, the cyclization of Ncp-A1 with Leu in C-terminal position is easier than the cyclization of Ncp-A2 with Phe. As a consequence, the proportion of the cyclic Leu-containing Ncp-A1 to the linear form of the peptide is higher.

Thus far, Ncps synthesis was reported in few *Nostoc* strains, and the structural diversity of the peptides was found to be low. Other classes of NRPs were detected in cyanobacteria representing different orders and genera, and within one class of the peptides numerous analogues were detected. For example, the number of naturally produced cyclic heptapeptide microcystins (MCs), is over 270 [40,41] and in one cyanobacterial strains even 47 MCs analogues were detected [40]. Cyanopeptolins are produced by many cyanobacterial taxa and so far more than 190 structural analogues of the peptides have been discovered [41]. In this work, cyanopeptolin gene cluster was identified in *N. edaphicum* CCNP1411 and thirteen products of the genes were previously reported [6]. These peptides contain seven amino acids and a short fatty acid chain, and only one element of the structure, 3-amino-6-hydroxy-2-piperidone (Ahp), is conserved [6]. The structural diversity of NRPs is generated by frequent genetic recombination events and point mutations in the NRP gene cluster. The changes in gene sequences affect the structure and substrate specificity of the encoded enzymes. The tailoring

enzymes can further modify the product, leading to even higher diversity of the synthesized peptides [42]. In case of Ncps, both the number of the producing organisms and the structural diversity of the peptides are limited. Ncp-M1 from *Nostoc* living in symbiosis with gastropod [16] is the only Ncp with structure distinctly different from Ncp-A1, Ncp-A2 and other Ncps described in this work.

The diversity within one class of bioactive metabolites offers a good opportunity for structure-activity relationship studies, without the need to synthesize the variants. The studies are of paramount importance when the efficacy and safety of a drug candidate are optimized. Therefore, in our future work, when sufficient quantities of pure Ncps are isolated, the activity of individual analogues against different cellular targets will be tested and compared, in order to select the lead compound for further studies.

3. Materials and Methods

3.1. Isolation, Purification and Culturing of *Nostoc* CCNP1411

Nostoc strain CCNP1411 was isolated in 2010 from the Gulf of Gdańsk, southern Baltic Sea, by Dr. Justyna Kobos. Based on the 16S rRNA sequence (GenBank accession number KJ161445) and morphological features, such as the shape of trichomes, cell size ($4.56 \pm 0.30 \mu\text{m}$ wide and $4.12 \pm 0.72 \mu\text{m}$ long) and lack of akinetes [43,44], the strain was classified to *N. edaphicum* species. Purification of the strain was carried out by multiple transfers to a liquid and solid (1% bacterial agar) Z8 medium supplemented with NaCl to obtain the salinity of 7.3 [45]. To establish the strain as a monoculture, free from accompanying heterotrophic bacteria, a third-generation cephalosporin, ceftriaxone (100 $\mu\text{g}/\text{mL}$) (Pol-Aura, Olsztyn, Poland) was used. In addition, the purity of the culture was regularly tested by inoculation on LA agar (solid LB medium with 1.5% agar) [46] and on agar Columbia +5% sheep blood (BTL Ltd. Łódź, Poland), a highly nutritious medium, recommended for fastidious bacteria. Cyanobacteria cultures were grown in liquid Z8 medium (100 mL) at $22 \pm 1 \text{ }^\circ\text{C}$, continuous light of $5\text{--}10 \mu\text{mol photons m}^{-2} \text{ s}^{-1}$. After three weeks of growth, the cyanobacterial biomass was harvested by passing the culture through a nylon net (mesh size 25 μm) and then freeze-dried before further processing.

3.2. Isolation and Sequencing of Genomic DNA

Genomic DNA of *N. edaphicum* CCNP1411 was isolated using SDS/Phenol method as described previously [47,48]. DNA quality control was performed by measuring the absorbance at 260/230 nm, template concentration was determined using Qubit fluorimeter (Thermo Fisher Scientific, Waltham, MA, USA), and DNA integrity was analyzed by 0.8% agarose gel electrophoresis and by PFGE using Biorad CHEF-III instrument (BioRad, Hercules, CA, USA).

Paired-end sequencing library was constructed using the NEB Ultra II FS Preparation Kit (New England Biolabs, Beverly, CA, USA) according to the manufacturer's instructions. The library was sequenced using an Illumina MiSeq platform (Illumina, San Diego, CA, USA) with 2×300 paired-end reads. Sequence quality metrics were assessed using FASTQC (<http://www.bioinformatics.babraham.ac.uk/projects/fastqc/>) [49].

The long reads were obtained using the GridION sequencer (Oxford Nanopore Technologies, Oxford, UK). Prior to long-read library preparation, genomic DNA was sheared into 30 kb fragments using 26 G needle followed by size selection on Bluepippin instrument (Sage Science, Beverly, MA, USA). DNA fragments above 20 kb were recovered using PAC30 kb cassette. 5 μg of recovered DNA was taken for 1D library construction using SQK-LSK109 kit and 0.5 μg of the final library was loaded into R9.4.1 flowcell and sequenced on MinION sequencer.

3.3. Genome Assembling

Raw nanopore data was basecalled using Guppy v3.2.2 (Oxford Nanopore Technologies, Oxford, UK). After quality filtering using NanoFilt [50] and residual adapter removal using Porechop (<https://github.com/rrwick/Porechop>), the obtained dataset was quality checked using NanoPlot [50]. Long nanopore reads were then assembled using Flye v2.6 [51]. Flye assembled contigs were further polished using Illumina sequencing reads and Unicycler_polish pipeline (<https://github.com/rrwick/Unicycler>).

3.4. Genome and NRPS Alignment

Genome assembly was annotated using the NCBI Prokaryotic Genome Annotation Pipeline [52] with the assistance of prokka [53] refine annotation, with additionally curated database comprised of sequences selected by Nostocales order from NCBI non-redundant and refseq_genomes (280 positions) databases, enriched by 35 NRPS/PKS clusters selected by cyanobacteria phylum. To create circular maps of *N. edaphicum* CCNP1411 genome, the CGView Comparison Tool [54] was engaged with additional GC skew and GC content analyses.

Selected span for potential NRPS cluster was confirmed with BLASTn, BLASTp [55] and antiSMASH [56]. ORFs start codons within a putative cluster were verified by the presence of ribosome binding sites, 4–12 nucleotides upstream of the start codon. Schematic comparison of ORF BLASTn from relative synthetases, AY167420.1 and CP026681.1, was visualized by EasyFig program (<http://mjsull.github.io/Easyfig/files.html>). Annotated regions of NRPS span were subjected for NCBI Conserved Domain Database search [57] with a set e-value threshold (10^{-3}), determining evolutionarily-conserved protein domains and motifs against CDD v3.18 database. Recognized motifs were selected using samtools v.1.9 and were subjected for protein structure and function prediction by I-TASSER [58], and results were confirmed with literature reports, PKS/NRPS Analysis Web-site prediction [59] and reevaluated using MEGAX suite [60]. Amino-acid sequence was visualized by BOXSHADE 3.2 program (https://embnet.vital-it.ch/software/BOX_form.html). Determination of domain ligand binding and active sites was achieved using COFACTOR and COACH part of I-TASSER analyses confirmed by MUSCLE amino acid alignment from MEGA X.

3.5. Data Deposition

Genomic sequences generated and analyzed in this study were deposited in the GenBank database under BioProject number: PRJNA638531.

3.6. Extraction and LC-MS/MS Analysis

For LC-MS/MS analyses of Ncps, the lyophilized (10 mg DW) biomass of *N. edaphicum* CCNP1411 was homogenized by grinding with mortar and pestle, and extracted in 1 mL of milliQ water, 20% methanol (pH 3.5, 6.0 and 8.0) and 50% methanol in water. The pH was adjusted with 0.5 M HCl and 1.0 M NaOH. In addition, the fresh material (500 mg FW) was extracted in 20% methanol in water. The samples were vortexed for 15 min and centrifuged at 14,000 rpm for 10 min, at 4 °C. The collected supernatants were directly analyzed by LC-MS/MS system.

The LC-MS/MS was carried out on an Agilent 1200 HPLC (Agilent Technologies, Waldbronn, Germany) coupled to a hybrid triple quadrupole/linear ion trap mass spectrometer QTRAP5500 (Applied Biosystems MDS Sciex, Concord, ON, Canada). The separation was achieved on a Zorbax Eclipse XDB-C18 column (4.6 mm ID × 150 mm, 5 µm; Agilent Technologies, Santa Clara, CA, USA). The extract components were separated by gradient elution from 10% to 100% B (acetonitrile with 0.1% formic acid) over 25 min, at a flow rate of 0.6 mL/min. As solvent A, 5% acetonitrile in MilliQ water with 0.1% formic acid was used. The mass spectrometer was operated in positive mode, with turbo ion source (5.5 kV; 550 °C). An information-dependent acquisition method at the following settings was used: for ions within the *m/z* range 500–1100 and signal intensity above the threshold of 500,000 cps

the MS/MS spectra were acquired within the m/z range 50–1000, at a collision energy of 60 eV and declustering potential of 80 eV. Data were acquired with the Analyst[®] Software (version 1.7 Applied Biosystems, Concord, ON, Canada).

4. Conclusions

Genes coding for subunits of the non-ribosomal peptide synthetase, in nostocyclopeptide-producing *N. edaphicum* CCNP1411, revealed differences in nucleotide compositions, compared to the previously described *npc* cluster of *Nostoc* sp. ATCC53789. Although the analysis of fragments of genes coding for active sites and ligand binding sites of the conserved protein domains derived from *N. edaphicum* CCNP1411 and *Nostoc* sp. ATCC53789 indicated identical amino-acid compositions, residues within adenylation domains and substrate binding sites were different between compared sequences. This finding may highlight sites prone to mutations within regions accounted for structure and substrate stability. Analysis of *npc* gene products in *N. edaphicum* CCNP1411 led to the detection of new nostocyclopeptide analogues. However, modifications in their structure were minor and limited to three positions of the heptapeptides. Although the naturally produced nostocyclopeptides were previously described as cyclic structures, in *N. edaphicum* CCNP1411 they are mainly present as linear peptide aldehydes, indicating a slow cyclization process.

Supplementary Materials: The following are available online at <http://www.mdpi.com/1660-3397/18/9/442/s1>. Figure S1: Structure and enhanced product ion mass spectrum of the cyclic nostocyclopeptide Ncp-A1 cyclo [Tyr+Gly+Gln+Ile+Ser+MePro+Leu] identified based on the following fragment ions: m/z 757 [M+H]; 739 [M+H-H₂O]; 729 [M+H-CO]; 721 [M+H-2H₂O]; 628 [M+H-MePro-H₂O]; 626 [M+H-Ile-H₂O]; 594 [M+H-Tyr]; 549 [Tyr+Gly+Gln+Ile+Ser+H]; 541 [M+H-(Ser+MePro)-H₂O]; 446 [M+H-(Ile+Ser+MePro)]; 428 [M+H-(Ile+Ser+MePro)-H₂O]; 386 [Gly+Gln+Ile+Ser+H]; 372 [MePro+Leu+Tyr+H]; 300 [Leu+Tyr+Gly+H-H₂O]; 209 [MePro+Leu+H]; 181 [MePro+Leu+H-CO]; 86-Ile/Leu immonium; 84 MePro immonium, Figure S2: Structure and enhanced product ion mass spectrum of the linear peptide aldehyde Ncp-A1-L (linear aldehyde of Ncp-A1) Tyr+Gly+Gln+Ile+Ser+MePro+Leu identified based on the following fragment ions: m/z 775 [M+H]; 757 [M+H - H₂O]; 739 [M+H-2H₂O]; 660 [M+H-Leu]; 549 [Tyr+Gly+Gln+Ile+Ser+H]; 531 [Tyr+Gly+Gln+Ile+Ser+H-H₂O]; 521 [Tyr+Gly+Gln+Ile+Ser+H-CO]; 532 [M+H-(MePro+Leu)-H₂O]; 462 [Tyr+Gly+Gln+Ile+H]; 434 [Tyr+Gly+Gln+Ile+H-CO]; 386 [Gly+Gln+Ile+Ser+H]; 349 [Tyr+Gly+Gln+H]; 301 [Gln+Ile+Ser+H-CO]; 227 [MePro+Leu+H]; 221 [Tyr+Gly+H]; 209 [MePro+Leu+H-H₂O]; 181 [MePro+Leu+H-H₂O-CO]; 148 [Tyr-NH₂]; 136 Tyr immonium; 86-Ile/Leu immonium; 84, 101 (immonium), 129 Gln; 84 MePro immonium, Figure S3: Structure and enhanced product ion mass spectrum of the cyclic nostocyclopeptide Ncp-A2 cyclo[Tyr+Gly+Gln+Ile+Ser+MePro+Phe] identified based on the following fragment ions: m/z 791 [M+H]; 773 [M+H-H₂O]; 763 [M+H-CO]; 755 [M+H-2H₂O]; 745 [M+H-CO-H₂O]; 678 [M+H-Ile]; 628 [M+H-Tyr]; 593 [M+H-(Ser+MePro)]; 549 [Tyr+Gly+Gln+Ile+Ser+H]; 531 [Tyr+Gly+Gln+Ile+Ser+H-H₂O]; 480 [M+H-(Ile+Ser+MePro)]; 462 [Tyr+Gly+Gln+Ile+H]; 406 [MePro+Phe+Tyr+H]; 379 [MePro+Phe+Tyr+H-CO]; 349 [Tyr+Gly+Gln+H]; 335 [Phe+Tyr+Gly+H-H₂O]; 312 [Ile+Ser+MePro+H]; 307 [Phe+Tyr+Gly+H-H₂O-CO]; 243 [MePro+Phe+H]; 215 [MePro+Phe+H-CO]; 158 [Gly+Gln+H-CO]; 132 Phe; 84 MePro immonium, Figure S4: Structure and enhanced product ion mass spectrum of the linear nostocyclopeptide aldehyde Ncp-A2-L (linear aldehyde of Ncp-A2) Tyr+Gly+Gln+Ile+Ser+MePro+Phe identified based on the following fragment ions: m/z 809 [M+H]; 791 [M+H-H₂O]; 773 [M+H-2H₂O]; 763 [M+H-CO-H₂O]; 660 [M+H-Phe]; 628 [M+H-Tyr-H₂O]; 549 [Tyr+Gly+Gln+Ile+Ser+H]; 531 [M+H-(MePro+Phe)-H₂O]; 462 [Tyr+Gly+Gln+Ile+H]; 434 [Tyr+Gly+Gln+Ile+H-CO]; 312 [Ile+Ser+MePro+H]; 261 [MePro+Phe+H]; 243 [MePro+Phe+H - H₂O]; 221 [Tyr+Gly+H], 193 [Tyr+Gly+ H-CO]; 148 [Tyr-NH₂]; 136 Tyr immonium; 84, 101 (immonium), 129 Gln; 84 MePro immonium, Figure S5: Proposed structure and enhanced product ion mass spectrum of cyclic nostocyclopeptide Ncp-E2 cyclo[Tyr+Gly+Gln+Ile+Ser+Pro+Leu] characterized based on the following fragment ions: m/z 743 [M+H]; 725 [M+H-H₂O]; 715 [M+H-CO]; 707 [M+H-2H₂O]; 697 [M+H - H₂O-CO]; 656 [M+H-Ser]; 638 [M+H-Ser-H₂O]; 628 [M+H-Ser-CO]; 612 [M+H-Ile-H₂O]; 549 [Tyr+Gly+Gln+Ile+Ser+H]; 541 [M+H-(Ser+Pro)-H₂O]; 531 [Tyr+Gly+Gln+Ile+Ser+H-H₂O]; 428 [M+H-(Ile+Ser+Pro)-H₂O]; 349 [Tyr+Gly+Gln+H]; 300 [Leu+Tyr+Gly+H-H₂O]; 195 [Pro+Leu+H]; 167 [Pro+Leu+H-CO]; 84 Gln; 70 Pro immonium, Figure S6: Proposed structure and enhanced product ion mass spectrum of the linear nostocyclopeptide aldehyde Ncp-E2-L (linear aldehyde of Ncp-E2) with general structure Tyr+Gly+Gln+Ile+Ser+Pro+Leu characterized based on the following fragment ions: m/z 761 [M+H]; 743 [M+H-H₂O]; 725 [M+H-2H₂O]; 549 [Tyr+Gly+Gln+Ile+Ser+H]; 532 [Tyr+Gly+Gln+Ile+Ser+H-H₂O]; 462 [Tyr+Gly+Gln+Ile+H]; 349 [Tyr+Gly+Gln+H]; 434 [Tyr+Gly+Gln+Ile+H-CO]; 300 [Ser+Pro+Leu+H]; 221 [Tyr+Gly+H]; 213 [Pro+Leu+H]; 195 [Pro+Leu+H-H₂O]; 148 [Tyr-NH₂]; 136 Tyr immonium; 84, 101 (immonium), 129 Gln; 70 Pro immonium, Figure S7: Proposed structure and enhanced product ion mass spectrum of cyclic nostocyclopeptide Ncp-E3 cyclo[Tyr+Gly+Gln+Val+Ser+MePro+Leu] characterized based on the following fragment ions: m/z 743 [M+H]; 725 [M+H-H₂O]; 715 [M+H-CO]; 707 [M+H - 2H₂O]; 697 [M+H-H₂O-CO];

645 [M+H-Val]; 580 [M+H-Tyr]; 527 [M+H-(Ser+MePro)-H₂O]; 428 [M+H-(Val+Ser+MePro)-H₂O]; 410 [M+H-(Val+Ser+MePro)-2H₂O]; 372 [Gly+Gln+Val+Ser+H]; 344 [Gly+Gln+Val+Ser+H-CO]; 300 [Leu+Tyr+Gly+H-H₂O]; 233 [Leu+Tyr+H-CO]; 209 [MePro+Leu+H]; 181 [MePro-Leu+H-CO]; 84 MePro immonium; 72 Val immonium, Figure S8: Relative contents of nostocyclopeptides extracted from 10 mg of lyophilized biomass of *N. edaphicum* CCNP1411 with 20% MeOH of different pH (3.5, 6 and 8)

Author Contributions: Conceptualization, H.M.-M. and G.W.; methodology, H.M.-M. and G.W.; software, M.G., J.G. and R.G.; validation, M.G., J.G. and R.G.; formal analysis, A.F. and M.G.; investigation, A.F. and M.G.; resources, data curation, M.G., H.M.-M., J.G. and R.G.; writing—original draft preparation, A.F. and M.G.; writing—review and editing, A.F., M.G.; H.M.-M. and G.W.; visualization, A.F. and M.G.; supervision, H.M.-M. and G.W.; project administration, H.M.-M.; funding acquisition, H.M.-M. All authors have read and agreed to the published version of the manuscript.

Funding: This research was funded by the National Science Centre in Poland 2016/21/B/NZ9/02304.

Conflicts of Interest: The authors declare no conflict of interest.

References

- Moore, R. Cyclic peptides and depsipeptides from cyanobacteria: A review. *J. Ind. Microbiol.* **1996**, *16*, 134–143. [[CrossRef](#)] [[PubMed](#)]
- Golakoti, T.; Ogino, J.; Heltzel, C.; Le Husebo, T.; Jensen, C.; Larsen, L.; Patterson, G.; Moore, R.; Mooberry, S.; Corbett, T.; et al. Structure determination, conformational analysis, chemical stability studies, and antitumor evaluation of the cryptophycins. Isolation of new 18 analogs from *Nostoc* sp. strain GSV 224. *J. Am. Chem. Soc.* **1995**, *117*, 12030–12049. [[CrossRef](#)]
- Boyd, M.; Gustafson, K.; McMahan, J.; Shoemaker, R.; O’Keefe, B.; Mori, T.; Gulakowski, R.; Wu, L.; Rivera, M.; Laurencot, C.; et al. Discovery of cyanovirin-N, a novel human immunodeficiency virus-inactivating protein that binds viral surface envelope glycoprotein gp120: Potential applications to microbicide development. *Antimicrob. Agents Chemother.* **1997**, *41*, 1521–1530. [[CrossRef](#)]
- Ploutno, A.; Carmeli, S. Nostocycline A, a novel antimicrobial cyclophane from the cyanobacterium *Nostoc* sp. *J. Nat. Prod.* **2000**, *63*, 1524–1526. [[CrossRef](#)]
- El-Sheekh, M.; Osman, M.; Dyan, M.; Amer, M. Production and characterization of antimicrobial active substance from the cyanobacterium *Nostoc muscorum*. *Environ. Toxicol. Pharmacol.* **2006**, *21*, 42–50. [[CrossRef](#)] [[PubMed](#)]
- Mazur-Marzec, H.; Fidor, A.; Cegłowska, M.; Wiczerzak, E.; Kropidłowska, M.; Goua, M.; Macaskill, J.; Edwards, C. Cyanopeptolins with trypsin and chymotrypsin inhibitory activity from the cyanobacterium *Nostoc edaphicum* CCNP1411. *Mar. Drugs* **2018**, *16*, 220. [[CrossRef](#)] [[PubMed](#)]
- Řezanka, T.; Dor, I.; Dembitsky, V. Fatty acid composition of six freshwater wild cyanobacterial species. *Folia Microbiol.* **2003**, *48*, 71–75. [[CrossRef](#)]
- Schwartz, R.; Hirsch, C.; Sesin, D.; Flor, J.; Chartrain, M.; Fromtling, R.; Harris, G.; Salvatore, M.; Liesch, J.; Yudin, K. Pharmaceuticals from cultured algae. *J. Ind. Microbiol.* **1990**, *5*, 113–124. [[CrossRef](#)]
- Gustafson, K.; Sowder, R.; Henderson, L.; Cardellina, J.; McMahan, J.; Rajamani, U.; Pannell, L.; Boyd, M. Isolation, primary sequence determination, and disulfide bond structure of cyanovirin-N, an anti-HIV (Human Immunodeficiency Virus) protein from the cyanobacterium *Nostoc ellipsosporum*. *Biochem. Biophys. Res. Commun.* **1997**, *238*, 223–228. [[CrossRef](#)]
- Okino, T.; Qi, S.; Matsuda, H.; Murakami, M.; Yamaguchi, K. Nostopeptins A and B, elastase inhibitors from the cyanobacterium *Nostoc minutum*. *J. Nat. Prod.* **1997**, *60*, 158–161. [[CrossRef](#)]
- Kaya, K.; Sano, T.; Beattie, K.; Codd, G. Nostocyclin, a novel 3-amino-6-hydroxy-2-piperidone containing cyclic depsipeptide from the cyanobacterium *Nostoc* sp. *Tetrahedron Lett.* **1996**, *37*, 6725–6728. [[CrossRef](#)]
- Mehner, C.; Müller, D.; Kehraus, S.; Hautmann, S.; Gütschow, M.; König, G. New peptolides from the cyanobacterium *Nostoc insulare* as selective and potent inhibitors of human leukocyte elastase. *ChemBioChem* **2008**, *9*, 2692–2703. [[CrossRef](#)] [[PubMed](#)]
- Golakoti, T.; Yoshida, W.; Chaganty, S.; Moore, R. Isolation and structure determination of nostocyclopeptides A1 and A2 from the terrestrial cyanobacterium *Nostoc* sp. ATCC53789. *J. Nat. Prod.* **2001**, *64*, 54–59. [[CrossRef](#)] [[PubMed](#)]
- Nowruzi, B.; Khavari-Nejad, R.; Sivonen, K.; Kazemi, B.; Najafi, F.; Nejadstari, T. Identification and toxicogenic potential of *Nostoc* sp. *Algae* **2012**, *27*, 303–313. [[CrossRef](#)]

15. Liaimer, A.; Jensen, J.; Dittmann, E. A genetic and chemical perspective on symbiotic recruitment of cyanobacteria of the genus *Nostoc* into the host plant *Blasia pusilla* L. *Front. Microbiol.* **2016**, *7*, 1963. [[CrossRef](#)] [[PubMed](#)]
16. Jokela, J.; Herfindal, L.; Wahlsten, M.; Permi, P.; Selheim, F.; Vasconcelos, V.; Døskeland, S.; Sivonen, K. A novel cyanobacterial nostocyclopeptide is a potent antitoxin against Microcystis. *ChemBioChem* **2010**, *11*, 1594–1599. [[CrossRef](#)]
17. Becker, J.; Moore, R.; Moore, B. Cloning, sequencing, and biochemical characterization of the nostocyclopeptide biosynthetic gene cluster: Molecular basis for imine macrocyclization. *Gene* **2004**, *325*, 35–42. [[CrossRef](#)]
18. Hoffmann, D.; Hevel, J.; Moore, R.; Moore, B. Sequence analysis and biochemical characterization of the nostopeptolide A biosynthetic gene cluster from *Nostoc* sp. GSV224. *Gene* **2003**, *311*, 171–180. [[CrossRef](#)]
19. Kopp, F.; Mahlet, C.; Grünewald, J.; Marahiel, M. Peptide macrocyclization: The reductase of the nostocyclopeptide synthetase triggers the self-assembly of a macrocyclic imine. *J. Am. Chem. Soc.* **2006**, *128*, 16478–16479. [[CrossRef](#)]
20. Enck, S.; Kopp, F.; Marahiel, M.; Geyer, A. The entropy balance of nostocyclopeptide macrocyclization analysed by NMR spectroscopy. *ChemBioChem* **2008**, *9*, 2597–2601. [[CrossRef](#)]
21. Herfindal, L.; Myhren, L.; Kleppe, R.; Krakstad, C.; Selheim, F.; Jokela, J.; Sivonen, K.; Døskeland, S. Nostocyclopeptide-M1: A potent, nontoxic inhibitor of the hepatocyte drug transporters OATP1B3 and OATP1B1. *Mol. Pharm.* **2011**, *8*, 360–367. [[CrossRef](#)]
22. Lee, W.; Belkhiri, A.; Lockhart, A.; Merchant, N.; Glaeser, H.; Harris, E.; Washington, M.; Brunt, E.; Zaika, A.; Kim, R.; et al. Overexpression of OATP1B3 confers apoptotic resistance in colon cancer. *Cancer Res.* **2008**, *68*, 10315–10323. [[CrossRef](#)] [[PubMed](#)]
23. Nishizawa, T.; Ueda, A.; Nakano, T.; Nishizawa, A.; Miura, T.; Asayama, M.; Fujii, K.; Harada, K.; Shirai, M. Characterization of the locus of genes encoding enzymes producing heptadepsipeptide micropeptin in the unicellular cyanobacterium Microcystis. *J. Biochem.* **2011**, *149*, 475–485. [[CrossRef](#)] [[PubMed](#)]
24. Rouhiainen, L.; Jokela, J.; Fewer, D.; Urmann, M.; Sivonen, K. Two alternative starter modules for the non-ribosomal biosynthesis of specific anabaenopeptin variants in *Anabaena* (cyanobacteria). *Chem. Biol.* **2010**, *17*, 265–273. [[CrossRef](#)] [[PubMed](#)]
25. Luesch, H.; Hoffmann, D.; Hevel, J.; Becker, J.; Golakoti, T.; Moore, R. Biosynthesis of 4-Methylproline in Cyanobacteria: Cloning of *nosE* and *nosF* and biochemical characterization of the encoded dehydrogenase and reductase activities. *J. Org. Chem.* **2003**, *68*, 83–91. [[CrossRef](#)] [[PubMed](#)]
26. Lambalot, R.; Walsh, C. Cloning, Overproduction, and Characterization of the *Escherichia coli* Holo-acyl Carrier Protein Synthase. *J. Biol. Chem.* **1995**, *270*, 24658–24661. [[CrossRef](#)]
27. Marchler-Bauer, A.; Derbyshire, M.; Gonzales, N.; Lu, S.; Chitsaz, F.; Geer, L.; Geer, R.; He, J.; Gwadz, M.; Hurwitz, D.; et al. CDD: NCBI's conserved domain database. *Nucleic Acids Res.* **2015**, *43*, d222–d226. [[CrossRef](#)]
28. Stachelhaus, T.; Mootz, H.; Marahiel, M. The specificity-conferring code of adenylation domains in nonribosomal peptide synthetases. *Chem. Biol.* **1999**, *6*, 493–505. [[CrossRef](#)]
29. Challis, G.; Ravel, J.; Townsend, C. Predictive, structure-based model of amino acid recognition by nonribosomal peptide synthetase adenylation domains. *Chem. Biol.* **2000**, *7*, 211–224. [[CrossRef](#)]
30. Stein, T.; Vater, J.; Kruff, V.; Otto, A.; Wittmann-Liebold, B.; Franke, P.; Panico, M.; McDowell, R.; Morris, H. The multiple carrier model of nonribosomal peptide biosynthesis at modular multienzymatic templates. *J. Biol. Chem.* **1996**, *271*, 15428–15435. [[CrossRef](#)]
31. Dehling, E.; Volkmann, G.; Matern, J.; Dörner, W.; Alfermann, J.; Diecker, J.; Mootz, H. Mapping of the Communication-Mediating Interface in Nonribosomal Peptide Synthetases Using a Genetically Encoded Photocrosslinker Supports an Upside-Down Helix-Hand Motif. *J. Mol. Biol.* **2016**, *428*, 4345–4360. [[CrossRef](#)]
32. Hacker, C.; Cai, X.; Kegler, C.; Zhao, L.; Weickmann, K.; Wurm, J.; Bode, H.; Wöhnert, J. Structure-based redesign of docking domain interactions modulates the product spectrum of a rhabdopeptide-synthesizing NRPS. *Nat. Commun.* **2018**, *9*, 4366. [[CrossRef](#)]
33. Richter, C.; Nietlispach, D.; Broadhurst, R.; Weissman, K. Multienzyme docking in hybrid megasynthetases. *Nat. Chem. Biol.* **2008**, *4*, 75–81. [[CrossRef](#)] [[PubMed](#)]

34. Haese, A.; Schubert, M.; Herrmann, M.; Zoicher, R. Molecular characterization of the enniatin synthetase gene encoding a multifunctional enzyme catalysing N-methyldepsipeptide formation in *Fusarium scirpi*. *Mol. Biol.* **1993**, *7*, 905–914. [[CrossRef](#)]
35. Marahiel, M.; Stachelhaus, T.; Mootz, H. Modular peptide synthetases involved in nonribosomal peptide synthesis. *Chem. Rev.* **1997**, *97*, 2651–2674. [[CrossRef](#)]
36. Chang, C.; Lohman, J.; Huang, T.; Michalska, K.; Bigelow, L.; Rudolf, J.; Jędrzejczak, R.; Yan, X.; Ma, M.; Babnigg, G.; et al. Structural Insights into the Free-Standing Condensation Enzyme SgcC5 Catalyzing Ester-Bond Formation in the Biosynthesis of the Eneidyne Antitumor Antibiotic C-1027. *Biochemistry* **2018**, *57*, 3278–3288. [[CrossRef](#)]
37. Du, L.; Lou, L. PKS and NRPS release mechanisms. *Nat. Prod. Rep.* **2010**, *27*, 255–278. [[CrossRef](#)] [[PubMed](#)]
38. Koketsu, K.; Minami, A.; Watanabe, K.; Oguri, H.; Oikawa, H. Pictet-Spenglerase involved in tetrahydroisoquinoline antibiotic biosynthesis. *Curr. Opin. Chem. Biol.* **2012**, *16*, 142–149. [[CrossRef](#)] [[PubMed](#)]
39. Liu, L.; Jokela, J.; Herfindal, L.; Wahlsten, M.; Sinkkonen, J.; Permi, P.; Fewer, D.; Døskeland, S.; Sivonen, K. 4-Methylproline guided natural product discovery: Co-occurrence of a 4-hydroxy- and 4-methylprolines in nostoweipeptins and nostopeptolides. *ACS Chem. Biol.* **2014**, *9*, 2646–2655. [[CrossRef](#)]
40. Bouaïcha, N.; Miles, C.; Beach, D.; Labidi, Z.; Djabri, A.; Benayache, N.; Nguyen-Quang, T. Structural diversity, characterization and toxicology of microcystins. *Toxins* **2019**, *11*, 714. [[CrossRef](#)]
41. Jones, M.; Pinto, E.; Torres, M.; Dörr, F.; Mazur-Marzec, H.; Szubert, K.; Tartaglione, L.; Dell’Aversano, C.; Miles, C.; Beach, D.; et al. Comprehensive database of secondary metabolites from cyanobacteria. *BioRxiv* **2020**. [[CrossRef](#)]
42. Meyer, S.; Kehr, J.; Mainz, A.; Dehm, D.; Petras, D.; Süßmuth, R.; Dittmann, E. Biochemical dissection of the natural diversification of microcystin provides lessons for synthetic biology of NRPS. *Cell. Chem. Biol.* **2016**, *23*, 462–471. [[CrossRef](#)] [[PubMed](#)]
43. Kondratyeva, N.V. Novyi vyd synio-zelenykh vodorostey—*Nostoc edaphicum* sp. n. [A new species of blue-green algae—*Nostoc edaphicum* sp. n. *Ukr. Bot. J.* **1962**, *19*, 58–65.
44. Komárek, J. *Süßwasserflora von Mitteleuropa. Cyanoprokaryota: 3rd Part: Heterocystous Genera*; Springer Spectrum: Berlin/Heidelberg, Germany, 2013; Volume 19, pp. 1–1130.
45. Kotai, J. *Instructions for Preparation of Modified Nutrient Solution Z8 for Algae*; Publication: B-11/69; Norwegian Institute for Water Research: Oslo, Norway, 1972; p. 5.
46. Bertani, G. Studies on lysogenesis. I. The mode of phage liberation by lysogenic *Escherichia Coli*. *J. Bacteriol.* **1951**, *62*, 293–300. [[CrossRef](#)] [[PubMed](#)]
47. Nowak, R.; Jastrzebski, J.; Kuśmirek, W.; Sałamatın, R.; Rydzanicz, M.; Sobczyk-Kopciół, A.; Sulima-Celińska, A.; Pauksztó, Ł.; Makowaczenko, K.; Płoski, R.; et al. Hybrid de novo whole genome assembly and annotation of the model tapeworm *Hymenolepis diminuta*. *Sci. Data* **2019**, *6*, 302. [[CrossRef](#)]
48. Wilson, K. Preparation of genomic DNA from bacteria. In *Current Protocols in Molecular Biology*; Ausubel, R., Bent, R.E., Eds.; Kingston: Fountain Valley, CA, USA; Wiley & Sons: New York, NY, USA, 1987; pp. 2.10–2.12.
49. Andrews, S. Babraham Bioinformatics, FastQC—A Quality Control Application for High Throughput Sequence Data. 2010. Available online: <http://www.bioinformatics.babraham.ac.uk/projects/fastqc/> (accessed on 11 February 2020).
50. De Coster, W.; D’Hert, S.; Schultz, D.; Cruets, M.; Van Broeckhoven, C. NanoPack: Visualizing and processing long-read sequencing data. *Bioinformatics* **2018**, *34*, 2666–2669. [[CrossRef](#)]
51. Kolmogorov, M.; Yuan, J.; Lin, Y.; Pevzner, P. Assembly of long, error-prone reads using repeat graphs. *Nat. Biotechnol.* **2019**, *37*, 540–546. [[CrossRef](#)]
52. Tatusova, T.; DiCuccio, M.; Badretdin, A.; Chetvernin, V.; Nawrocki, E.; Zaslavsky, L.; Lomsadze, A.; Pruitt, K.; Borodovsky, M.; Ostell, J. NCBI prokaryotic genome annotation pipeline. *Nucleic Acids Res.* **2016**, *44*, 6614–6624. [[CrossRef](#)]
53. Seemann, T. Prokka: Rapid prokaryotic genome annotation. *Bioinformatics* **2014**, *30*, 2068–2069. [[CrossRef](#)]
54. Grant, J.; Arantes, A.; Stothard, P. Comparing thousands of circular genomes using the CGView comparison tool. *BMC Genom.* **2012**, *13*, 202. [[CrossRef](#)]
55. Altschul, S.; Madden, T.; Schäffer, A.; Zhang, J.; Zhang, Z.; Miller, W.; Lipman, D. Gapped BLAST and PSI-BLAST: A new generation of protein database search programs. *Nucleic Acids Res.* **1997**, *25*, 3389–3402. [[CrossRef](#)] [[PubMed](#)]

56. Medema, M.; Blin, K.; Cimermanic, P.; de Jager, V.; Zakrzewski, P.; Fischbach, M.; Weber, T.; Takano, E.; Breitling, R. antiSMASH: Rapid identification, annotation and analysis of secondary metabolites biosynthesis gene clusters in bacterial and fungal genome sequences. *Nucleic Acids Res.* **2011**, *39*, w339–w346. [[CrossRef](#)]
57. Marchler-Bauer, A.; Lu, S.; Anderson, J.; Chitsaz, F.; Derbyshire, M.; DeWesse-Scott, C.; Fong, J.; Geer, L.; Geer, R.; Gonzales, N.; et al. CDD: A conserved database for the functional annotation of proteins. *Nucleic Acids Res.* **2011**, *39*, d225–d229. [[CrossRef](#)] [[PubMed](#)]
58. Yang, J.; Yan, R.; Roy, A.; Xu, D.; Poisson, J.; Zhang, Y. The I-TASSER Suite: Protein structure and function prediction. *Nat. Methods* **2015**, *12*, 7–8. [[CrossRef](#)] [[PubMed](#)]
59. Bachmann, B.; Ravel, J. Methods for in silico prediction of microbial polyketide and nonribosomal peptide biosynthetic pathways from DNA sequence data. *Methods Enzymol.* **2009**, *458*, 181–217.
60. Kumar, S.; Stecher, G.; Li, M.; Knyaz, C.; Tamura, K. MEGA X: Molecular Evolutionary Genetics Analysis across computing platforms. *Mol. Biol. Evol.* **2018**, *35*, 1547–1549. [[CrossRef](#)]



© 2020 by the authors. Licensee MDPI, Basel, Switzerland. This article is an open access article distributed under the terms and conditions of the Creative Commons Attribution (CC BY) license (<http://creativecommons.org/licenses/by/4.0/>).

Supplementary Material: *Nostoc edaphicum* CCNP1411 from the Baltic Sea – a new producer of nostocyclopeptides

Anna Fidor ¹, Michał Grabski ², Jan Gawor ³, Robert Gromadka ³, Grzegorz Węgrzyn ², Hanna Mazur-Marzec ^{1*}

¹ Division of Marine Biotechnology, Faculty of Oceanography and Geography, University of Gdansk, Marszałka J. Piłsudskiego 46, PL-81378 Gdynia, Poland; anna.fidor@phdstud.ug.edu.pl (A.F.);

² Department of Molecular Biology, University of Gdansk, Wita Stwosza 59, 80-308 Gdansk, Poland; grzegorz.wegrzyn@biol.ug.edu.pl (G.W.); michal.grabski@phdstud.ug.edu.pl (M.G.);

³ Institute of Biochemistry and Biophysics, Polish Academy of Sciences, DNA Sequencing and Oligonucleotide Synthesis Laboratory, Warsaw, Poland; gaworj@ibb.waw.pl (J.G.); robert@ibb.waw.pl (R.G.)

* Correspondence: hanna.mazur-marzec@ug.edu.pl; Tel.: +48 -58-523-66-21; +609-419-132 (H.M.M.)

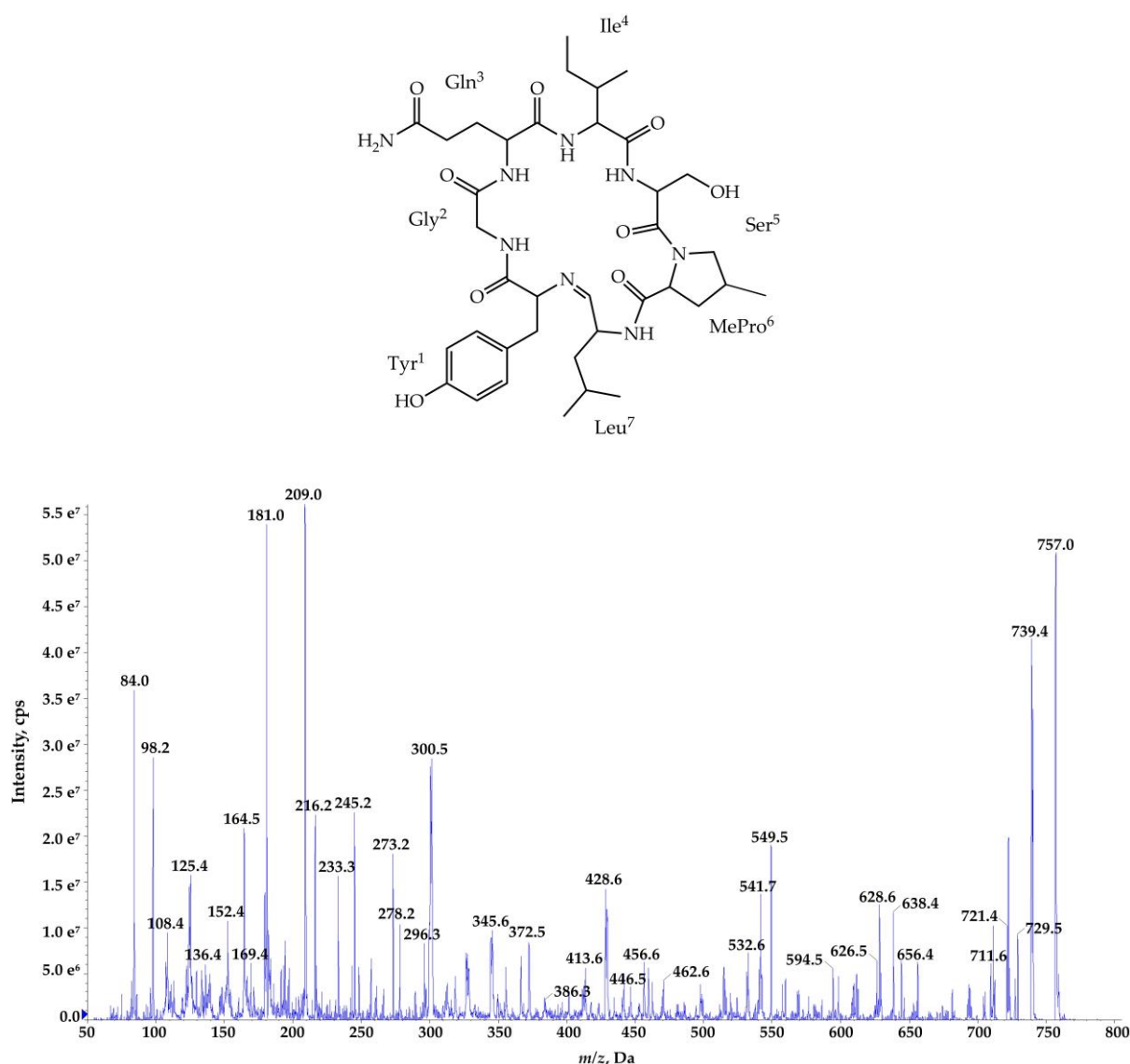


Figure S1: Structure and enhanced product ion mass spectrum of the cyclic nostocyclopeptide **Ncp-A1** cyclo[Tyr+Gly+Gln+Ile+Ser+MePro+Leu] identified based on the following fragment ions: m/z 757 [M+H]; 739 [M+H – H₂O]; 729 [M+H – CO]; 721 [M+H – 2H₂O]; 628 [M+H – MePro – H₂O], 626 [M+H – Ile – H₂O]; 594 [M+H – Tyr]; 549 [Tyr+Gly+Gln+Ile+Ser+H]; 541 [M+H – (Ser+MePro) – H₂O], 446 [M+H – (Ile+Ser+MePro)]; 428 [M+H – (Ile+Ser+MePro) – H₂O]; 386 [Gly+Gln+Ile+Ser+H]; 372 [MePro+Leu+Tyr+H]; 300 [Leu+Tyr+Gly+H – H₂O]; 209 [MePro+Leu+H]; 181 [MePro+Leu+H – CO]; 86 – Ile/Leu immonium; 84 MePro immonium.

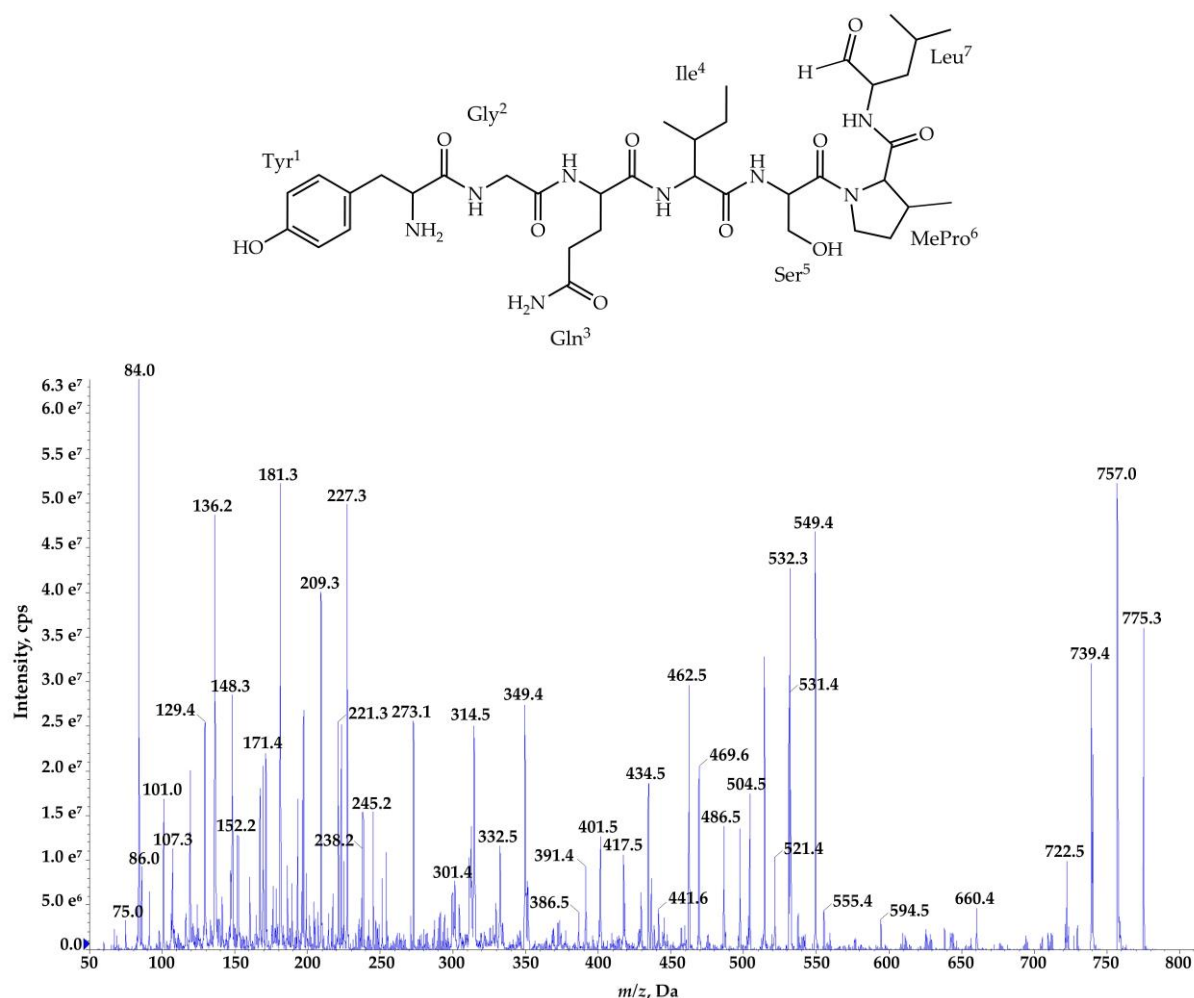


Figure S2: Structure and enhanced product ion mass spectrum of the linear peptide aldehyde **Ncp-A1-L** (linear aldehyde of **Ncp-A1**) Tyr+Gly+Gln+Ile+Ser+MePro+Leu identified based on the following fragment ions: m/z 775 [M+H]; 757 [M+H – H₂O]; 739 [M+H – 2H₂O]; 660 [M+H – Leu]; 549 [Tyr+Gly+Gln+Ile+Ser+H]; 531 [Tyr+Gly+Gln+Ile+Ser+H – H₂O]; 521 [Tyr+Gly+Gln+Ile+Ser+H – CO]; 532 [M+H – (MePro+Leu) – H₂O]; 462 [Tyr+Gly+Gln+Ile+H]; 434 [Tyr+Gly+Gln+Ile+H – CO]; 386 [Gly+Gln+Ile+Ser+H]; 349 [Tyr+Gly+Gln+H]; 301 [Gln+Ile+Ser+H – CO]; 227 [MePro+Leu+H]; 221 [Tyr+Gly+H]; 209 [MePro+Leu+H – H₂O]; 181 [MePro+Ile+H – H₂O – CO]; 148 [Tyr – NH₂]; 136 Tyr immonium; 86 – Ile/Leu immonium; 84, 101 (immonium), 129 Gln; 84 MePro immonium.

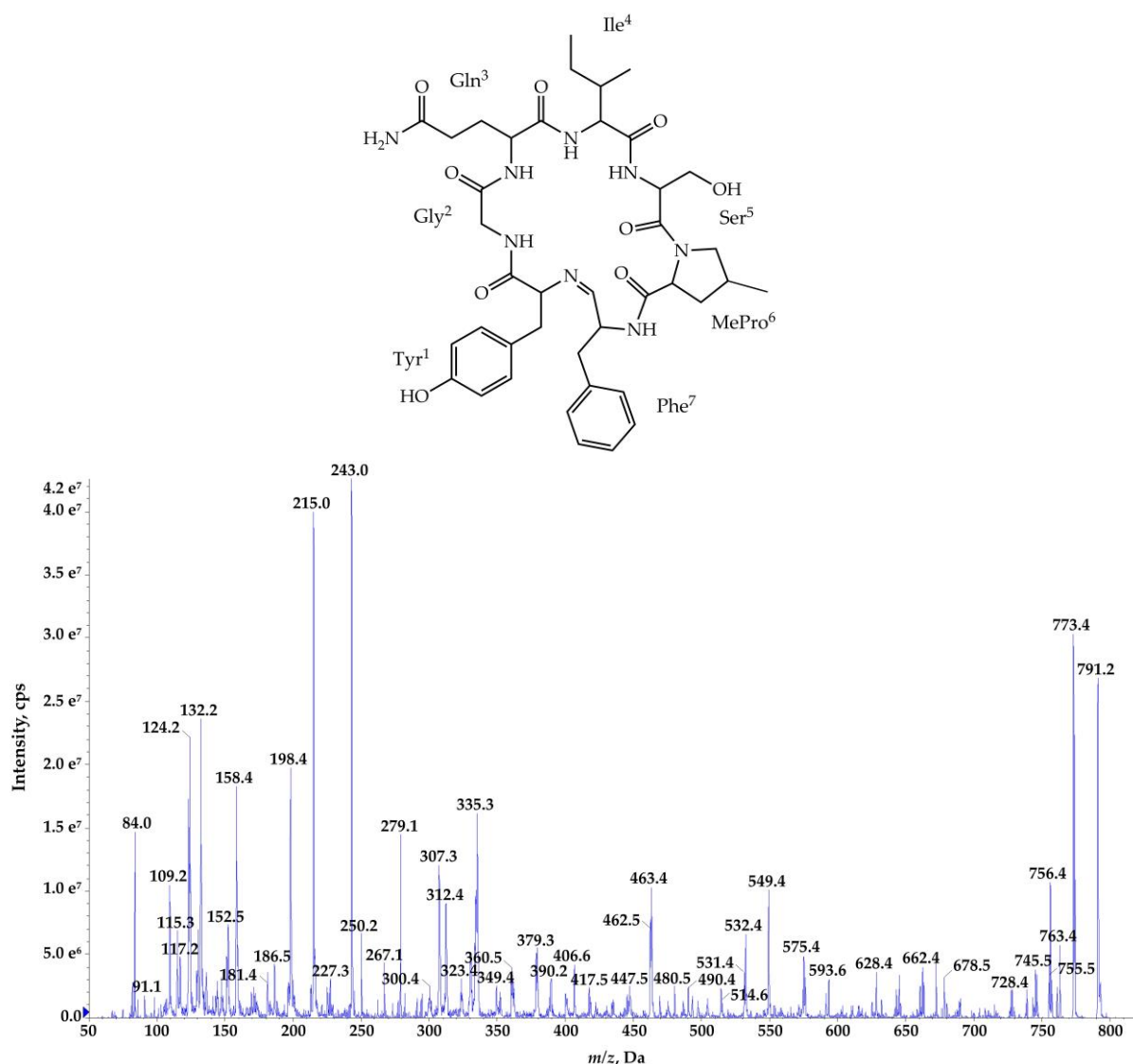


Figure S3: Structure and enhanced product ion mass spectrum of the cyclic nostocyclopeptide **Ncp-A2** cyclo[Tyr+Gly+Gln+Ile+Ser+MePro+Phe] identified based on the following fragment ions: m/z 791 [M+H]; 773 [M+H – H₂O]; 763 [M+H – CO]; 755 [M+H – 2H₂O]; 745 [M+H – CO – H₂O]; 678 [M+H – Ile]; 628 [M+H – Tyr]; 593 [M+H – (Ser+MePro)]; 549 [Tyr+Gly+Gln+Ile+Ser+H]; 531 [Tyr+Gly+Gln+Ile+Ser+H – H₂O]; 480 [M+H – (Ile+Ser+MePro)]; 462 [Tyr+Gly+Gln+Ile+H]; 406 [MePro+Phe+Tyr+H]; 379 [MePro+Phe+Tyr+H – CO]; 349 [Tyr+Gly+Gln+H]; 335 [Phe+Tyr+Gly+H – H₂O]; 312 [Ile+Ser+MePro+H]; 307 [Phe+Tyr+Gly+H – H₂O – CO]; 243 [MePro+Phe+H]; 215 [MePro+Phe+H – CO]; 158 [Gly+Gln+H – CO]; 132 Phe; 84 MePro immonium.

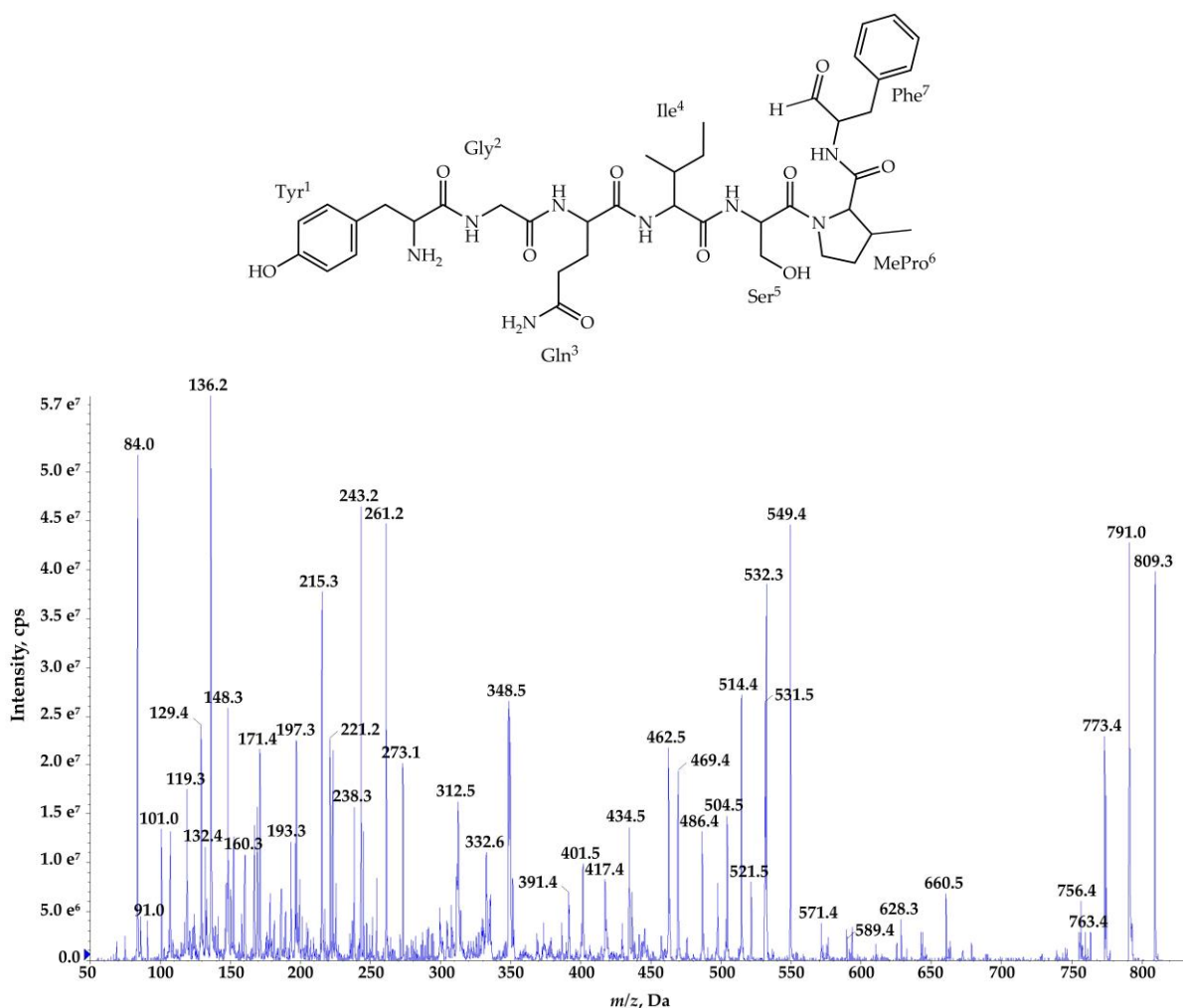


Figure S4: Structure and enhanced product ion mass spectrum of the linear nostocyclopeptide aldehyde **Ncp-A2-L** (linear aldehyde of **Ncp-A2**) Tyr+Gly+Gln+Ile+Ser+MePro+Phe identified based on the following fragment ions: m/z 809 [M+H]; 791 [M+H – H₂O]; 773 [M+H – 2H₂O]; 763 [M+H – CO – H₂O]; 660 [M+H – Phe]; 628 [M+H – Tyr – H₂O]; 549 [Tyr+Gly+Gln+Ile+Ser+H]; 531 [M+H – (MePro+Phe) – H₂O]; 462 [Tyr+Gly+Gln+Ile+H]; 434 [Tyr+Gly+Gln+Ile+H – CO]; 312 [Ile+Ser+MePro+H]; 261 [MePro+Phe+H]; 243 [MePro+Phe+H – H₂O]; 221 [Tyr+Gly+H], 193 [Tyr+Gly+H – CO]; 148 [Tyr – NH₂]; 136 Tyr immonium; 84, 101 (immonium), 129 Gln; 84 MePro immonium.

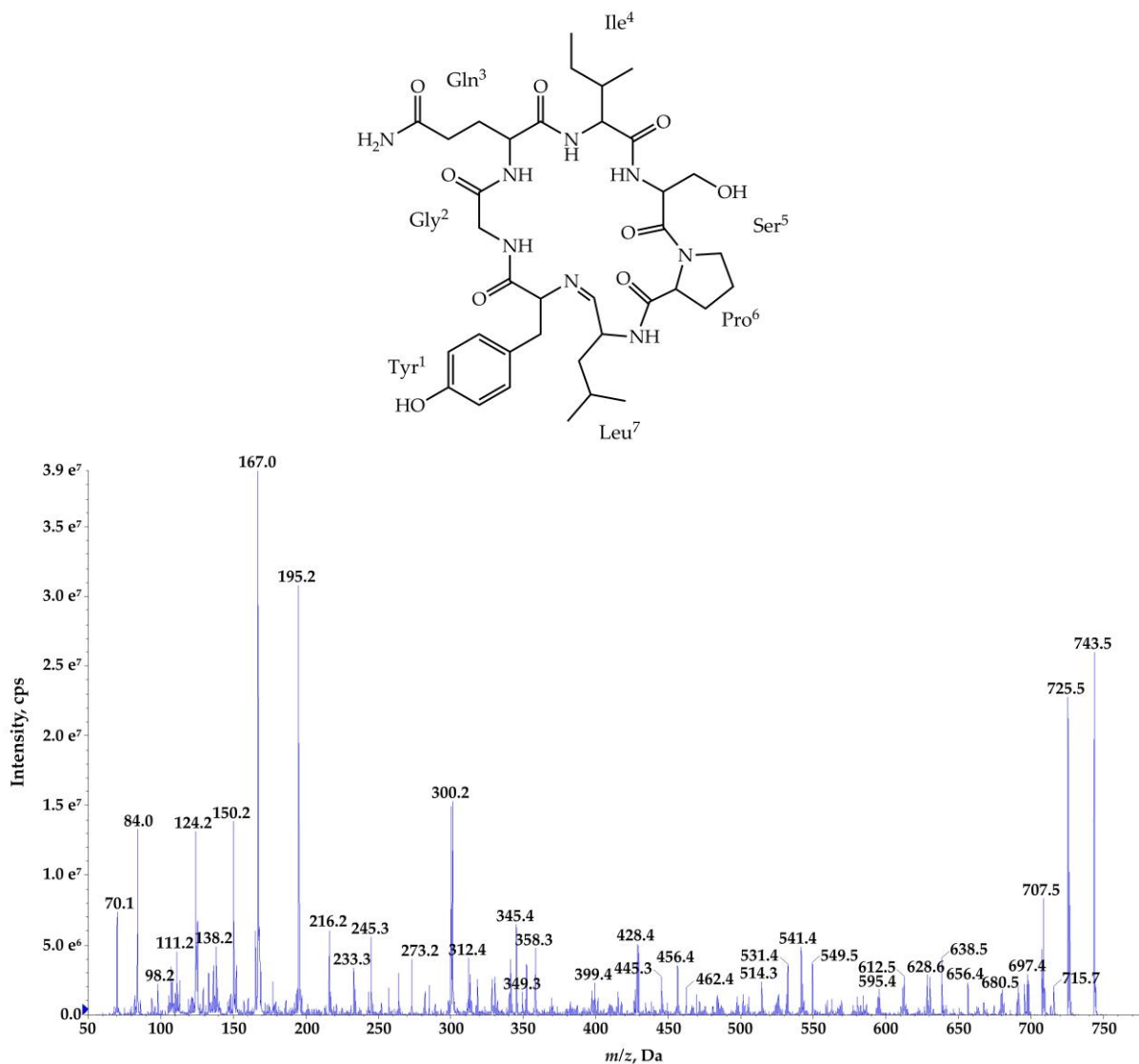


Figure S5: Proposed structure and enhanced product ion mass spectrum of cyclic nontocyclopeptide **Ncp-E2** cyclo[Tyr+Gly+Gln+Ile+Ser+Pro+Leu] characterized based on the following fragment ions: m/z 743 [M+H]; 725 [M+H - H₂O]; 715 [M+H - CO]; 707 [M+H - 2H₂O]; 697 [M+H - H₂O - CO]; 656 [M+H - Ser]; 638 [M+H - Ser - H₂O]; 628 [M+H - Ser - CO]; 612 [M+H - Ile - H₂O]; 549 [Tyr+Gly+Gln+Ile+Ser+H]; 541 [M+H - (Ser+Pro) - H₂O]; 531 [Tyr+Gly+Gln+Ile+Ser+H - H₂O]; 428 [M+H - (Ile+Ser+Pro) - H₂O]; 349 [Tyr+Gly+Gln+H]; 300 [Leu+Tyr+Gly+H - H₂O]; 195 [Pro+Leu+H]; 167 [Pro+Leu+H - CO]; 84 Gln; 70 Pro immonium.

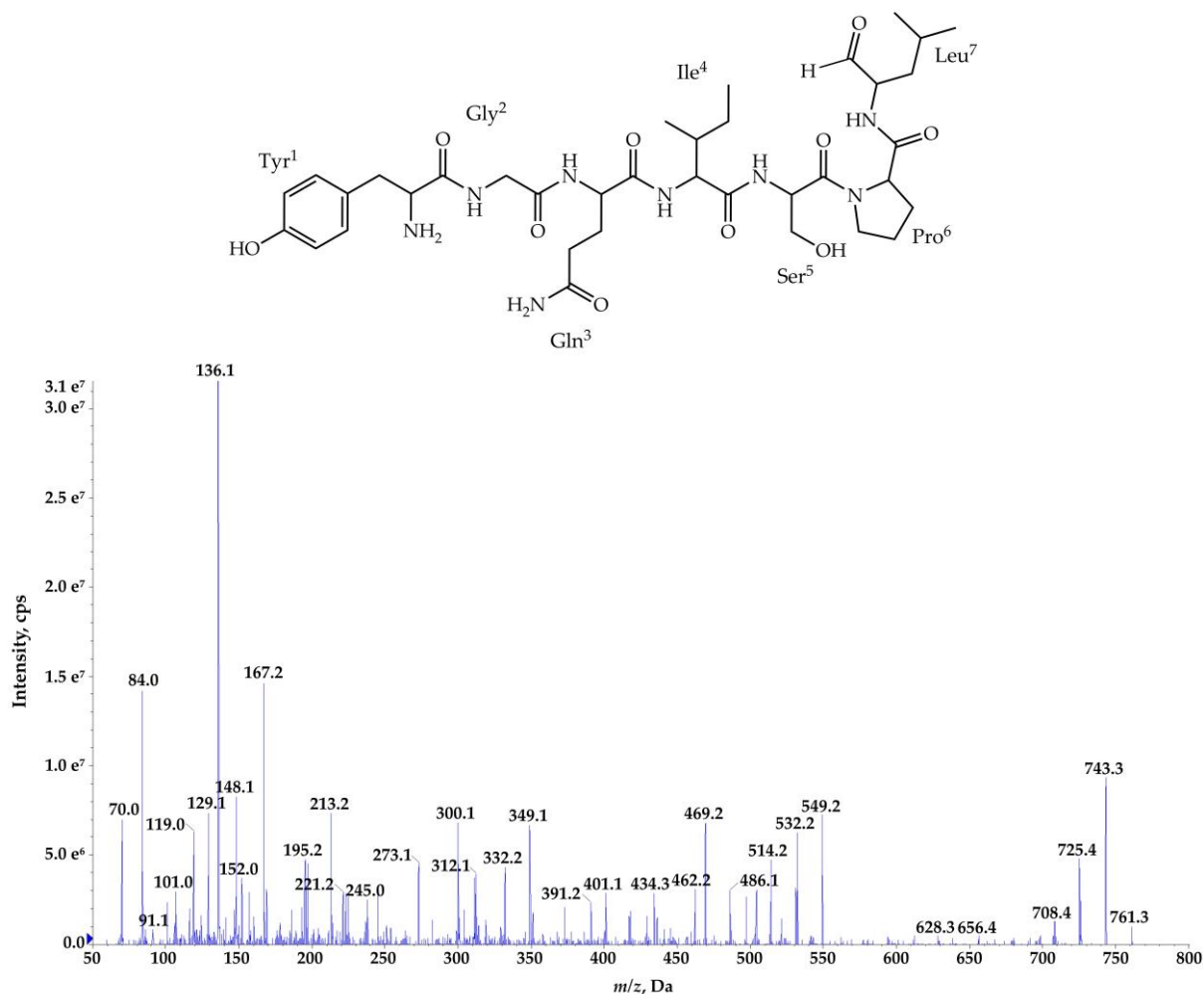


Figure S6: Proposed structure and enhanced product ion mass spectrum of the linear nostocyclopeptide aldehyde **Ncp-E2-L** (linear aldehyde of **Ncp-E2**) with general structure Tyr+Gly+Gln+Ile+Ser+Pro+Leu characterized based on the following fragment ions: m/z 761 [M+H]; 743 [M+H - H₂O]; 725 [M+H - 2H₂O]; 549 [Tyr+Gly+Gln+Ile+Ser+H]; 532 [Tyr+Gly+Gln+Ile+Ser+H - H₂O]; 462 [Tyr+Gly+Gln+Ile+H]; 349 [Tyr+Gly+Gln+H]; 434 [Tyr+Gly+Gln+Ile+H - CO]; 300 [Ser+Pro+Leu+H]; 221 [Tyr+Gly+H]; 213 [Pro+Leu+H]; 195 [Pro+Leu+H - H₂O]; 148 [Tyr - NH₂]; 136 Tyr immonium; 84, 101 (immonium), 129 Gln; 70 Pro immonium.

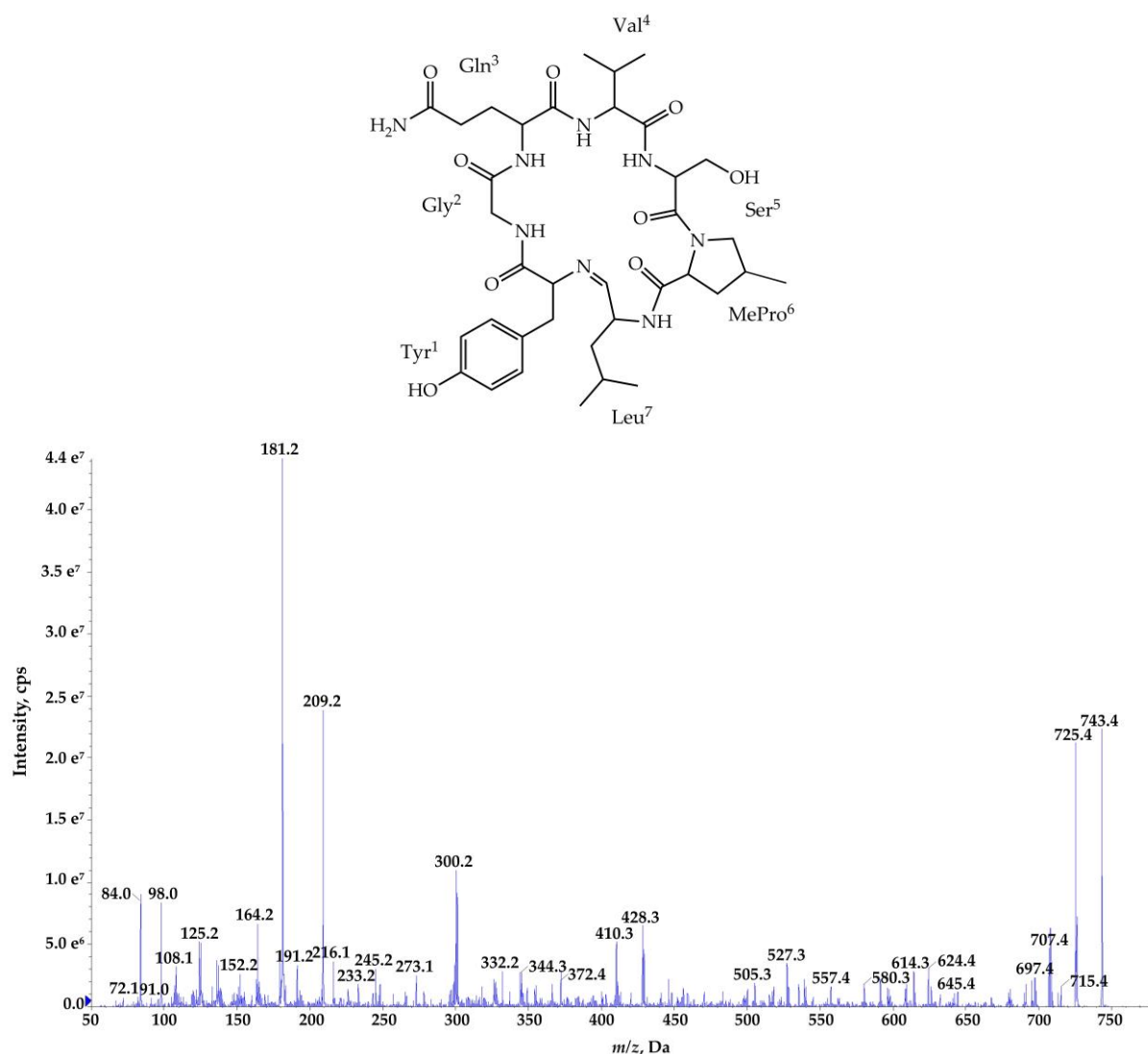


Figure S7: Proposed structure and enhanced product ion mass spectrum of cyclic nostocyclopeptide **Ncp-E3** cyclo[Tyr+Gly+Gln+Val+Ser+MePro+Leu] characterized based on the following fragment ions: m/z 743 [M+H]; 725 [M+H – H₂O]; 715 [M+H – CO]; 707 [M+H – 2H₂O]; 697 [M+H – H₂O – CO]; 645 [M+H – Val]; 580 [M+H – Tyr]; 527 [M+H – (Ser+MePro) – H₂O]; 428 [M+H – (Val+Ser+MePro) – H₂O]; 410 [M+H – (Val+Ser+MePro) – 2H₂O]; 372 [Gly+Gln+Val+Ser+H] ; 344 [Gly+Gln+Val+Ser+H – CO]; 300 [Leu+Tyr+Gly+H – H₂O]; 233 [Leu+Tyr+H – CO]; 209 [MePro+Leu+H]; 181 [MePro – Leu+H – CO]; 84 MePro immonium; 72 Val immonium.

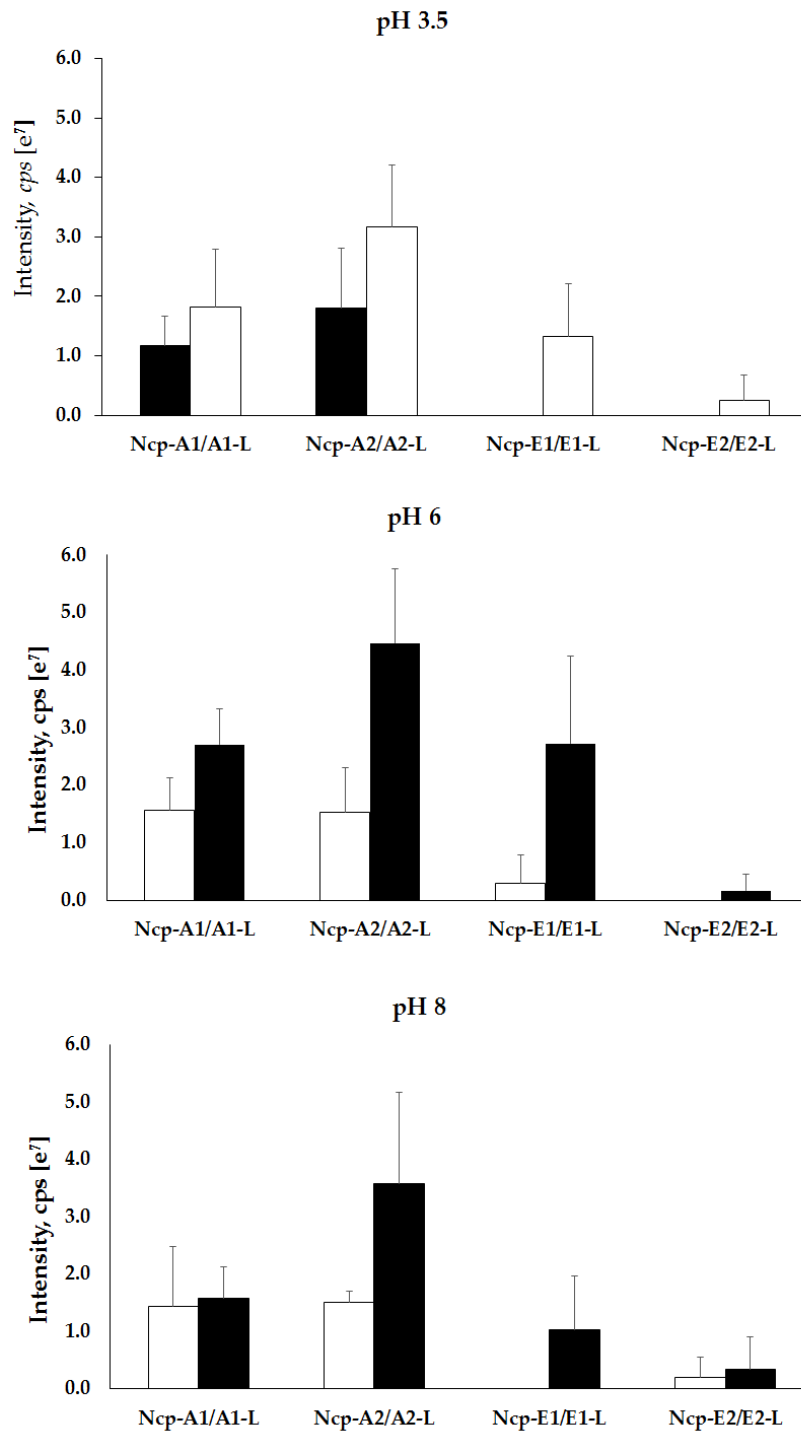


Figure S8: Relative cell contents of nostocyclopeptides extracted from 10 mg of lyophilized biomass of *N. edaphicum* CCNP1411 with 20% MeOH in different pH (3.5, 6 and 8).

Statement of Co-Authorship

Conceptualization: Hanna Mazur-Marzec, Grzegorz Węgrzyn
Methodology: Hanna Mazur-Marzec, Grzegorz Węgrzyn
Software: Michał Grabski, Jan Gawor, Robert Gromadka
Validation: Michał Grabski, Jan Gawor, Robert Gromadka
Formal analysis: Anna Fidor, Michał Grabski
Investigation: Anna Fidor, Michał Grabski
Resources and data curation: Michał Grabski, Jan Gawor, Robert Gromadka, Hanna Mazur-Marzec
Writing – original draft preparation: Anna Fidor, Michał Grabski
Writing – review and editing: Anna Fidor, Michał Grabski, Hanna Mazur-Marzec, Grzegorz Węgrzyn
Visualization: Anna Fidor, Michał Grabski
Supervision: Hanna Mazur-Marzec, Grzegorz Węgrzyn

I, the undersigned, acknowledge the above contribution of work undertaken for the published work "*Nostoc edaphicum* CCNP1411 from the Baltic Sea – a new producer of nostocyclopeptides" (*Marine Drugs*, 2020, DOI:10.3390/md18090442) contributing to the dissertation "Peptides produced by the Baltic cyanobacterium *Nostoc edaphicum* CCNP1411 – structure and biological activity".

My contribution to the work was: LC-MS/MS analyses, investigation, writing the original manuscript, edition of manuscript, data visualization.

.....

(Anna Fidor)

Statement of Co-Authorship

Conceptualization: Hanna Mazur-Marzec, Grzegorz Węgrzyn
Methodology: Hanna Mazur-Marzec, Grzegorz Węgrzyn
Software: Michał Grabski, Jan Gawor, Robert Gromadka
Validation: Michał Grabski, Jan Gawor, Robert Gromadka
Formal analysis: Anna Fidor, Michał Grabski
Investigation: Anna Fidor, Michał Grabski
Resources and data curation: Michał Grabski, Jan Gawor, Robert Gromadka, Hanna Mazur-Marzec
Writing – original draft preparation: Anna Fidor, Michał Grabski
Writing – review and editing: Anna Fidor, Michał Grabski, Hanna Mazur-Marzec, Grzegorz Węgrzyn
Visualization: Anna Fidor, Michał Grabski
Supervision: Hanna Mazur-Marzec, Grzegorz Węgrzyn

I, the undersigned, acknowledge the above contribution of work undertaken for the published work "*Nostoc edaphicum* CCNP1411 from the Baltic Sea – a new producer of nostocyclopeptides" (*Marine Drugs*, 2020, DOI:10.3390/md18090442) contributing to the dissertation "Peptides produced by Baltic cyanobacterium *Nostoc edaphicum* CCNP1411 - structure and biological activity".

My contribution to the work was design of the study, methodology development, data interpretation and edition of manuscript.



(Hanna Mazur-Marzec)

Statement of Co-Authorship

Conceptualization: Hanna Mazur-Marzec, Grzegorz Węgrzyn
Methodology: Hanna Mazur-Marzec, Grzegorz Węgrzyn
Software: Michał Grabski, Jan Gawor, Robert Gromadka
Validation: Michał Grabski, Jan Gawor, Robert Gromadka
Formal analysis: Anna Fidor, Michał Grabski
Investigation: Anna Fidor, Michał Grabski
Resources and data curation: Michał Grabski, Jan Gawor, Robert Gromadka, Hanna Mazur-Marzec
Writing – original draft preparation: Anna Fidor, Michał Grabski
Writing – review and editing: Anna Fidor, Michał Grabski, Hanna Mazur-Marzec, Grzegorz Węgrzyn
Visualization: Anna Fidor, Michał Grabski
Supervision: Hanna Mazur-Marzec, Grzegorz Węgrzyn

I, the undersigned, acknowledge the above contribution of work undertaken for the published work "*Nostoc edaphicum* CCNP1411 from the Baltic Sea – a new producer of nostocyclopeptides" (*Marine Drugs*, 2020, DOI:10.3390/md18090442) contributing to the dissertation "Peptides produced by Baltic cyanobacterium *Nostoc edaphicum* CCNP1411 - structure and biological activity".

The contribution to the work was participation in genetic analyzes, writing the original draft, editing of the manuscript, visualization and discussion of the results.



(Michał Grabski)

Statement of Co-Authorship

Conceptualization: Hanna Mazur-Marzec, Grzegorz Węgrzyn
Methodology: Hanna Mazur-Marzec, Grzegorz Węgrzyn
Software: Michał Grabski, Jan Gawor, Robert Gromadka
Validation: Michał Grabski, Jan Gawor, Robert Gromadka
Formal analysis: Anna Fidor, Michał Grabski
Investigation: Anna Fidor, Michał Grabski
Resources and data curation: Michał Grabski, Jan Gawor, Robert Gromadka, Hanna Mazur-Marzec
Writing – original draft preparation: Anna Fidor, Michał Grabski
Writing – review and editing: Anna Fidor, Michał Grabski, Hanna Mazur-Marzec, Grzegorz Węgrzyn
Visualization: Anna Fidor, Michał Grabski
Supervision: Hanna Mazur-Marzec, Grzegorz Węgrzyn

I, the undersigned, state that my contribution to the published work:

Fidor A, Grabski M, Gawor J, Gromadka R, Węgrzyn G, Mazur-Marzec H. *Nostoc edaphicum* CCNP1411 from the Baltic Sea - A new producer of nostocyclopeptides. *Marine Drugs* 2020; 18(9): 442. doi:10.3390/md18090442.

was as follows: participation in planning the study, expertise in analyzing biological and genomic data, and discussion of the results.


prof. dr hab. Grzegorz Węgrzyn

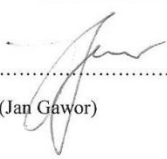
.....
(Grzegorz Węgrzyn)

Statement of Co-Authorship

Conceptualization: Hanna Mazur-Marzec, Grzegorz Węgrzyn
Methodology: Hanna Mazur-Marzec, Grzegorz Węgrzyn
Software: Michał Grabski, Jan Gawor, Robert Gromadka
Validation: Michał Grabski, Jan Gawor, Robert Gromadka
Formal analysis: Anna Fidor, Michał Grabski
Investigation: Anna Fidor, Michał Grabski
Resources and data curation: Michał Grabski, Jan Gawor, Robert Gromadka, Hanna Mazur-Marzec
Writing – original draft preparation: Anna Fidor, Michał Grabski
Writing – review and editing: Anna Fidor, Michał Grabski, Hanna Mazur-Marzec, Grzegorz Węgrzyn
Visualization: Anna Fidor, Michał Grabski
Supervision: Hanna Mazur-Marzec, Grzegorz Węgrzyn

I, the undersigned, acknowledge the above contribution of work undertaken for the published work "*Nostoc edaphicum* CCNP1411 from the Baltic Sea – a new producer of nostocyclopeptides" (*Marine Drugs*, 2020, DOI:10.3390/md18090442) contributing to the dissertation "Peptides produced by Baltic cyanobacterium *Nostoc edaphicum* CCNP1411 - structure and biological activity".

The contribution to the work was participation in sequencing and genome analysis.


.....
(Jan Gawor)



Warsaw, 01.04.2022

Statement of Co-Authorship

Conceptualization: Hanna Mazur-Marzec, Grzegorz Węgrzyn

Methodology: Hanna Mazur-Marzec, Grzegorz Węgrzyn

Software: Michał Grabski, Jan Gawor, Robert Gromadka

Validation: Michał Grabski, Jan Gawor, Robert Gromadka

Formal analysis: Anna Fidor, Michał Grabski

Investigation: Anna Fidor, Michał Grabski

Resources and data curation: Michał Grabski, Jan Gawor, Robert Gromadka, Hanna Mazur-Marzec

Writing – original draft preparation: Anna Fidor, Michał Grabski

Writing – review and editing: Anna Fidor, Michał Grabski, Hanna Mazur-Marzec, Grzegorz Węgrzyn

Visualization: Anna Fidor, Michał Grabski

Supervision: Hanna Mazur-Marzec, Grzegorz Węgrzyn

I, the undersigned, acknowledge the above contribution of work undertaken for the published work "*Nostoc edaphicum* CCNP1411 from the Baltic Sea – a new producer of nostocyclopeptides" (*Marine Drugs*, 2020, DOI:10.3390/md18090442) contributing to the dissertation "Peptides produced by Baltic cyanobacterium *Nostoc edaphicum* CCNP1411 - structure and biological activity".

The contribution to the work was participation in sequencing and genome analysis.

(Robert Gromadka)

Publication 4



Communication

Nostocyclopeptides as New Inhibitors of 20S Proteasome

Anna Fidor ¹, Katarzyna Cekała ², Ewa Wieczerek ², Marta Ceglowska ³, Franciszek Kasprzykowski ², Christine Edwards ⁴ and Hanna Mazur-Marzec ^{1,*}

- ¹ Division of Marine Biotechnology, Institute of Oceanography, University of Gdańsk, Marszałka Józefa Piłsudskiego 46, PL-81378 Gdynia, Poland; anna.fidor@phdstud.ug.edu.pl
- ² Department of Biomedical Chemistry, Faculty of Chemistry, University of Gdańsk, Wita Stwosza 63, PL-80308 Gdańsk, Poland; jedrzejewskakatarzyna.92@gmail.com (K.C.); ewa.wieczerek@ug.edu.pl (E.W.); franciszek.kasprzykowski@ug.edu.pl (F.K.)
- ³ Institute of Oceanology, Polish Academy of Sciences, Powstańców Warszawy 55, PL-81712 Sopot, Poland; mceglowska@iopan.pl
- ⁴ School of Pharmacy and Life Sciences, Robert Gordon University, Aberdeen AB10 7GJ, UK; c.edwards@rgu.ac.uk
- * Correspondence: hanna.mazur-marzec@ug.edu.pl

Abstract: Nostocyclopeptides (Ncps) are a small class of bioactive nonribosomal peptides produced solely by cyanobacteria of the genus *Nostoc*. In the current work, six Ncps were isolated from *Nostoc edaphicum* strain CCNP1411. The bioactivity of these compounds was tested in vitro against 20S proteasome, a proteolytic complex that plays an important role in maintaining cellular proteostasis. Dysfunction of the complex leads to many pathological disorders. The assays indicated selective activity of specific Ncp variants. For two linear peptide aldehydes, Ncp-A2-L and Ncp-E2-L, the inhibitory effects on chymotrypsin-like activity were revealed, while the cyclic variant, Ncp-A2, inactivated the trypsin-like site of this enzymatic complex. The aldehyde group was confirmed to be an important element of the chymotrypsin-like activity inhibitors. The nostocyclopeptides, as novel inhibitors of 20S proteasome, increased the number of natural products that can be considered potential regulators of cellular processes.

Keywords: 20S proteasome inhibitors; cyanobacteria; *Nostoc*; nostocyclopeptides



Citation: Fidor, A.; Cekała, K.; Wieczerek, E.; Ceglowska, M.; Kasprzykowski, F.; Edwards, C.; Mazur-Marzec, H.

Nostocyclopeptides as New Inhibitors of 20S Proteasome. *Biomolecules* **2021**, *11*, 1483. <https://doi.org/10.3390/biom11101483>

Academic Editor: Olivier Coux

Received: 1 September 2021
Accepted: 5 October 2021
Published: 8 October 2021

Publisher's Note: MDPI stays neutral with regard to jurisdictional claims in published maps and institutional affiliations.



Copyright: © 2021 by the authors. Licensee MDPI, Basel, Switzerland. This article is an open access article distributed under the terms and conditions of the Creative Commons Attribution (CC BY) license (<https://creativecommons.org/licenses/by/4.0/>).

1. Introduction

The 26S proteasome is a large (2.4 MDa), multifunctional and ATP-dependent enzymatic complex with chymotrypsin-like (CT-L), trypsin-like (T-L), and caspase-like (C-L) activities [1–4]. In eukaryotic organisms, it recognizes and degrades proteins with covalently attached ubiquitin (8.5 kDa protein) [5,6]. The 26S proteasome is composed of a 20S barrel-shaped core particle (700 kDa) responsible for proteolytic activity and one or two 19S (890 kDa) regulatory subunits with ubiquitin-binding sites [3,4,7]. The 20S proteasome also occurs as a free complex that degrades proteins in the ubiquitin-independent pathway [8,9]. In humans, the dysfunction of this proteolytic machinery leads to changes in protein profile and, ultimately, to serious health problems. Therefore, proteasome regulators are explored as promising therapeutic agents for a range of diseases (e.g., cancer, autoimmune disorders, inflammation, malaria) [10–12]. The majority of the known 20S proteasome inhibitors belongs to peptide-based structures such as peptide aldehydes, boronates, epoxyketones, or peptide vinyl sulfones [13–15]. Some of the active compounds are of natural origin. Leupeptin, isolated from several strains of Gram-positive bacteria of the order *Actinomycetales*, inhibits T-L activity of the 20S proteasome [16]. Tyropeptin A, a peptide aldehyde produced by the soil *Streptomycetales* of the genus *Kitasatospora*, strain MK993-dF2, inhibits mainly CT-L activity [17,18]. Marine fungus *Peicillium fellutanum* is a producer of fellutamide B, a strong inhibitor of CT-L activity (IC₅₀ 9.4 nM) with mild effects on T-L (IC₅₀ 2.0 μM) and C-L (IC₅₀ 1.2 μM) activities [19]. The proteasome inhibition within the nanomolar to the

micromolar range of IC_{50} was also documented for metabolites isolated from cyanobacteria *Symploca* sp., *Scytonema hofmannii*, and *Nostoc*.

In our preliminary studies, fractions from *Nostoc edaphicum* CCNP1411 containing nostocyclopeptides (Ncps) inhibited the chymotrypsin-like activity of the 20S proteasome. Ncps constitute a small group of nonribosomal peptides solely produced by cyanobacteria of the genus *Nostoc*. The biological activity of the peptides was reported in several studies. According to Golakoti et al. [20], Ncp-A1 and Ncp-A2 have cytotoxic activity against human colorectal adenocarcinoma (LoVo) and human nasopharyngeal (KB) cell lines (IC_{50} ca. 1 μ M). Another nostocyclopeptide variant, Ncp-M1, was shown to inhibit the transport of toxic microcystin-LR and nodularin into hepatocytes by blocking organic anion transporter polypeptides, OATP1B1, and OATP1B3. These polypeptides are also overexpressed in cancer cells [21,22]. The role of Ncp-M1 and its analogs as antitumor agents and as tools to study membrane transport was proposed [21,23,24].

Given the pharmaceutical potential of Ncps, the recognition of their action on different cellular targets is important. In the current work, the effects of Ncps on the 20S proteasome were explored. To determine structure-activity relationship, six different Ncps isolated from the Baltic cyanobacterium *N. edaphicum* CCNP1411 were tested, including linear and cyclic Ncp variants.

2. Materials and Methods

2.1. Organism, Extraction, and Isolation of Compounds

Nostoc edaphicum strain CCNP1411 (GenBank Accession Number: PRJNA638531) was isolated from the Gulf of Gdańsk, southern Baltic Sea. The cyanobacterium was grown in a Z8 medium enriched with NaCl [25]. The culture was kept in 2 L flasks at 22 ± 1 °C and light of 5–10 μ mol photons $m^{-2} s^{-1}$. After three weeks, the biomass was harvested using a nylon net (mesh size 25 μ m).

The freeze-dried biomass of CCNP1411 (20 g) was homogenized and extracted four times with 75% methanol (MeOH) in MilliQ water (4×150 mL) by vortexing for 30 min. The extracts were centrifuged at $12,000 \times g$ for 15 min at 4 °C. Combined supernatants were diluted with MilliQ water to achieve the final concentration of MeOH < 10%. Isolation of Ncps was performed using the HPLC system (Shimadzu Corporation, Kyoto, Japan). During all chromatographic runs, the absorbance was monitored at 210 nm and 270 nm. The diluted sample was loaded onto a preconditioned 120 g SNAP KP-C18-HS column (100 Å, 30 μ m) (Biotage, Uppsala, Sweden). The flash chromatography was performed with a mobile phase consisting of MilliQ water (phase A) and 100% MeOH (phase B) using a step gradient from 10 to 100% B over 180 min (flow rate 12 mL min^{-1}). The volume of the fractions collected was 40 mL. Ncps-containing fractions were pooled, concentrated, and separated on Jupiter Proteo C12 column (250 \times 21.2 mm; 90 Å; 4 μ m) (Phenomenex, Torrance, CA, USA). The mobile phase was composed of 5% CH_3CN in MilliQ water (phase A) and 100% CH_3CN (phase B), both containing 0.1% of formic acid (flow rate 12 mL min^{-1}). The chromatographic run (15–100% B) took 110 min, and 2 mL fractions were collected. All fractions containing Ncps mixture were combined, concentrated, and subjected to further separation under modified conditions. The gradient started at 15% B and for the first hour the content of phase B increased by 1% every 15 min up to 19% B. This concentration was maintained for the next 20 min, and then within 30 min, it increased linearly to 100% B. Pure Ncps (Ncp-A2 and Ncp-E4-L) were present in fractions eluted in the range 15–25% of phase B.

The remaining fractions containing Ncps were pooled, and the other four individual peptides were isolated using an analytical Agilent HPLC 1200 Series system (Agilent Technologies, Santa Clara, CA, USA) with a diode array detector (DAD) operating at 210 and 270 nm. Ncp-A1 was isolated using Jupiter Proteo C12 column (250 \times 4.6 mm, 90 Å, 4 μ m) (Phenomenex, Torrance, CA, USA), while Ncp-A2-L, Ncp-E2, and its linear analog Ncp-E2-L, were isolated on Zorbax Eclipse XDB-C18 column (4.6 \times 150 mm; 80 Å; 5 μ m) (Agilent Technologies, Santa Clara, CA, USA). During all analytical chromatographic runs, the same

mobile phase (at flow rate 0.5 mL min^{-1}) was used as for the preparative separations. Ncps were eluted when the mobile phase contained 16–43% B. Identification and purity of peptides in individual fractions and subfractions were achieved by LC-MS/MS analysis at each purification step. Analyses were carried out using Agilent 1200 HPLC (Agilent Technologies, Santa Clara, CA, USA) coupled to a QTRAP5500 triple-quadrupole/linear ion trap mass spectrometer (Applied Biosystems MDS Sciex, Concord, ON, Canada), as previously described [26]. Chromatographic separation was performed on a Zorbax Eclipse XDB-C18 column ($4.6 \times 150 \text{ mm}$; 80 \AA ; 5 \mu m) using gradient elution with the same mobile phase as for the HPLC-DAD analyses. The mass spectrometer operated under the positive Turbo Ion Spray ionization mode (5.5 kV , $550 \text{ }^\circ\text{C}$). Tandem mass spectra were acquired at collision energy 60 V .

2.2. NMR Analysis

The 1D ^1H NMR and 2D homo- and heteronuclear NMR (COSY, TOCSY, ROESY, HSQC, and HMBC) were acquired with the application of Bruker Avance III spectrometers, 500 MHz and 700 MHz (Bruker, Billerica, MA, USA). Spectra were recorded in $\text{H}_2\text{O}:\text{D}_2\text{O}$ (9:1). NMR data were processed and analyzed by TopSpin (Bruker, Billerica, MA, USA) and SPARKY software (3.114, Goddard and Kneller, freeware <https://www.cgl.ucsf.edu/home/sparky>).

2.3. Human 20S Inhibition Assay

The 20S proteasome inhibition assay was performed following the procedure of Czerwonka et al. [27]. Human 20S proteasome (h20S) isolated from erythrocytes was used. Latent h20S was activated with 0.01% SDS (sodium dodecyl sulfate). The final concentration of the proteasome was 1 \mu g mL^{-1} (1.4 nM). The fluorogenic substrates, Suc-LLVY-AMC, Boc-LRR-AMC, and Z-LLE-AMC, were used as probes in the chymotrypsin-like, trypsin, and caspase-like activity assays, respectively, at a final concentration of 100 \mu M . Stock solutions of Ncps (10 mM) were prepared in dimethyl sulfoxide (DMSO) and were tested in the concentration range of 5 to 50 \mu M . The content of DMSO never exceeded 3% of the final reaction volume. The assays were performed in a 96-well plate in 50 mM TrisHCl, pH 8.0, at $37 \text{ }^\circ\text{C}$. The percentage of the substrate hydrolysis was measured by the amount of the released AMC (aminomethyl coumarin) using Tecan Infinite M200 Pro ($\lambda = 380\text{--}460 \text{ nm}$) spectrofluorimeter (Tecan Trading AG, Männedorf, Switzerland). The fluorescence measurements were performed at 2-min intervals for 60 min. The activity of h20S in the presence of isolated Ncps was calculated in relation to the control (DMSO). The known proteasome inhibitor PR11 [28] was used to ensure the correctness of the assay. The peptide at the final concentration of 0.2 \mu M decreases the relative CT-L activity of the h20S to 6% of the control.

3. Results and Discussion

Thus far, the presence of Ncps was reported in five strains of *Nostoc* isolated from different habitats [20,23,29–31]. This includes two Baltic strains: XSPORK 13A producing the cyclic Ncp-M1 [23] and CCNP1411 producing 10 other Ncps variants [31]. The putative structures of the five linear and five cyclic Ncps variants produced by CCNP1411 were elucidated based on mass spectra fragmentation patterns [31]. Two of the cyclic forms, Ncp-A1 and Ncp-A2, enclosed by imino linkage between the *N*-terminal amine group of conserved Tyr and *C*-terminal aldehyde group of Leu or Phe, were previously identified in *Nostoc* sp. ATCC53789 isolated from lichen [20]. In position 6 of the Ncps from CCNP1411, 4-methylproline (MePro) or Pro is present, while Ile or Val is in position 4 (Figure 1). In the current study, we were able to isolate 6 out of 10 Ncps produced by CCNP1411 (Table 1): three cyclic variants (Ncp-A1, Ncp-A2, and Ncp-E2), two linear aldehyde forms of the cyclic variants (Ncp-A2-L and Ncp-E2-L), and the six-amino acid peptide Ncp-E4-L lacking the aldehyde group in the *C*-terminus. In the case of four other Ncps produced by CCNP1411 (Ncp-A1-L, Ncp-E1, Ncp-E1-L, Ncp-E3), their purity and/or quantities were not sufficient

for inclusion in the study. Ncp-A2-L (Figure 1) was the only variant obtained in sufficient amounts for NMR analyses. The ^1H NMR spectrum of Ncp-A2-L displayed a typical pattern of a peptide. The COSY, TOCSY, and HMBC experiments allowed for the identification of the residues in Ncp-A2-L as Tyr, Gly, Gln, Ile, Ser, MePro, and phenylalanine (Phe-H) (Table 2, Figures 1 and S1–S5). The amino acid sequence was confirmed by TOCSY data. The presence of two aromatic amino acid residues was recognized by the signals occurring in the aromatic region of the spectrum (δ_{H} 6.78–7.26 ppm). One of them was identified as tyrosine-based on the AA'BB' spin system between the aromatic protons (Tyr-H5/5' and Tyr-H6/6', JH, H = 8.0 Hz). The second aromatic residue was identified as phenylalanine based on the TOCSY interaction between 34, 35, and 36 protons and the HMBC correlation from two diastereotopic methylene protons 32a (δ_{H} 2.57 ppm) and 32b (δ_{H} 2.98 ppm) to the aromatic 34/34' carbons (Figures S3 and S5). The 4-methyl group of the proline residue was identified based on the ^1H NMR doublet signal at δ 0.82 ppm (protons 29) and the HMBC correlation between the methyl protons with 26 (δ_{C} 37.3 ppm) and 28 (δ_{C} 55.0 ppm) carbons (Figures S1 and S5). The signal at δ_{H} 9.46 ppm was assigned to phenylalanine aldehyde proton. The occurrence of the studied compound in the linear form was further confirmed by the lack of the ROESY correlation between tyrosine and phenylalanine residues.

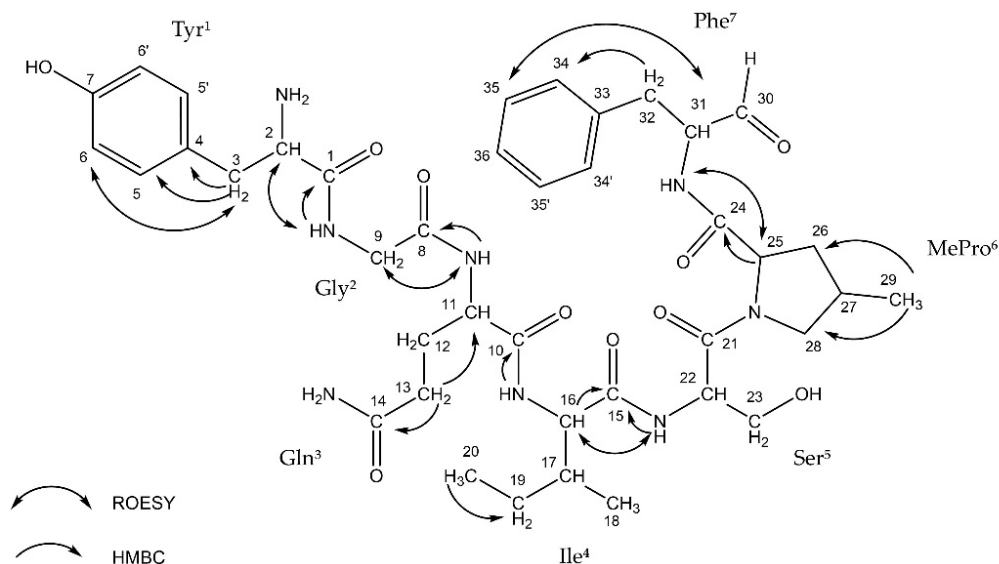


Figure 1. ROESY and HMBC correlations in nostocyclopeptide Ncp-A2-L.

Table 1. Structures of six nostocyclopeptide-variants isolated from *Nostoc edaphicum* CCNP1411 as pure compounds.

Peptide Name	Molecular Mass	Structure
Ncp-A1	756	[Tyr ¹ +Gly ² +Gln ³ +Ile ⁴ +Ser ⁵ +MePro ⁶ +Leu ⁷]
Ncp-A2	790	[Tyr ¹ +Gly ² +Gln ³ +Ile ⁴ +Ser ⁵ +MePro ⁶ +Phe ⁷]
Ncp-A2-L	808	Tyr ¹ +Gly ² +Gln ³ +Ile ⁴ +Ser ⁵ +MePro ⁶ +Phe-H ⁷
Ncp-E2	742	[Tyr ¹ +Gly ² +Gln ³ +Ile ⁴ +Ser ⁵ +Pro ⁶ +Leu ⁷]
Ncp-E2-L	760	Tyr ¹ +Gly ² +Gln ³ +Ile ⁴ +Ser ⁵ +Pro ⁶ +Leu-H ⁷
Ncp-E4-L	676	Tyr ¹ +Gly ² +Gln ³ +Ile ⁴ +Ser ⁵ +MePro ⁶

Table 2. Nuclear Magnetic Resonance (NMR) Spectroscopic Data for Ncp-A2-L (Tyr-Gly-Gln-Ile-Ser-MePro-Phe-H).

Residue	Position	δ_C , type	δ_H (J in Hz)	ROESY	HMBC ^a
Tyr	1				
	2	169.9, C			
	3	54.6, CH	4.13, t (6.9, 6.9)	NH(1), 6	
	4	36.0, CH ₂	3.04, dd (7.3, 12.9)	6	
	5/5'	125.5, C			
	6/6'	130.9, CH	6.78, d (8.0)		2, 4, 5
	7	115.9, CH	7.04, d (8.0)	2, 3	
	NH ₂ OH	155.3, C			
Gly	8	170.7, C			
	9	42.4, CH ₂	3.84, m	NH(2)	
	NH(1)		8.46, t (5.6, 5.6)	2	1
Gln	10				
	11	173.1, C		NH(3)	
	12a	53.2, CH	4.30, m		10
	12b	27.2, CH ₂	1.88, m		
	13		1.99, m		
	14	31.1, CH ₂	2.26, t (7.3, 7.3)		11, 12, 14
	NH(2) NH ₂	178.0, C	8.25, d (7.6)	9	8
Ile	15	173.4, C			
	16	58.2, CH	4.09, t (8.1, 8.1)	NH(4)	17
	17	36.0, CH	1.77, m		
	18	14.7, CH ₃	1.08, d (6.6)		
	19	24.6, CH ₂	1.32, m		
	20	10.0, CH ₃	0.79, t (7.3, 7.3)	22	17, 19
	NH(3)		8.21, d (6.8)	11	10
Ser	21				
	22	n.o.			
	23a	n.o.	4.59, m	20	
	23b	61.0, CH ₂	3.69, m		
	NH(4) OH		3.77, m 8.31, d (5.1)	16	15
MePro	24	173.8, C			
	25	61.3, CH	4.15, dd (8.1, 9.3)		24
	26	37.3, CH ₂	2.13, m		
	27	33.1, CH	2.04, m		
	28a	55.0, CH ₂	2.84, t (10.5, 10.5)	NH(5)	
	28b		3.86, m		26
	29	15.2, CH ₃	0.82, d (6.6)		26, 28
Phe-H	30		9.46, s		
	31	n.o.	4.01, m	35	
	32a	55.5, CH	2.57, dd (10.6, 14.0)	34	34/34'
	32b	34.2, CH ₂	2.98, dd (4.0, 14.5)		
	33			32	
	34/34'	137.9, C	7.26, m		
	35/35'	129.5, CH	7.15, d (7.2)	31	
	36 NH(5)	128.7, CH 126.6, CH	7.18, m 7.46, d (9.3)	25	24

^a HMBC correlations are given from proton(s) stated to the indicated carbon atom.

In our preliminary studies with the application of the human 20S proteasome, the Ncp-containing fractions of CCNP1411 inhibited CT-L activity at micromolar concentrations. In the current work, to unequivocally state which of the cyanobacterial metabolites are responsible for this activity, the six isolated Ncps were assayed. For three cyclic Ncps (Ncp-A1, Ncp-A2, Ncp-E2) and the six-amino acid linear variant without an aldehyde

group (Ncp-E4-L), no effects on CT-L activity of the human 20S proteasome were observed (Figure 2A). This activity was inhibited only by two linear peptide aldehydes, Ncp-A2-L and Ncp-E2-L, applied at 50 μ M (Figure 2A). As the two Ncps differ in position 6 (Pro/MePro) and the C-terminal amino acid (Leu/Phe), it can be concluded that these residues do not affect the CT-L activity. Nostocyclopeptide Ncp-E2-L, as well as the widely used synthetic proteasome inhibitor MG-132 [32,33], contain the aldehyde group on C-terminal Leu. The potent activity of MG-132 (IC_{50} 0.11 μ M) [34] was attributed to the formation of the hemiacetal covalent bond between the aldehyde group of C-terminal Leu and the hydroxyl group of Thr1 present in the active site of the proteasome [35]. Another bioactive linear nostocyclopeptide from CCNP1411, Ncp-A2-L, also has the C-terminal amino acid aldehyde (Phe), which again confirms the importance of the aldehyde group for the CT-L inhibition [14,36]. Due to the limited amounts of the isolated Ncps, their effects on T-L and C-L activities were examined with no replications. In the assays, only the cyclic Ncp-A2 showed concentration-dependent inhibition of T-L activity (Figure 2B) and had weak effects on C-L activity (Figure 2C). The other Ncp variants had no clear effects on the two proteolytic sites.

The two linear Ncps, Ncp-A2-L and Ncp-E2-L, moderately decreased the CT-L activity (IC_{50} ca. 50 μ M), compared with several known aldehyde-containing proteasome inhibitors [13]. However, this moderate potency of the Ncps is compensated by their high specificity. Unlike many other peptide aldehydes, which inhibit a wide range of proteases [13,36], the two Ncps interacted with the CT-L site but did not modify the T-L and C-L activities.

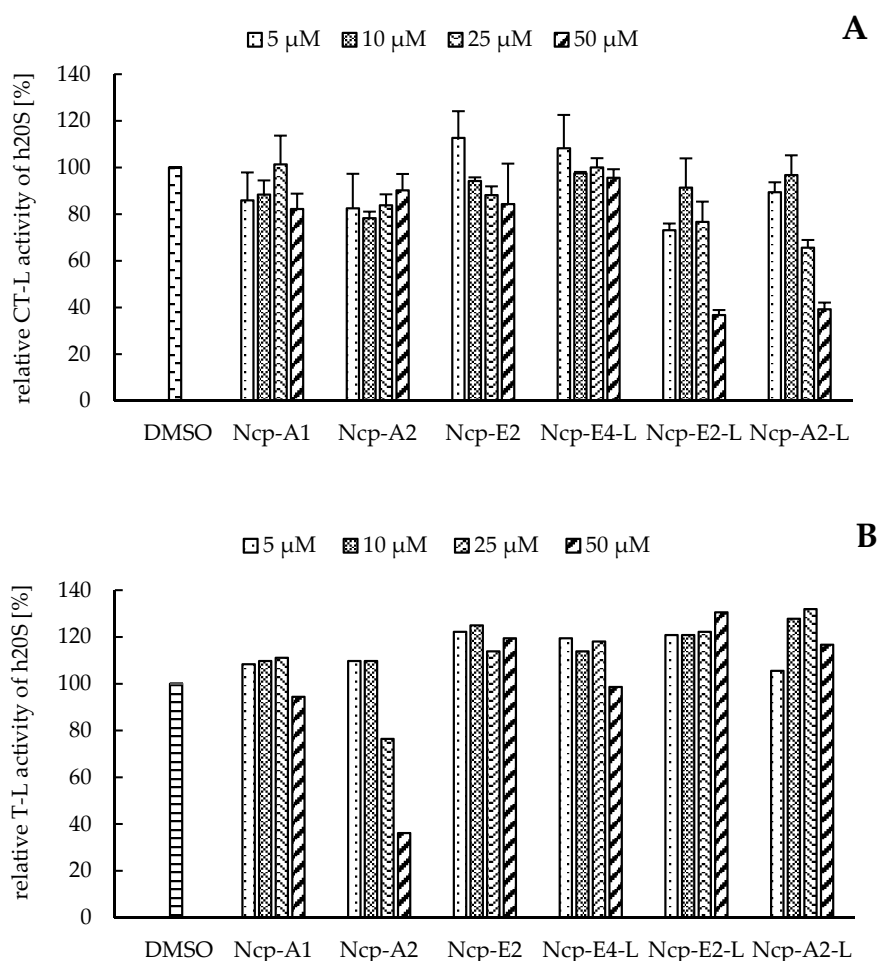


Figure 2. Cont.

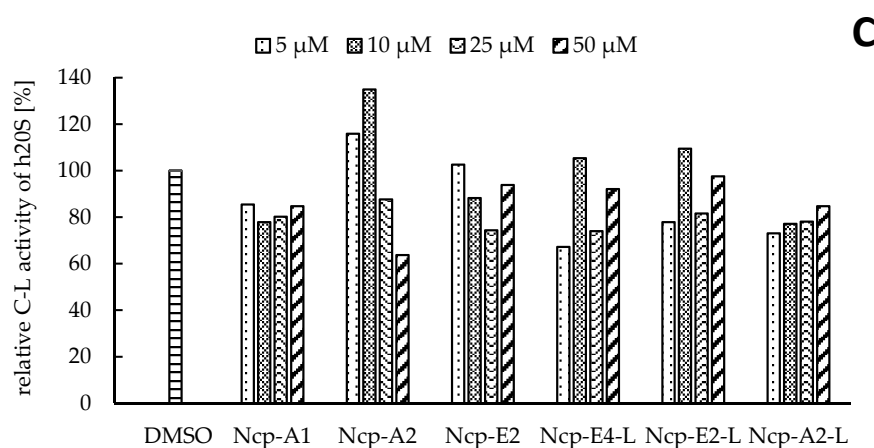


Figure 2. The effects of cyclic and linear (L) nostocyclopeptides (Ncps) on the CT-L (A), T-L (B), and C-L (C) activities of the human 20S proteasome. DMSO was used as a control, and PR11 was used to ensure the correctness of the assay. In the CT-L activity assay, all Ncp variants were tested in triplicate.

Among cyanobacteria metabolites, α,β -epoxyketones carmaphycin A and B, isolated from *Symploca* sp., were found to inhibit CT-L activity of the *Saccharomyces cerevisiae* 20S proteasome at low nanomolar concentrations [37]. The authors suggested that the sulfoxide/sulfone moieties in the methionine-derived residues of the inhibitor are crucial for the interaction with the enzyme complex. Nostodione A from *Scytonema hofmannii*, which inhibits CT-L activity (IC_{50} 50 μ M), contains indole moiety fused with diketone system [38]. Other cyclic metabolites from cyanobacteria have demonstrated inhibitory effects against 20S complex. For example, scytonemide A from *S. hofmannii*, a cyclic peptide characterized by the presence of a unique imino linkage, inhibited catalytic activity of proteasome at IC_{50} 96 nM [39]. Kronic et al. [39] suggested that Gln residue contributed to structural conformation in this peptide, enabling optimal binding at the active site. On the other hand the presence of an imine enabled the formation of a covalent bond. *Nostoc*-derived (*Nostoc* sp. UIC 10022A) cylindrocyclophanes were active against the 20S proteasome in a wide range of activities (IC_{50} 2.2–100 μ M). According to the authors, dichloromethyl moiety was crucial to achieving a higher level of inhibition [40].

The proteasome is an important drug target in a variety of diseases [10–12]. Currently, three proteasome inhibitors, approved by the American Food and Drug Administration (FDA), are clinically used for the treatment of multiple myeloma (MM) and mantle cell lymphoma (MVL) patients: bortezomib (Velcade) [41], carfilzomib (Kyprolis) [42] and ixazomib (Ninlaro) [43]. Unfortunately, despite the initial promising effects and high efficacy of the proteasome inhibitors in MM treatment, in many patients, resistance has developed. Moreover, some patients do not respond to this treatment, or the side effects of the drugs are too severe [44–47].

Currently, the application of proteasome inhibitors in the treatment of other diseases, e.g., in autoimmune disorders, inflammation, or malaria, is explored [4,48]. Further studies are also performed to better understand the effect of specific proteasome inhibitors on general protein homeostasis. In parallel, screening for novel agents with a potential therapeutic application as regulators of the 20S proteasome and other components of the ubiquitin-proteasome system is continued [49,50]. Regardless of the low potency, Ncps still can be considered as starting points for drug development. As in the case of many bioactive natural products, their activity and selectivity can be optimized by structural modifications so that the final compound can demonstrate a better therapeutic potential.

4. Conclusions

Nostoc edaphicum strain CCNP1411 produces 10 nostocyclopeptides, including cyclic and linear forms. In the current work, the effect of six isolated Ncps structural variants

on the activity of the human 20S proteasome was examined. The results indicate the differences in the activity of the cyclic and linear Ncp variants and show their selectivity in interaction with the proteasome active sites. Two of the linear peptides, Ncp-A2-L and Ncp-E2-L, inhibited the CT-L activity of the enzymatic complex without any effect on T-L and C-L sites. On the other hand, the cyclic Ncp-A2 had an inhibitory effect on T-L activity. The study also confirmed the importance of an aldehyde group for the interaction with the active center responsible for the CT-L activity. This is the first report on the inhibitory effect of Ncps on the 20S proteasome, which is an important drug target in various diseases.

Supplementary Materials: The following are available online at <https://www.mdpi.com/article/10.3390/biom11101483/s1>. Figure S1: ¹H NMR spectrum of Ncp-A2-L in H₂O:D₂O (9:1), Figure S2: COSY spectrum of Ncp-A2-L in H₂O:D₂O (9:1), Figure S3: TOCSY spectrum of Ncp-A2-L in H₂O:D₂O (9:1), Figure S4: HSQC spectrum of Ncp-A2-L in H₂O:D₂O (9:1), Figure S5: HMBC spectrum of Ncp-A2-L in H₂O:D₂O (9:1).

Author Contributions: Conceptualization: A.F. and H.M.-M.; methodology: H.M.-M., C.E. and F.K.; formal analysis: A.F., H.M.-M. (LC-MS/MS); A.F., M.C., F.K. and C.E. (extraction, fractionation, isolation of compounds); K.C. and A.F. (20S inhibition assay); writing original draft preparation: A.F.; writing review and editing: A.F., H.M.-M., E.W., C.E., K.C., M.C. and F.K.; visualization: A.F. and E.W.; supervision: H.M.-M.; project administration: H.M.-M.; funding acquisition: H.M.-M. All authors have read and agreed to the published version of the manuscript.

Funding: This research was funded by the National Science Centre in Poland 2016/21/B/NZ9/02304 and the statutory program of the Institute of Oceanology, PAN (grant No.II.3).

Institutional Review Board Statement: Not applicable.

Informed Consent Statement: Not applicable.

Data Availability Statement: Not applicable.

Conflicts of Interest: The authors declare no conflict of interest.

References

1. Kisselev, A.F.; Callard, A.; Goldberg, A. Importance of the different proteolytic sites of the proteasome and the efficacy of inhibitors varies with the protein substrate. *J. Biol. Chem.* **2006**, *281*, 8582–8590. [[CrossRef](#)]
2. Adams, J. The proteasome: Structure, function, and role in the cell. *Cancer Treat. Rev.* **2003**, *29*, 3–9. [[CrossRef](#)]
3. Deshmukh, F.K.; Yaffe, D.; Olshina, M.A.; Ben-Nissan, G.; Sharon, M. The contribution of the 20S proteasome to proteostasis. *Biomolecules* **2019**, *9*, 190. [[CrossRef](#)]
4. Sherman, D.J.; Li, J. Proteasome inhibitors: Harnessing proteostasis to combat disease. *Molecules* **2020**, *25*, 671. [[CrossRef](#)] [[PubMed](#)]
5. Ciechanover, A.; Brundin, P. The ubiquitin proteasome system in neurodegenerative diseases: Sometimes the chicken, sometimes the egg. *Neuron* **2003**, *40*, 427–446. [[CrossRef](#)]
6. Ciechanover, A. Proteolysis: From the lysosome to ubiquitin and the proteasome. *Nat. Rev.* **2005**, *6*, 79–86. [[CrossRef](#)]
7. Bedford, L.; Paine, S.; Sheppard, P.W.; Mayer, R.J.; Roelofs, J. Assembly, structure and function of the 26S proteasome. *Trends Cell Biol.* **2010**, *20*, 391–401. [[CrossRef](#)] [[PubMed](#)]
8. Orłowski, M.; Wilk, S. Ubiquitin-independent proteolytic functions of the proteasome. *Arch. Biochem. Biophys.* **2003**, *415*, 1–5. [[CrossRef](#)]
9. Hwang, J.; Winkler, L.; Kalejta, R.F. Ubiquitin-independent proteasomal degradation during oncogenic viral infections. *Biochim. Biophys. Acta* **2011**, *1816*, 147–157. [[CrossRef](#)]
10. Tundo, G.R.; Sbardella, D.; Santoro, A.M.; Coletta, A.; Oddone, F.; Grasso, G.; Milardi, D.; Lacal, P.M.; Marini, S.; Purrello, L.; et al. The proteasome as a druggable target with multiple therapeutic potentialities: Cutting and non-cutting edges. *Pharmacor. Ther.* **2020**, *213*, 107579. [[CrossRef](#)] [[PubMed](#)]
11. Verbrugge, S.E.; Scheper, R.J.; Lems, W.F.; de Gruijl, T.D.; Jansen, G. Proteasome inhibitors as experimental therapeutics of autoimmune diseases. *Arthritis Res. Ther.* **2015**, *17*, 17. [[CrossRef](#)]
12. Cao, Y.; Zhu, H.; He, R.; Kong, L.; Shao, J.; Zhuang, R.; Xi, J.; Zhang, J. Proteasome, a promising therapeutic target for multiple diseases beyond cancer. *Drug Des. Devel. Ther.* **2020**, *14*, 4327–4342. [[CrossRef](#)]
13. de Bettignies, G.; Coux, O. Proteasome inhibitors: Dozens of molecules and still counting. *Biochimie* **2010**, *92*, 1530–1545. [[CrossRef](#)]
14. Ma, Y.; Xu, B.; Fang, Y.; Yang, Z.; Cui, J.; Zhang, L.; Zhang, L. Synthesis and SAR study of novel peptide aldehydes as inhibitors of 20S proteasome. *Molecules* **2011**, *16*, 7551–7564. [[CrossRef](#)]

15. Harer, S.L.; Bhatia, M.S.; Bhatia, N.M. Proteasome inhibitors mechanism; source for design of newer therapeutic agents. *J. Antibiot.* **2012**, *65*, 279–288. [[CrossRef](#)]
16. Oerlemans, R.; Berkers, C.; Assaraf, Y.G.; Scheffer, G.L.; Peters, G.J.; Verbrugge, S.E.; Cloos, J.; Slootstra, J.; Meloen, R.H.; Shoemaker, R.H.; et al. Proteasome inhibition and mechanism of resistance to a synthetic, library-based hexapeptide. *Investig. New Drugs* **2018**, *36*, 797–809. [[CrossRef](#)]
17. Momose, I.; Sekizawa, R.; Hashizume, H.; Kinoshita, N.; Homma, Y.; Hamada, M.; Iinuma, H.; Takeuchi, T. Tyropeptins A and B, new proteasome inhibitors produced by *Kitasatospora* sp. MK993-dF2. *J. Antibiot.* **2001**, *54*, 997–1003. [[CrossRef](#)]
18. Momose, I.; Sekizawa, R.; Iinuma, H.; Takeuchi, T. Inhibition of proteasome activity by tyropeptin A in PC12 cells. *Biosci. Biotechnol. Biochem.* **2002**, *66*, 2256–2258. [[CrossRef](#)]
19. Hines, J.; Groll, M.; Fahnstock, M.; Crews, C.M. Proteasome inhibition by fellutamide B induces nerve growth factor synthesis. *Chem. Biol.* **2008**, *15*, 501–512. [[CrossRef](#)]
20. Golakoti, T.; Yoshida, W.; Chaganty, S.; Moore, R. Isolation and structure determination of nostocyclopeptides A1 and A2 from the terrestrial cyanobacterium *Nostoc* sp. ATCC53789. *J. Nat. Prod.* **2001**, *64*, 54–59. [[CrossRef](#)]
21. Lee, W.; Belkhir, A.; Lockhart, A.C.; Merchant, N.; Glaeser, H.; Harris, E.I.; Washington, M.K.; Brunt, E.M.; Zaika, A.; Kim, R.B.; et al. Overexpression of OATP1B3 confers apoptotic resistance in colon cancer. *Cancer Res.* **2008**, *68*, 10315–10323. [[CrossRef](#)]
22. Svoboda, M.; Wleck, K.; Taferner, B.; Hering, S.; Stieger, B.; Tong, D.; Zeillinger, R.; Thalhammer, T.; Jäger, W. Expression of organic anion-transporting polypeptides 1B1 and 1B3 in ovarian cancer cells: Relevance for paclitaxel transport. *Biomed. Pharmacother.* **2011**, *65*, 417–426. [[CrossRef](#)]
23. Jokela, J.; Herfindal, L.; Wahlsten, M.; Permi, P.; Selheim, F.; Vasconcelos, V.; Døskeland, S.; Sivonen, K. A novel cyanobacterial nostocyclopeptide is a potent antitoxin against *Microcystis*. *ChemBioChem* **2010**, *11*, 1594–1599. [[CrossRef](#)]
24. Herfindal, L.; Myhren, L.; Kleppe, R.; Krakstad, C.; Selheim, F.; Jokela, J.; Sivonen, K.; Døskeland, S. Nostocyclopeptide-M1: A potent, nontoxic inhibitor of the hepatocyte drug transporters OATP1B3 and OATP1B1. *Mol. Pharm.* **2011**, *8*, 360–367. [[CrossRef](#)]
25. Kotai, J. *Introduction for Preparation of Modified Nutrient Solution Z8 for Algae*; Norwegian Institute for Water Research Publication: Oslo, Norway, 1972.
26. Mazur-Marzec, H.; Fidor, A.; Cegłowska, M.; Wiczerzak, E.; Kropidłowska, M.; Goua, M.; Macaskill, J.; Edwards, C. Cyanopeptolins with trypsin and chymotrypsin inhibitory activity from the cyanobacterium *Nostoc edaphicum* CCNP1411. *Mar. Drugs* **2018**, *16*, 220. [[CrossRef](#)]
27. Czerwonka, A.; Fiołka, M.J.; Jędrzejewska, K.; Jankowska, E.; Zając, A.; Rzeski, W. Pro-apoptotic action of protein-carbohydrate fraction isolated from coelomic fluid of the earthworm *Dendrobaena veneta* against human colon adenocarcinoma cells. *Biomed. Pharmacother.* **2020**, *126*, 110035. [[CrossRef](#)]
28. Gaczyńska, M.; Osmulski, P.A.; Gao, Y.; Post, M.J.; Simons, M. Proline- and arginine-rich peptides constitute a novel class of allosteric inhibitors of proteasome activity. *Biochemistry* **2003**, *42*, 8663–8670. [[CrossRef](#)]
29. Nowruzi, B.; Khavari-Nejad, R.; Sivonen, K.; Kazemi, B.; Najafi, F.; Nejadstattari, T. Identification and toxigenic potential of *Nostoc* sp. *Algae* **2012**, *27*, 303–313. [[CrossRef](#)]
30. Liamer, A.; Jensen, J.; Dittman, E. A genetic and chemical perspective on symbiotic recruitment of cyanobacteria of the genus *Nostoc* into the host plant *Blasia pusilla* L. *Front. Microbiol.* **2016**, *7*, 1963. [[CrossRef](#)]
31. Fidor, A.; Grabski, M.; Gawor, J.; Gromadka, R.; Węgrzyn, G.; Mazur-Marzec, H. *Nostoc edaphicum* CCNP1411 from the Baltic Sea—a new producer of nostocyclopeptides. *Mar. Drugs* **2020**, *18*, 442. [[CrossRef](#)]
32. Guo, N.; Zhilan, P. MG 132, a proteasome inhibitor, induces apoptosis in tumor cells. *Asia Pac. J. Clin. Oncol.* **2013**, *9*, 6–11. [[CrossRef](#)]
33. Zhang, L.; Hu, J.J.; Gong, F. MG 132 inhibition of proteasome blocks apoptosis induced by severe DNA damage. *Cell Cycle* **2011**, *10*, 3515–3518. [[CrossRef](#)]
34. Hasegawa, M.; Kinoshita, K.; Nishimura, C.; Matsumura, U.; Shionyu, M.; Ikeda, S.; Mizukami, T. Affinity labeling of the proteasome by a belactosin A derived inhibitor. *Bioorg. Med. Chem. Lett.* **2008**, *18*, 5668–5671. [[CrossRef](#)]
35. Kisselev, A.F.; van der Linden, W.A.; Overkleeft, H.S. Proteasome inhibitors: An expanding army attacking a unique target. *Chem. Biol.* **2012**, *19*, 99–115. [[CrossRef](#)]
36. Kisselev, A.F.; Goldberg, A. Proteasome inhibitors: From research tools to drug candidates. *Chem. Biol.* **2001**, *8*, 739–758. [[CrossRef](#)]
37. Pereira, A.R.; Kale, A.J.; Fenley, A.T.; Byrum, T.; Debonsi, H.M.; Gilson, M.K.; Valeriote, F.A.; Moore, B.S.; Gerwick, W.H. The carmaphycins: New proteasome inhibitors exhibiting an α,β -epoxyketone warhead from a marine cyanobacterium. *ChemBioChem* **2012**, *13*, 810–817. [[CrossRef](#)]
38. Shim, S.H.; Chlipala, G.; Orjala, J. Isolation and structure determination of a proteasome inhibitory metabolite from a culture of *Scytonema hofmannii*. *J. Microbiol. Biotechnol.* **2008**, *18*, 1655–1658.
39. Kronic, A.; Vallat, A.; Mo, S.; Lantvit, D.D.; Swanson, S.M.; Orjala, J. Scytonemides A and B, cyclic peptides with 20S proteasome inhibitory activity from the cultured cyanobacterium *Scytonema hofmannii*. *J. Nat. Prod.* **2010**, *29*, 1927–1932. [[CrossRef](#)]
40. Chlipala, G.E.; Sturdy, M.; Kronic, A.; Lantvit, D.D.; Shen, Q.; Porter, K.; Swanson, S.M.; Orjala, J. Cyliindrocyclophanes with proteasome inhibitory activity from the cyanobacterium *Nostoc* sp. *J. Nat. Prod.* **2010**, *73*, 1529–1537. [[CrossRef](#)]
41. Field-Smith, A.; Morgan, G.J.; Davies, F.E. Bortezomib (VelcadeTM) in the treatment of multiple myeloma. *Ther. Clin. Risk Manag.* **2006**, *2*, 271–279. [[CrossRef](#)]

42. Herndon, T.M.; Deisseroth, A.; Kaminskas, E.; Kane, R.C.; Koti, K.M.; Rothmann, M.D.; Habtemariam, B.; Bullock, J.; Bray, J.D.; Hawes, J.; et al. Food and Drug Administration approval: Carfilzomib for the treatment of multiple myeloma. *Clin. Cancer Res.* **2013**, *19*, 4559–4563. [[CrossRef](#)]
43. Shirley, M. Ixazomib: First global approval. *Drugs* **2016**, *76*, 405–411. [[CrossRef](#)] [[PubMed](#)]
44. Bai, Y.; Su, X. Updates to the drug-resistant mechanism of proteasome inhibitors in multiple myeloma. *Asia-Pac. J. Clin. Oncol.* **2021**, *17*, 29–35. [[CrossRef](#)]
45. Kim, K.B. Proteasomal adaptations to FDA-approved proteasome inhibitors: A potential mechanism for drug resistance. *Cancer Drug Resist.* **2021**, *4*, 634–645.
46. Moreau, P.; Richardson, P.G.; Cavo, M.; Orłowski, R.Z.; Sam Miguel, J.F.; Palumbo, A.; Harousseau, J.-L. Proteasome inhibitors in multiple myeloma: 10 years later. *Blood* **2012**, *120*, 947–959. [[CrossRef](#)]
47. Pancheri, E.; Guglielmi, V.; Wilczynski, G.M.; Malatesta, M.; Tonin, P.; Tomelleri, G.; Nowis, D.; Vattemi, G. Non-hematologic toxicity of bortezomib in multiple myeloma: The neuromuscular and cardiovascular adverse effects. *Cancers* **2020**, *12*, 2540. [[CrossRef](#)]
48. Cromm, P.M.; Crews, C.M. The proteasome in modern drug discovery: Second life of highly valuable drug target. *ACS Cent. Sci.* **2017**, *3*, 830–838. [[CrossRef](#)] [[PubMed](#)]
49. Mofers, A.; Selvaraju, K.; Gubat, J.; D’Arcy, P.; Linder, S. Identification of proteasome inhibitors using analysis of gene. *Eur. J. Pharmacol.* **2020**, *889*, 173709. [[CrossRef](#)]
50. Shen, X.; Wu, C.; Lei, M.; Yan, Q.; Zhang, H.; Zhang, L.; Wang, X.; Yang, Y.; Li, J.; Zhu, Y.; et al. Anti-tumor activity of a novel proteasome inhibitor D395 against multiple myeloma and its lower cardiotoxicity compared with carfilzomib. *Cell Death Dis.* **2021**, *12*, 429. [[CrossRef](#)]

Supplementary Material: Nostocyclopeptides as new inhibitors of 20S proteasome

Anna Fidor ¹, Katarzyna Cekała ², Ewa Wieczerek ², Marta Ceglowska ³, Franciszek Kasprzykowski ², Christine Edwards ⁴, Hanna Mazur-Marzec ^{1*}

¹ Division of Marine Biotechnology, Institute of Oceanography, University of Gdańsk, Marszałka Józefa Piłsudskiego 46, PL-81378 Gdynia, Poland; anna.fidor@phdstud.ug.edu.pl (A.F.); hanna.mazur-marzec@ug.edu.pl (H.M-M.)

² Department of Biomedical Chemistry, Faculty of Chemistry, University of Gdańsk, Wita Stwosza 63, PL-80308 Gdańsk, Poland; jedrzejewskakatarzyna92@gmail.com (K.C.); ewa.wieczerek@ug.edu.pl (E.W.); franciszek.kasprzykowski@ug.edu.pl (F.K.)

³ Institute of Oceanology, Polish Academy of Sciences, PowstańcówWarszawy 55, PL-81712 Sopot, Poland; mceglowska@iopan.pl

⁴ School of Pharmacy and Life Sciences, Robert Gordon University, Aberdeen AB10 7GJ, UK; c.edwards@rgu.ac.uk (C.E.)

* Correspondence: hanna.mazur-marzec@ug.edu.pl (H.M-M.)

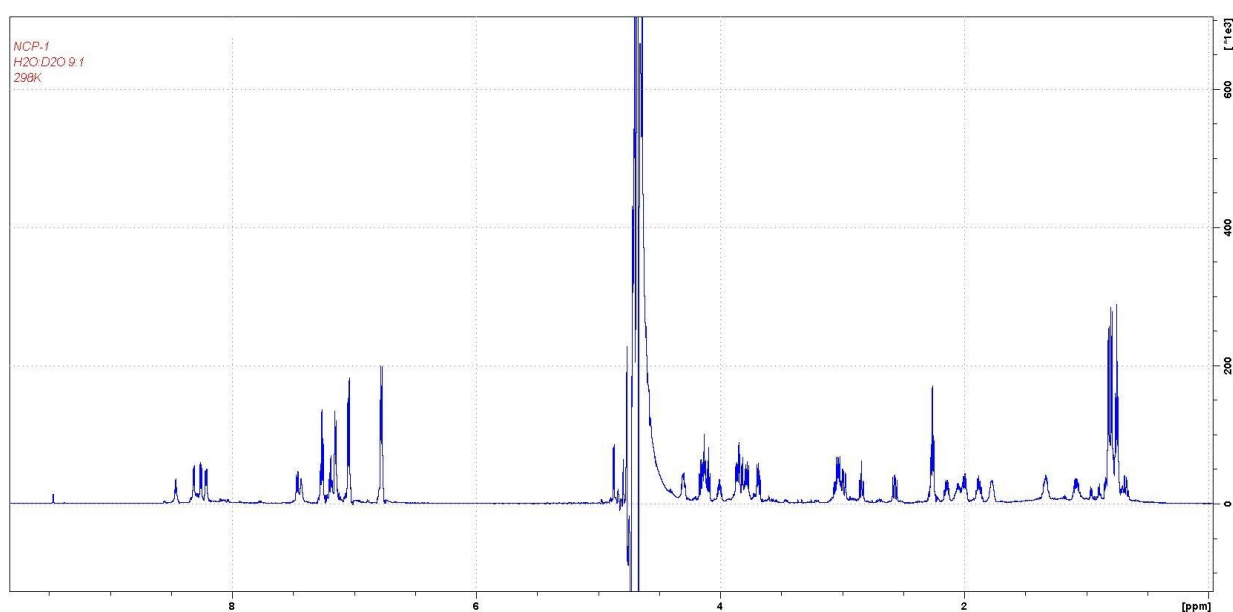


Figure S1: ¹H NMR spectrum of Ncp-A2-L in H₂O:D₂O (9:1)

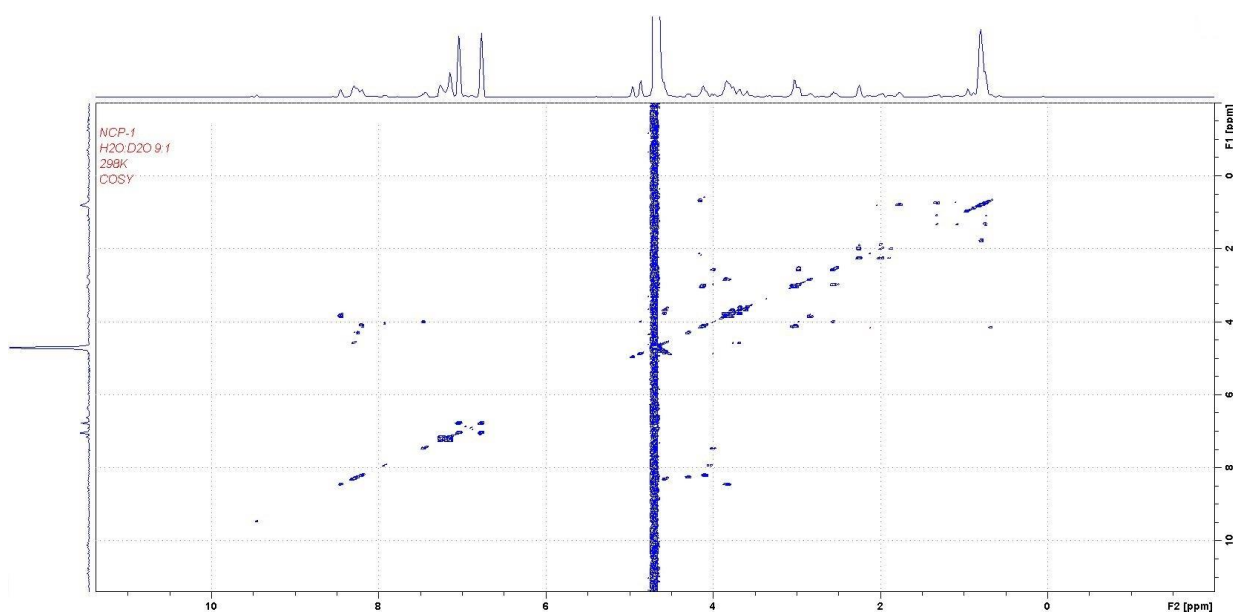


Figure S2: COSY spectrum of Ncp-A2-L in H₂O:D₂O (9:1)

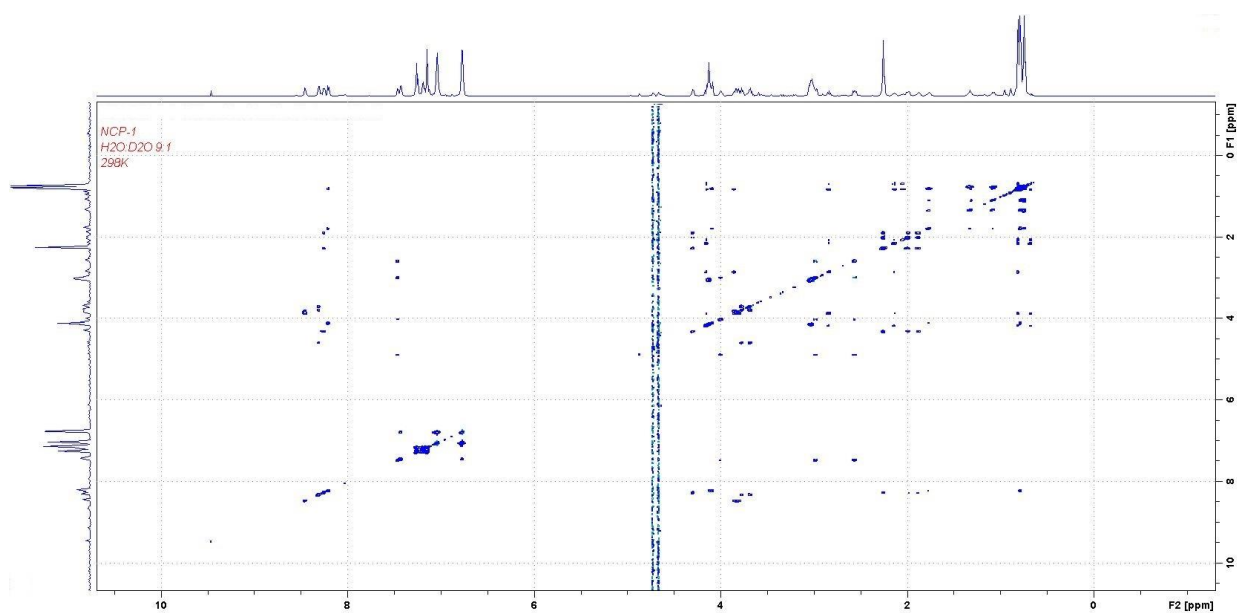


Figure S3: TOCSY spectrum of Ncp-A2-L in H₂O:D₂O (9:1)

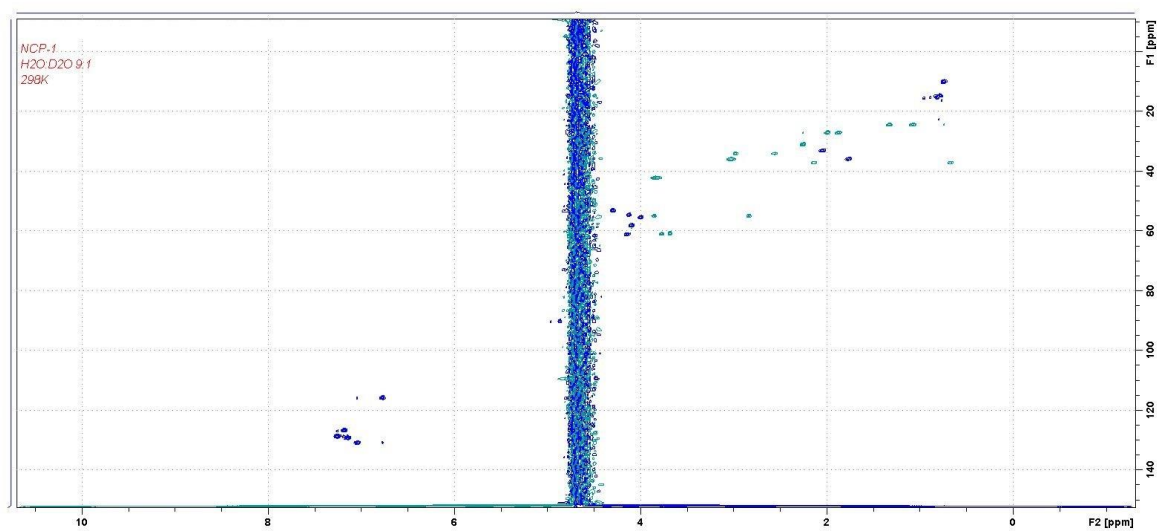


Figure S4: HSQC spectrum of Ncp-A2-L in H₂O:D₂O (9:1)

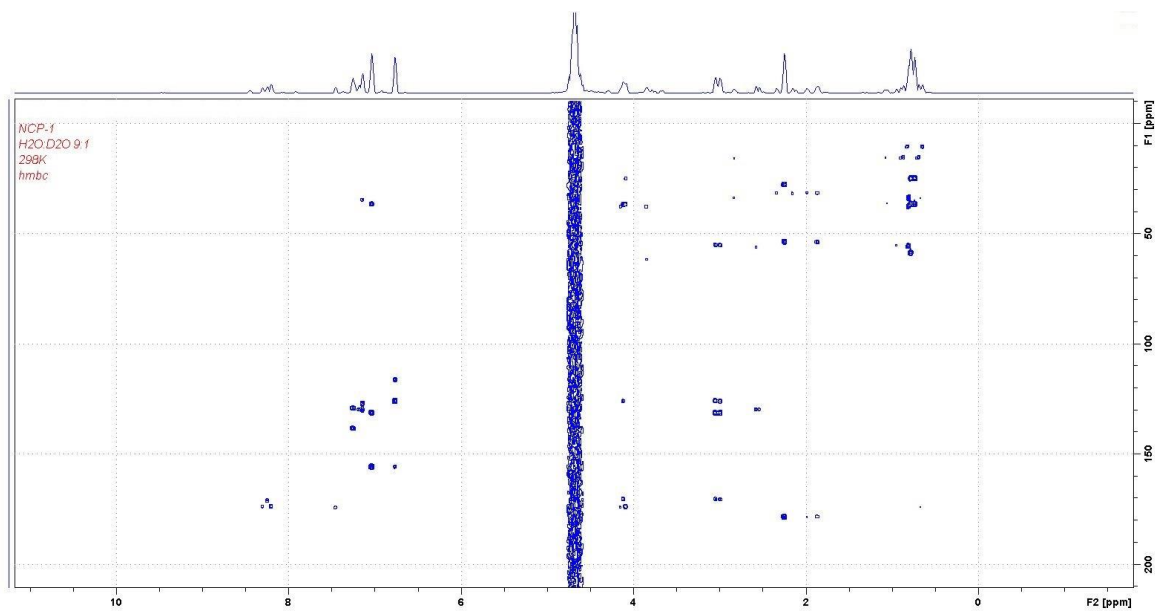


Figure S5: HMBC spectrum of Ncp-A2-L in H₂O:D₂O (9:1)

Statement of Co-Authorship

Conceptualization: Anna Fidor, Hanna Mazur-Marzec
Methodology: Hanna Mazur-Marzec, Christine Edwards, Franciszek Kasprzykowski
LC-MS/MS analysis: Anna Fidor, Hanna Mazur-Marzec
Extraction, fractionation, isolation of compounds: Anna Fidor, Marta Ceglowska, Franciszek Kasprzykowski, Christine Edwards
20S inhibition assay: Katarzyna Cekała, Anna Fidor
Writing – original draft preparation: Anna Fidor
Writing – review and editing: Anna Fidor, Hanna Mazur-Marzec, Ewa Wiczerzak, Katarzyna Cekała, Christine Edwards, Marta Ceglowska, Franciszek Kasprzykowski
Visualization: Anna Fidor, Ewa Wiczerzak
Supervision: Hanna Mazur-Marzec

I, the undersigned, acknowledge the above contribution of work undertaken for the published work "Nostocyclopeptides as new inhibitors of 20S proteasome" (*Biomolecules*, 2021, DOI:10.3390/biom11101483) contributing to the dissertation "Peptides produced by the Baltic cyanobacterium *Nostoc edaphicum* CCNP1411 - structure and biological activity".

My contribution to the work was: conceptualization, LC-MS/MS analyses, extraction, fractionation and isolation of pure compounds, 20S inhibition assays, writing the original draft, edition of the manuscript and visualization of data.

.....
(Anna Fidor)

Statement of Co-Authorship

Conceptualization: Anna Fidor, Hanna Mazur-Marzec
Methodology: Hanna Mazur-Marzec, Christine Edwards, Franciszek Kasprzykowski
LC-MS/MS analysis: Anna Fidor, Hanna Mazur-Marzec
Extraction, fractionation, isolation of compounds: Anna Fidor, Marta Ceglowska, Franciszek Kasprzykowski, Christine Edwards
20S inhibition assay: Katarzyna Cekała, Anna Fidor
Writing – original draft preparation: Anna Fidor
Writing – review and editing: Anna Fidor, Hanna Mazur-Marzec, Ewa Wiczerzak, Katarzyna Cekała, Christine Edwards, Marta Ceglowska, Franciszek Kasprzykowski
Visualization: Anna Fidor, Ewa Wiczerzak
Supervision: Hanna Mazur-Marzec

I, the undersigned, acknowledge the above contribution of work undertaken for the published work "Nostocyclopeptides as new inhibitors of 20S proteasome" (*Biomolecules*, 2021, DOI:10.3390/biom11101483) contributing to the dissertation "Peptides produced by Baltic cyanobacterium *Nostoc edaphicum* CCNP1411 - structure and biological activity".

My contribution to the work was conceptualization, methodology development and edition of manuscript.



.....
(Hanna Mazur-Marzec)

Statement of Co-Authorship

Conceptualization: Anna Fidor, Hanna Mazur-Marzec
Methodology: Hanna Mazur-Marzec, Christine Edwards, Franciszek Kasprzykowski
LC-MS/MS analysis: Anna Fidor, Hanna Mazur-Marzec
Extraction, fractionation, isolation of compounds: Anna Fidor, Marta Ceglowska, Franciszek Kasprzykowski, Christine Edwards
20S inhibition assay: Katarzyna Cekała, Anna Fidor
Writing – original draft preparation: Anna Fidor
Writing – review and editing: Anna Fidor, Hanna Mazur-Marzec, Ewa Wiczerzak, Katarzyna Cekała, Christine Edwards, Marta Ceglowska, Franciszek Kasprzykowski
Visualization: Anna Fidor, Ewa Wiczerzak
Supervision: Hanna Mazur-Marzec

I, the undersigned, acknowledge the above contribution of work undertaken for the published work "Nostocyclopeptides as new inhibitors of 20S proteasome" (*Biomolecules*, 2021, DOI:10.3390/biom11101483) contributing to the dissertation "Peptides produced by Baltic cyanobacterium *Nostoc edaphicum* CCNP1411 - structure and biological activity".

The assessment of my and PhD candidate (Anna Fidor) contribution to the work is 5 % and 60 %.


.....
(Katarzyna Cekała)

Statement of Co-Authorship

Conceptualization: Anna Fidor, Hanna Mazur-Marzec
Methodology: Hanna Mazur-Marzec, Christine Edwards, Franciszek Kasprzykowski
LC-MS/MS analysis: Anna Fidor, Hanna Mazur-Marzec
Extraction, fractionation, isolation of compounds: Anna Fidor, Marta Ceglowska, Franciszek Kasprzykowski, Christine Edwards
20S inhibition assay: Katarzyna Cekała, Anna Fidor
Writing – original draft preparation: Anna Fidor
Writing – review and editing: Anna Fidor, Hanna Mazur-Marzec, Ewa Wieczerzak, Katarzyna Cekała, Christine Edwards, Marta Ceglowska, Franciszek Kasprzykowski
Visualization: Anna Fidor, Ewa Wieczerzak
Supervision: Hanna Mazur-Marzec

I, the undersigned, acknowledge the above contribution of work undertaken for the published work "Nostocyclopeptides as new inhibitors of 20S proteasome" (*Biomolecules*, 2021, DOI:10.3390/biom11101483) contributing to the dissertation "Peptides produced by Baltic cyanobacterium *Nostoc edaphicum* CCNP1411 - structure and biological activity".

The assessment of my and PhD candidate (Anna Fidor) contribution to the work is 6 % and 60 %.



(Ewa Wieczerzak)

Statement of Co-Authorship

Conceptualization: Anna Fidor, Hanna Mazur-Marzec
Methodology: Hanna Mazur-Marzec, Christine Edwards, Franciszek Kasprzykowski
LC-MS/MS analysis: Anna Fidor, Hanna Mazur-Marzec
Extraction, fractionation, isolation of compounds: Anna Fidor, Marta Ceglowska, Franciszek Kasprzykowski, Christine Edwards
20S inhibition assay: Katarzyna Cekała, Anna Fidor
Writing – original draft preparation: Anna Fidor
Writing – review and editing: Anna Fidor, Hanna Mazur-Marzec, Ewa Wieczerzak, Katarzyna Cekała, Christine Edwards, Marta Ceglowska, Franciszek Kasprzykowski
Visualization: Anna Fidor, Ewa Wieczerzak
Supervision: Hanna Mazur-Marzec

I, the undersigned, acknowledge the above contribution of work undertaken for the published work "Nostocyclopeptides as new inhibitors of 20S proteasome" (*Biomolecules*, 2021, DOI:10.3390/biom11101483) contributing to the dissertation "Peptides produced by Baltic cyanobacterium *Nostoc edaphicum* CCNP1411 - structure and biological activity".

The assessment of my and PhD candidate (Anna Fidor) contribution to the work is 4 % and 60 %.



(Marta Ceglowska)

Statement of Co-Authorship

Conceptualization: Anna Fidor, Hanna Mazur-Marzec
Methodology: Hanna Mazur-Marzec, Christine Edwards, Franciszek Kasprzykowski
LC-MS/MS analysis: Anna Fidor, Hanna Mazur-Marzec
Extraction, fractionation, isolation of compounds: Anna Fidor, Marta Ceglowska, Franciszek Kasprzykowski, Christine Edwards
20S inhibition assay: Katarzyna Cekała, Anna Fidor
Writing – original draft preparation: Anna Fidor
Writing – review and editing: Anna Fidor, Hanna Mazur-Marzec, Ewa Wieczerzak, Katarzyna Cekała, Christine Edwards, Marta Ceglowska, Franciszek Kasprzykowski
Visualization: Anna Fidor, Ewa Wieczerzak
Supervision: Hanna Mazur-Marzec

I, the undersigned, acknowledge the above contribution of work undertaken for the published work "Nostocyclopeptides as new inhibitors of 20S proteasome" (*Biomolecules*, 2021, DOI:10.3390/biom11101483) contributing to the dissertation "Peptides produced by Baltic cyanobacterium *Nostoc edaphicum* CCNP1411 - structure and biological activity".

The assessment of my and PhD candidate (Anna Fidor) contribution to the work is 5 % and 60 %.



(Christine Edwards)

Statement of Co-Authorship

Conceptualization: Anna Fidor, Hanna Mazur-Marzec

Methodology: Hanna Mazur-Marzec, Christine Edwards, Franciszek Kasprzykowski

LC-MS/MS analysis: Anna Fidor, Hanna Mazur-Marzec

Extraction, fractionation, isolation of compounds: Anna Fidor, Marta Ceglowska, Franciszek Kasprzykowski, Christine Edwards

20S inhibition assay: Katarzyna Cekała, Anna Fidor

Writing – original draft preparation: Anna Fidor


Writing – review and editing: Anna Fidor, Hanna Mazur-Marzec, Ewa Wieczerzak, Katarzyna Cekała, Christine Edwards, Marta Ceglowska, Franciszek Kasprzykowski

Visualization: Anna Fidor, Ewa Wieczerzak

Supervision: Hanna Mazur-Marzec

I, the undersigned, acknowledge the above contribution of work undertaken for the published work "Nostocyclopeptides as new inhibitors of 20S proteasome" (*Biomolecules*, 2021, DOI:10.3390/biom11101483) contributing to the dissertation "Peptides produced by Baltic cyanobacterium *Nostoc edaphicum* CCNP1411 - structure and biological activity".

My contribution to the work was methodology development, compounds isolation and edition of manuscript.



(Franciszek Kasprzykowski)

8. APPENDIX

OŚWIADCZENIE

Ja, niżej podpisana Anna Fidor (nr albumu: 004871), doktorantka Środowiskowych Studiów Doktoranckich na Wydziale Oceanografii i Geografii (Uniwersytet Gdański) oświadczam, iż przedłożona przeze mnie praca doktorska „Peptides produced by the Baltic cyanobacterium *Nostoc edaphicum* CCNP1411 – structure and biological activity” („Peptydy produkowane przez bałtycką cyjanobakterię *Nostoc edaphicum* CCNP1411 – struktura i aktywność biologiczna”) została wykonana samodzielnie, przedstawia wyniki badań wykonanych pod kierunkiem Prof. dr hab. Hanny Mazur-Marzec (promotor), nie narusza praw autorskich, interesów prawnych i materialnych innych osób.

.....

(data, własnoręczny podpis)